Sea-urchin inspired wet bioadhesives - a multidisciplinary quest towards biomimicry

R Santos

Biomedical and Oral Sciences Research Unit (UICOB), School of Dentistry of the University of Lisbon, Portugal

INTRODUCTION: Adhesive mechanisms are beginning to be deciphered in some marine organisms that attach permanently with a cement (mussels, barnacles) or use a viscous film to move and adhere (limpets). However, this is far from being true for sea urchins, that attach strongly but temporarily to the substratum. Sea urchins are exclusively benthic animals and to withstand hydrodynamic forces rely on hundreds of independent adhesive organs, their adoral tube feet, specialized in locomotion and anchoring. Tube feet consist of two functional units: a disc, which makes contact with the substratum, and a stem, which connects the disc to the test. Therefore, the tenacity with which an individual can anchor to a surface is determined by the strength of its numerous tube feet which, in turn, depends on the tensile strength of the stem and the adhesive power of the disc. The later is determined by the chemical properties of an adhesive secretion that is able to functionally assemble underwater and displace water, ions, and weakly bound polyions, properties that are rarely achieved by synthetic adhesives. In addition, sea urchins also possess an effective de-adhesive secretion that rapidly releases the tube feet in order to begin a new attachment-detachment cycle. This de-adhesive secretion is believed to contain enzymes, which catalytic activity promotes breaking of the bonds established between the adhesive and the disc, thus leaving a circle of adhesive material (footprint) strongly attached to the substrate.

METHODS & RESULTS: More than 10 years of research combining morphological and biomechanical techniques have provided evidence that tube feet discs attach with a tenacity (adhesive force per unit area) similar to other marine and commercial adhesives, being able to cope with different substrate chemistries and roughness, thus ensuring strong adhesion irrespective of substratum profile or chemistry. These findings demonstrated that sea urchins tube feet have evolved to resist hydrodynamic loads and deal with the unpredictability of the substratum, which has not yet been achieved by any synthetic (chemical-based) adhesive when applied in an underwater environment. More recently, techniques such as proteomics and mass spectrometry, demonstrated that tube feet are unique mechano-sensory adhesive organs and highlighted putative adhesive proteins. Work is in progress to identify the genes coding for these adhesive proteins in order to produce recombinant analogues or partial adhesive motifs that can be used to design new dental bioadhesives inspired on millions of years of optimization through biological selection.

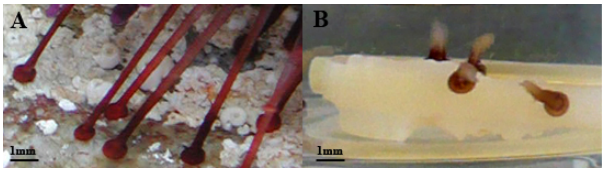

Fig. 1: Images of sea urchin tube feet attaching underwater to the surface of a rock (A) and to enamel and dentine in a human tooth slice both in (B).

DISCUSSION & CONCLUSIONS: Adhesives produced by marine attaching organisms have attracted attention as a paradigm of strong and versatile underwater adhesion. Given the similarity between the oral environment and the wave swept seashore it is highly probable that water-efficient marine adhesives can be valuable sources of inspiration to develop new dental adhesives. Although a number of improved dental adhesives have become available commercially there are still a number of unsolved problems, reinforcing the need to develop new biomimetic adhesives based on the knowledge of the molecular mechanisms underlying marine adhesion.

ACKNOWLEDGEMENTS: Fundação para a Ciência e Tecnologia for financing; COST Action TD0906 (http://www.cost-bioadhesives.org/) and several colleagues and scientists, in particular Dr. Patrick Flammang, for their valuable contribution over the years.

Evaluation of synthetic bone substitute engineered with amniotic epithelial cells in bone regeneration

A Polimeni[1], S Tetè[2], EF Gherlone[3]

[1]Dept of Oral Science, University "La Sapienza", Rome, Italy. [2]Dept of Medical ,Oral and Biotechnological Science, University "G. d'Annunzio, Chieti, Italy. [3]Dept of Dentistry, Vita Salute University, San Raffaele Hospital, Milan, Italy.

INTRODUCTION: The objective of this study was to in vitro and in vivo evaluate the efficacy, safety and flexibility of an innovative cell-based tissue engineering approach for bone regeneration. Tissue engineering is an area of multidisciplinary research aimed at regenerating tissues and restoring organ functionality by means of the transplant of cells and tissues developed in vitro or by stimulating cellular growth in a synthetic matrix. The generated vital tissue should ideally be immunologically, functionally, structurally and mechanically identical to native tissue. In recent years, the efforts in this area focused on the characterization of the regenerative properties of different sources of stem cells by studying embryonic and adult stem cells, but both cell types exhibit critical elements that have, until now, limited their clinical application. For this reason it was necessary to find an alternative source of cells for regenerative purpose. Amniotic derived cells (ADSs) are used in this study. ADSs are an intermediate stage between embryonic stem cells and lineage-restricted adult progenitor cells. Their high proliferation rate together with their differentiation potential into cells of all 3 embryonic germ layers (ectoderm, endoderm and mesoderm) are important advantages over most of the known adult stem cell sources. Our research includes the selection of a stem cell niche with characteristics suitable for tissue regeneration, that is the amniotic epithelium, the development of a suitable synthetic tridimensional scaffolds in order to build a biocomplex with stem cells, and the evaluation of the osteo-regenerative potential of the obtained biocomplex for pre-clinical application.

METHODS: Novel cell constructs, made by stem cells and synthetic tridimensional scaffolds (hydroxiapatite and beta-tricalcium phosphate in a 30/70 ratio or mineralized, solvent-dehydrated bone allografts), were prepared for in vitro and in vivo tests, through the direct rapid prototyping technique dispense-plotting. For preclinical setting, sheep was chosen as animal model, because of its high translational value. The oAEC (ovine amniotic epithelial cells) were collected from amnions of sheep slaughtered at approximately 3 month of pregnancy. In order to achieve 3D scaffold loading, $10x10^6$ labeled oAEC were inseminated on single blocks of synthetic bone substitute (~1.4 cm^3). Bilateral sinus augmentation procedure are carried out with an extra-oral approach. Animals were euthanatized 45 and 90 days after surgery and block section were obtained. Sinus explants were fixed in 4% paraformaldehyde solution and analyzed with the micro Computerized Tomography (micro-CT) technique in order to evaluate the biomaterial integration into the host tissue. The fixed explants were also processed for histological and immunohistological analyses in order to detect the progression of healing at different time.

RESULTS: The results of this study suggest that scaffold integration and bone deposition are positively influenced by the oAEC loading. Maxillary sinuses treated with the engineered biocomplexes displayed a limited inflammatory response and an accelerated process of angiogenesis.

DISCUSSION & CONCLUSIONS: Transplanted oAEC were able to significantly increase the quantity of newly deposited bone tissue, as well as to stimulate a widespread process of angiogenesis and osteogenesis, which represent crucial events successfully guiding tissue. In addition, oAEC seem to be also able to directly participate in the process of bone deposition, as suggested by the presence of themselves entrapped within the newly deposited bone matrix.

REFERENCES: [1] B. Stevens, Y. Yang, A. Mohandas, et al (2008) *J Biomed Mater Res B.* **85**:573. [2] S. Hollister (2005) **4**:518. [3] U. Deisinger, S. Hamisch, M. Schumacher, et al (2008) *Key Engineering Materials* **361**:915.

ACKNOWLEDGEMENTS: This study was partly funded by PRIN 20102ZLNJ5.

An overview of biomimetic approaches for biomedical adhesives development

P Flammang, M Demeuldre, E Hennebert

Biology of Marine Organisms and Biomimetics, Research Institute for Biosciences, University of Mons, Belgium

INTRODUCTION: Many natural bioadhesives perform in ways that man-made products simply cannot match. Marine adhesives, for instance, work most effectively underwater and are universal in their performance to substrates of varying composition and structure. They could therefore potentially inspire novel, superior adhesives for a large range of biomedical applications. Indeed, similarities exist between the marine and human physiologic environments, and a strategy that works well in one context may be useful in the other. Yet, because biomimetic efforts are only possible when composition and key molecular components of biological adhesives are understood, so far only a very limited number of organisms have been used for the development of bio-inspired adhesives.

COMPOSITION OF NATURAL ADHESIVES: Numerous marine invertebrates produce highly viscous or solid adhesive secretions, made up of complex blends of proteins associated with or without other components. The diversity of marine adhesives is huge but, to date, only a very limited number of marine organisms have been studied in detail. The best-characterized marine bioadhesives are those from the mussel and the sandcastle worm. Mussels produce a byssus, which consists of a bundle of proteinaceous threads. Their distal ends, mediating adhesion to the substratum, are made up of a mixture of six major proteins known as foot proteins. The sandcastle worm is a tube-dwelling invertebrate that builds its shelter by assembling sand grains and shells fragments with an adhesive consisting of five major proteins. Studies on mussel and tubeworm proteins have revealed molecular convergences such as low complexity sequences, strongly skewed amino acid compositions, repeating peptide motifs, and the presence of post-translationally modified amino acids. Among the latter, DOPA is the most thoroughly investigated as it plays important interfacial and cross-linking roles in the adhesives.

PRODUCTION OF BIOMIMETIC ADHESIVES: For most applications (including biomedical applications), harvesting the natural adhesive is an unrealistic solution. To bypass the problem of obtaining adhesive proteins directly from marine organisms, research into the production of bio-inspired adhesives has developed in two different directions: the production of recombinant adhesive proteins and the incorporation of functional adhesive motifs, mostly DOPA, to chemically synthesized polymers (Fig. 1). Other remarkable properties of natural cements, such as the capacity to form complex coacervates, to self-assemble and to cross-link, have been mimicked for the underwater delivery and in situ curing of the biomimetic adhesives. Most bio-inspired adhesives developed within the last 5 years have focused on biotechnological and biomedical applications. Different formulations have been tested as adhesives and sealants for surgery, as coatings to functionalize biomaterials and scaffolds, or as self-adhesive hydrogels for drug delivery.

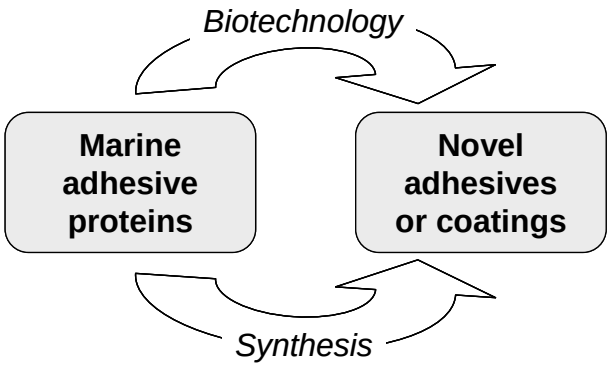

Fig. 1: The two ways of producing biomimetic adhesives: recombinant DNA technology and chemical synthesis of polymeric chains incorporating key reactive groups.

PERSPECTIVES: The production of adhesives suitable for medical applications is far from being mastered on an industrial scale. On the other hand, fundamental research in the field of biological and biomimetic bonding has made enormous progress. This will certainly result in new bio-inspired adhesive designs for a whole range of niche applications.

REFERENCES: E. Hennebert, et al. (2012) Lessons from sea organisms to produce new biomedical adhesives in *Biomimetic Approaches for Biomaterials Development* (ed. J.F. Mano) Wiley-VCH, pp 273-291.

Analysis and Fabrication of nanofur for biomimetic applications

M Röhrig, M Schneider, H Louvin, A Hopf, M Worgull, H Hölscher

Institute of Microstructure Technology, Karlsruhe Institute of Technology (KIT), Germany

INTRODUCTION: Various technical surfaces are inspired by plants or insects covered with dense hair of nanometer thickness [1]. The large-scale fabrication of these surfaces, however, is challenging. Here, we introduce a highly scalable and cost-effective molding technique for the fabrication of dense nanofur. In this way we tune the wettability of polycarbonate from hydrophilic to superhydrophobic. By mechanically structuring the nanofur we change the local wettability and create liquid traps. Furthermore, we use these surfaces for the creation of slippery liquid infused surfaces (SLIPS) [2] inspired by the pitchers plant [3].

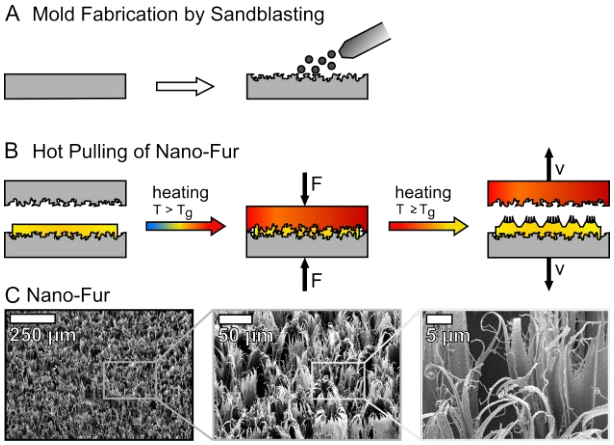

Fig. 1: Fabrication of nanofur by hot pulling. **A** *A steel-plate serves as mold and the required roughness and undercuts are generated by sandblasting.* **B** *The heated mold is pressed onto the foil and the polymer softens and fills the cavities of the mold. By retracting the heated mold, the softened polymer elongates and forms a cratered surface covered with high aspect ratio nanohairs.* **C** *SEM micrographs showing the fractal surface topography of nanofur fabricated from polycarbonate.*

METHODS: The hot pulling process relinquishes expensive mold inserts since demolding forces are utilized to form high aspect ratio micro- and nanostructures. Sandblasted steel-plates serve as mold insert as well as counter-plate in the fully automated process (Fig. 1A). The mold insert is heated to a temperature exceeding the glass transition temperature of the material (144° C for polycarbonate). When this pre-defined temperature is attained, the mold insert is moved towards the opposing polycarbonate foil which is fixed. As soon as the mold insert is in contact with the polycarbonate, softening of the polymer begins (Fig. 1A). Once the mold insert reaches the chosen depth of penetration and the pre-defined holding-time is elapsed, the heated mold insert is retracted from the polymer with a controlled velocity. Therefore, the softened polymer elongates during demolding and forms a cratered surface covered with high aspect ratio nanohairs (Fig. 1C).

RESULTS: Interestingly, the hydrophilic polycarbonate can be transformed to a super-hydrophobic surface by hot pulling (Fig. 2). Therefore, the nanofur surfaces are applicable for a wide variety of applications inspired by nature like SLIPS [2].

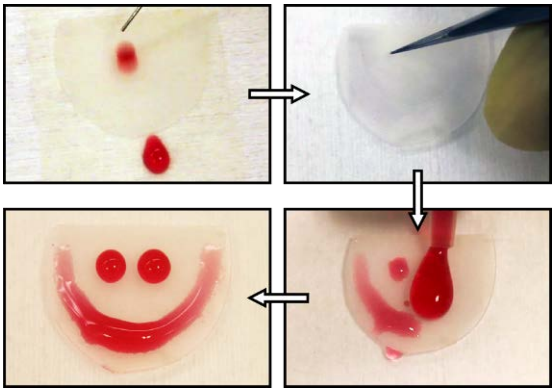

Fig. 2: A flat polycarbonate surface is hydrophobic but hot pulling of a very dense fur of nanoscale hairs results in a super-hydrophobic surface. Destroying the nanohairs by scratching makes the sample hydrophilic again. These zones serve now as reservoirs for water like in this example where a smiley is scratched into the foil.

REFERENCES: [1]B. Bhushan, et al. (2009) *Phil. Trans. R. Soc. A*, 1631 [2]S. Wong et al. (2011) *Nature* **477**, 443. [3]H. F. Bohn et al. (2004) PNAS 101, 14138.

ACKNOWLEDGEMENTS: This work was carried out with the support of the Karlsruhe Nano Micro Facility (KNMF, www.kit.edu/knmf), a Helmholtz Research Infrastructure at Karlsruhe Institute of Technology (KIT, www.kit.edu).

Versatile functional surfaces and interfaces via direct reaction of bioinspired catechols

J Saiz-Poseu[1], B García[2], J Sedó[1], J Hernando[3], F Busqué[3], D Ruiz-Molina[1]

[1]Centro de Investigación en Nanociencia y Nanotecnología, Campus UAB, 08193, Cerdanyola del Valles, Spain [2]Fundación Privada ASCAMM, Unidad de Nanotecnología, ParcTecnològic del Vallès, Av. UniversitatAutònoma, 23 - 08290 Cerdanyola del Vallès, Spain. [3]Chemistry Department, Universitat Autònoma de Barcelona, Campus UAB 08193, Cerdanyola del Vallès, Spain., druiz@cin2.es

INTRODUCTION: Mussel-adhesive proteins have been the subject of intensive scientific research associated to their remarkable ability to strongly adhere to virtually all surfaces. Albeit diverse in structure, this behavior has been attributed to their varying amounts of the non-essential catecholic aminoacid DOPA. Since this discovery, an ever-increasing number of bioinspired catechol-based polymers have been used for the fabrication of water-resistant adhesives, protective layers, primers for functional adlayers and nanoscale coatings, among others [1]. Herein we report a new approach for the preparation of catechol-based colloids and functional coatings based on a simple polymerization process in the presence of ammonia [2]. This strategy represents a significant advance in combining many advantages of methods reported previously: ease of preparation, solubility in appropriate solvents and a high ratio of adhesive (catecholic)-to-functional moieties.

METHODS: In a typical experiment, a large molar excess of aqueous ammonia was slowly added under vigorous stirring in the presence of air to a solution of the 4-heptadecylcatechol (0.2 % , w/v) in methanol, at 40 ºC. Thin-layer chromatography (TLC) was used to follow the reaction, showing that the majority of monomer had already reacted after 3 hours, and consumed quantitatively within 24 hours, after which a dark-brown amorphous solid could be extracted with chloroform and isolated by evaporation.

RESULTS AND DISCUSSION: As a proof of concept, the first molecule of choice was a catechol bearing a long alkyl chain. The material resulting from its reaction with ammonia is shown to spontaneously structure in the form of nanoparticles a few hundred nanometers in diameter in water, which easily stick to several different interphases, especially textiles, affording stable NP coatings.

On the other side, when this material is dissolved in non-polar solvents such as hexane, robust coatings on a representative variety of substrates, both at the nano-/macroscale are obtained, by means of a quick and *ex situ* approach without any pretreatment or modification. Whereas catechol monomers bearing a long alkyl chain afford coatings with a persistent hydrophobic character, it was shown that this methodology can be extended to several other catechols with different ring pendant groups, providing varied surface functionalities such as oleophobic/hydrophilic, anti-fouling, anti-bacterial activities and water remediation.

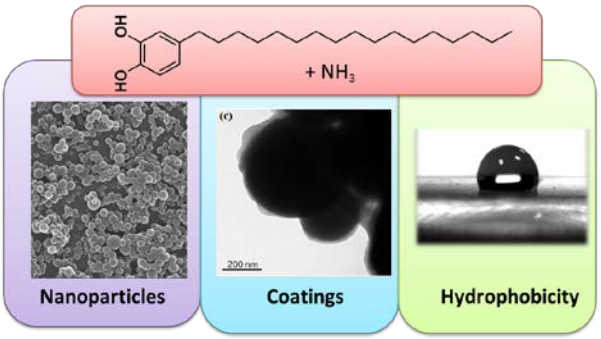

Fig.1. Examples of the different nanostructures and coatings obtained with our new methodology together with a representative example of one of the possible applications: hydrophobicity.

REFERENCES: [1]J. Sedó, J. Saiz-Poseu, F. Busqué and D. Ruiz-Molina. *Adv. Mater*. **2013**, *25*, 653–701. [2]J. Saiz-Poseu, J. Sedó, B. García, C. Benaiges, T.Parella , R. Alibés , J. Hernando, F. Busqué and D. Ruiz-Molina. *Adv. Mater*. **2013**, *25*, 2066–2070. [3]M. Guardingo, J. Sedó, J. Faraudo, A. Verdaguer, F. Busqué and D. Ruiz-Molina. *Small*. Submitted.

ACKNOWLEDGMENTS: This work was supported by MICINN through projects MAT2012-38318-C03-02, MAT2012-38319-C02-01, CTQ2010-15380 and CTQ2009-07469.

How do sea cucumber Cuvierian tubules become sticky? A comparative histological approach

M Demeuldre[1], R Wattiez[2], E Hennebert[1], P Flammang[1]

[1]Biology of marine organisms and Biomimetics [2]Proteomics and Microbiology, Research Institute for Biosciences, University of Mons, Belgium.

INTRODUCTION: Marine bioadhesive research has been gaining increasing interest because of its high potential for the development of novel adhesives for biomedical applications like in surgery or in dentistry. Both fields indeed require adhesives working in wet environment where a "classical glue" cannot operate. Currently permanent adhesion is the most investigated type of adhesion but in the search for new models, we are studying Cuvierian tubules, a specialized defense system occurring in some species of sea cucumbers. When these animals are stressed, they expel a few tubules, which lengthen considerably and become sticky upon contact with any object, immobilizing potential predators. The material secreted by theses tubules has the particularity to become immediately sticky unlike permanent adhesion material. In this study, we investigated the interface between tubules and the substrate to show how the glue is produced and released.

METHODS: Individuals of *Holothuria forskali* and *Holothuria maculosa* were collected by scuba diving in Roscoff (France) and by snorkeling in Toliara (Madagascar), respectively. Cuvierian tubules were fixed in 3% glutaraldehyde in 0.1M cacodylate buffer at three different stages: (*i*) before expulsion, (*ii*) after expulsion but before contact and (*iii*) after expulsion and contact. They were then postfixed with 1% osmium tetroxide in 0.1M cacodylate buffer, embedded in Spurr resin, sectioned transversally or longitudinally and observed in transmission electron microscopy (TEM). For scanning electron microscopy (SEM), Cuvierian tubules were forced to be expelled on different substrates (glass, Teflon®, mica) and then detached manually leaving Cuvierian tubules glue prints on the surface. These prints were fixed in Bouin's fluid and prepared by critical-point drying and sputter-coating before observation.

RESULTS AND DISCUSSION: Cuvierian tubules were observed at different stages during their elongation and adhesion process. Although the tubules from the two species present differences in their quiescent state, these tend to disappear as soon as tubules elongate. Indeed, in *H. forskali*, the mesothelium, the layer responsible for adhesion, is composed of two cell layers: an inner folded layer of granular cells and an outer layer of peritoneocytes. *H. maculosa*, on the other hand, possesses a mesothelium with well-developed peritoneocytes but reduced granular cells. Moreover, an additional layer of a third voluminous cells type is sandwiched in-between. When Cuvierian tubules elongate without contact, peritoneocytes, and the third cell type in *H. maculosa*, disintegrate and granular cells become the most external. Finally, when they make contact with a surface, granular cells release the content of their granules and the glue is formed. Cuvierian tubule glue prints from the two species were observed in order to understand the structure and formation of the adhesive. In *H. forskali*, prints present a heterogeneous aspect due to variations in the quantity of deposited material within a same patch. This can be explained a contamination of the glue with other tubule components (collagen fibres, granules of granular cells) which may occur when tubules are detached. The glue itself seems to be composed of 60-80 nm globular nanostructure deposited as a thin film. No difference was observed between the substrates regarding glue structure but Cuvierian tubules were less sticky on Teflon than on glass or mica, which is reflected by the lower quantity of adhesive attached on this material. In *H. maculosa*, glue prints present the same structure but a fibrillar network was frequently observed covering the glue and "contaminant" granules from granular cells were not as abundant as in *H. forskali*. Thus, although peritoneocytes possess mucous granules which are labelled by anti-glue antibodies, only the contents of granular cells seem to enter in the composition of the glue in both species. The role of peritoneocytes and of the new cell type is still unknown.

REFERENCES: P. Becker and P. Flammang (2010) Unravelling the sticky threads of sea cucumbers – A comparative study on Cuvierian tubule morphology and histochemistry in *Biological Adhesive System* (eds J. von Byern & I. Grunwald) Spinger, pp 87-98.

Analysis of the adhesion of hierarchical fibrillar structures using finite element simulations

F Bosia[1], S Colella[1], NM Pugno[2]

[1] *Department of Physics, University of Torino, Italy* [2] *Laboratory of Bio-Inspired & Graphene Nanomechanics , School of Biosciences, Department of Mechanical, Environmental and Civil Engineering, University of Trento*

INTRODUCTION: Gecko adhesion to surfaces has been widely studied in recent years, including their ability to adapt to both rough and smooth surfaces. The analysis of the terminal elements of gecko paws and their specific structure and topology has led to the development of bioinspired synthetic fibrillar dry adhesives, including mushroom-shaped tips for optimizing adhesion.

To model the expected adhesion and detachment behaviour of multiple contacts, in the past we have derived a theory of multiple peeling[1], extending the pioneering energy-based single peeling theory of Kendall, including large deformations and pre-stretching. In this contribution, we study the problem of the adhesion of single and multiple contacts using Finite Element Method (FEM) analysis, with the aim of determining optimal configurations.

METHODS: We perform FEM simulations using the Structural Mechanics module in COMSOL Multiphysics 4.3. Various geometries are considered:

- Single, double and multiple peeling of fibrils in contact with a flat surface, with variable peeling angle and controlled pre-stress.
- Multiple peeling of fibril hierarchical structures
- Adhesion and peeling of single and multiple mushroom-like elements

Both material and geometric nonlinearities are included in the analysis, as well as the influence of pulling angle. The influence of complex hierarchical configurations is discussed and compared to previous calculation results using multiple-peeling theory.

RESULTS: Calculated results show good agreement with the analytic theory, and the simulation method allows the analysis to be extended to further cases and more complex geometries. The influence of contact splitting, pre-stress and hierarchical structured is discussed in terms of efficiency of the considered adhesive structure. Further data, e.g. the distribution of mechanical stresses, are also included in the analysis.

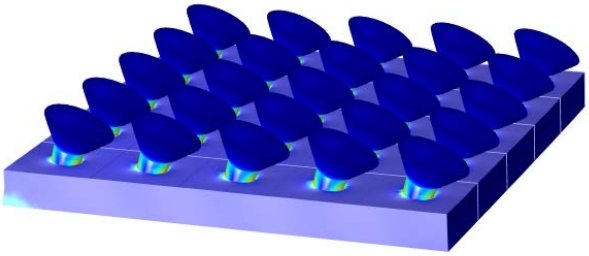

Fig. 1: Geometry of one of the considered structured surfaces, based on mushroom-like adhesive elements. Colour scale represents calculated Von Mises stresses when a specific peeling force is applied.

DISCUSSION & CONCLUSIONS: The simulation method allows in-depth analysis of the efficiency of the adhesive behaviour of multiple contacts, arranged in simple or hierarchical structures. The results could contribute to the development and optimization strategies for bio-inspired adhesive surfaces.

REFERENCES: [1]N.M. Pugno (2011) *Int. J. Fract.* **171**:185-193.

ACKNOWLEDGEMENTS: This work is supported by the ERC Ideas Starting grant n 279985 “BIHSNAM—Bio-inspired Hierarchical Super Nanomaterials”.

Nano forsterite biocomposites for biomedical application: Mechanical properties and bioactivity

G Furtos[1], MA Naghiu[2], H Declercq[3], M Cornelissen[3], M Gorea[2], C Prejmerean[1], M Tomoaia-Cotisel[2]

[1]*Raluca Ripan Institute of Research in Chemistry, Babes-Bolyai University, Cluj-Napoca, Romania*
[2]*Faculty of Chemistry and Chemical Engineering, Babes-Bolyai University, Cluj-Napoca, Romania*
[3]*Department of Anatomy, Embryology, Histology and Medical Physics, Ghent University, Ghent, Belgium*

INTRODUCTION: Addition of bioactive particles to non biodegradable polymer matrix could improve mechanical properties, biocompatibility and bioactivity properties of biocomposites, may promote new bone growth at interface with implant, and in time to increase in the *in vivo* longevity of the prosthesis. Forsterite (Mg_2SiO_4) is member mineral of the Olivine group based on the magnesia–silica system and showed *in vitro* good bioactivity and biocompatibility, providing the opportunity to be a material that may be used as bioactive bone repair materials [1,2]. Forsterite ceramics had higher fracture toughness (K_{IC} = 2.4 MPa $m^{1/2}$) [2] compared with hydroxyapatite ceramics (K_{IC} = 0.6–1.0 MPa $m^{1/2}$) and higher than lower limit reported for bone implant [3].

METHODS: Forsterite (Mg_2SiO_4) nano powders were prepared by sol–gel method using magnesium nitrate and TEOS were used as starting magnesium and silicon precursor. Nano powder was characterized by TEM, X-ray and granulometry. Forsterite powder was used to obtain different new self-curing biocomposites by mixing nano forsterite powder (5 (C5F), 10 (C10F), 15(C15F), 30 (C30F), 50(C50F), 70 (C70F) %wt.) with bis-GMA and TEG-DMA monomers. The newly nano forsterite biocomposites were investigated for mechanical properties: compressive strength (CS), compressive modulus (CM), diametral tensile strength (DTS), flexural strength (FS) and flexural modulus (FM) and structural investigation (SEM and AFM) before and after 1 month in simulated body fluid (SBF). The amount of viable cells attached on the polymer and biocomposites discs after 1 day were tested.

RESULTS: Mechanical tests values of forsterite composite were not significantly different ($p > 0.05$). The CS values were between 128.70 to 167.49 MPa. Addition of forsterite until 50% wt. to polymer matrix led to an increase in CS values, in the following order: Polymer (P) < C5F < C70F < C10F < C15F < C50F. The mean comparing using Tukey test showed a statistically significant different between CS value of P samples and value of C30F and respectively C50F samples ($p < 0.05$). CM increase with addition of forsterite from 1.49 to 2.75 GPa and statistically significant different when materials were compared with C50F and C70F ($p < 0.05$). DTS test showed values between 25.45 to 31.55 MPa and a statistically significant difference was registered between C50F and C70F ($p < 0.05$). FS ranged from 59.47 to 83.20 MPa after 24h and decrease after 1 month between 50.04 to 77.73 MPa. The highest of FS values (83.20 MPa) was registered for C50F. After 1 month of storage all materials decrease FS. The trends in these CM values were similar to those seen in the FM and they may all be related to the increases in filler content within composite materials. CM values were between 2.05 to 8.60 GPa and decrease after 1 month of SBF storage between 1.94 to 7.37 GPa. CS, CM and FM values were correlated with forsterite volume fraction (%) from composites. There was established a direct correlation between the percentage of fillers and CS, CM and FM of forsterite resin composites (r^2_{CS} = 0.90, r^2_{CM}=0.94, r^2FM = 0.99, r^2FM= 0.99).

DISCUSSION & CONCLUSIONS: The results reveal that the mechanical properties increase with addition of forsterite filler. The CS, FS, DTS increase until addition of 50%wt. forsterite and for CM and FM 70%wt. forsterite. AFM and SEM investigation confirm biomineralization of new biocomposites could be used for biomedical application. Biological tests showed an improving cell adhesion with increasing of forsterite powder.

REFERENCES: [1]M. Kharaziha, M.H. Fathi, (2009) Ceram. Int. 35, 2449-2454. [2]S. Ni, L. Chou, J. Chang (2007) Ceram. Int. 33, 83-88. [4]W. Suchanek, M. Yoshimura (1998) J. Mater. Res. 13 94–117.

Calcification of natural polymer biomaterials: understanding the mechanisms of calcium phosphate precipitation

MM Beppu, CG Aimoli, DO Lima

School of Chemical Engineering, University of Campinas, Brazil

INTRODUCTION: Manipulation of molecules to create materials of unexpected properties is the cutting edge of Materials Science and Engineering. Conversely, it is also almost as old as life itself. Bone, teeth, shells of crustaceans, chorals; all those are examples of materials that are obtained through the interaction of typically biological materials – such as proteins or carbohydrates – with inorganic compounds, notably calcium, phosphate and carbonate. Understanding how these compounds are formed is a key to emulate nature in vitro and design materials that fulfill our own purposes. The understanding of how macromocules act in precipitation of inorganic phases is the key knowledge that is needed to stablish the foundation to mimic nature and produce materials with high mechanical modulus besides outstanding optical and thermal properties.

METHODS: This Lecture compiles the results of our *in vitro* investigations on how the addition of small amounts of biopolymers (7-70ppm) influences the precipitation of calcium phosphate: chitosan and alginate were chosen whilst they are polissacharides that presents respectively, amino and carboxyl groups, the most common functions in biopolymers.

RESULTS: Results show the strong effect of natural polymers to organize inorganic phases that are formed *in situ.* Apparently, the key to natural mineralization lies in two aspects: molecular recognition and self-assembly. The former may be exemplified as the action of certain molecular groups, such as hydroxyl and amine. These structures act as templates where crystals are formed. The first step in crystal development is the formation of a nucleus. In homogeneous nucleation, the effect of minerals supersaturation must overcome the interfacial free energy of the nucleus/liquid interface (IFEN, interfacial free energy of nucleation). Nevertheless, the active groups present in biopolymers may act as sites where free energy of nucleation is reduced, *i.e.*, heterogeneous nucleation occurs. Since we are dealing with biopolymers, which are usually large molecules containing more than one active group, their spatial conformation may shield certain groups in a way that diffusion of minerals is too slow, or further crystal growth cannot be attained. Even if these groups offer a lower free energy of nucleation, they become kinetically unavailable. This is the first step to understand self-assembly.

DISCUSSION & CONCLUSIONS: The results lead to the conclusion that alginate action is dynamic, where alginate molecules act as templates to nucleation, and most of the biopolymer remains in solution even when all calcium phosphate has precipitated. However, despite the effect on phase composition being mainly related to the system's kinetics, alginate does present thermodynamic interaction with the precipitates. Biopolymers in solution do not present a random conformation. Their 3-D structure is a direct result from molecular forces acting among active groups. The way these groups are organized in the molecule and how they react to medium's characteristics, such as pH and temperature, ultimately determine its conformation. Nevertheless, as inorganic ions are introduced, they affect molecular structure. One example is the ionotropic effect, characterized by the formation of a biopolymeric reticular gel enclosing divalent ions such as Ca^{2+} or Mg^{2+}. An outstanding consequence is that inorganic-organic composites assemble themselves in small structures that are alike to each other, and may, in turn, form greater structures. It is probable that is acts reducing the free energy of nucleation, as in heterogeneous nucleation processes. On the other hand, the role of small amounts of Chitosan effect was found to be more intense than alginate´s in terms of influence (compared to blank samples) and also in orientation of the inorganic phase that was obtained. These results may indicate that polymers shall have interactions but just enough to conduct ions to molecular recognition and correct epitaxy to orient crystals. Strong interactions would end up binding the species and making then unavailable for further oriented growth. The results indicate cells might present similar influences in mineralization systems.

ACKNOWLEDGEMENTS: The authors thank FAPESP, CAPES, CNPq and LNLS.

Towards the identification of the proteins involved in sea star adhesion

E Hennebert[1], M Demeuldre[1], R Wattiez[2], P Ladurner[3], P Flammang[1]

[1]Biology of Marine Organisms and Biomimetics, University of Mons, Belgium [2]Proteomics and Microbiology, University of Mons, Belgium [3]Institute of Zoology, University of Innsbruck, Austria

INTRODUCTION: Sea stars can adhere strongly but temporarily to a variety of substrata using an adhesive secreted by their tube feet. Proteins are the main components of the organic fraction of this adhesive material and presumably play a key role in sea star adhesion, as evidenced by the removal of adhesive footprints from surfaces after a treatment with trypsin [1]. After analysis by SDS-PAGE, the protein fraction from the adhesive material of *Asterias rubens* separates into about 25 protein bands of which 11, named "Sea star footprint proteins" (Sfps), were not identified in databases and presumably correspond to novel adhesive proteins. Tandem mass spectrometry analysis of these protein bands yielded 43 de novo-generated peptide sequences [2]. In this study we further characterized some of these proteins in terms of sequence and function.

METHODS: Degenerate oligonucleotide primers were designed on the basis of one of the peptides obtained by MS/MS [1] and were used in RT-PCR to amplify the sequence of the cDNA coding for the protein from which the peptide derives. In parallel, a BLAST search was performed with the peptide sequence in the sea star tube foot transcriptome (purchased from GIGA-Genomics; Liège, Belgium).

Proteins were extracted from whole tube feet and analysed by SDS-PAGE. The gel lane was entirely cut up into successive sections, and all the pieces were analysed by mass spectrometry.

Four sets of polyclonal antibodies were raised against four peptides encoded by the cDNA sequence obtained with the biomolecular techniques. They were used in immunoblot on the proteins extracted from footprints and from whole tube feet, as well as in immunohistochemistry on tube foot longitudinal sections.

RESULTS: The two biomolecular techniques used allowed the recovery of a same cDNA sequence whose ORF translates into a 3921 amino acid protein, with a calculated molecular weight of 436 kDa. The protein sequence contains 5 coagulation factor domains, 3 von Willebrand factor domains, 3 galactose binding lectin domains, 2 C8 domains, and 3 trypsin inhibitor like cystein rich domains.

The MS/MS data obtained for proteins extracted from whole tube feet were searched for peptides matching the 436 kDa protein. According to the piece of the lane analysed, all the peptides retrieved derived specifically from one of four main large fragments of the protein sequence. These fragments corresponded respectively to the Nterm, Nterm-middle, Cterm-middle or Cterm part of the sequence, the cleavage sites appearing to occur just in the front of the 3 von Willebrand factor domains.

Two of the four sets of polyclonal antibodies directed against one peptide selected in each of the four fragments specifically labelled the tube foot adhesive cells, confirming the adhesive function of the protein (Fig. 1). The four sets of antibodies labelled proteins extracted from the footprints and from the tube feet with a same apparent molecular weight as that of the corresponding fragments.

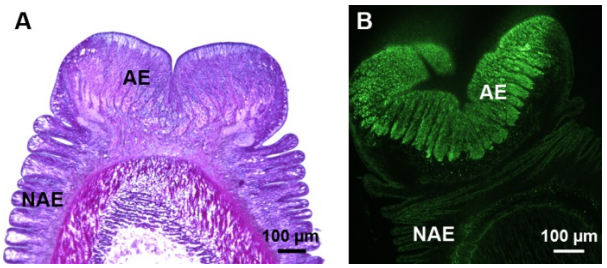

Fig. 1: Longitudinal sections through tube feet of the sea star A. Rubens *stained for histology (A) and immunolabelled with polyclonal antibodies directed against a peptide from the 1st fragment of the 436 kDa protein sequence (B). AE: adhesive epidermis, NAE: non-adhesive epidermis.*

DISCUSSION & CONCLUSIONS: The results suggest that the putative 436 kDa protein coded by a unique mRNA would be processed to yield four distinct proteins. The adhesive function of these proteins is evidenced by their localisation in tube foot adhesive cells and by the presence of domains specifically found in proteins with an adhesion role.

REFERENCES: [1] P. Flammang (1996) Adhesion in echinoderms in *Echinoderm Studies Vol. 5* (eds M. Jangoux and J.M. Lawrence) Balkema, pp 1-60. [2] E. Hennebert, R. Wattiez, J. Waite and P. Flammang (2012) *Biofouling* **28(3)**, 289-303.

Human skin surface model material substrate for *in-vitro* adhesion assays

M Haber, I Lir

Biota Ltd., Or Akiva, Israel

INTRODUCTION: Adhesion to living tissues is an important parameter for evaluation of the appropriateness for use of tissue adhesives and sealants [1]. However, the use of living or *ex-vivo* human or animal tissues as substrates for adhesion assays is very problematic due to ethical issues, limited availability, high variability and low reproducibility. Use of synthetic substrates provides precise and consistently reproducible results, but without clinical relevance. We have developed a human skin surface model material substrate for *in-vitro* adhesion assays. The model material provides accurate and consistently reproducible clinically relevant results [2].

METHODS: Human skin simulating composition consisting of gelatin, hydroxyethyl cellulose (HEC) and ProLipid®141(ISP), plasticized by glycerol and cross-linked by formaldehyde was formulated. The functionality of the model material components are described in Table 1.

Table 1. Functionality of components

Component	Function
Gelatin	Simulate skin biochemistry
HEC	Modify mechanical properties
Glycerol	Increase elasticity
Formaldehyde	Improve hydrolytic stability
ProLipid	Sebum-like hydrophobicity

Films with thickness of 100±5 µm, having human skin-like topography, have been obtained by casting aqueous formulations on human skin negative silicone replica and air drying [3]. Mechanical properties of the films were measured by tensile tests (ASTM 882-97). The surface properties of the films were evaluated by the static contact angle method (ASTM D 724-99 modified). The validity of the model was tested by lap-shear (ASTM 1002-94) and 180°-peel (ASTM D 903-93) adhesion tests using commercial surgical tapes Micropore™ (3M) and Transpore™ (3M). Each of the tapes was applied on the surface of either the model (*in vitro* tests) or a forearm skin of healthy volunteers (*in vivo* tests).

RESULTS: The model material properties have been tailored by modification of components ratios and the degree of cross-linking thus enabling variability of real human skin. The cross-linking effect of formaldehyde allows converting the gelatin solution to a water-swellable but water-insoluble matrix. The amount of glycerol and HEC in the composition determines the mechanical properties of the model material. Adhesion assay using human volunteers' skin and the model provide similar results, as described in table 2 and 3.

Table 2. Skin vs. model peel adhesion assays

Substrate	Peel strength, N/mm	
	Transpore	Micropore
Human skin	0.50±0.16	0.34±0.07
Model	0.39±0.10	0.30±0.10

Table 3. Skin vs. model lap-shear adhesion assays

Substrate	Lap-shear strength, MPa	
	Transpore	Micropore
Human skin	0.08±0.01	0.08±0.05
Model	0.09±0.02	0.10±0.02

Substrate, adhesive, conditions of the joint preparation and applied test have significant affects on adhesion properties. Peel strength was found higher than lap-shear strength for the all substrates tested. In all cases, interfacial adhesive failure was noticed, i.e., failure occurring at the interface between the adhesive and the surface.

DISCUSSION & CONCLUSIONS: Human skin surface model material that mimics human skin's surface biochemical composition, structure and topography, was developed. The results of the lap-shear and 180°-peel adhesion tests confirm the similarity of the developed model material and human skin in terms of debonding strength of surgical tapes peel and shear removal. The model is versatile and its properties can be tailored to simulate diverse human skin types by adjustment of the model's components proportions. The developed material was tested to provide accurate and reproducible clinically relevant results, and as a substrate for evaluation of algal-bioadhesives properties.

REFERENCES: [1]ASTM F2458. [2]I. Lir, M. Haber, H. Dodiuk-Kenig (2007) *J. Adhesion Sci. Technol.*, **21**:1497–1512. [3]J.C. Charcoudian (1988) *J. Soc. Cosmet. Chem.*, **39:**225-234.

ACKNOWLEDGEMENTS: This work was supported in part by grant G5RD-CT-2001-00542 from the European Union.

Nanostructured bioinspired dry adhesives

S Akerboom, M Kamperman

Laboratory of Physical Chemistry and Colloid Science, Wageningen University, Dreijenplein 6, 6703 HB Wageningen, the Netherlands

INTRODUCTION: The key strategy in many natural attachment systems is the incorporation of patterns, i.e. fibrillar surfaces or subsurface structures. For example, the toes of a gecko have millions of micron-sized fibrils packed closely together and each fibril branches into hundreds of nanosized spatula-shaped structures [1]. We develop nanofabrication processes based on self-assembly, which will allow the fabrication of polymeric nanosized fibrillar arrays (gecko-mimic) or subsurface patterns (grasshopper-mimic) with complex 3D structures, hard to achieve with top-down methods. Here, we developed biomimetic nanostructured surfaces using colloidal self-assembly.

METHODS: Negatively charged polystyrene particles, 1.15 μm in diameter, were synthesized using a surfactant-free emulsion polymerization and spread on an air-water interface, see Figure 1. This monolayer served as a template for polydimethylsiloxane (PDMS). A syringe with a blunt tip needle filled with PDMS was used to apply PDMS to the side of the Petri dish containing the monolayer of particles. PDMS was allowed to crosslink at RT for 2 days, resulting in layers of 0.2-0.6 mm thick. To remove the template particles from the PDMS mold, we first applied Scotch Magic Tape, which removes the largest portion of templating particles. The remaining colloids were removed by soaking the sample in N-methyl-2-pyrrolidone (NMP) for 1 hour, followed by dipping the samples in NMP 30 times in an ultrasonic bath.

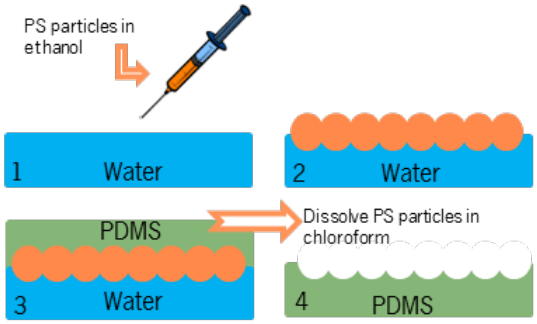

Fig. 1: Fabrication of nanopatterned polydimethylsiloxane (PDMS) using colloidal lithography directly at the air/water interface.

RESULTS: Figure 2 shows scanning electron microscopy (SEM) images of a crystalline monolayer of polystyrene particles and the complete removal of the particles after treatment with NMP.

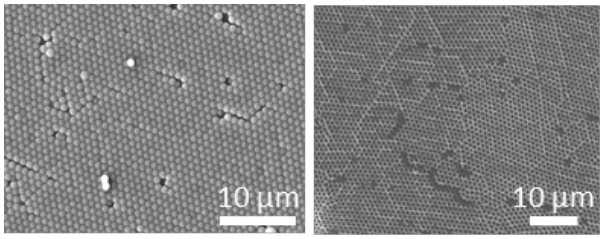

Fig. 2: Scanning electron microscopy (SEM) images of crystalline monolayer and resulting nanostructured surface.

To optimize the order of the colloidal monolayer and to control the immersion depth of the particles, the pH of the subphase was varied systematically. The charges on the particles originate from carboxyl groups with pK_{a1}=3.85 and pK_{a2}=5.44. The order showed a rapid increase when the pH of the subphase was higher than the first dissociation constant of the carboxyl groups on the surface. This way, different subphase conditions were used to control the topography of PDMS surfaces.

DISCUSSION & CONCLUSIONS: Colloidal lithography directly at the air/water interface resulted in a variety of nanostructured surfaces. We are particularly interested in hour-glass shaped pillars, because this particular fibril size and shape is expected to result in significantly enhanced adhesion, because stress concentrations will be decreased at the pillar edges, thereby increasing the toughness of the system. These biomimetic microstructured surfaces have great potential for a variety of applications such as adhesives, self-cleaning surfaces and anti-fouling coatings.

REFERENCES: [1] M. Kamperman, E. Kroner, A. del Campo, R.M. McMeeking, E. Arzt (2010) *Adv Eng Mater* **12**:335-348.

ACKNOWLEDGEMENTS: S.A. and M.K. acknowledge Netherlands Organization for Scientific Research (NWO) for financial support.

Investigation of modified a-C:H film coatings for biomedical applications

Y Ohgoe, A Homma, KK Hirakuri, A Funakubo, Y Fukui

Tokyo Denki University

INTRODUCTION: Carbon-based coatings are widely expected as biocompatible materials. Hydrogenated amorphous carbon (a-C:H) films are used for various purposes such as increasing wear resistance of mechanical parts of artificial hip and knee joints, increasing the corrosion resistance of orthodontic archwires, and imparting antithrombotic properties to stents [1,2]. Several recent attempts were made to modify the characteristics of a-C:H film coating by adding elements, such as oxygen, nitrogen, and fluorine, into the films for each application [3,4]. In this study, we investigated an effect of nitrogen doping and fluorine doping of a-C:H film on cell behavior and hemolytic performance, respectively [4,5].

METHODS: Nitrogen doping of a-C:H (a-C:H:N) film was deposited on segmented polyurethane (SPU) scaffold fibre (φ1μm) sheet by radio frequency (r.f.) plasma chemical vapour deposition (CVD) method. NIH-3T3 cells were used to estimate the cellular responses on the a-C:H:N film. The cells were seeded on the a-C:H:N film surfaces and incubated at 37 °C in an atmosphere consisting of 5% CO_2 and 95% air with a relative humidity of 100%. The cells were cultured in the D-MEM for 3 days. During the cell culture, cell behavior on the scaffold fiber was analyzed at intervals of 10 minutes for 72 hours by time-lapse imaging system. On the other hand, fluorine doping of a-C:H (antibacterial a-C:H:F) film was deposited on impeller surface of an artificial heart blood (SUS 304) by ionization method [5]. To estimate the hemolytic performance of the blood pump with the a-C:H:F film coating, the amount of the hemolysis was measured using a mock circulatory system with 500 ml of pig blood. The blood circulation was conducted for 180 min with a blood flow rate of 5 L/min, a pimp head of 100 mmHg, and an impeller speed at 1100 [rpm] [6].

RESULTS: The smooth surface fiber of the SPU scaffold had become noticeably wrinkled by the a-C:H:N film coating. Additionally, a-C:H:N film coating had been changed to hydrophilic side by C=O bonds. Compared with non-doping of a-C:H film, it was observed that the a-C:H:N film coating had a facilitatory effect on cell behavior and cell growth. The nitrogen doping improved physical and chemical characteristics of the a-C:H film coating for cell culture on the scaffold. On the other hand, a-C:H:F film coating surface had been changed to hydrophobic side by C-F bonds. The effect of the fluorine doping was increased to more negative potentials on the a-C:H film surfaces. As a result, it was shown that the amount of the hemolysis was reduced 20% with decreasing the surface energy of the blood contacting surface.

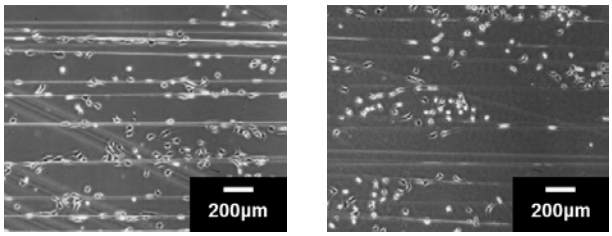

With a-C:H:N coating Without coating

Fig. 1: Images of cells on the SUP Scaffold fiber – analysis of cell behavior on scaffold fiber

DISCUSSION & CONCLUSIONS: It was observed that nitrogen content of the a-C:H:N film was possible to control cells behavior on the scaffold fiber and induced cell growth. On the other hand, fluorine atoms are very electronegative and so will carry some degree of negative charge. The a-C:H:F film coating is expected as a surface modification technique for biomaterials. In this study, it has been demonstrated that addition of selective elements into a-C:H films is possible to advance of the characteristics of a-C:H film coating for biomedical applications.

REFERENCES: [1]R. K. Roy, et al (2009) *Vacuum* **83**: 1179-1183. [2]R.K. Roy, K.R. Lee (2007) *J. Biomed. Mater. Res. Part B* **83B**: 72-84. [3] T. Hasebe, et al (2007) *New Diamond and Frontier Carbon Technology* **17**: 263-279. [4] P. Yang, N. Huang, Y. X. Leng et al (2006), *NIM B* **242**: 22-25. [4]Y. Ohgoe, et al (2013) *MRS Proceedings* **1498**: mrsf12-1498-l09-30. [5]Y. Ohgoe, et al (2012) *NDNC 2012 Abstract*: 2.

ACKNOWLEDGEMENTS: This research was partially supported by the Research Institute for Science and Technology, Tokyo Denki University.

An antimicrobial and biocompatible peptide surface coating

AR Leong[1,2], N Cole[1], N Kumar[3], MD Willcox[1]

[1] *School of Optometry and Vision Science, University of New South Wales, NSW.* [2] *Brien Holden Vision Institute, Sydney NSW, Australia.* [3] *School of Chemistry, University of New South Wales, NSW, Australia*

INTRODUCTION: Implanted medical devices were associated with an estimated 2 million infections and 80 000 deaths, and an economic cost of $3 billion, in the USA in 2004 [1]. Given the difficulty in treating implant-associated infections without surgery [2], an anti-infective surface coating for medical implants is urgently required. Current technology in this area raises concerns with regard to broad-spectrum efficacy and antibiotic resistance [3]. Integration with host tissue is another challenge for surgical implants; close tissue integration promotes long-term implant success by allowing a robust immune response at the tissue-implant interface [4]. Thus, the ideal surface for implanted medical devices is both antimicrobial and tissue-compatible.

METHODS: A cationic antimicrobial peptide (CAP) was covalently attached to polymer substrates to examine its effect on bacteria and mammalian cells. CAP was attached *via* its primary amines to carboxyl groups of hydroxyethyl methacrylate–methacrylic acid (HEMA–MMA) using 1-(3-dimethylaminopropyl)-3-ethylcarbodiimide. The coated surfaces were exposed to clinical isolates of *Staphylococcus epidermidis*, *Staphylococcus aureus*, or *Pseudomonas aeruginosa* for 24 h. Samples were rinsed, and then vortexed to dissociate adherent bacteria, which were enumerated via agar plate colony counts. CAP was attached *via* its single cysteine residue to amine groups of a plasma polymerised heptylamine film on a fluorinated ethylene propylene (FEP) substrate, using succinimidyl-4-[N-maleimidomethyl]-cyclohexane-1-carboxylate. HaCaT human keratinocytes were added to these surfaces and their activity was observed. The growth medium was Dulbecco's Modified Eagle Medium with 10% serum. After 96 h, keratinocytes were stained to assess viability.

RESULTS: CAP-coated HEMA–MMA compared to blank HEMA–MMA showed reductions in adhesion for each bacterial species tested (Table 1).

Table 1. Log reductions of viable bacteria adherent to CAP-coated HEMA–MMA.

Bacterial Species	Mean log reduction ± SD
S. epidermidis	3.6 ± 0.5
S. aureus	2.6 ± 0.3
P. aeruginosa	1.8 ± 0.2

Human keratinocytes were able to adhere and proliferate to a greater extent on CAP-coated FEP-heptylamine than on FEP-heptylamine (Figure 1).

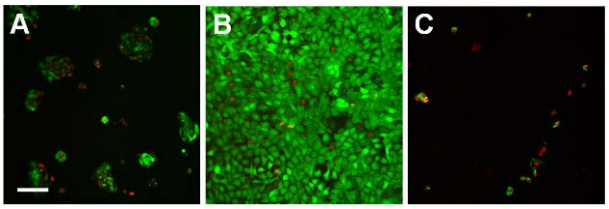

Fig. 1: Confocal microscopy images of HaCaT cells on heptylamine (A), heptylamine–CAP (B), and a process control (C). The cytoplasms of viable cells appear green and the nuclei of non-viable cells appear red. Bar 100 μm.

DISCUSSION & CONCLUSIONS: Our *in vitro* experiments demonstrate lethal activity of our CAP surface against Gram-positive and Gram-negative bacterial species, and show that the surface is conducive to mammalian cell attachment. This forms the basis of a promising coating for surgically implanted devices. Our current *in vitro* work aims to develop a single surface that combines both of these properties. Future *in vivo* experiments will test the anti-infective and tissue-integrative properties of this surface using a mouse model of implanted biomaterials.

REFERENCES: [1] R.O. Darouiche (2004) *N Engl J Med* **350**:1422-1429. [2] M. Schierholz, J. Beuth (2001) *J Hosp Infect* **49**:87-93. [3] K.S. Rabindranath, T. Bansal, J, Adams, et al (2009) *Nephrol Dial Transplant* **24**:3763-3774. [4] A.G. Gristina (1994) *Clin Orthop Relat Res* **298**:106-118.

PCL coatings on magnesium alloy

L Altomare[1], L Petrini[2], F Migliavacca[1], S Farè[1]

[1]*Dipartimento di Chimica, Materiali, Ing. Chimica 'G. Natta', Politecnico di Milano, Italy*
[2]*Dipartimento di Ingegneria Civile e Ambientale, Politecnico di Milano, Italy*

INTRODUCTION: Magnesium (Mg) and its alloys are metal materials investigated for the fabrication of biodegradable implants, thanks to their low thrombogenicity and well-known biocompatibility. Moreover, Mg might represent a possible alternative to biodegradable polymers thanks to its better mechanical properties. [1]. The main purpose of the present work is the design, fabrication and characterization of a polycaprolactone (PCL) coating on a substrate in Mg AZ31 alloy (3% Al, 1% Zn, 0.2% Mn) via dip coating technique.

METHODS: To perform the dip coating, three different solutions of PCL in trichloromethane were prepared (10, 7 and 5% w/v). The dipping and extraction rate of the substrates from the polymer solution were 60, 100 and 200 mm/min. The evaluation of the coating morphology was performed by scanning electron microscope, thickness measurements were carried out observing sample sections by optical microscope. Samples were immersed in phosphate buffered saline (PBS) and degradation was evaluated by pH measurements and ion release analysis.

RESULTS: The 10% w/v concentration of the PCL solution was excluded because preliminary tests showed the formation of coatings with a surface morphology inadequate to the continuity and homogeneity requirements. Coating thickness increases with the concentration of the polymer solution (from 5 to 7% w/v) maintaining a constant speed. However, it decreases for dipping and extraction rate greater than 100 mm/min (Fig. 1), in agreement with the literature [2].

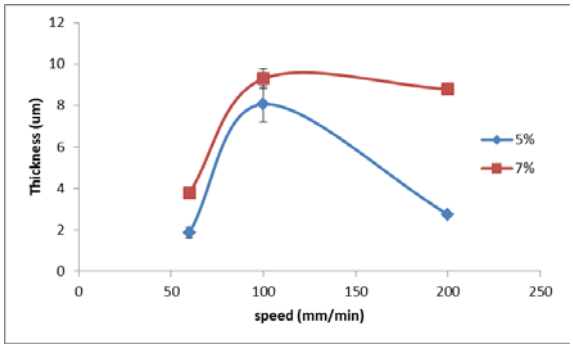

Figure 1. PCL coating thickness related to solution viscosity and speed of extraction rate of the substrate.

The kinetics of degradation of the coated AZ31 specimens in PBS significantly improved after PCL coating, as shown in figure 2. At the same time-points, a lower pitting corrosion (Fig. 2b) was evidenced for PCL coated samples compared to the uncoated ones (Fig. 2a). A pH increase was observed for all samples even though it was lower for samples coated with PCL.

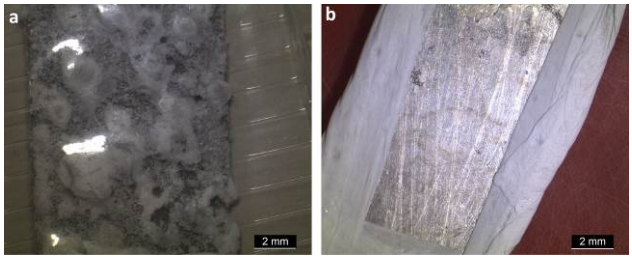

Figure2: AZ31alloy without (a) and with (b)PCL coating

DISCUSSION & CONCLUSIONS: PCL coatings on Mg AZ31 alloy were continuous, homogeneous and smooth after the optimization of the dip-coating parameters. However, imperfections persisted along the edges of the specimens, thus determining a rapid corrosion of the metallic substrate during the degradation tests. Optical microscopy observations showed a PCL coating thickness homogeneous and consistent with that used for coronary stents (5 to 10 μm). Adhesion tests with a home-made scratch test apparatus are under investigation. Optimization of dip coating for complex shape, such as metallic stent, need to be performed.

REFERENCES: [1] H. Hermawan, et al. (2010) *Acta Biomaterialia*, 6. [2] H. Fang, et al. (2008) *Materials Letters*, 62.

ACKNOWLEDGEMENTS: The authors would like to thank Fondazione CaRiTRO for partially funding the research project.

Nanocrystal iron film prepared using a filtered cathodic vacuum arc for improving biocompatibility of vascular devices

J Wang[1,2], H Sun, YH He[1], Y Yun[2], N Huang[1]

[1] Key Lab. of Advanced Materials Technology, Ministry of Education, Southwest Jiaotong University, China. [2] Engineering Research Center for Revolutionizing Metallic Biomaterials, North Carolina A & T State University, NC,USA. Email: nhuang@263.net

INTRODUCTION: Biodegradable iron materials have a high potential for vascular stent applications. Achieving tunable surface for cell and blood compatibility remains a challenge. Bulk nanocrystal iron exhibited good biocompatibility [1]. Here, nanocrystal iron (NC-Fe) film was prepared and investigated for surface bioactivity.

METHODS: NC-Fe flim were deposited onto polished silicon wafer (100) by filtered cathode vacuum arc deposition (FCVAD). A radio frequency power of 300 W, a substrate pulsed bias of −150 V, Ar flow of 20 sccm, and deposition time of 20 min were controlled. The structure and morphology of this film were studied. The viability of endothelial cells (ECs) and the adhesion and activation of platelet were assayed.

RESULTS & DISCUSSION: The structure of NC-Fe film was shown in Fig. 1a. The α-Fe (110) peak was detected from NC-Fe film compared with bulk pure iron. According to line profile analysis, an average crystallite size of ~14.5 nm was calculated. The surface morphology of the film was fairly smooth without metal drop (Fig. 1b), which suggested a high deposition quality.

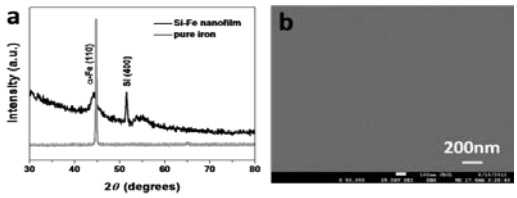

Fig. 1. (a) X-ray diffraction pattern of NC-Fe film deposited on a silicon substrate compared to that of bulk pure iron. (b) Surface SEM image of NC-Fe film.

For cytocompatibility tests, the initial attachment (4 h) and upper proliferation (1 and 3 days) of ECs on the NC-Fe film were significantly superior to that on 316L stainless steel (SS), silicon (Si), and pure iron surface. Corresponding, cell count, cell area coverage ratio, projected area per cell, and minor/major axis ratio showed an excellent activity of ECs. A lower concentration of iron ion can produce a favorable effect on the metabolic activity of ECs. But this concentration over 50 μg/ml expresses toxicity to cells [2]. It was indicated that the amount of released iron ions was controlled appropriately on the NC-Fe film, which presented a preferable promotion for better adhesion and proliferation of ECs.

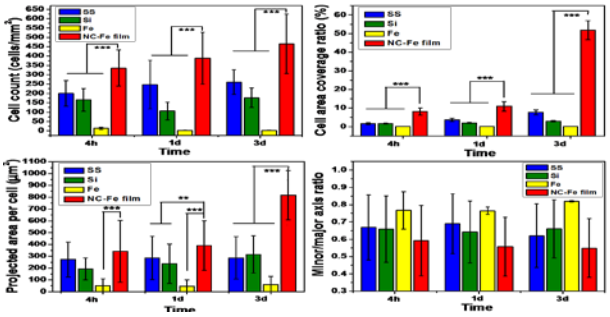

Fig. 2. Amounts, cover ratio, projected area per cell and minor/major axis ratio of ECs on the samples surfaces after 4 hours, 1 and 3 days of culture.

For hemocompatibility tests, there were a large number of adherent platelets on SS and Si surface, and most were adhered, aggregated and activated to the extent of fully spreading state. The morphologies of platelets were destroyed on pure iron due to rapid surface corrosion. By contrast, a few round platelets adhered on the NC-Fe film surface, i.e., no spreading as an activation sign.

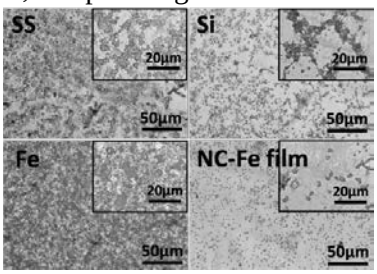

Fig. 3. The morphologies of adherent platelets on the samples surfaces incubated in PRP for 2 hours.

CONCLUSIONS: Nanocrystal iron film, as a biodegradable metal film, was fabricated by FCVAD. It showed a good biocompatibility with high ECs activity and low coagulation. This study offers a promising approach for the development of bioactive metallic interface.

REFERENCES: 1 F. L. Nie, Y. F. Zheng, S. C. Wei et al (2010) *Biomed. Mater* **5**:065015. 2 S. F. Zhu, N. Huang, L. Xu et al (2009) *Mat. Sci. Eng. C* **29**:1589.

ACKNOWLEDGEMENTS: China Scholarship Council 201207000016 and PhD Innovation Fund of SWJTU 2011.

PEG-b-cationic polycarbonate diblock copolymer as antibacterial and antifouling coating for intravascular catheters

X Ding[1,2], C Yang[1], JL Hedrick[3], YY Yang[1]

[1]*Institute of Bioengineering and Nanotechnology, Singapore* [2] *NUS Graduate School for Integrative Sciences & Engineering (NGS), Singapore* [3] *IBM Almaden Research Center, USA*

INTRODUCTION: The infections caused by medical devices, especially catheter-associated infections (CAIs), are the major challenges in hospitals. Various catheter coating methods have been studied to prevent the CAIs. However, it is difficult to obtain an effective and facile coating without elevating the toxicity of the catheter surfaces. In this study, we simply coated diblock copolymers of poly(ethylene glycol) (PEG) and cationic antimicrobial polycarbonate onto silicone rubber via a reactive polydopamine (PDA) coating to render antimicrobial and antifouling surface properties [1].

METHODS: The polymers with various compositions were synthesized through metal-free organocatalytic ring-opening polymerization of MTC-OPrBr and MTC-OEt monomers [2] using HS-PEG-OH as the macroinitiator in the presence of TU and DBU as catalysts. The resulting polymers were quaternized with trimethylamine to obtain HS-PEG-cationic polycarbonate diblock copolymers (HS-PEG-PCN). X-ray photoelectron spectroscopy (XPS) and quartz crystal microbalance (QCM) were used to characterize surface properties. Methicillin-susceptible Staphylococcus aureus (MSSA) and methicillin-resistant Staphylococcus aureus (MRSA) isolates – leading causes of intravascular CAIs – were employed to evaluate the antibacterial and antifouling activities of the polymer coatings. In addition, protein adsorption on the surfaces was tested by QCM, and platelet adhesion were examined by scanning electron microscopic (SEM).

RESULTS: Static contact angle and XPS measurements proved the successful coating of the diblock copolymers, and quartz crystal microbalance results showed that the coating thickness increased as polymer concentration increased. Polymer coatings with a hydrophobic component effectively killed planktonic MSSA and MRSA in solution and prevented their fouling on silicone rubber surface. Live/dead cell staining experiments revealed that polymer coatings with optimal polymer compositions possessed significantly higher antifouling activity than PEG coating. In addition, SEM studies showed that the polymer coating inhibited *S. aureus* biofilm formation over a period of 7 days. Furthermore, the polymer coating caused no significant hemolysis, and there was no blood protein absorption or platelet adhesion observed.

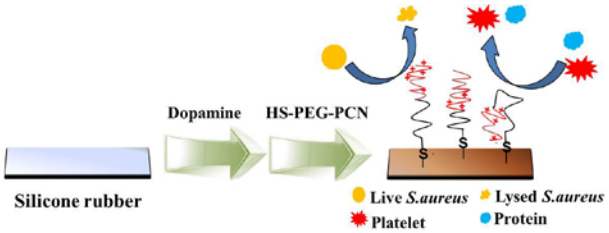

Fig. 1: The making of antibacterial and antifouling polymer coating on silicone rubber surfaces.

DISCUSSION & CONCLUSIONS: A series of PEG-b-cationic polycarbonates have been successfully synthesized and grafted onto silicone rubber surface through an active polydopamine coating layer. The polymer coatings with hydrophobic components kill MSSA and MRSA in solution and efficiently prevent surface fouling. These coatings inhibit biofilm formation without causing significant hemolysis, blood protein absorption or platelet adhesion. These findings suggest great potential for PEG-b-cationic polycarbonates as antifouling and antibacterial coatings for intravascular catheters.

REFERENCES: [1]X. Ding, C Yang, TP Lim, et al (2012) *Biomaterials* **33**: 6593–603. [2]RC Pratt, F Nederberg, RM Waymouth et al (2008) *Chem Commun* **44**:114-6.

Titanium-alloyed DLC layers for implants

L Joska[1], J Fojt[1], V. Cvrcek[2], V Brezina[3]

[1] Institute of Chemical Technology in Prague, Faculty of Chemical Technology, Technicka 5, Prague, CR. [2]Czech Technical University in Prague, Faculty of Electrical Engineering, Prague, CR. [3] Masaryk University, Faculty of Medicine, Brno, CR.

INTRODUCTION: Layers based on diamond-like carbon offer two ways of application in medicine. Excellent tribological properties can take advantage on friction areas of big joint replacements, and they may also serve on the other hand as bio-inert barrier layers on implants made of materials likely to cause a negative response of the organism (e.g. CoCrMo alloys in dentistry). One of the current aims in the field of implantology is to achieve the fastest possible osseointegration, which requires that the implanted surfaces should be bioactive. The study was focused on the evaluation of interaction of titanium-alloyed DLC layers with model body fluids and on assessment of the influence of alloying on their bioactivity.

METHODS: DLC layers with three levels of titanium concentration were prepared for testing. The tests were carried out in buffered physiological solution and the same fluid with fluoride ions added, environment interesting for applications in dentistry. Special attention was directed on the tests performed in simulated body fluid (SBF). The layers were characterized by scanning electron microscopy and photoelectron spectroscopy. Processes on the DLC(Ti) layer-simulated body solutions phase boundary were monitored by electrochemical impedance spectroscopy. The surface colonization with MG63 cells was also tested within the study.

RESULTS: Layers with three different titanium concentrations of 3.4, 10.2 a 23.6 % at. were obtained. Considering the thickness of layers, calotest method determined the thickness of functional DLC(Ti) layers to be 0.6-0.8 μm, the chemical composition was determined by photoelectron spectroscopy. Carbon was partly bound in a form of carbides. The electrochemical study (measurement of EIS spectra was repeated every 24 hours, the length of exposures was always 168 hours) proved the significant impact of alloying on the impedance/electrochemical response. Considering its inertness, only reactions of the environment components proceed on an unalloyed DLC layer exposed in physiological saline solution. The presence of titanium induced the change to a typical course corresponding to a passive surface. Addition of fluoride ions resulted in a dramatic change in the course of the spectra. A drop in impedance confirmed known instability of titanium oxides in an environment containing fluorides, which also applied in the case of titanium bound in a DLC layer. Measurements proved a difference in behaviour of DLC and DLC (Ti) coating during the exposure in simulated body fluid. Hydroxyapatite practically did not precipitate on unalloyed layers at all. On the contrary, photoelectron spectroscopy identified the presence of the Ca-P compound on specimens with titanium alloyed coatings. This process was well detectable by EIS spectrometry – during the exposures, the module increased and the phase decreased in the low-frequency part of the spectra. The colonization test showed a slight increase in the occupation of the alloyed DLC(Ti) layer surfaces with cells as compared with unalloyed layers. Surprisingly, the most important change was detected on a layer with 23.6% of titanium, where approximately 5.9 % of the alloying element is bound in carbide. At the same time, higher colonization was noted on specimens whose surface was jet-blasted prior to the coating in comparison with polished surfaces.

DISCUSSION & CONCLUSIONS: A significant change in behaviour of coated systems was achieved by alloying DLC layers with titanium. The interaction of coatings with model body fluids was unambiguously determined by titanium and its electrochemical behaviour. The presence of titanium, without any other chemical processing, e.g. activation in alkali, lead to both initiation of hydroxyapatite formation during the exposure in SBF and the increase of cell colonization. These facts are promising in terms of the use of titanium alloyed barrier DLC layers in e.g. dental implantology.

ACKNOWLEDGEMENTS: This study was carried out as a part of the P108/10/1782 project (Czech Science Foundation).

Bioactive coatings with low-fouling, non-thrombogenic but cell-adhesive properties, using chondroitin sulphate

S Lerouge[1,2], P Thalla[1,2], P Lequoy[1,2], H Fadlallah[1,2], B Liberelle[3], H Savoji[2,3], MR Wertheimer[3], G De Crescenzo[4], Y Merhi[5]

[1] Ecole de technologie supérieure (ETS), Dept. of Mechanical Engineering [2] CHUM Research Center (CRCHUM) [3] Dept. of Engineering Physics [4]Dept. of Chemical Engineering, École Polytechnique de Montréal [5]Montreal Heart Institute, Montréal, Canada

INTRODUCTION: Low-fouling sublayers are increasingly used to immobilize growth factors (GF) or bioactive molecules, because they can prevent their denaturation and loss of bioactivity. Low-fouling coatings can also serve as non-thrombogenic surfaces that could be used in vascular substitutes; however, the *in vivo* efficiency of a non-fouling as a non-thrombogenic surface is usually limited by poor stability. Coatings that promote endothelial cell (e.g. HUVEC) adhesion and retention are more promising. Regrettably, coatings used for this purpose (collagen, fibronectin, etc) generally exhibit thrombogenic properties. The aim of the present study was to demonstrate the advantages of chondroitin sulphate (CS) as a sublayer combining low-fouling, low-thrombogenicity and cell adhesive properties.

METHODS: CS was covalently grafted using carbodiimide chemistry on a thin coating with a high concentration of primary amines (7.5%), created by low-pressure plasma deposition ("LP") [1]. This permits identical surface composition on any type of substrate. Two other types of low-fouling surfaces were prepared for comparison: 1) Star PEG with N- hydroxy succinamide (NHS) terminal groups; and 2) carboxymethylated dextran (CMD) [2]. Water contact angle, ellipsometry and XPS analyses were used to optimize and characterize the surfaces.

Low-fouling properties were assessed by Quartz Crystal Microbalance with Dissipation (QCM-D). A stable baseline was achieved in PBS prior to the injection of fibrinogen (340 kDa), albumin (66 kDa) solution or serum for 2 h, followed by rinsing with PBS for 30 min. Protein adsorption was monitored by changes in frequency (Δf) and dissipation (ΔD).

Adhesion, growth and survival of HUVEC were assessed on CS, CMD and PEG surfaces. Tissue culture polystyrene plates (TCPS) and PET films were used as controls. CS and CMD surfaces were also further modified by immobilization of epidermal growth factor (EGF), to evaluate CS as a sublayer for GF.

Platelet adhesion was studied by whole blood perfusion assays [3], on control and modified surfaces (CS, LP, PET), before or after HUVEC growth on these. CellVue® Red and CD61-FITC were used to visualize HUVEC and blood platelets respectively, after 15 minutes of perfusion. On each type of surface, the density of HUVEC was compared with its initial value, to determine the percentage of cells remaining on the surface after perfusion. SEM was used to assess platelet aggregation and activation.

RESULTS: PEG, CMD and CS all present low-fouling properties, the highest reduction of protein adsorption being obtained on CMD. Platelet adhesion assays showed that LP is thrombogenic, while PEG, CMD and CS all drastically decreased adhesion and activation of platelets ($p<0.001$). While HUVEC adhesion and growth were found to be very limited on PEG and CMD, it reached similar values on CS as on the positive control (TCPS). More important, cell retention during perfusion with blood was found to be excellent on CS (ca. 90%), but poor on PET control (<30%, $p<0.05$). When EGF was immobilized on CS and CMD, data once again showed a clear advantage of CS+EGF, on which cell adhesion and survival were drastically improved compared with CMD+EGF (60%, versus 3% of cells remaining after 7 days in serum-free media; $p<0.001$).

DISCUSSION AND CONCLUSIONS: While PEG and CMD non-fouling surfaces are limited by poor cell adhesion, CS exhibits very favorable properties as a coating for vascular implants, either alone or in combination with GF. It may help form a complete, stable endothelium and may help prevent vascular graft occlusion. Yet, additional studies are required to further assess its stability, non-thrombogenic properties and cell-adhesion mechanisms.

REFERENCES: [1]Truica-Marasescu et al. *PPaP* 5, 2008. [2]Liberelle et al. *Bioconjugate Chem* 21, 2010. [3]Merhi et al. *JBMR* 34, 1997.

ACKNOWLEDGEMENTS: This work is being funded by NSERC/CIHR and CRC.

Thin films with controlled fibroin fibril deposition for contact with cells

MA Moraes[1,3], T Crouzier[2], MM Beppu[1], M Rubner[3]

[1] *School of Chemical Engineering, University of Campinas, Campinas, Brazil* [2] *Department of Biological Engineering, Massachusetts Institute of Technology, Cambridge, USA.* [3] *Department of Materials Science and Engineering, Massachusetts Institute of Technology, Cambridge, USA*

INTRODUCTION: Silk fibroin (SF) is a protein extracted from silkworm cocoons that is able to form fibrils in layer-by-layer (LbL) thin films (successive deposition of polymers on a substrate) and is promising for applications in biomedical field [1]. A nanofibrous scaffold, with unidirectional fiber orientation, is a good candidate for reconstruction of damaged muscle tissue. In tissues like muscle, cell alignment is crucial for the formation of organized myotubes and reconstruction of the anisotropic tissue with similar mechanical behavior [2]. The aim of this work was to create layer-by-layer assembled ultra-thin multilayer films with controlled deposition of aligned SF fibrils using chitosan (CHI – good H-bond capability, low charge density) or poly(allylamine hydrochloride) (PAH - low H-bond capability, high charge density) as counterparts for LbL assembly. Also, we analyzed the ability of such films to be used as pattern to guide myoblasts attachment and proliferation.

METHODS: Silk fibroin solution was prepared according to our previously published method [1] and diluted to 0.15g/L. CHI was dissolved in 0.25M acetic acid and PAH in ultrapure water. CHI and PAH were used in a concentration of 1 g/L and at pH 6. For film preparation, the substrates were immersed in the CHI or PAH solution and SF solution alternately. After each polymer deposition, three rinse steps in ultrapure water and one drying step (essential for film formation) at room conditions were used. The films were analyzed after deposition of 20-bilayers by ellipsometry and optical microscopy, in bright field mode. The ability of SF aligned fibrils to guide cell adhesion and proliferation was tested with C2C12 myoblasts.

RESULTS: Thin films of $(CHI/SF)_{20}$ and $(PAH/SF)_{20}$ were uniform and had a dry thickness of 143 nm and 188 nm, respectively. We could control SF fibril formation by changing the assembly partner. LbL films deposited with CHI had uniform and aligned SF fibrils (d ≈ 200 nm), while in PAH films no fibrils were observed (Figure 1a). Myoblasts were seeded on the surface of the films. The cells attached, spread and proliferated to reach confluence after 7 days of (Figure 1b), but were randomly oriented on the films. Myoblasts proliferated more in the films with CHI than with PAH, showing a better compatibility.

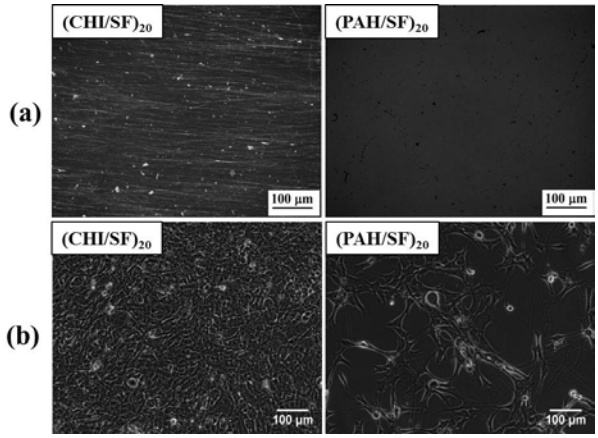

Fig. 1: (a) Optical microscope images (bright field) of films with fibrils (CHI/SF) and without fibrils (PAH/SF) and (b) C2C12 myoblasts proliferation after incubation for 7 days.

DISCUSSION & CONCLUSIONS: It was possible to prepare LbL thin films by successive deposition of CHI or PAH and SF and to control the deposition of SF aligned fibrils within the films. The assembly partner, the chemical interactions and the drying step during deposition are the key factors controlling fibril deposition. C2C12 myoblasts did not follow the pattern imposed by SF fibrils, probably because fibrils are embedded in the film and the alignment of surface topography is too small to be recognized by cells. Despite not guiding the cells, as expected, the films were not toxic to cells and can be used as coatings for biomedical devices, drug delivery and biosensors with specific target molecules.

REFERENCES: [1]G. Nogueira, et al. (2010) *Langmuir* **26**:8953-8958. [2] A. Cooper, et al. (2010) *J Mater Chem* **20**:8904-8911.

ACKNOWLEDGEMENTS: The authors thank to CAPES and CNPq (Brazil) for financial support.

The effect of fibronectin/phosphorylcholine coatings on PTFE substrates on endothelial cells adhesion and hemocompatibility properties

V Montaño[1,2], P Chevallier[1], D Mantovani[1], E Pauthe[2]

[1] Laboratory for Biomaterials and Bioengineering (CRC I), Dept. of Min-Met-Materials Eng., & University Hospital Research Center, Laval University, Quebec city, Canada [2] ERRMECe, Dept. of Biology, University of Cergy-Pontoise, France

INTRODUCTION: When a biomaterial is implanted in the human body, its surface interacts with the surrounding biological tissues and fluids. In the case of cardiovascular materials, it is desired to stimulate endothelialization and to avoid thrombus formation. Numerous works have been performed on the improvement of one of these performances separately: hemocompatibility or endothelialization. In order to obtain both properties simultaneously, our original approach is to combine two biomolecules with complementary properties in one coating: fibronectin (FN) to enhance endothelialization [1,2] and phosphorylcholine (PRC) because of its non thrombogenic properties [3].

METHODS: PTFE film was cleaned before used. Two approaches are proposed to prepare FN and PRC coatings. Both of them start with FN adsorption on PTFE surfaces. After this adsorption, PRC is added either activated to form a covalent bond with FN or not activated to be simply adsorbed. Coatings characterization was performed through X-Ray Photoelectron Spectroscopy (XPS), immunostaining of FN with polyclonal and monoclonal antibodies and Scanning Electronic Microscopy (SEM). The biological properties were assessed by the adhesion of endothelial cells (EC) for endothelialization behaviour and platelets adhesion/activation and clotting time though the free hemoglobin method for hemocompatibility properties.

RESULTS: XPS results evidenced the presence of both biomolecules on the different coatings. Furthermore, a desorption of FN was observed when PRC previously activated is added to form a covalent bond. Immunostaing confirmed the presence of FN and also the availability of cell binding domain on the surface. SEM images show the formation of complexes when PRC is activated. Coated surfaces improved EC adhesion and spreading compared to the uncoated one (see Figure 1). A remarkable diminution on platelets adhesion and activation was observed on coated samples. Moreover, coated PTFE surfaces showed diminutions of the clotting time when in contact

with blood. All coatings seemed to improve the hemocompatibility properties and no significant differences were detected in the presence of PRC.

Fig. 1: Adhesion test of EC on different surfaces: a) uncoated PTFE, b) FN coating, c) FN and PRC adsorption; d) FN adsorption-PRC grafting.

DISCUSSION & CONCLUSIONS: Two different coatings have been prepared containing phosphorylcholine and fibronectin on a PTFE film. Physicochemical and biochemical characterization have

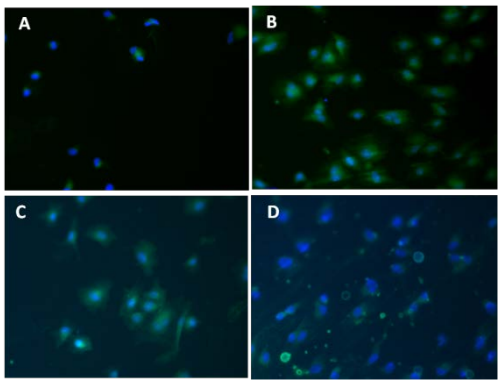

demonstrated the presence of both biomolecules on the coatings. The influence of biomolecules grafting/adsorption on the improvement of biological performances of the surfaces have been proved through endothelial cells adhesion as well as hemocompatibility tests. Further experiments are required in order to assess the stability of the coating under flux onto metallic surfaces.

REFERENCES: [1]K.Vallières et al. (2007) *Macromol. Biosci*. 7, 738–745. [2]L. Baujard-Lamotte, et al. (2008) *Colloids and Surfaces B: Biointerfacesz.* 63 129–137. [3]A.L. Lewis et al. (2002). *Biomaterials*. 23 1697–1706A.

ACKNOWLEDGEMENTS: To E. Camand-Pesnel, S. Hamour, R. Agniel and to the blood donors for their collaboration on the performance of the experiments.

Effect of Collagen type-I on the rate of osseointegration of Ca-containing biodegradable Mg-Zr based alloys

D Mushahary[1], C Wen[2], JM Kumar[3], N Harishankar[4], G Pande[3], P Hodgson[1], Y Li[1]

[1] Institute for Frontier Materials, Deakin University, Victoria, Australia [2] Faculty of Engineering and Industrial Sciences, Swinburne University of Technology, Victoria. Australia [3] CSIR-Centre for Cellular and Molecular Biology, Hyderabad, India [4] National Institute of Nutrition (ICMR), Hyderabad, India

INTRODUCTION: Mg-Zr based biodegradable implants alloyed with Ca were investigated to assess their biocompatibility and efficacy in bone formation and osseointegration. Bare alloys, containing Ca, exhibited low surface energy, poor corrosion-resistance, reduced osteoinduction and bone integration activity [1, 2]. Upon coating with Collagen type-I, these alloys demonstrated enhanced performance as an implant material that are suitable for rapid and efficient new bone tissue induction with optimal mineral content and cellular properties.

METHODS: Collagen type-I was extracted from rat tail [3] and was characterized by FT-IR spectroscopy using a control sample. Alloys were dip-coated with Collagen type-I and the thickness of the coated protein was measured by profilometer. Coated alloys were characterized using X-Ray Diffraction (XRD) and Scanning Electron Microscopy (SEM). The free surface energy and wettability of the coated alloys were determined from the contact angles of polar solvents on the surface of the alloys. *In vivo* bone formation around the implants in rabbit femur was investigated by measuring the Bone Mineral Content/Density (BMC/BMD) of the implanted region using Dual-Energy X-Ray Absorptiometry (DXA) and new bone mineralization was visualized by histological and immuno-histochemical analysis.

RESULTS: Results show that Mg-Zr-Ca alloys, when coated with Collagen-I have a tendency to form superior trabecular bone structure, with better osteoinduction around the implants, as compared to the control and uncoated ones. Further, surface modification improved the surface energy of these alloys and the mineral content of the implanted region of femur bone in experimental animals. Both the uncoated [2] and surface modified Mg-Zr based alloys integrated with the host tissue and did not cause any undesirable side effects. Fig. 1 shows Hematoxylin and Eosin stained newly formed bone tissue around Mg-Zr-Ca alloy after 3 months and 1 month implantation for the uncoated and coated implants, respectively.

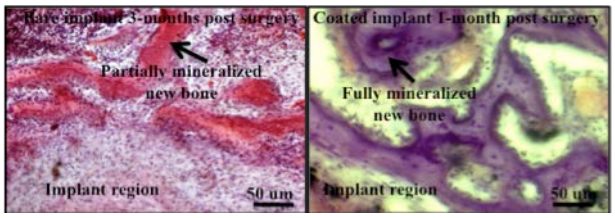

Fig. 1: Hematoxylin and Eosin stained newly formed bone tissue around Mg-Zr-Ca alloy 3 months and 1 month post-implantation respectively, in rabbit femur. The coated implant shows more rigid and mineralized trabecular bone formation (right) as compared to the bare implant (left) that forms less mineralized new bone tissue upon implantation.

DISCUSSION & CONCLUSIONS: This study demonstrated that surface modification of Mg-Zr-Ca alloys using Collagen type-I benefit the osseointegration and the formation of a new trabecular bone structure around the implants. Further, surface modification of these alloys could osseointegrate at an even earlier implanted period compared to the bare implants. Although *in vitro* results did not indicate any improvement in the cell behaviour for the surface modified Ca-containing alloys, the *in vivo* osseointegration rate was significantly enhanced. Hence, Collagen type-I coating on Mg-Zr-Ca alloys is a promising method for expediting new bone formation *in vivo* and enhancing osseointegration in biodegradable implant applications.

REFERENCES: [1]Y. Li, C. Wen, D. Mushahary, et al (2012) *Acta Biomater* **8**:3177-88. [2]D. Mushahary, S. Ragamouni, Y. li, et al (2013) *Inter J Nanomedicine* (In press). [3]N. Rajan, J. Habermehl, M.F. Cote et al (2006) *Nat Protoc* **1**:2753-8.

ACKNOWLEDGEMENTS: The authors acknowledge the financial support from the Australia-India Strategic Research Fund (AISRF) BF030031 to CW and PH and GAP 0311 to GP.

Optimum cross-section for hydroxyapatite/collagen nanocomposite-coated subperiosteal devices

M Uezono[1, 2, 3], K Takakuda[3], M Kikuchi[4], S Suzuki[1], K Moriyama[1]

[1] *Department of Maxillofacial Orthognathics, Graduate School of Tokyo Medical and Dental University, Tokyo, JP.* [2] *JSPS Research Fellow, Tokyo, JP.* [3] *Institute of Biomaterials and Bioengineering, Tokyo Medical and Dental University, Tokyo, JP.* [4] *International Center for Materials Nanoarchitectonics, National Institute for Material Science, Tsukuba, JP.*

INTRODUCTION: In our previous study [1], we reported hydroxyapatite/collagen nanocomposite-coating (HAp/Col) achieved rapid osseo-integration of titanium rod onto bone surface. The bone-bonding strength of this rod, however, was not enough for clinical use. The objective of this study was to discover the effective cross-sectional geometry of rods to increase the bone-bonding strength utilizing rat carvalia model.

METHODS: Two types of HAp/Col coated titanium rod specimens with circular (Cr) and semi-circular (Sc) cross-sectional geometry were prepared. Experimental animals were 12-week-old male SD rats. The specimens were placed under periosteum of their calvaria. The bone-forming capability of specimens was evaluated after four weeks placement via histological observations and bonding strength tests.

RESULTS & DISCUSSION: In the histological observations, both of Cr and Sc rods were almost completely surrounded by new bone tissues (Fig1, 2). Although significant difference between Cr and Sc was not detected in the bone contact ratios, Sc group demonstrated about three times greater strength than Cr group with significant difference in the bonding strength tests.

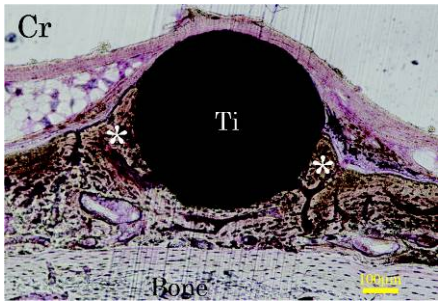

Fig. 1: Typical image of Cr group – undecalcified section with villanueva stain. Newly formed bone (*) was observed in the vicinity of the rod (Ti).

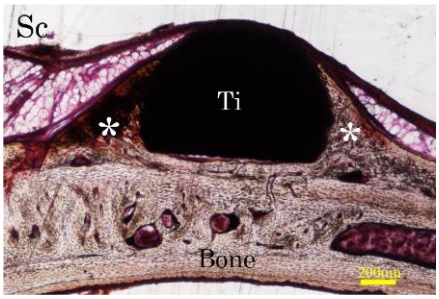

Fig. 2: Typical image of Sc group – undecalcified section with villanueva stain. The rod (Ti) was covered with newly formed bone (*).

CONCLUSIONS: In the animal experiment utilizing rat calvaria, the rod of semi-circular cross-section was discovered to have superior bone-bonding strength. The use of such rods will be conveniently adopted for the development of devices for clinical use.

REFERENCES: [1]M. Uezono, K. Takakuda, M. Kikuchi, et al (2013) *J Biomed Mater Res B Appl Biomater* DOI: 10.1002/jbm.b.32913.

ACKNOWLEDGEMENTS: This study was partially supported by a Grant-in-Aid for Scientific Research (B) No. 23300163, Scientific Research (C) No. 24593083, Grant-in-Aid for JSPS fellows No. 24-9937 from the Ministry of Education, Culture, Sports, Science and Technology of Japan.

Nanoengineered plasma polymer films

K Vasilev

Mawson Institute and School of Engineering, University of South Australia, Mawson Lakes Campus, Mawson Lakes, SA 5099, Australia

INTRODUCTION: Plasma polymerisation is an attractive technique for deposition of thin functional coatings useful for various applications. Benefits of this technique include solvent free deposition and independence from the substrate material when few nanometres of plasma polymer have been deposited [1]. Of particular interest to our group and others are applications in the field on biomaterials. In order to open new horizons for plasma polymers we developed the field of nanoengineered plasma polymer films where we integrate nanoparticles and nanostructures with plasma polymers to create new more advanced biomaterials. Examples of such applications are antibacterial coatings, drug delivery platforms and cell guidance surfaces. These abstract outlines several applications.

METHODS: We deposit plasma polymers under low pressure, typically 1 x 10^{-1} mbar using parallel plate plasma chamber configuration described in ref [1]. Specific surfaces designed in gradient manner are prepared in a plasma chamber described for the first time in [2]. Surface gradients are generated by tailoring the chemical composition in the plasma phase which is done through controlling the flow rate of two monomers. Plasma polymer is deposited through a 1 mm slot in a mask placed over a substrate which is moving with controlled speed.

RESULTS: The generation of advanced nanoengineered plasma polymer films began with the fabrication of nanocavities into plasma polymer films via tempering with nanoparticles [3]. This work was a pure "scientific curiosity" but demonstrated the possibility to combine plasma polymerisation and electrostatic immobilisation of nanoparticles, to incorporate nanoparticles into plasma polymer films and transport ions and molecules out (and potentially in) of plasma polymers. This inspired several interesting applications.

One application was the generation of tunable plasma polymer films loaded with silver nanoparticles [4]. The films were fist loaded with silver ion by immersion in $AgNO_3$ which was followed by reduction of these ions to silver nanoparticles. We demonstrated that by tuning the rate of release of the silver ions from the films we can tune the coatings completely antibacterial but tolerant to mammalian cells. This strategy was further developed to delivering and release of conventional antibiotics [5].

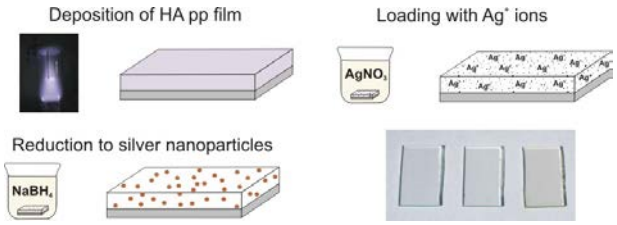

Fig. 1. Generation of silver nanoparticles loaded plasma polymer films. The brownish colour of the glass slide on the left is due to the loaded silver nanoparticles.[4]

A substrate independent method for generation of surface gradients that we developed involves modification of a substrate with an uniform coating of a plasma polymer layer carrying targeted functionalities and subsequent immersion of this substrate with a controlled speed into a solution of nanoparticles or ligands [6]. We used such surface to study the effect of surface nanotopography and stiffness on cellular behaviour [7,8].

DISCUSSION & CONCLUSIONS: We have combined plasma polymers, which were typically regarded as a continuous pinhole-free coating, with nanoparticles to create nanoengineered films useful for various applications. This concept creates new opportunities for plasma polymers and generations of more advanced coatings.

REFERENCES: [1]K. Vasilev et al. (2009) *Chem Commun* 3600 – 3602. [2]J. D. Whittle et al. (2003) *Chem Commun* **2**: 1766. [3]K. Vasilev et al. (2009) J *Phys Chem B* **113**: 7059-7063. [4]K. Vasilev et al. (2010) *Nano Lett* **10**: 202-207. [5]K. Vasilev, et al. (2011) *ACS Appl Mater & Interf* 3:4831. [6]R. V. Goreham, et al. (2012) *Thin Solid Films* **528**: 106–110. [7]I Hopp et al (2013) *Biomaterials* **34**(21): 5070–5077. [8]R. V. Goreham, A. Mierczynska-Vasilev, L. Smith, et al RSC Adv (2013) DOI: 10.1039/C3RA23193C.

Surface functionalization of metallic biomaterials with antibacterial compounds

D Rodriguez, FJ Gil

Biomaterials, Biomechanics and Tissue Engineering group, Technical University of Catalonia (Barcelona-TECH), Barcelona, Spain; Biomedical Research Networking Centre in Bioengineering, Biomaterials and Nanomedicine (CIBER-BBN), Spain

INTRODUCTION: Bacterial infection is a prominent cause of implant failure [1]. A common treatment strategy is the use of antibiotics. The rise of multidrug resistant bacteria, however, poses serious concerns to this strategy [2]. Looking for strategies that prevent bacteria colonization of metallic implant surfaces is an alternative [3]. Two approaches aimed to prevent the formation of bacterial biofilm on metallic implant surfaces were studied: 1) development of antifouling surfaces based on poly(ethylene glycol) (PEG), and 2) formation of surface coatings with antimicrobial compounds with broad-spectrum activity against bacteria and slow bacteria resistance response (i.e. coatings with silver nanoparticles and surface grafting with antimicrobial peptides (AMP)).

METHODS: A plasma equipment (Diener electronic GmbH) operating at 13.56MHz, pulsed regime, was used to polymerize a precursor (tetraglyme) in a low-pressure argon atmosphere. Plasma-activated titanium surfaces were covered with a PEG coating with this process.

Silver-coated titanium samples were prepared by two processes. A pulsed electrochemical anodizing process (ParStat 2273 potentiostat) deposited silver on titanium from complexed silver in aqueous solution. A second process precipitated silver nanoparticles in acidic chitosan solution at high temperature. Titanium samples were dip-coated with the chitosan-nanoparticle solution.

Antibacterial activity of a lactoferrin-derived AMP was also studied. Smooth titanium samples were activated with NaOH and silanized with either CPTES or APTES silane for covalently anchoring the lactoferrin-derived AMP.

The treated surfaces were examined with FE-SEM, FIB and TEM. Roughness was measured by white-light interferometry and wettability by contact angle. Surface chemical composition was evaluated with SEM/EDS, FTIR, XPS and ToF-SIMS techniques. The antibacterial effect of the surface treatments on adhesion and biofilm formation was evaluated on two bacterial strains present in oral biofilms (*Streptococcus sanguinis* and *Lactobacillus salivarius*). Cell adhesion and cytotoxicity (LDH) on treated surfaces were determined through *in vitro* cell culture using fibroblasts.

RESULTS: A layer of PEG was deposited on titanium by plasma treatment as confirmed by FTIR and FIB. Both protein adsorption and bacteria adhesion decreased with the presence of the layer. A reduction in cell viability was found for treated surfaces.

Presence of silver on anodized titanium samples was confirmed by XPS and visualized as localized deposits in FE-SEM imaging. TEM showed the presence of silver nanoparticles dispersed in the chitosan matrix. A reduction in bacteria adhesion correlated to silver presence was observed for treated surfaces.

A coating of silanized peptide on titanium was formed with both APTES and CPTES silanes. A significant reduction in biofilm formation was found for the samples coated with APTES-silanized peptide (table 1).

Table 1. Luminiscence of biofilms (BacTiter-Glo Reagent) on control and treated samples (1d).

Luminescence (a.u.)	S.sanguinis	L.salivarius
Control (Ti)	425±20	41000±6500
Ti-APTES-AMP	80±5	10500±6000

DISCUSSION & CONCLUSIONS: Surface treatments with remarkable antibacterial properties have been developed. These surfaces are promising candidates for *in vivo* applications.

REFERENCES: [1] J.W. Costerton, L. Montanaro, C.R. Arciola (2005) *Int J Artif Organs* **28**:1062-8. [2] P.S. Stewart, J.W. Costerton (2001) *The Lancet*, **358**:135-8. [3] K. Vasilev, J. Cook, H.J. Griesser (2009) *Expert Rev Med Devices* **6**:553-67.

ACKNOWLEDGEMENTS: These results are part of Maria Godoy-Gallardo and Judit Buxadera PhD theses. The peptides were produced by Dr. Carles Mas-Moruno. Funding from the MICINN Spanish Ministry (Project MAT2009-13547) and Fundación Ramón Areces (project 'Biosellado') is acknowledged.

Innovative Cu and Cu/TiO_2 ultrathin adhesive films deposited by HIPIMS inducing accelerated inactivation of *E. coli, MRSA* under solar and actinic light

S Rtimi, C Pulgarin, J Kiwi

Ecole Polytechnique Fédérale de Lausanne, EPFL-SB-ISIC-GPAO, Station 6, CH-1015, Lausanne, Switzerland

INTRODUCTION: Antimicrobial surfaces can reduce/eliminate hospital-acquired infections (HAI) acquired on contact with bacteria surviving for long times in hospital facilities. Cu and TiO_2/Cu films prepared by sol-gel show low adhesion since they can be wiped off by a cloth or thumb. Sputtering of nano-particulate highly oxidative Cu/Cu_2O/CuO and TiO_2 films are shown in this study to lead to uniform, resistant antibacterial films.

METHODS: Sputtering of Cu and TiO_2/Cu samples on highly stable polyester fabrics were performed by direct current (DC), pulsed (DCP)[1] and high ionized pulse plasma magnetron sputtering (HIPIMS)[1]. The evaluation of the bacterial inactivation kinetics in the dark and under light irradiation was carried out according to ISO standards for *E. coli*[1] and by the recently developed methods in Lausanne on MRSA[2]. The Cu-polyester surfaces were characterized by: electron microscopy (EM), atomic force microscopy (AFM), X ray-photoelectron-spectroscopy (XPS), X-ray fluorescence (XRF), diffuse reflectance spectroscopy (DRS), droplet contact angle (CA), and ion-coupled plasma mass spectrometry (ICP-MS).

RESULTS AND DISCUSSIONS: Thickness were carried out for the target TiO_2/Cu 60%/40% for samples sputtered 150s leading to fast bacterial inactivation. The composite film was 38 nm thick, equivalent to ~190 layers, each of 0.2 nm X-ray fluorescence (XRF) indicated a composition 0.29% wt Cu_2O/CuO and a 0.45% wt TiO_2 per weight polyester[3]. Under actinic light, Figure 1 traces 3, 4 and 5 show the bacterial inactivation as the sputtering time was increased up to 150s. Sputtering for 300s induces bacterial inactivation taking longer times than the sample sputtered for 150s. Therefore, the amount of Cu^0 is not the main species leading to bacterial inactivation. This sample presents the highest amount of Cu-sites held in exposed positions interacting with *E. coli*. The bactericide action is faster than when TiO_2 and Cu were sputtered separately on polyester.

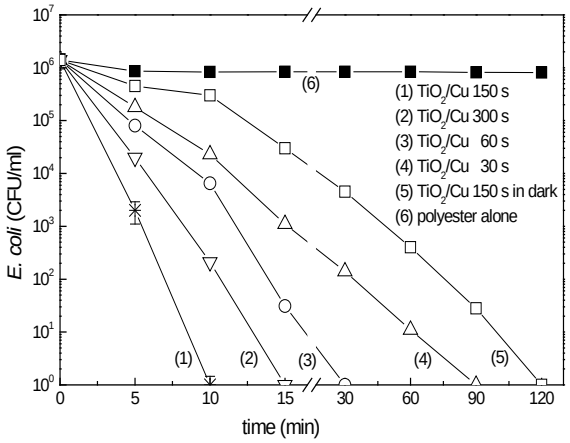

Fig. 1. E coli survival on TiO_2/Cu polyester under Osram Lumilux 18W/827 light (4.2 mW/cm^2).

Figure 2 presents the inactivation time *vs* thickness for DCP and HIPIMS TiO_2/Cu sputtered films. Figure 2 shows the reduction for the HIPIMS TiO_2/Cu layer thickness compared to DC/DCP deposited layer to inactivate bacteria.

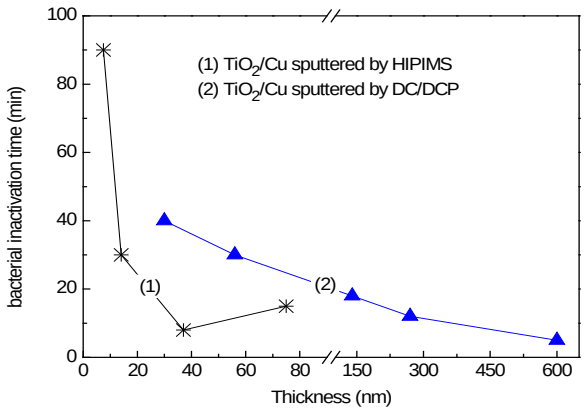

REFERENCES: [1]*E. Kusiak et al (2011)* E. coli inactivation by HIPIMS sputtered surfaces *J. Phys Chem. C.*, **115***: 21113-21119.* [2]L. Rio et al (2012) Cu-sputtered surfaces inactivation of methicillin resistant MRSA, *J. Appl. Microb*. **78***: 8176-8182* [3]S. Rtimi et al (2012) Innovative TiO_2/Cu surfaces inactivating bacteria, *ACS Appl. Mater. & Interf. **4**: 5234-5240*

ACKNOWLEDGEMENTS: We thank the EPFL, the Limpid FEP-7 Collaborative European Project NMP 2012.2.2.2-6 and the COST Action TD 0906 for support of this work.

Highly stable, dual effect antibacterial coatings deposited via a hybrid plasma process

M Cloutier[1,2], R Tolouei[1], O Lesage[1,2], S Turgeon[1], L Lévesque[1], M Tatoulian[2], D Mantovani[1]

[1] *Laboratory for Biomaterials and Bioengineering* (CRC I), *Dept. of Min-Met-Materials Eng., & University Hospital Research Center, Laval University, Quebec city, Canada* [2] *Laboratoire de Génie des Procédés Plasmas et Traitements de Surface, ENSCP, Paris, France*

INTRODUCTION: The design of antibacterial materials is now increasingly moving towards surface modification methods and mainly based on three chief strategies: the reduction of bacterial adhesion, the controlled release of biocides and the grafting of contact-killing surface molecules[1-2]. However, a regular drawback of most of these engineered materials is their lack of stability (rapid leaching of biocide agent, loss of surface grafted molecules, etc.) when exposed to harsh operating conditions, which limit their long-term effectiveness. One possibility to overcome these limitations is offered by plasma technologies. Strongly adherent and cohesive coatings with a tunable set of properties can be deposited on various substrates and loaded with the desired biocides. Herein, we report an innovative approach for the production of silver-doped Diamond-like Carbon (Ag-DLC) films to act as highly stable antibacterial coatings.

METHODS: Silicon and 316L stainless steel were used as substrates. Coatings were deposited using a hybrid Plasma Enhanced Chemical Vapor Deposition – Physical Vapor Deposition (PECVD-PVD) reactor. Methane and hydrogen were used as PECVD precursors of the DLC films, while silver was incorporated via simultaneous PVD sputtering. XPS and Auger spectroscopy were used to study the structure and chemistry of the Ag-DLC coatings. Topographical and mechanical properties were assessed with AFM, SEM and optical microscopy. Atomic Absorption Spectroscopy (AAS) was used to study the silver release. Biological tests, using standardized quantitative methods and Live/Dead assays with *E. Coli*, were used to investigate the antibacterial activity and bacterial anti-adhesive properties of the studied surfaces.

RESULTS: Mechanically stable hydrogenated DLC coatings were obtained on both silicon and stainless steel, with an adjustable silver percentage. The films (80-100 nm) showed little damage after exposition to abrasion, sonication and autoclaving. Both pure DLC and Ag-DLC films exhibited reduced bacterial adherence compared with stainless steel, due to the DLC's higher hydrophobicity and nanosmoothness. However, only the Ag-DLC coatings with a silver percentage over 1.5% showed a significant bactericidal effect against *E. Coli*. The effect was directly related to the silver ions release from the coatings.

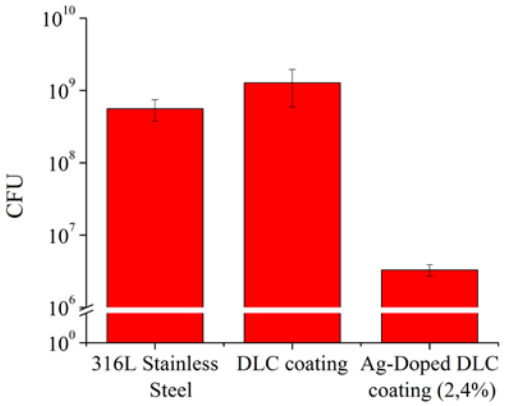

Fig. 1: E. Coli bacterial activity after 4 hours contact with the tested surface, followed by 24 hours post-contact incubation.

DISCUSSION & CONCLUSIONS: Ag-DLC coatings displayed a dual effect against bacteria by both reducing bacterial adhesion and gradually releasing silver ions. Their superior mechanical stability, especially against intense sterilization treatment such as autoclaving, would make them interesting options as bioactive surfaces for healthcare environments.

REFERENCES: [1] J.A. Lichter, K.J. Van Vliet and M.F. Rubner (2009) *Macromolecules* **42**:8573-86. [2] K. Vasilev, J. Cook and H. J. Griesser (2009) *Expert Rev Med Devic* **6:**553-67.

ACKNOWLEDGEMENTS: The authors would like to acknowledge the financial support of the Natural Sciences and Engineering Research Council of Canada and the Canadian Space Agency. The authors are also thankful for the guidance and assistance from Dr P. Chevallier.

Antibiofouling microfiltration membranes prepared by plasma-induced hydrophilic surface modifications

Y Han[1,2], JC Cho[2], MH Jung[3], YH Lee[1]

[1] Center for Water Resource Cycle, Korea Institute of Science and Technology [2] Department of Environmental Sciences, Hankuk University of Foreign Studies [3] Department of Physics, Sogang University, South Korea

INTRODUCTION: Polyvinylidene fluoride has been widely used in microfiltration (MF) membranes. Because of its hydrophobicity, PVDF can easily adsorb proteins and many other organic molecules during the membrane separation process, resulting in membrane biofouling. In our study, we demonstrate the plasma-induced grafting of hydrophilic monomers onto MF PVDF membrane surfaces and internal pores. The flux profiles and antibiofouling performances of the surface-modified membranes were compared with a pristine PVDF membrane.

METHODS: The pristine hydrophobic PVDF membrane (pore size of 0.45 μm, Durapore) were selected. The hydrophilization experiment was carried out in a custom-built plasma apparatus. The plasma-induced grafting of hydrophilic monomers (i.e., acrylic acid(AA), ammonia) onto membrane surfaces in the solution vessel was carefully performed under various operational conditions (0.02~0.3 wt%, monomer, 0~10 min, 50~700 W, 60 Hz). The permeation flux of the membranes was investigated in batch and cross-flow filtration systems. The chemical compositions of the membranes were characterized using XPS, FT-IR, SEM, AFM, contact angle analysis [1,2].

RESULTS: In the FT-IR spectrum, the strong absorption peak attributed -C=O and -NH/-NH_2 were observed for plasma-induced acrylate and ammonia grafted membranes, respectively. This indicates the grafting of hydrophilic monomers onto the membrane surfaces were occurred extensively. The morphology of the surface-modified membranes examined using SEM was almost identical to that of the pristine membrane, as shown in Fig. 1. The pure DDI water flux of the surface-modified membranes was consistently higher than that of the pristine membrane. The permeation flux of the protein (BSA) and mixed microorganisms solution though the surface-modified membranes was up to 68% higher than the pristine membrane, which resulted in much lower membrane fouling resistance values compared with that of the pristine membrane (Table 1).

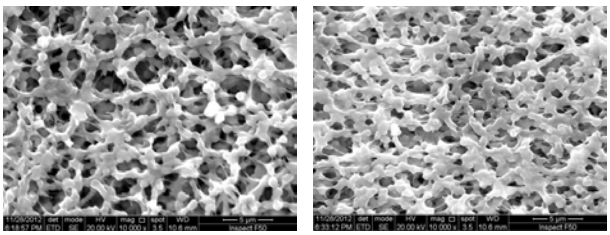

Fig. 1: SEM Images of the pristine PVDF membrane (left) and the ammonia grafted PVDF membrane (right) prepared at ammonia concentrations of 0.3 wt%.

Table 1. Estimated membrane resistance values.

Sample	Membrane resistance (R, $10^{10}m^{-1}$)	
	Intrinsic (R_m)	Fouling (R_f)
Pristine PVDF	1.62	7.44
0.02 wt% AA	1.63	5.76
0.05 wt% AA	1.41	2.71
0.10 wt% AA	1.39	2.54
0.10 wt% NH_3	1.50	2.83
0.30 wt% NH_3	1.35	2.39

DISCUSSION & CONCLUSIONS: Batch and cross-flow fouling experiments showed that the plasma-induced surface-modified hydrophilic MF PVDF membranes were notably less susceptible to biofouling of protein and mixed microorganisms than the pristine PVDF membrane.

REFERENCES: [1] R.F. Susanti, Y.S. Han, J. Kim, Y.H. Lee, R. G. Carbonell (2013) *J Membr Sci* **440**:88-97. [2] D. Gao, T. Zhang, C.Y. Tang, W. Wu, C. Wong, Y.H. Lee, D.H. Yeh, C.S. Criddle (2010) *J Membr Sci* **364**:331-338.

ACKNOWLEDGEMENTS: This research was based on work supported by Center for Water Resource Cycle at KIST and by KEITI (Korea Environmental Industry & Technology Institute) (Project No. 192-091-001).

Antifungal activity of hyaluronic acid / chitosan nanostructured films containing silver ions

TB Taketa[1], RSN Brilhante[2], JJC Sidrim[2], MM Beppu[1]

[1] School of Chemical Engineering, University of Campinas, Campinas SP. [2] Specialized Medical Mycology Center, Federal University of Ceará, Fortaleza CE

INTRODUCTION: Layer-by-layer **(**LbL) is a bottom-up technique for the construction of films with micro/nanometric thicknesses. In most cases, the fundamental driving force for the formation of these films is originated from the electrostatic interaction between oppositely charged species. The LbL technique is widely developed to give adequate answer to precise needs in different fields, including nontoxic, biodegradable and suitable antimicrobial surfaces for biomedical applications. The aim of this work was to evaluated the antifungal activity of the LbL coatings (with and without silver ions) containing natural polymers against *Candida albicans* strain.

METHODS: Polyelectrolyte multilayers were assembled onto glass substrates, with a PEI pre-coating. All polymer solutions were prepared with Milli-Q® water (1 g/L, pH 3). The slides were sequentially dipped in each respective polyelectrolyte solution (chitosan (CHI) or hyaluronic acid (HA)) for 15 min and subsequently rinsed three times with pure water (same pH as the polyelectrolyte dipping solutions) for 2, 1 and 1 min, respectively. Samples were dried at ambient conditions. The (HA/CHI) multilayers contained 10 bilayers. As a post-assembly treatment, films were rinsed in a silver acetate solution (1000 ppm, pH 7). Anticandidal assays were based on the protocol discussed by Sidrim and Rocha[1]. Briefly, three streaks of Candida albicans were made on corn-meal agar with Tween 80 in a petri dish. The slides were transferred to dishes and were positioned over the streaks made in the agar. The samples were stored at 30 °C. Observations under an optical microscope were made after 20 and 96 hours of culture.

RESULTS: For $(HA/CHI_3)_{10}$ coatings, after only 20 hours of growth, it was possible to observe the yeast filamentation. After 7 days of culture, we observed a greater proliferation of yeast in the medium, with the presence of bunches of blastoconidia and a large quantity of pseudohyphae with terminal chlamydospores. On the other hand, coatings containing Ag^+ completely inhibited the growth of Candida albicans after 7 days of contact. The same system, with alginate as a substitute for the HA, did not present the same effiency against *C. albicans* (data not shown). HA/CHI multilayers allow the incorporation of a higher silver content, as verified by EDX analysis (data not shown).

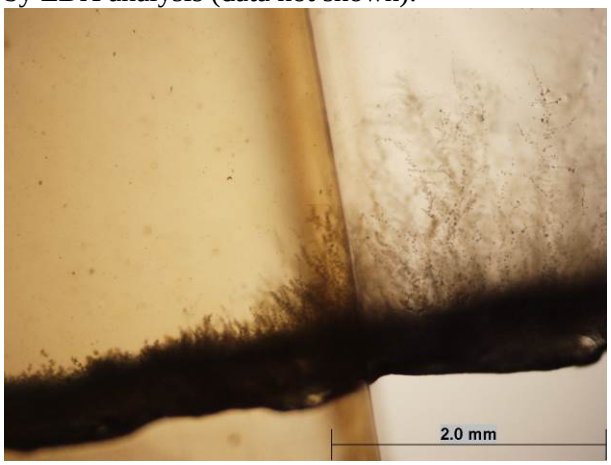

Fig. 1: Activity of $(HA/CHI3)_{10}Ag^+$ coating against the fungus. In the region below the slide (left side), no growth of the microorganism is observed. In the region of agar (right side), growth is pronounced.

DISCUSSION & CONCLUSIONS: The mode of action of silver ions involves the inactivation of proteins linked to the fungus cell wall, the interference with the electron and solute transport systems and inhibition of respiratory enzymes that promote the generation of reactive oxygen species [2]. In addition, silver causes the winding of DNA into a more condensed structure that presents a low replicative capacity [3]. The synergistic use of natural polymers and LbL technique was possible, in a simple and versatile way, enabling the construction of nanostructured films with promising application as antifungal surfaces.

REFERENCES: [1]J.J.C. Sidrim et al.(2004) *Micologia Médica à Luz de Autores Contemporâneos*, Guanabara Koogan Press. [2] B.S. Atiyeh, et al. (2007) Burns, 33:139-148. [3] Q.L. Feng, *et al.* (2000) Journal of Biomedical Materials Research, 52:662-668.

ACKNOWLEDGEMENTS: CAPES, CNPq, FAPESP and Specialized Medical Mycology Center (CEEM).

Adsorption, system release and antimicrobial properties of chlorhexidine on nanohydroxyapatite coatings

J Barros[1,2], L Grenho[1,2], CM Manuel[2,3,4], OC Nunes[1,3], LF Melo[2,3], FJ Monteiro[1,2], MP Ferraz[1,5]

[1] INEB – Instituto de Engenharia Biomédica, Universidade do Porto, Porto, Portugal [2]FEUP – Faculdade de Engenharia, Universidade do Porto, Porto, Portugal [3]ULP – Universidade Lusófona do Porto, PortugaL [4]LEPAE – Laboratório de Engenharia dos processos, ambiente e energia. Departamento de Engenharia Química, Universidade do Porto, Porto, Portugal [5]CEBIMED – Centro De estudos em Biomédica, Universidade Fernando Pessoa, Porto, Portugal

INTRODUCTION: Nanohydroxyapatite possesses exceptional biocompatibility and bioactivity with respect to bone cells and tissues, and for this reason, it has been used as a coating for orthopedic implants or as a bone substitute[1]. Unfortunately, this feature may also encourage bacterial adhesion and biofilm formation. Recently, there has been interest in the functionalisation of implant surfaces with antimicrobials, to reduce the likelihood of bacterial infestation and colonization of the surrounding tissues. Chlorhexidine digluconate (CHX) is a common antimicrobial agent used for a wide range of medical applications[2]. In this study, the adsorption of chlorhexidine digluconate (CHX) to nanohydroxyapatite sintering at 830ºC discs (nanoHA830) and release system from these surfaces was investigated. The *in vitro* antimicrobial activity of CHX associated with nanoHA was also evaluated.

METHODS: CHX in different concentrations (5-1500 mg/L) were adsorbed on nanoHA830 agitated gently at 37ºC for 24 hours. The supernatant was then analyzed by UV spectrophotometry. Adsorption isotherms for CHX adsorption to nanoHA830 were plotted as CHX mass adsorbed per unit surface area as a function of CHX equilibrium concentration in solution, after adsorption[3]. Release system was measured in CHX-nanoHA disc coatings by submersion of these discs into saline solutions and measuring chlorhexidine UV absorbency versus time. Control experiment using CHX-free ceramic samples was performed under the same experimental conditions (negative control). All tests were performed in triplicate. The antimicrobial efficacy of the amount of CHX release was evaluated. Minimum inhibitory concentration (MIC) value of chlorhexidine was determined for *S.aureus* ATCC 25923 and *E.coli* ATCC 25922, according to what was defined by Clinical and Laboratory Standards Institute (CLSI)[4]. The biomaterial surfaces with and without CHX were studied by scanning electron microscopy (SEM).

RESULTS: CHX adsorbed onto nanoHA discs exhibited Langmuir-type adsorption isotherms, with a linear plots and a good correlation (R^2 = 0.996). The morphological effect studied by SEM showed that CHX did not cause morphological changes to the nanoHA surfaces. The CHX-nanoHA disc coatings showed a slow release over time for a period of several days, being the amount of CHX released higher than MIC values for both bacteria used. The samples obtained from release studies were tested in *S.aureus* ATCC 25923 and *E.coli* ATCC 25922 strains, showing antimicrobial activity, revealing that binding to nanoHA did not affect antimicrobial activity of CHX.

DISCUSSION & CONCLUSIONS: These results showed that CHX-nanoHA disc coatings might provide good alternatives for antibiotics delivery. They also suggest that a pre-implantation treatment with chlorhexidine solution might provide post-operative antimicrobial capability at the implant site.

REFERENCES: [1]Ferraz *et al, J Biomed Mater Res A* 2007;81: 994-1004. [2]Barbour *et al, Col Surf A*, 2007;307:116-120. [3]Giménez-Martín et al, Cellulose 2009;16:467-479. [4]Clinical and Laboratory Standards Institute (CLSI), 2010; M100-S20.

ACKNOWLEDGEMENTS: This work was financed by FEDER funds through the *Programa Operacional Factores de Competitividade* – COMPETE and by Portuguese funds through FCT in the framework of the project NaNOBiofilm (PTDC/SAU-BMA/111233/2009).

Antibacterial activity of nanohydroxyapatite containing zinc oxide nanoparticles

L Grenho[1,2], FJ Monteiro[1,2], MP Ferraz[1,3]

[1]INEB - Instituto de Engenharia Biomédica, Universidade do Porto, Porto, Portugal [2] DEMM, Faculdade de Engenharia, Universidade do Porto, Porto, Portugal [3] CEBIMED - Centro de Estudos em Biomedicina, Universidade Fernando Pessoa, Porto, Portugal

INTRODUCTION: Biofilms play a crucial role in healthcare-associated infections, especially those related to implants or medical devices. Strategies are therefore needed to develop the next generation of implant surfaces capable of preventing bacterial adhesion [1]. Zinc oxide (ZnO) is a known antibacterial agent [2] and nanohydroxyapatite (nanoHA) is a promising bioceramic to be used in bone regeneration scaffolds, to fill small bone defects or as coating for orthopedic implants, due to its chemical similarities with mineral bone [3]. The addition of ZnO nanoparticles to form a biocomposite material may thus reduce undesirable bacteria activity. In the present work, ZnO was associated to nanoHA structure and its influence on bacterial proliferation and biofilm formation were investigated.

METHODS: Two different ZnO nanopowders with mean particle size of < 100nm and < 50nm (Sigma-Aldrich) were tested. ZnO particles were integrated into nanoHA powder (Fluidinova S.A., Portugal) at weight percentages (wt.%) of 0, 2, 10 and 25%. The composite powders were uniaxially pressed to cylindrical samples and heat-treated at 830ºC for 15 min. The composites were studied by scanning electron microscopy (SEM) and X-ray photoelectron spectroscopy. To evaluate the bacterial proliferation and biofilm formation, *Staphylococcus aureus* ATCC 25923 and *Escherichia coli* ATCC 25922 were seeded onto the nanocomposite samples in tryptic soy broth, for 24 h at 37ºC. Optical density (OD) readings and colony forming units (CFU) after sonication were the selected methods of analysis.

RESULTS: Surface morphology of the composites as observed by SEM revealed that ZnO particles were homogeneously dispersed within the nanoHA matrix (Fig. 1). Concerning the composites antibacterial activity, a strong and significant reduction on the biofilm formation was noticed for the several tested composites. The inclusion of 25 wt.% ZnO (< 50 nm) reduced biofilm growth by approximately 98% for *S. aureus* and 99% for *E. coli*. Concerning the effect of various nanoHA-ZnO composites on the growth of *S. aureus* and *E. coli*, the OD data after 24h of incubation indicated a significant reduction in total bacteria counts for bacteria cultured in the presence of the composites compared to those cultured onto pure ceramic samples. The results also indicated that antibacterial efficiency increased with increasing ZnO concentration for both studied bacteria.

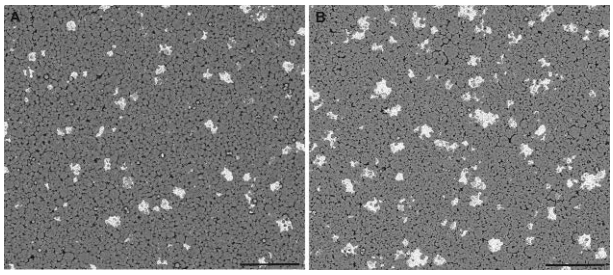

Fig. 1: Back scattering electrons images collected by SEM of nanoHA-ZnO composites heat-treated at 830ºC with different amounts of ZnO (< 100 nm): 10 wt.% (a) and 25 wt.% (b). Scale bar 50 µm.

DISCUSSION & CONCLUSIONS: The data clearly suggest that composites formulated with ZnO nanoparticles with smaller sizes (< 50 nm) showed a significant growth inhibition at just 2 wt.%, whereas for composites with relatively larger ZnO particles (< 100 nm) the same effect was just observed for 10-25 wt.%. The enhanced bioactivity of smaller particles may be attributed to the higher surface area/volume ratio, which results in the generation of a larger number of active oxygen species that may cause fatal damage to microorganisms. Therefore, in the future, nanoHA-ZnO composites should be further studied to be implanted and prevent microorganisms from attaching and forming biofilms in some indwelling medical devices.

REFERENCES: [1] J.T. Seil et al. (2011) *Acta Biomater* **6**:2579-84. [2] K.R. Raghupathi et al. (2011) *Langmuir* **27**:4020-8. [3] M.P. Ferraz et al. (2004) *J Appl Biomater Biomech* **2**:74-80.

ACKNOWLEDGEMENTS: *FEDER* and *FCT*.

Osteoconductivity of crosslinked biomimetic LbL films atop nano/microstructured Ti-6Al-4V

B Labat, S Morin-Grognet, F Gaudière, L Bertolini-Forno, JP Vannier, G Ladam, H Atmani

La2B – MERCI EA 3829, Centre Universitaire d'Evreux, Université de Rouen, 27002 Evreux, France

INTRODUCTION: Controlling physical, chemical, and biological properties for biomimicry of bone biomaterial engineering is a key challenge. In the present work, we combined (i) nano/micro-roughness of a titanium alloy (TA6V), (ii) biomimetic LbL films composed of poly-l-lysine (PLL) and chondroitin sulfate A (CSA) [1,2] and (iii) genipin (GnP), a natural crosslinker for LbL films [3]. Osteoconductivity of the substrates was assessed through adhesion, proliferation and early/late differentiation of pre-osteoblast MC3T3-E1.

METHODS: *Substrates preparation and surface characterization:* TA6V samples were nano/micro-structured by acid-etching (named *AE*) and then, coated with LbL films composed of $(CSA/PLL)_6$±CSA. The films were used either native or crosslinked with GnP. QCM-D was used to monitor the LbL films buildup. AFM and contact angle were performed to determine their topography and wettability. *Morphology:* MC3T3-E1 cells were observed for nucleus (DAPI) and actin-cytoskeleton (FITC-phalloidin) three hours after seeding by using fluorescence microscopy. *Proliferation:* Alamar Blue® assay was performed to evaluate the cell growth. *Osteogenic differentiation:* ALP activity of MC3T3-E1 was monitored over 14 days, and mineralization of the extracellular matrix was assessed by Alizarin Red S staining (2%) and confocal Raman microspectroscopy.

RESULTS: Acid-etching generated rough surfaces (*Ra*=350 nm and *Rt*=1.5 µm) (Fig. 1A). Cells cultured onto native LbL films poorly anchored (Fig. 1B) and were less proliferating (Fig. 2A). Conversely, cell adhesion and proliferation were enhanced onto GnP-treated LbL films with a slight promoting effect of roughness. Fig. 2B shows sparse mineralized nodules identified as hydroxyapatite (HAp) by Raman spectroscopy, after 40 days of culture.

DISCUSSION & CONCLUSIONS: The highly hydrated CSA/PLL biomimetic films were stiffened upon crosslinking with GnP allowing favourable initial cell anchoring. Additionally, the combination of roughness and biomimetic GnP crosslinked CSA/PLL films constitutes a successful approach for bone tissue engineering as it enhanced short-, mid- and long-term pre-osteoblast processes. Further progress of this strategy by using drug-eluting LbL architectures is envisaged.

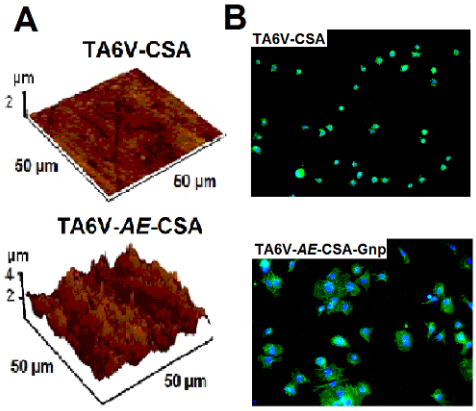

Fig.1: (A) 3D AFM images of the substrates before and after acid-etching (AE) coated with native CSA ending films - (B) Fluorescence images of cell morphology: nuclei (blue) and F-actin (green) at 3hrs.

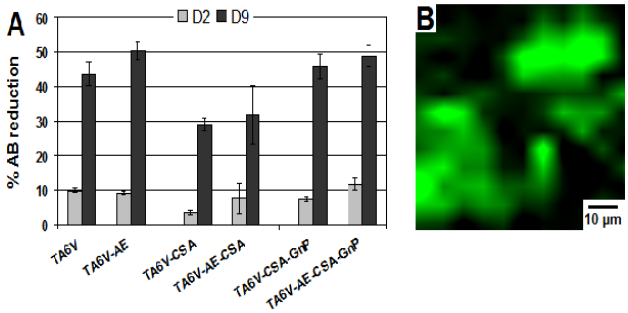

Fig. 2: (A) Proliferation of MC3T3-E1 cells atop TA6V and TA6V-AE coated with native or GnP-treated CSA ending films. (B) Mineralization: RAMAN mapping for HAp (ν=960 cm^{-1}-green) atop native CSA/PLL film.

REFERENCES: [1] Decher, G. (1997) *Science*, **277**, 1232–37. [2] F. Gaudière, I. Masson, S. Morin-Grognet, et al. (2012), *Soft Matter*, **8**, 8327–37. [3] A. L. Hillberg, C. A. Holmes and M. Tabrizian, (2009), *Biomaterials*, **30**, 4463–70.

ACKNOWLEDGEMENTS: This work was partially supported by the Grand Evreux Agglomération and the Conseil Général de l'Eure.

In vitro biocompatibility and *in vivo* antibacterial effect of nanohydroxyapatite and zinc oxide granules (nanoHA/ZnO)

L Grenho[1,2*], CL Salgado[1,2*], MH Fernandes[3], FJ Monteiro[1,2], MP Ferraz[1,4]

[1] *INEB, Instituto Nacional de Engenharia Biomédica, Porto.* [2] *FEUP, Faculdade de Engenharia, Departamento de Engenharia Metalúrgica e Materiais, Universidade do Porto, Porto.* [3] *FMDUP, Faculdade de Medicina Dentária, Departamento de Farmacologia, Universidade do Porto, Porto.* [4] *Universidade Fernando Pessoa, Porto. * Contributed equally*

INTRODUCTION: Orthopaedics is currently the largest market of biomaterials worldwide and implant-related infections remain the first reasons for bone implant failure [1]. Within the increase in antibiotic-resistant strains, recent prophylactic strategies have been developed, including pre-coating of devices with peptide antibiotics [2], but there is also a need for alternative strategies. Recent studies have focused on developing prosthetic materials that reduce adhesion or survival of bacteria with new therapeutic targets like ions, such as zinc [3,4]. The objective of this study was to evaluate the *in vitro* biocompatibility of nanoHA granules with and without ZnO and the antibacterial effect *in vivo* (*Staphylococcus aureus* infection).

METHODS: The porous granules were prepared using the polyurethane sponge impregnation method. Two types of slurries were prepared using pure nanohydroxyapatite (nanoHA), nanoHA with 2 Wt% of ZnO. The infiltrated sponges were sintered: heating rate of 1°C/min until 600°C (1h), followed by 4°C/min until 830°C (1h). For the *in vitro* study, human osteoblast-like cells linage (MG63) was cultured with complete α-MEM. The cells were seeded $5x10^4$cell/well and the viability was evaluated after 1 and 3 days with resazurin assay. NanoHA granules with and without ZnO (2%) were implanted subcutaneously on male Wistar rats. After closing the injury, a cell suspension was injected. After 1 and 3 days, the animals were euthanized and the tissue was homogenized. *S. aureus* CFU's were counted with serial dilutions of the obtained suspension.

RESULTS:

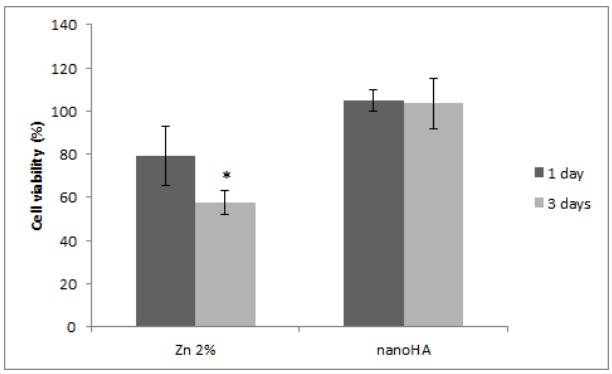

Fig. 1: Resazurin assay results showing the viable MG63 cells on different samples after 1 and 3 days of culture. (*) represent significant difference at $p<0.05$ with respect to control (TCPS - 100%).

DISCUSSION & CONCLUSIONS: Multiple comparisons between the samples proved that the granules with zinc cultured for 3 days were observed to have statistically significant difference with respect to control (TCPS). The antibacterial effect on the animals was observed after 3 days of both materials implantation. NanoHA/ZnO material showed better antibacterial properties and could be considered as suitable for hard tissue replacement material.

REFERENCES: [1] C. Romanò et al. (2013) *J. Chemotherapy* **25**:67-80. [2] L. Sánchez-Vásquez et al (2013) *Biochimica et Biophysica Acta* **1830**: 3427–3436. [3] J. L. Suárez-Franco et al (2013) *J Nanomaterials* **361249**: 1-7. [4] N. Saha et al (2012) *J Biomed Mat Res B* **100B**: 256-264.

ACKNOWLEDGEMENTS: The authors acknowledge financial support by FEDER (COMPETE) through FCT for funding (project NaNOBiofilm - PTDC/SAU-BMA/111233/2009, PhD grant SFRH/BD/72866/2010 and Post-doc grant SFRH/BPD/84443/2012).

Electrophoretic Deposition of Graphene Oxide Reinforced Chitosan–Hydroxyapatite Composite Coatings for Biomedical Applications

Y Shi, M Li, Q Liu, Z Jia, X Xu, Y Cheng, Y Zheng, T Xi, S Wei

Center for Biomedical Materials and Tissue Engineering, Academy for Advanced Interdisciplinary Studies, Peking University, Beijing, China

INTRODUCTION: Graphene oxide (GO) has attracted enormous attention as nanofillers in biocomposites, due its high mechanical property, biocompatibility, antibaterial property and good dispersibility. In order to harness the versatile properties of GO, electrophoretic deposition (EPD) was employed to prepare GO/ hydroxyapatite/ chitosan composite coatings on Ti, as a simple and cost-effective method. Hydroxyapatite (HA, $Ca_{10}(PO_4)_6(OH)_2$) is a bioactive ceramic, with chemical and physical similarity to that of natural apatite in hard tissues. And HA is generally combined with chitosan (CS) to mimick the mineral portion as well as the organic portion of natural bone. However their low mechanical properties cannot meet the clinical requirements in load-bearing areas. Therefore, in our research, GO is introduced and co-deposited with HA/CS using EPD method, as a reinforcing phase.

METHOD: Electrodeposition was performed from CS solutions in a mixed ethanol-water solvent (20/80vol%) containing HA and 0~2 wt% GO. The deposition was investigated by Zetasizer Nano ZS90 and transmission electron microscope (TEM). The resulting nanocomposite coatings were further characterized by Raman spectra and water contact angle measurements.

RESULT:

Due to the presence of chitosan, rod-like HA nanoparticles accumulate with each other. While after adding GO, HA particles distribute randomly on the surface and edge of GO, leading to a more stable dispersion, which was verified by the increased ζpotential of the solutions.

Raman analysis confirms the existences of GO and HA. The water angle analysis indicates that higher GO contents could result in more hydrophilic coatings.

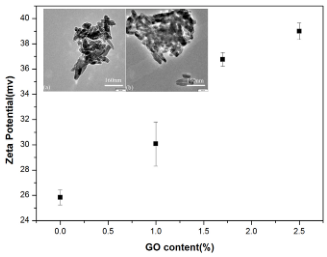

Figure 1.Zeta potential of CS-HA suspension with different GO contents. The inset shows the TEM morphologies of HA-CS(a), HA-CS-GO(b)

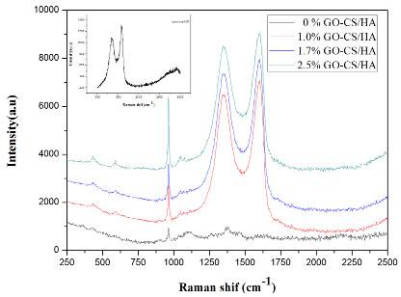

Figure 2.Raman spectra of the resulting coatings and the pristine GO sheet (shown as inset).

DISCUSSION & CONCLUSIONS: GO/HA/CS composites with different GO contents were successfully deposited on the Ti substrate through one-step electrophoretic deposition. The addition of GO can improve the surface hydrophilicity and is beneficial to the application of HA bioactive coating. The obtained GO/HA/CS composites coatings show great potential in major load-bearing applications (e.g. total joint replacement.

REFRENCES: [1]Hailong Fan, et al(2010) *Biomacromolecules* 11:2345–2351. [2]K. randfield, F. Sun, M. FitzPatrick, M. Cheong, I. Zhitomirsky(2009) *Surface & Coatings Technology* 203:1481-1487. [3]Ming Fang et al(2010) *Langmuir* 26(22)：16771–16774.

Bacterial behavior on micro-patterned surfaces

Y Leng[1], X Ge[1], M Yang[1], X Lu[2]

[1]*Department of Mechanical Engineering, The Hong Kong University of Science and Technology, Hong Kong* [2]*Key Lab. of Advanced Materials, Ministry of Education, Southwest Jiaotong University, Chengdu, China*

INTRODUCTION: Controlling biomaterial-centered infection is crucial for regenerative medicine, because the bacterial infection on an implant surface results in the implantation failure eventually. Bacterial adhesion on the implant *in vivo* has been proven to be an initial and important step for the subsequent bacterial proliferation and infection. Thus, modifying the implant surface, *i.e.* biomaterial surface, might be an effective way in inhibiting the biomaterial-centered infection. A number of surface parameters can affect the bacterial adhesion, including surface topography, chemistry, electrical charge, and wettability. In the present study, we investigated the surface topographical effects on bacterial behavior.

METHODS: We employed the photolithography and dry etching methods to generate regular two distinctive micro-patterns on silicon: pillar and honeycomb with a size range of 1 to 20 μm. *Escherichia coli* (*E.coli*) and *Staphylococcus aureus* (*S.aureus*), which represent two different shapes (rod and sphere), were used as bacterial models. The patterned surface was cultured with bacteria for various periods of time (30 min, 12 h, and 24h) to study bacterial adhesion and proliferation on the topographic patterns.

RESULTS: A single specimen, which consisted of different surface areas including one flat area and patterned areas with various sizes, was reliably revealed topographic effects on bacterial behavior. Experimental results indicate the differences of bacterial adhesion and growths on various patterned surfaces. For example, Figure 1 shows *E. coli* behavior on the pillar patterns with size from 0.6 μm to 20 μm; and Figure 2 shows E. coli behavior on the honeycomb patterns with feature size from 0.5 ~ 10 μm. Significant reduction of bacterial adhesion, growth and proliferation can be achieved when the pattern feature size is in the range of 0.6~0.8 μm for pillar and 1.0 μm for honeycomb patterned surfaces.

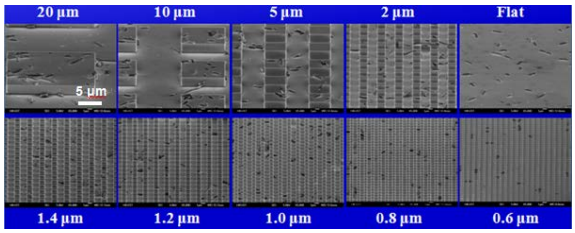

Fig. 1: Typical SEM images of Si_E.coli_10[5] CFU/mL_24 h.

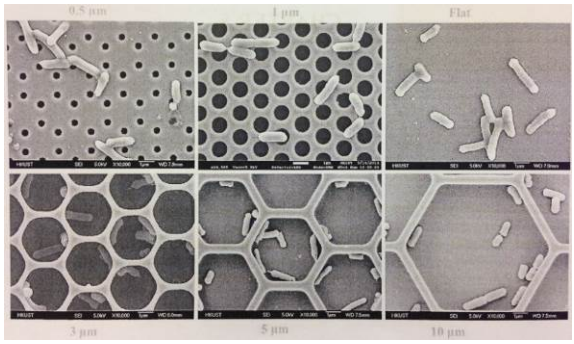

Fig. 2: SEM images of E.coli adhesion on honeycomb patterned surfaces after 24 h incubation.

CONCLUDING REMARKS: In this systematic study, we carefully make the all types of surfaces possessing the same chemical composition, wettability and zeta potential to eliminate possible variables which could affect the bacterial behavior. Thus, we can reveal the truly bacterial responses to topographic surface features. After comprehensive comparison and analysis, we conclude that (1) micro-patterned surface can manipulate bacterial adhesion partially because of physical confinement effects. (2) Significant reduction of bacterial adhesion, growth and proliferation can be achieved when the topographic feature size decreases down to the level of single or sub-micrometer.

ACKNOWLEDGEMENTS: This work was supported by Research Grants Council of Hong Kong FSGRF13EG58/HKUST615408.

Utilization of NO coupled iron oxide nanoparticles for an antibacterial treatment

M Talantikit[1], A Leduc[2], J Barbeau[2], LH Yahia[1]

[1]*Laboratoire d'Innovation et d'Analyse de Bioperformances, Ecole Polytechnique, Montréal, Québec* [2]*Laboratoire de contrôle des infections, Université de Montréal, Montréal, Québec*

INTRODUCTION: Occidental population tends to live longer inducing the use of medical and orthopedics implants. Resistant bacteria can contaminate implants, leading to the apparition of nosocomial infections (NI). Common treatment against bacteria is the use of antibiotics. But a long contact of antibiotics with bacteria can cause resistance. Adding to it, bacteria can produce a biofilm (polysaccharides layer, practically impossible to destruct). This project will allow developing an antibacterial treatment on implants surface and medical instruments to prevent nosocomial infections. Iron oxide nanoparticles (Fe_3O_4) were chosen because they have interesting properties that can be exploited (hyperthermia, magnetism). Using nanoparticles can be a nice solution to kill those resistant bacteria. This project will allow developing a antibacterial treatment on implants surface and medical instruments to prevent NI.

METHODS: *Nanoparticles preparation:* Nanoparticles were prepared by Dr Sophie Laurent (Belgium)

Antibacterial assay: To determine the minimal inhibitory concentration (MIC) a microbiology test was done. It consists to find the lowest concentration of an antimicrobial that will visibly lower the growth of bacteria after an overnight incubation. Two strains of bacteria were studied: *Staphylococcus aureus (*Gram+ bacteria) and *Escherichia coli* (Gram- bacteria). A serial dilution of the nanoparticles was done (3, 1.5, 0.75 and 0.375mg/mL). A control negative was done (NPs + media culture). This experiment was done with SPIONs, SPIONs + NO, and CuO as a positive control (because know as a strong antimicrobial). *Nitrosation of SPIONs* NPs were functionalized with NO.

RESULTS: The results for the copper oxide were as predicted. Copper is known to be an important antimicrobial. The MIC was clearly visible at a low concentration for both strains of bacteria (with a better susceptibility for the Gram+ bacteria).

The toxic effect of iron oxide, functionalized with NO, is visible too (less than the copper one). The toxic effect is more important for bacteria Gram+ than Gram-. At lowest concentration, for *S.aureus*, 30% of bacteria were killed, compared to 60% at the highest concentration of nanoparticles. For *E.coli*, it was observable a diminution of more than 40% of bacteria growth at the highest concentration.

DISCUSSION & CONCLUSIONS: These results are definitely promising. To increase the percentage of bacteria killing (or even total destruction) it's possible to increase the NO doses at the surface of the nanoparticles. Some other experiments must be done with different NO doses to determine a lethal threshold against bacteria.

REFERENCES: BARBEAU Jean, GAUTHIER Carl, PAYMENT Pierre, « Biofilms, infectious agents, and dental unit waterlines: a review », *Can J Microbiology*, 1998, 1019-1028

FIGUEROLA Albert, DI CORATO Riccardo, MANNA Liberato, PELLEGRINO Teresa, « From iron oxide nanoparticles towards advanced iron-based inorganic materials designed for biomedical applications », *Pharmacological Research*, 2010, 126-143

STEWART Phillip S, COSTERTON J William, « Antibiotic résistance of bacteria in biofilms », *The Lancet*, 2001, Vol 358

ZIEBUHR Wilma, HENNIG Susanne, ECKART Martin, KRANZLER Hennes, BATZILLA Christoph, KOZISKAYA Svetlana, « Nosocomial infections by *Staphylococcus epidermis:* how a commensal bacterium turns into a pathogen », *Antimicrobial Agents*, 2006, S14-S20

ZHANG, MANSOURI S, MBEH D. A., YAHIA L'Hocine, SACHER E. and VERES T., "Nitric Oxide Delivery by Core/Shell Superparamagnetic Nanoparticle Vehicles with Enhanced Biocompatibility". Langmuir 28(35):12879-12885, 2012.

ACKNOWLEDGEMENTS:
This work was supported by FQRNT. We thank Sophie Laurent for the preparation of SPIONs.

Towards anti-biofilm surfaces

SH Hakobyan, O Rzhepishevska, R Ruhal, M Ramstedt

Department of Chemistry, Umeå University, 901 87 Umeå, Sweden

INTRODUCTION: Antibiotics are often inefficient for treatment of chronic infections associated with bacterial biofilms that build-up on, for example, catheters and prosthetics. Biofilms are organized clusters of bacterial cells that are attached to a surface and produce extracellular substances that mediate bacterial attachment and protect the cells. Biofilms are responsible for approximately 80% of all microbial infections, and cause 100,000 deaths annually in the USA alone [1]. One way to prevent biofilm formation is to modify properties of surfaces that bacteria attach to, for example, by coating the surface with a layer of polymer brushes. Polymer brushes are thin polymer films where the polymer chains are tethered to the surface of an underlying substrate [2]. Another way to combat biofilms is to treat bacteria with chemicals that specifically prevent biofilm formation. Ga(III) ions inhibit biofilm formation and kill both planktonic and biofilm bacteria due to their chemical similarity to biologically important Fe(III). Ga(III) is most efficient when stabilized in a complex with other molecules [3].

METHODS: Polymer brushes were prepared following the surface-initiated polymerization strategy by using controlled Atom Transfer Radical Polymerisation (ATRP) technique. The thickness of polymer brushes were less than 0.5 µm. Speciation and equilibria of the Ga(III)-hydrazone system were determined by potentiometric titration and UV-VIS spectrometry. Biofilms of *Pseudomonas aeruginosa* were grown in a flow chamber and confocal images of biofilm were taken *in vivo* after staining with fluorescent dye.

RESULTS & DISCUSSION: In this project we have seen that polymer brushes with negative charge reduce attachment of bacteria and change architecture of its biofilm. We have also studied hydrazones, which are a class of organic molecules, that have antivirulent effects and can form complexes with Ga(III). Our preliminary results show that presence of Ga(III) greatly increases stability of hydrazones and Ga-hydrazone complexes have pronounced antibacterial properties (tested against *P. aeruginosa).*

Our future plans is to combine polymer brushes and soluble antibiofilm compounds in long-lasting antibiofilm surfaces by incorporation of Ga-hydrozone complexes into negatively charged polymer brushes or covalent attachment onto anti-fouling brushes.

REFERENCES: [1] R. Klevens, J.R. Edwards, et al (2007) *2002 Public health rep* **122**:160-66. [2] M. Ramstedt, B. Ekstrand-Hammarström, et al (2009) *Biomaterials* **30**:1524-31. [3] O. Rzhepishevska, B. Ekstrand-Hammarström, et al (2011) *Antimicrob Agents Chemother* **55**:5568-80

.

Biocompatible antimicrobial surfaces based on metals – vancomycin complexes

M Varisco[1], PS Brunetto[1], KM Fromm[1]

[1] *Department of Chemistry, University of Fribourg, Fribourg, Switzerland*

INTRODUCTION: The number of people requiring internal fixation devices or joint replacement grows every year. Different types of intervention exist and hundreds of thousands of patients are submitted to them every year. The problem of infection is important: for some intervention it can be up to 20 % of the cases,[1, 2] increasing the costs and inducing pain (or even death) to the patients.

One way to prevent this infection is to protect the surfaces of the implants by coatings. Metal ions like silver(I) or copper(II), known for their antimicrobial properties[3] and antibiotics such as vancomycin can be combined (figure 1). Till today there is no evidence of bacterial resistance to this synergic action.

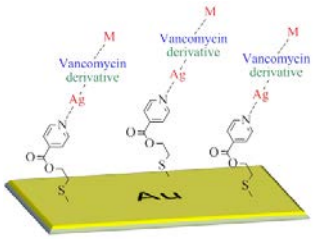

Figure 1: schematic representation of the coating.

To coat the vancomycin onto surfaces, a modification is needed. A bioactive derivative (IPV, figure 2), was attached in a non-covalent way to the surfaces through an organic linker and silver(I). Afterwards, silver(I) ions were complexed with the antibiotics for the final surface functionalization.

Figure 2: schematic representation of the derivative.

METHODS: We used a gold (111) surface as model surface to attach our vancomycin derivatives. It was synthetized starting from a flexible biocompatible linker (8-ammino-3,6-dioxaoctanoate functionalised with a pyridinyl group) and vancomycin. This new antibiotics and the complex formed with $Ag(NO_3)$ were characterised by mass spectrometry and UV/Vis spectrometry.

The modified surfaces were characterized by Scanning Electron Microscopy (SEM), immunofluorescence detection and X-ray reflection. Release of antibiotics was studied using UV/Vis spectrometry and Inductively Coupled Plasma - Optical Emission Spectroscopy.

RESULTS: Surface analysis of the coated specimens showed a good attachment of the antibiotic to the surface leading to both micro- and nano-structured topology. Both metal and antibiotic molecule were released over a period of one month. The antimicrobial activity, the cytotoxicity and soft-tissue integration were evaluated and will be discussed. Furthermore other study on the vancomycin derivative will be taken into account.

DISCUSSION & CONCLUSIONS: The study based on our modified surface showed promising results. Both metals and antibiotic were successfully attached to the surface showing a good antimicrobial activity and biocompatibility. This technique could be very useful to diminish the problem of biofilm formation.

REFERENCES: [1]A. Trampuz, A. F. Widmer (2006) *Infect Diseases* ***19****:349.* [2]L. M. Baddour et al. (2003) *Circulation* **108**:2015. [3]P. S. Jarret (1994) *Metal Based Drugs* **5-6**:467.

ACKNOWLEDGEMENTS: The author thanks the Swiss National Science Foundation for most generous support and Teva Pharmaceuticals for the vancomycin.

Inhibition of initial bacterial adhesion to titanium by lactoferrin

F Nagano-Takebe[1], H Miyakawa[2], F Nakazawa[2], K Endo[1]

[1] Health Sciences University of Hokkaido, School of Dentistry, Division of Biomaterials and Bioengineerings [2] Health Sciences University of Hokkaido, School of Dentistry, Division of Oral Microbiology

INTRODUCTION: Modification of implant abutment surfaces with antibacterial molecules is effective to prevent peri-implantitis. We have already demonstrated that early bacterial adhesion on titanium surfaces was substantially reduced by adsorption of an antibacterial molecule, human lactoferrin (LF) [1]. However, in the oral cavity, adsorbed LF could be replaced by salivary proteins. The aim of this study was to confirm the effect of adsorbed LF with a saliva coating.

METHODS: Titanium disks were mirror polished and prepared as follows. For the "Control group", disks were soaked in distilled water for 24 h. For the "LF group", disks were soaked in LF solution (0.1 mg/mL) for 24 h. For the "Saliva group", half of the Control group was incubated with artificial saliva containing mucin [2] for 1 h at 37°C. For the "LF-saliva group", half of the LF group was incubated with artificial saliva for 1 h at 37°C.

To confirm adsorption of LF, samples were incubated with a rabbit anti-human LF antibody for 1 h. A secondary antibody, FITC labeled goat antibody to rabbit IgG, was conjugated for 1 h. Samples were observed by confocal laser scanning microscopy. The adsorption of LF was evaluated by measuring the mean gray value of the images as fluorescence intensity using Image J software. Data were statistically analyzed by one-way ANOVA and Games-Howell post hoc test.

For the bacterial adhesion experiment, samples were placed in 12-well plate and anaerobically incubated for 2 h with *Streptococcus gordonii* (*S.gordonii*) in PBS adjusted to give 2×10^9 cfu/well. Samples were washed with PBS and then stained with 0.1% crystal violet. After washing with PBS, samples were dissolved in 99.5% ethanol and the optical density of each solution at 595 nm was measured. Data were statistically analyzed by two-way ANOVA.

All experiments were repeated independently at least three times.

RESULTS: Figure 1A shows the fluorescence intensity of the samples (n=30). The mean gray values of the LF and LF-saliva groups were significantly higher than those of the Control and Saliva groups ($p<0.01$). There was no significant difference between the LF and LF-saliva groups ($p>0.05$).

Figure 1B shows the results for the bacterial adhesion test (n=7). The adhesion of *S.gordonii* was significantly increased by saliva coating ($p<0.01$) and significantly decreased by adsorption of LF ($p<0.01$). There was no interaction between adsorbed LF and the saliva coating ($p=0.561$). Adsorption of LF inhibited bacterial adhesion regardless of the saliva coating.

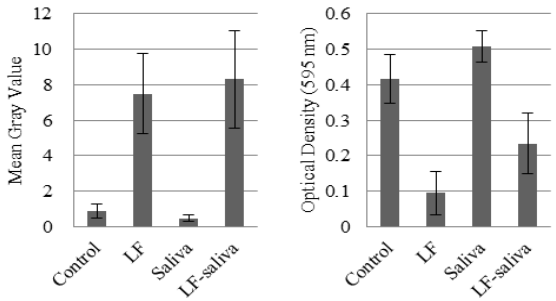

(A) (B)

Fig. 1: (A) Fluorescence intensity, and (B) Adhesion of S. gordonii

DISCUSSION & CONCLUSIONS: Our study showed that adsorbed LF remained on titanium surfaces after incubation in saliva. The remaining LF inhibited bacterial adhesion to the titanium surface. The adsorption of LF on abutment materials is therefore effective to prevent peri-implantitis.

REFERENCES: [1]F. Nagano, M. Hashimoto, K. Endo et al (2012) *Japanese Society for Dental Materials and Devices* **31**:358. [2] C. Russell and W. A. Coulter (1975) *Applied Microbiology* **29**:141-144.

ACKNOWLEDGEMENTS: This study was supported by JSPS KAKENHI (Grant Numbers 23792289)

Hydrogel coatings with tunable surface exposure of hydroxyapatite

D Moreau[1], Y Auriac[1], M Betbeder[1], DN Ku[2], L Corté[1]

[1] *Centre des Matériaux CNRS UMR 7633, Mines Paristech, Evry, France.* [2] *George W. Woodruff School of Mechanical Engineering, Georgia Institute of Technology, Atlanta, GA, USA*

INTRODUCTION: Injuries and damages of soft connective tissues such as ligaments, tendons, or cartilage can usually not be healed and most often require a reconstruction using natural grafts, durable synthetic implants or degradable tissue-engineered scaffolds. To restore proper physiological function, it is crucial that these reconstructed tissues are well anchored to the bone tissues of the treated joint. In particular, for synthetic implants, failures at the bone-implant interface often remain a limitation.[1] For bone prosthetics such as hip implants, coating by osseoconductive ceramics has been shown to significantly improve the strength of the anchorage to bone.[2] How this approach can be applied to softer tissue substitutes currently motivates strong research efforts.[2] In particular, the design of coatings that contain bioceramics to enhance osseoconduction while still adhering properly to the soft implant remains a challenge. To address this question we investigate the potential of composite coatings made of hydroxyapatite particles (HAp) dispersed in a hydrogel matrix.
The studied hydrogel matrix consists of a cross-linked network of (poly)vinyl-alcohol (PVA) macromolecules swollen with water. These PVA hydrogels are biocompatible, non degradable and exhibit a soft elastic behaviour very similar to that of connectives tissues.[3] In particular, recent works have shown that assemblies of PVA hydrogel fibres can reproduce closely the tensile response of ligaments.[4] With this work, we apply our findings to these PVA fibres with the aim to ensure a strong anchorage of the implant in bone tunnels by promoting osseoconduction.

METHODS: PVA/HAp composites were prepared by dispersing micro HAp (5-60µm) in PVA aqueous solution at various concentrations. Physical cross-linking of the PVA matrix was achieved by the freezing-thawing method.[3] Both bulks and coating were produced by molding and soaking of PVA fibres, respectively. The morphology and surface of these composites was characterized by optical and scanning electron microscopy. The adhesion strength of the coating to hydrogel fibres was investigated by pull-out tests.

RESULTS: The exposure of HAp at the surface of PVA/HAp coatings was characterized by SEM imaging in backscattered electron mode. The surfaces of PVA fibres coated with different compositions of PVA/HAp hydrogel are given in Fig.1. These observations show how the HAp (in white) can be increasingly exposed by reducing the ratio of PVA over HAp in the coating solution.

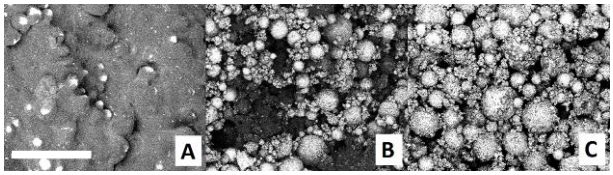

Fig. 1: Backscattered e^- imaging of coatings with different PVA/HA weight ratios: 0.9 (A), 0.23(B), 0.1 (C). (Scale bar=100µm)

The mechanical properties of these coatings were characterized experimentally. In particular, pull-out tests of PVA fibres embedded in a PVA/HAp bulk reveal an increase in adhesion between the fibers and the coating after PVA cross-linking.

DISCUSSION & CONCLUSIONS: By varying the composition and elaboration processes, PVA/HAp coatings were created where the coating thickness varies from tens to hundreds of microns and the exposure of HAp can be tuned from 0 to almost 100%. Moreover, mechanical tests show that the PVA hydrogel matrix of the coating can be cross-linked to pure PVA hydrogel substrate to provide a strong adhesion between the coating and the implant. The results of ongoing *in vivo* experimentation in a rabbit model to assess coating osseoconductivity may be presented.

REFERENCES: [1]Mascarenhas *et al.* (2008) *McGill Journal of Medicine* 11(1): 29–37. [2] Li *et al.* (2011) *Applied Surface Science* 257 (2011) 9371– 9376. [3] Peppas *et al.* (2000) *Advances in Polymer Science* Vol.153. [4] Bach *et al.* (2013) *Journal of Biomechanics*, in press.

ACKNOWLEDGEMENTS: Financial support from Mines-Paristech and Carnot Mines Institute is gratefully acknowledged.

Zwitterionic polymer brushes as dynamic cell-active interfaces: synthesis and characterization by imaging ellipsometry

E Vaselli[1], MG Santonicola[1,2]

[1] *Center for Advanced Biomaterials for Healthcare@CRIB, Istituto Italiano di Tecnologia, Italy*
[2] *Materials Science and Technology of Polymers, MESA+ Institute for Nanotechnology, University of Twente, The Netherlands*

INTRODUCTION: Biocompatible interfaces based on polymers that are covalently attached to surface at one end (polymer brushes) offer several advantages in the development of cell-active platforms for *in vitro* assays [1]. Robust functional surfaces are often needed for reproducible assays that can be reused for several days. In addition, switchable biointerfaces may be easily prepared by growing brushes of field-responsive polymers that can be reversibly controlled by external stimuli [2-3]. In a previous study, Santonicola and colleagues showed that it is possible to modulate the interaction of zwitterionic polymer interfaces with cell-model bilayer lipid membranes by controlling the polymer architecture [4]. Here we present the preparation of brush-modified chips based on zwitterionic PSBMA for cell-active assays, and we investigate the morphology of the hydrated polymer brush interface obtained at different polymerizations conditions using *in situ* imaging ellipsometry.

METHODS: Polymer brushes of zwitterionic PSBMA were grafted onto gold-coated glass slides using atom transfer radical polymerization (ATRP) from surface-bound thiolated initiators as previously reported [4]. Polymer-modified chips were characterized with a KSV-CAM 200 setup for water contact angle measurements, and by FTIR spectroscopy using a Bruker VERTEX 70V spectrometer. Imaging ellipsometry investigations were performed with the EP3-SE spectroscopic nulling ellipsometer (Accurion GmbH) equipped with a liquid cell with temperature control and a spectroscopy lamp for multiple-wavelengths spectra. Analysis of the measured ellipsometric angles was performed with the commercial software supplied with the instrument using a multi-layer model for flat film on glass substrate.

RESULTS: In imaging ellipsometry, thickness maps (*Fig. 1 right*) and refractive index maps of the hydrated polymer surfaces were extracted from the simultaneous fitting of the ellipsometric angles measured at fixed angle in the wavelength range 400-1000 nm. Results show that ATRP reactions regulated by high activator/deactivator ratios give rise to more homogeneous polymer brushes with higher density and lower surface roughness than those obtained at lower ratios. The swelling in water and therefore the mechanical properties of the hydrated polymer layers are remarkably different. The effect of the initiator SAM composition on the swelling of the grafted brushes was also investigated, revealing optimal conditions with more diluted SAMs.

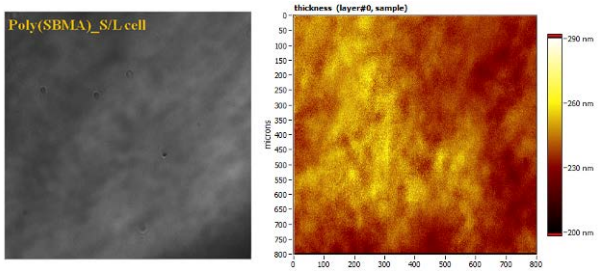

Fig. 1: Ellipsometric contrast image (left) and fitted thickness map (right) of swollen PSBMA brush interface prepared by surface-initiated ATRP on gold-coated glass chip in water at 25℃.

DISCUSSION & CONCLUSIONS: Currently the development of cell-active assays is greatly limited by the lack of information on how the properties of underlying polymer substrates relate to cell behaviour. Non-invasive imaging ellipsometry can be successfully used to characterize conformation and optical properties of polymer coatings in their hydrated state. The role of the different zwitterionic PSBMA brush structures on cell behaviour is under investigation.

REFERENCES: [1] J.E. Raynor, J.R. Capadona, et al. (2009) *Biointerphases* **4**: FA3-FA16. [2]M.G. Santonicola, G.W. de Groot, M. Memesa, et al. (2010) *Langmuir* **26**:17513-17519. [3]A. Mizutani, A. Kikuchi, et al. (2008) *Biomaterials* **29**:2073-2081. [4] M.G. Santonicola, M. Memesa, A. Meszyńska, et al. (2012) *Soft Matter* **8**:1556-1562.

Effect of cell culture media on nanoparticle-protein complexes: perspectives on cellular response

DA Mbeh[1], TS Djavanbakht[1], L Tabet [2], K Maghni[2], E Sacher[3], LH Yahia[1]

[1]LIAB, École Polytechnique de Montréal, Montréal, Qc, Canada H3C 3A7 [2]Hôpital du Sacré-Cœur de Montréal, 5400, boul. Gouin Ouest Montréal, Qc, Canada [3]RQMP, École Polytechnique de Montréal, Montréal, Qc, Canada H3C 3A7.

INTRODUCTION: Nanoparticles (NPs) are used as contrast agents, for drug delivery, etc [1]. Biological responses in the presence of NPs result from interactions that depend on their physico-chemical properties , the biological medium and the phenomenon of proteins adsorption that form a protein layer (the saw called corona) [2]. Qualitative and quantitative studies of this corona are still rare, but necessary to understand how these interactions can be controlled, so that the potential of NPs can be fully exploited and safely used. We propose to understand the mechanism of adsorption of proteins and correlate their physicochemical characteristics and biocompatibility.

METHODS: We performed an accurate investigation of the biophysicochemical properties of spherical iron oxide NPs upon incubation in cell culture media supplemented with the protein source FBS (fetal bovine serum). A range of spectroscopic and microscopic techniques were applied in order to describe the corona formed by dispersing the NPs in the cell culture media. We hypothesized that the nature of SPIONs and suspending media elicit the formation of different corona that, in turn, may exert different biological effects in interacting with cells. To assess such hypothesis, we performed viability assays on A549 cell line exposed to the NPs.

RESULTS: We demonstrated that the presence of corona reduced agglomeration of NPs. Spectroscopic analyses showed the adsorption of proteins onto the SPIONs. We also observed that the cellular response depends on the type of adsorbed proteins. These results show that beyond a physico-chemical characterization of NPs, an understanding of the effect of culture media, blood and other biological fluids, which may come into contact with the NPs is crucial for the assessment of their nanotoxicology.

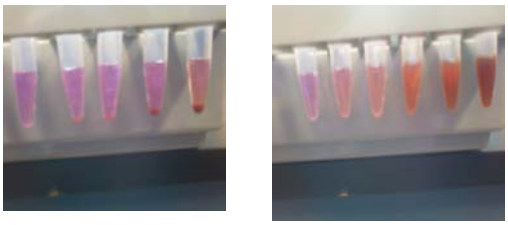

Fig 1: Left- (Fe3O4@COOH in the culture medium + serum-free supplement) and Right - (Fe3O4 @ COOH in the culture medium + FBS). This picture shows how the presence of proteins in the medium reduced agglomeration of NPs, and their subsequent sedimentation.

DISCUSSION & CONCLUSIONS: Our results demonstrate that Protein-NP interactions are mediated by different parameters such as the different composition of the cell culture media, surface composition of the NPs among others.

REFERENCES: [1] Z. P. Chen, R. Z. Xu et al (2009) *Nanoscale Res Lett* **4**:204–209. [2]W. J. Stark. (2011) *Angew Chem Int Ed Engl.* **50(6)**:1242-58.

ACKNOWLEDGEMENTS: The authors gratefully acknowledge Fonds québécois de la recherche sur la nature et les technologies (FQRNT) and Natural Sciences and Engineering Research Council of Canada (NSERC) for their financial support and Canada Foundation for Innovation(CFI) for the equipment made available to us.

.

Thermo-mechanical and spectroscopic characterization of chitosan/PEO/levan ternary blend films for bioactive coatings

M Sennaroglu Bostan[1], E Mutlu[2], H Kazak[2], SS Keskin[3], E Toksoy Oner [2], MS Eroglu[1,4]

[1] *Department of Chemical Engineering, Marmara University, Istanbul, Turkey* [2] *Department of Bioengineering, Marmara University, Istanbul, Turkey* [3] *Department of Environmental Engineering, Istanbul, Marmara University, Turkey* [4] *TUBITAK-UME, Chemistry Group Laboratories, Kocaeli, Turkey*

INTRODUCTION: Binary blend films of chitosan, PEO and levan have been attracting a considerable interest in biomedical and food applications [l,2]. Therefore, ternary blend films are expected to have a higher potential since chitosan and levan may enhance mechanical and thermal stability of PEO films while reducing the water solubility and minimizing the crystallinity via intermolecular hydrogen bonding. Considering these facts, this study focused on preparation of ternary blend films of chitosan, PEO and levan to establish their morphological, thermo-mechanical, surface and biological properties.

METHODS: Chitosan was prepared by deacetylation of chitin of shrimp shell. Levan was produced by microbial fermentation of *Halomonas smyrnensis* AAD6^T cultures [3]. Poly(ethylene oxide), PEO (300.000) was supplied from Sigma Aldrich and used as received. Films were prepared by solution casting with the compositions detailed in Table 1.

Table 1. Composition of blend films

Sample code	Chitosan/PEO/Levan (w/w/w)
CPL1	78.3/8.7/13
CPL2	69.6/17.4/13
CPL3	60.9/26.1/13
CPL4	52.2/34.8/13

FT-IR spectra were recorded on a Thermo Nicolet 6700 FT-IR spectrophotometer. Thermal gravimetric analysis (TGA) were conducted using Pyris6 Perkin Elmer Thermal Analyzer System. DSC measurements were performed using Perkin Elmer Jade DSC at a heating rate of 10 ^oC/min under argon atmosphere (20 ml/min flow rate). DMA measurements were conducted using Diamond model Dynamic Mechanical Analyzer (DMA) supplied by Perkin Elmer-Seiko (Japan). Film samples were analyzed by an X-ray diffractometer (RIGAKU® D/MAX2200/PC) to obtain X-ray diffraction patterns.

RESULTS: Hydrogen bonding between blend components was evidenced as the absorption frequency of $-NH_2$ groups of pure chitosan shifted to lower wave-number in the blend (from 1588 to 1544 cm^{-1}), indicating an intermolecular interaction of chitosan with PEO and levan. DTG peak temperatures of pure levan, chitosan and PEO were observed at 240, 390 and 417 ^oC, respectively. The T_gs of the blend films decreased with increasing PEO contents approaching toward the T_g of PEO, which is about -20 ^oC (Fig. 1). The characteristic peaks of PEO were not observed in diffraction patterns when PEO content was less than 26.1% (CPL3), which could be considered as a further proof of the suppression of PEO crystallinity *via* hydrogen bonding, which has a significant effect on the overall crystallinity of the blend films.

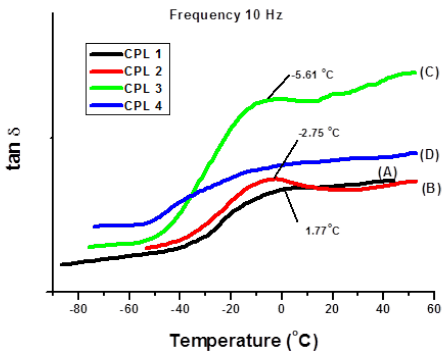

Fig. 1. Loss tangent (tan δ) curves of the blend samples

DISCUSSION & CONCLUSIONS: Ternary blend films are expected to have high potential to find uses as active food packaging, hemodialysis membrane and artificial skin materials.

REFERENCES: [1] J. Li et al. (2010) *Carbohydr Polym.*, 79, 786–791. [2] JR Barone and M Medynets (2007) *Carbohydr Polym., 69*, 554–561. [3] A. Poli et al. (2009) *Carbohydr Polym*, 78, 651.

ACKNOWLEDGEMENTS: This study was supported by TUBITAK (111M232) and Marmara Univ. Research Fund (FEN-C-DRP-030912-0306).

Photochemical modification of collagen and silk fibroin films for potential biomedical applications

A Sionkowska[1], S Lazare[2]

[1] *Faculty of Chemistry, Nicolaus Copernicus University, Torun, Poland* [2] *Institut des Sciences Moléculaires (ISM) UMR, University Bordeaux 1, France*

INTRODUCTION: Silk fibroin is a biopolymer spun into fibers by some arthropods such as spiders. Pure silk fibroin is biocompatible, can degrade slowly *in vivo*, supports attachment and proliferation of many cells and supports osteoblastic differentiation. Collagen is a most abundant protein in animals. It is the main protein of connective tissue and the main component of the skin. As an extracellular matrix protein it is widely used as a biomaterial for tissue regeneration and implantation. Both, collagen and silk fibroin can be processed into films and scaffolds to improve tissue regeneration in skin, nerve, bone and cartilage [1,2]. During UV-irradiation of biopolymers, the excited molecules can be formed in the first stage, and then the secondary processes such as chain scission, cross-linking, and oxidation take place [3]. Such photochemical reactions may lead to surface modification of thin biopolymer films. In the present work the modification of the surface of collagen films and silk fibroin films by UV-irradiation is presented.

METHODS: Collagen was obtained in our laboratory from tail tendons of young albino rats. After washing in distilled water the tendons were dissolved in 0.4M acetic acid solution. Silk fibroin was dissolved in organic solvent and thin films were obtained by solution casting method. The surface properties of biopolymer films after KrF excimer laser irradiation (λ = 248 nm) were investigated by scanning electron microscopy (SEM) and optical microscopy.

RESULTS: After UV-irradiation of collagen films and silk fibroin films several alterations can be observed. For films treated with KrF excimer laser emitting radiation with λ = 248 nm these alterations are rather big. In Fig. 1 one can see the surface of silk fibroin film after treatment by laser light. The contact angle measurements and values of surface free energy showed that the wettability of biopolymer films was changed by UV irradiation. The increase of polarity of samples indicates an efficient photooxidation on the surface upon UV irradiation.

The laser irradiation of the used specimens caused an expansion of materials above their surface with pronounced symptoms of its melting. Laser treatment of collagen films and silk fibroin films led to formation of a three dimensional polymer "micro-foam" structure with interconnected pores.

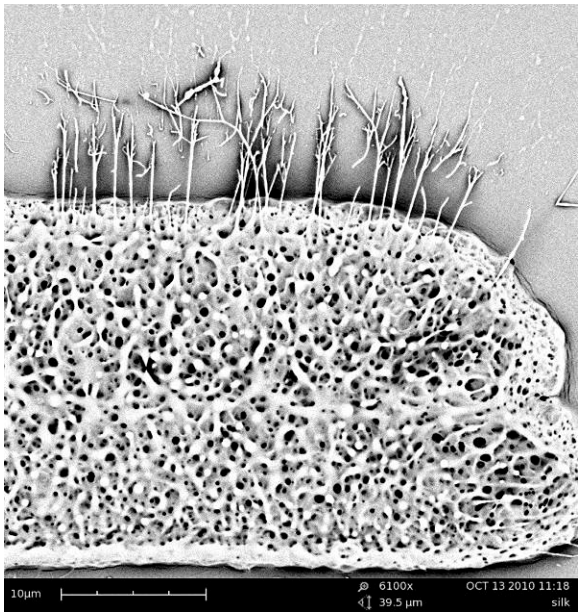

Fig. 1: SEM image of silk fibroin film after ns laser irradiation (energy fluence was 1,1J/cm^2)

DISCUSSION & CONCLUSIONS: The laser irradiation of biopolymer films can be considered as clean technique for their surface modification. Modified biopolymer surface due to the presence of interconnecting pores can be more biocompatible and can be easy for proliferation by living cells.

REFERENCES: [1] M.Vert (2007) Prog. Polym. Sci. **32**: 755-761. [2]A. Sionkowska (2011) Prog. Polym. Sci. **36**: 1254. [3] S. Lazare, A. Sionkowska, A. Planecka, M. Zaborowicz, A. Planecka, J. Lopez, M. Dijoux, C. Loumena, N-C. Hernandez (2012) Appl. Phys. A, 2012; **106**: 67

ACKNOWLEDGEMENTS: Financial support from the Rector of Nicolaus Copernicus University Grant is gratefully acknowledged.

Comparison of extracellular matrix proteins on the cellular response after covalent immobilization onto titanium using plasma polymerized allylamine

M Heller[1,3], PW Kämmerer [3], J Brieger[3], B Al-Nawas[3], R Förch[1,2]

[1]Max Planck Institute for Polymer Research, Mainz, Germany. [2]IMM Institut für Mikrotechnik Mainz, Mainz, Germany. [3]Universitätsmedizin der Johannes Gutenberg Universität, Mainz, Germany.

INTRODUCTION: Biomimetic surface modifications of biomaterials are a promising approach to stimulate cellular behavior such as adhesion, proliferation and differentiation, which is particularly important for the osseointegration of different medical implants [1]. In the current study the extracellular matrix (ECM) proteins collagen and laminin were immobilized covalently onto titanium via the linker molecules α, ω-bis-*N*-hydroxysuccinimide polyethylene glycol. The Ti surface was previously preconditioned with a thin layer of plasma polymerized allylamine. The modified surfaces were seen to stimulate the adhesion of human umbilical cord endothelial cells (HUVECs) and human osteoblasts (HOBs).

METHODS: *Materials:* Titanium samples (Alfa Aesar, 99.7 % purity, area 1 cm²) were serial sanded, acid etched and oxidized to eliminate contaminations from the manufacturing steps. Chemicals and Collagen (Sigma-Aldrich), Laminin (Santa Cruz Biotechnology); HUVECs were isolated from umbilical cords using a standard protocol and HOBs were purchased from Promocell. *Plasma polymerization* of allylamine (pp-AA) was carried out for 5 minutes using a monomer pressure of 0.1 mbar and an input power of 100 W. *Immobilization of ECM proteins* was conducted in two steps. First the cross-linker was incubated for 15 minutes using a concentration of 5% (w/v) in PBS pH 7.4. Afterwards collagen or laminin were incubated for 1 h using a concentration of 500 µg/ml in PBS. *Cell experiments* were performed in triplicate seeding 50000 cells on each sample and analyzing cell adhesion after 1and 3 days using calcein staining. Percentage of cell coverage was analyzed using ImageJ (NIH, Bethestha, USA).

RESULTS: Cell adhesion (Fig. 1) on collagen modified titanium is distinctly enhanced in the case of HUVECs and HOBs at all investigation times compared to the titanium control. On laminin modified samples HUVECs did not show improved cell adhesion, whereas HOBs reveal a strong enhancement of cell adhesion compared to non-modified titanium. The values of the percentage of cell coverage (Table 1) correspond to the results of Figure 1.

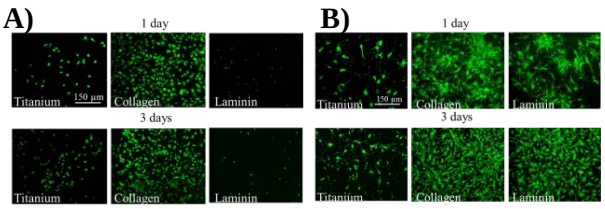

Fig 1: Cell adhesion of A) HUVECs and B) HOBs on collagen and laminin modified titanium after 1 and 3 days.

Cell type	time [days]	titanium [%]	collagen [%]	laminin [%]
HUVECs	1	4.0	48.1	0.8
	3	8.8	35.2	0.5
HOBs	1	8.5	66.2	40.4
	3	33.4	82.6	71.1

Table 1: Percentage of cell coverage on modified and non-modified titanium.

Cell adhesion to extracellular matrix is integrin mediated. The binding specificity of these cell surface receptors depends on the combination of α and β subunits of different integrin molecules [2]. Different integrin classes are responsible for the interaction with the RGD-peptide containing collagen or to laminin, suggesting that HUVECs used in this work do not express laminin-binding integrins and can therefore not interact with the laminin molecules on the surface. HOBs seem to express both, RGD and laminin binding integrin receptors, thats why cell adhesion is enhanced on both modified samples.

CONCLUSIONS: It was possible to selectively influence the adhesion of HUVECs and HOBs on modified Ti surfaces, by offering surfaces decorated with different ECM proteins via covalent bonds. The results suggest that laminin-binding integrins are absent (or of low density) in the currently used HUVECs.

REFERENCES: [1] P.W. Kämmerer & M. Heller et al (2011) *Eur Cell Mater* **21:**364-72. [2] R.O. Hynes (2002) *Cell* **110:**673-87.

ACKNOWLEDGEMENT: Max Planck Graduate Center mit der Johannes Gutenberg Universität Mainz.

Grafting of dextran copolymers for a long-term stable stent coating

EC Michel[1,2], V Montaño[1,3], P Chevallier[2], A Labbé-Barrère[1], D Letourneur[1], D Mantovani[2]

[1] *Lab. for Biomaterials and Bioengineering (CRC-I), Dept. Min-Met-Materials Eng. & University Hospital Research Center, Laval University, Quebec City, Canada* [2] *INSERM U698, Laboratoire de Bio-ingénierie de Polymères Cardiovasculaires, Université Paris 13, France* [3] *ERRMECe, Dept. of Biology, University of Cergy-Pontoise, France*

INTRODUCTION: Metallic intravascular stents are medical scaffolds commonly used as mechanical support for diseased arteries. Nevertheless, complications remain and different proactive coatings, which are however prone to delamination after stent deployment, are investigated. Thus, the aim of this project is to covalently graft a dextran-polybutylmethacrylate copolymer, which has already demonstrated interesting results towards cell proliferation [1], on a stainless steel (SS) substrate previously coated by a plasma-deposited fluorocarbon film (CF_x). In order to covalently graft the copolymer on substrates, dextran was activated by carboxymethylation reaction (CMD) prior copolymerization [2]. This last reaction should be well controlled in order to optimize the grafting on plasma-aminated CF_x-SS substrates without losing the biological activity of dextran. Consequently, different substitution degrees (SD) of dextran were used, then the activation and grafting steps were fully characterized and the biological properties were investigated with blood contact and cells adhesion tests.

METHODS: CMD synthesis is previously described [2]. Three different CMD, using dextran 70 000 g/mol, were synthesized with SD of 0.2, 0.4 and 1. To graft polymers, CF_x-SS substrates were immersed in 2 mg/mL aqueous CMD solutions along with 1-ethyl-3-(3-dimethylaminopropyl) carbodiimide and N-hydroxysuccinimide overnight and vigorously rinsed with 1M NaCl and deionized water. ^{1}H NMR, FTIR, X-ray photoelectron spectroscopy and contact angle analyses were used to characterize CMD polymers. To perform biological tests, polymers were grafted to PTFE films as model of CF_x coating. Coagulation time of samples was studied using the hemoglobin free methodology and cells adhesion tests were carried with endothelial cells (EC) and smooth muscle cells (SMC).

RESULTS & DISCUSSION: Dextran activation was confirmed by IR peak at 1690 cm^{-1} (C=O of carboxyl moieties) and ^{1}H NMR peaks between 4.0-4.2 ppm from CH_2-COOH. Regardless the CMDs, their grafting efficiency were confirmed by XPS results: decrease of fluorine concentration and an increase in oxygen component. The hydrophilic character provided by CMD grafting had therefore an influence on cells adhesion as well as on the clotting time compared to unmodified Teflon film. Indeed, EC adhesion was significantly improved on CMD0.2-Teflon (Fig. 1) and the maximum effect on coagulation time was reached after 40 min. In opposite, whatever the CMD substitution degree, poor SMC adhesion was observed.

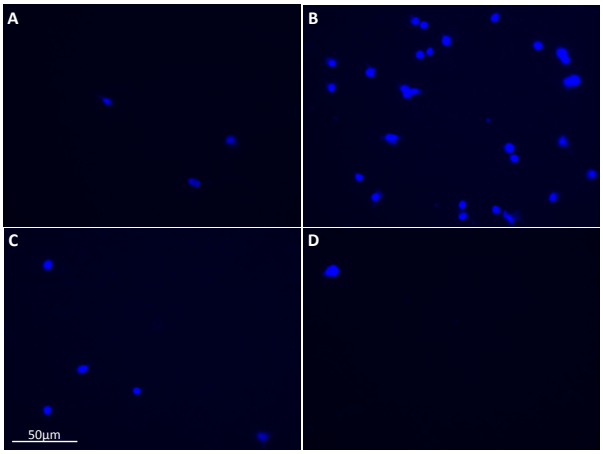

Fig. 1: Adhesion tests of EC on PTFE films: a) uncoated and grafted with b) CMD 0.2, c) CMD 0.4, d) CMD 1.

CONCLUSIONS: These preliminary results exhibited that low modified dextran keeps its biological activity when grafted on surfaces. Therefore, CMD-PBMA copolymers with low CMD substitution degree will be synthesized and grafted on substrates, and then fully characterized towards coating stability and biological activity.

REFERENCES: [1]S. M. Derkaoui, A. Labbé, P. Chevallier et al (2012) *Acta Biomateriala* **8**:3509-15. [2] E.C. Michel, P. Chevallier, A. Barrère et al (2011) *Adv. Mat. Res.* **409**:164-9.

ACKNOWLEDGEMENTS: This work was supported by Inserm-FRSQ, the Quebec Ministry for International Relations, the CFQCU and the Research Center of University hospital.

Self-assembly of fatty acids on hydroxylated aluminum surface: Nanoscale organization and effect on protein adsorption

I Liascukiene[1], SJ Asadauskas[1], N Aissaoui[2], JF Lambert[2], J Landoulsi[2]

[1] *Center for Physical Sciences and Tecnology, Institute of Chemistry, A. Gostauto 9, LT-01108 Vilnius, Lithuania* [2] *Laboratory of surface Reactivity, University of Pierre & Marie Curie, – Paris VI, 4 Place Jussieu, Case 178, 75252 Paris cedex 05, France.*

INTRODUCTION: Fatty acids (FA) are among lipids that have attracted much interest in studies dealing with the adsorption of biomolecules and their behavior at interfaces (self-assembly, organization, etc). The mechanism by which FA interact with surfaces has been described in many reports, revealing the ability of these molecules to attach to oxide surfaces through their carboxylate head groups. In a previous study [1], we have shown that the self-assembly of oleic acid and linoleic acid on a superficially hydroxylated aluminum surface led to the formation of ordered nanostructures. In the present study, we investigate the stability of self-assembled FA layers in a variety of media with biological interest and the adsorption behavior of plasmatic proteins on this nanostructured surface.

METHODS: A variety of FA, differing by either the length of the alkyl chain or the level of unsaturation, was adsorbed on hydroxylated aluminum substrate. The stability of the self-assembled layers was examined in air and in aqueous media. The adsorption of human serum albumin (HSA) and fibrinogen (Fg) was performed on FA-modified aluminum substrate at room temperature and at 37°C. The surface was characterized by PM-IRRAS and water contact angle (WCA). AFM was also used to record high resolution images in view of probing the nanoscale organization of the surface and the subsequent protein adsorption.

RESULTS: PM-IRRAS results showed that the self-assembly of FA on the hydroxylated aluminum surface occurs through the formation of coordinative bonded carboxylate species and WCA angles displayed values around 120°, indicating a clear hydrophobic character of the surface. Conditioning FA-modified surface in different media greatly influenced the surface wettability and the nanoscale organization as evidenced by WCA measurements (Table 1) and AFM images (Fig.1), respectively. The adsorption of HSA and Fg was performed on the FA-modified surfaces at different concentrations, indicating noticeable differences in their behavior.

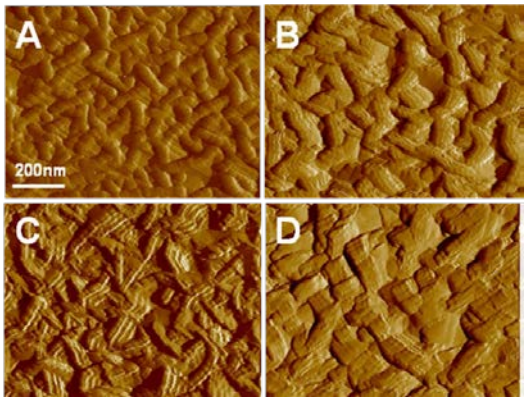

Fig. 1: AFM images of hydroxylated aluminum surface before (A) and after the adsorption of oleic acid (B) and further conditioning in H_2O (C) or PBS (D) for 24 h.

Table 1. Water contact angle values of oleic acid-modified aluminum surfaces after conditioning for 24h in different media

Conditioning media	Water contact angle (°)
Air	132.5(±2.49)
H_2O	103.5(±2.73)
H_2O_2 (10 mM)	103.1(±5.16)
NaCl (3.5 %)	81.9(±1.38)
PBS	bdl

DISCUSSION & CONCLUSIONS: FA interact strongly with the hydroxylated aluminum through their deprotonated carboxylic acid head groups. We observed formation of highly regular lines on the surface, presumably due to the self-assembly and self-organization of the FA molecules. Conditioning these self-assembled layers in different media provided a better understanding of the surface-FA interactions. The obtained surfaces were used to investigate the behavior of proteins on nanoscale organized surface.

REFERENCES: [1]I. Liascukiene, N. Aissaoui, S. J. Asadauskas, et al (2012) *Langmuir* **28**:5116-24.

Effect of protein grafting on the hydrolytic degradation of lactide and caprolactone based biodegradable elastomeric terpolymer

A Larrañaga[1,2], AA Guay-Bégin[2], P Chevallier[2], G Sabbatier[2], J Fernández[1], G Laroche[2], JR Sarasua[1]

[1] Department of Mining-Metallurgy Engineering and Materials Science, University of the Basque Country (UPV/EHU) & BERC POLYMAT, Bilbao, Spain. [2] Centre de recherche du CHUQ, Hôpital Saint-François d´Assise, Quebec, Canada. jr.sarasua@ehu.es

INTRODUCTION: Thermoplastic biodegradable polymers displaying an elastomeric behavior and mechanical consistency are greatly appreciated for the regeneration of soft tissues and for various medical devices [1,2]. However, while the selection of a suitable base material is determined by mechanical and biodegradation considerations, there are the surface properties of the biomaterial that are responsible for the biological response [3, 4]. In this work bovine serum albumin (BSA) was covalently grafted on the surface of a biodegradable terpolymer composed of ε-caprolactone (CL), D-lactide (D-LA) and L-lactide (L-LA) (PLCL). Finally, the effect of surface modification on the hydrolytic degradation of the material was investigated for a period up to 63 days.

METHODS: As illustrated in Figure 1, amino functionalities were introduced on the surface of polymer films by an atmospheric plasma treatment under N_2+H_2 discharge. Plasma treated samples were then submerged in phosphate buffered saline (PBS) (pH=7.4) containing 2-3 mg mL^{-1} of sulfo-SMPB (sulfosuccinimidyl-4-(p-maleimidophenyl) butyrate) for 2 h at 4ºC. After grafting, films were washed with PBS and subsequently submerged in a BSA solution to covalently attach this protein to the surface of the biodegradable terpolymer. The modified surface was characterized by means of X-ray Photoelectron Spectroscopy (XPS), static contact angle measurements and atomic force microscopy (AFM). Finally, a hydrolytic degradation study of pristine terpolymer (PLCL), plasma modified PLCL (P-PLCL) and albumin grafted PLCL (BSA-PLCL) in phosphate-buffered saline (PBS) at 37ºC was carried out for a period up to 63 days. The changes in water absorption, weight loss, crystallinity, phase structure and molecular weight of the samples were studied using differential scanning calorimetry (DSC), gel permeation chromatography (GPC) and weight measurements.

RESULTS: According to XPS, AFM and static contact angle measurements, BSA was satisfactorily immobilized on the surface of the terpolymer, being the degree of albumin surface coverage (Γ_{BSA}) ~35%.

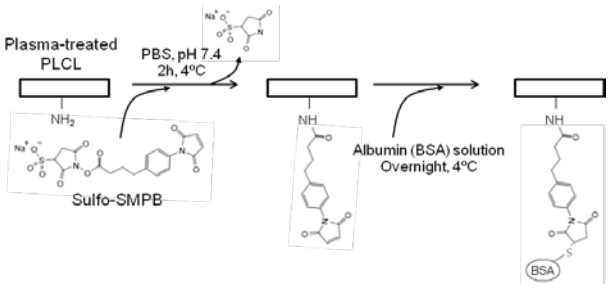

Fig. 1: Schematic representation of the covalent grafting of BSA on the surface of plasma-treated biodegradable terpolymer.

The presence of albumin on the surface of the terpolymer clearly affected the hydrolytic degradation behaviour. As an illustration, after 28 days submerged in PBS, the molecular weight of the non-treated sample decreased from an initial molecular weight of $101.6x10^3$ to $30.2x10^3$ g mol^{-1}, whereas the albumin grafted sample reached a value of $46.6\ x10^3$ g mol^{-1}.

DISCUSSION & CONCLUSIONS: In this work a procedure to covalently bond biologically active molecules to the surface of biodegradable polymers is presented. The presence of these molecules clearly affected the degradation behavior of the polymer.

REFERENCES: [1]S. François, N. Chafké, B. Durand, G. Laroche (2009) *Acta Biomaterialia* **5**:2418-28. [2]R. Sartoneva, S. Haimi, S. Miettinen et al. (2011) *Journal of the Royal Society Interface* **8**:671-77. [3]K. Valliéres, E. Petitclerc, G. Laroche (2007) *Macromolecular Bioscience* **7**:738-45.[4] M. Crombez, P. Chevallier, R.C. Gaudreault et al. (2005) *Biomaterials* **26**: 7402-09.

ACKNOWLEDGEMENTS: A. L. acknowledges a research mobility grant from UPV/EHU.

Mechanism of interaction of oligopeptides with copper surfaces: Sticking versus strapping

J Landoulsi[1], A Berquand[2], C Méthivier[1], CM Pradier[1]

[1] *Laboratory of surface Reactivity, University of Pierre & Marie Curie, – Paris VI, France* [2] *Bruker Nano GmbH, Dynamostrasse, Germany*

INTRODUCTION: Oligopeptides are increasingly recognized as relevant biomolecules for the modification of solid surfaces in the fields of biomaterials, including for biosensing, drug delivery systems, implantings, etc. This is due to the ability of peptides to have specific affinities with various materials. However, the mechanism by which peptides are able to be anchored directly on the surface remains not well understood.

METHODS: The interaction of Gly-Pro-Glu and Gly-Cys-Glu peptides on copper surface was monitored *in situ* using QCM-D and electrochemical tests. The adsorbed phase was then characterized either in the dried state using PM-IRRAS and XPS, or in the hydrated state using AFM. In addition to topographical features, AFM was used for probing nanomechanical properties of the adlayer formed in the presence of Gly-Cys-Glu peptide. For this purpose, we used a mode, recently developed, which allows a direct mapping of a variety of surface properties, including stiffness and adhesion, to be probed simultaneously with topographical images.[1-2]

RESULTS: The adsorption of Gly-Cys-Glu was evidenced by both XPS (significant increase of nitrogen molar concentration and presence of sulphur) and PM-IRRAS analyses (appearance of amide bands characteristic of peptidic links). By contrast, the presence of Gly-Pro-Glu on the copper surface could not be detected. AFM images showed that the surface was kept almost unchanged after the adsorption of Gly-Pro-Glu (Fig. 1A), while a noticeable modification with Gly-Pro-Glu peptide was observed (Fig.1B), revealing the formation of dense and closely packed nanoparticles with fairly regular size (height ~ 8 nm). *In situ* QCM-D monitoring unexpected behaviour, suggesting layer dissolution in one case (Fig. 1C) and a mass deposition in the other case (Fig. 1D). These results are in agreement with electrochemical tests performed under open circuit conditions. Furthermore, under electrochemical control, it appears that the adsorption behavior of peptides is influenced by the applied potential values.

Nanomechanical properties of the Gly-Cys-Pro peptide adlayer were probed at the same time as imaging, by means of peak force tapping, as detailed elsewhere.[1] Results showed that the presence of the peptide adlayer decreases noticeably the stiffness of the surface (DMT Young's modulus ~106 GPa on bare copper compared to 0.06 GPa in the presence of the adsorbed Gly-Cys-Glu peptide).

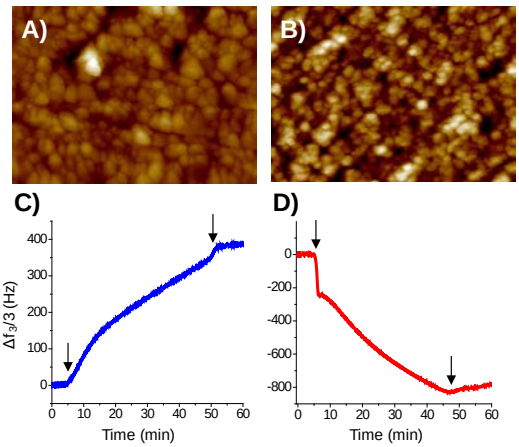

Fig. 1: (A-B) AFM height images recorded (A) prior to and (B) after the adsorption of Gly-Cys-Glu. (C-D) Frequency shifts recorded upon interaction of (A) Gly-Pro-Glu and (D)Gly-Cys-Glu.

DISCUSSION & CONCLUSIONS: All these findings evidenced that though both peptides strongly interact with the copper surface, the mechanism of interaction is radically different. Gly-Pro-Glu did not adsorb on the copper surface; it rather likely forms a "soluble peptide-copper complex" thus enhancing the dissolution rate of copper ions. By contrast, Gly-Cys-Glu formed an adlayer through a strong interaction between thiol groups, originating from cystein, and copper atoms, as evidenced by electrochemical measurements. The composition and the nanomechanical properties of the adlayer suggest the formation of an "insoluble peptide-copper complex" which remains stable on the surface.

REFERENCES: [1] J. Landoulsi, V. Dupres (2013) *PCCP* **15**, 8429. [2] J. Adamcik, A. Berquand et al (2011) *App Phys Lett* **98**: 193701.

Copper biosorption on immobilized *Saccharomyces cerevisiae* biomass

F Di Caprio[1], P Altimari[1], D Uccelletti[2], F Pagnanelli[1], L Toro[1]

[1]Dipartimento di Chimica, Università "Sapienza" di Roma, Roma, Italia. [2]Dipartimento Biologia e Biotecnologie "C. Darwin", Università "Sapienza" di Roma, Roma, Italia

INTRODUCTION: Biosorption represents a competitive technological alternative for heavy metal removal. This technique exploits the property of certain bio-molecules (or types of biomass) to bind and concentrate selected ions or other molecules from aqueous solutions[1]. The main advantage of biosorption, compared to traditional sorption techniques, is the application of an inexpensive adsorbing material. The scarce mechanical strength and the difficulties of separation from liquid make however, impractical the direct large scale application of non-living biomasses. Immobilization of the biomass within mechanically stable matrices is needed in industrial practice. The choice of the immobilization matrix is of fundamental importance as it determines not only the mechanical stability but also the possibility of the immobilized biomass to participate in the heavy metal removal. In this contribution, the biosorption of copper onto a non-living *Saccharomyces cerevisiae* wild strain biomass immobilized in calcium alginate matrices is investigated.

METHODS: Beads of calcium alginate with immobilized biomass were obtained by dropping a biomass suspension (biomass concentration of 0.2 g/ml) with sodium alginate (3% w/v) into a solution of $CaCl_2$ (20% w/w). Dropping was performed by a peristaltic pump at flow rate of 1.56 ml/min. Beads of calcium alginate without biomass were also prepared by dropping a sodium alginate solution (3% w/v) into $CaCl_2$ (20% w/w) solution. To characterize biosorption kinetics, batch tests were performed under magnetic stirring with 0.35 g of beads added to 80 ml of copper solution. Initial copper concentration of 50 and 150 ppm were considered. Biosorption isotherms were determined by performing batch tests with initial copper concentration ranging between 10 and 120 mg/L at pH=4 and pH=6. For this purpose, the pH was periodically corrected during the test by addition of NaOH or HCl.

RESULTS: Results of the analysis of biosorption kinetics are displayed in Fig. 1. To assess sustainability, the evolution of adsorbed copper for amount of calcium alginate composing the employed beads is reported. The main cost is indeed determined by calcium alginate while biomass can be collected at zero or even negative cost. For sake of clarity, only data corresponding to initial copper concentration $C_{0,Cu}$=50 ppm are shown.

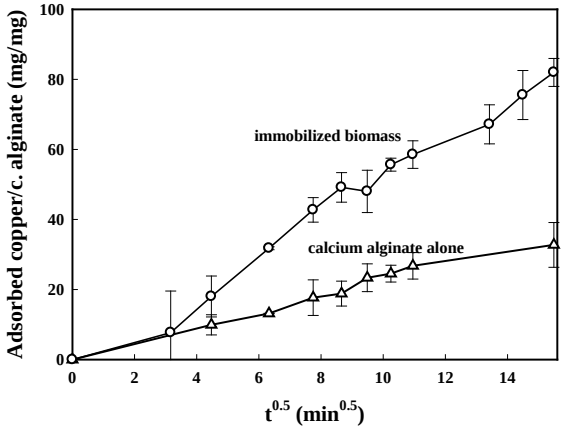

Fig. 1: Evolution of adsorbed copper onto beads of calcium alginate ($C_{0,Cu}$=50 ppm).

Analysis of equilibrium isotherms (not shown) evidenced that the biosorption capacity of beads with immobilized biomass at copper concentration around 30 ppm was 42 and 31 mg/g at pH=4 and pH=6 respectively.

DISCUSSION & CONCLUSIONS: It is apparent from Fig. 1 that biomass immobilization can largely reduce the amount of employed calcium alginate thus leading to significant cost savings. The analysis of biosorption kinetics also evidences that the dependence of the adsorbed metal on the square root of time does not follow a linear path revealing the emergence of an anomalous diffusion. A two-stage sorption behaviour is in particular found evidencing a significant influence of swelling on biosorption kinetics. Accounting for this mechanism is fundamental for mathematical modelling of biosorption columns realized through beads packing. Finally, we note that increasing pH leads to a growth in biosorption capacity evidencing a significant influence of ionic exchange mechanisms on biosorption.

REFERENCES: [1]J. Wang, C. Chen (2006) *Biotechnology Advances*, 24 427–451.

Conformation of bovine submaxillary mucin on hydrophobic surface

KI Pakkanen, JB Madsen, S Lee

Department of Mechanical Engineering, Technical University of Denmark, DK-2800, Kgs. Lyngby, Denmark

INTRODUCTION: Mucins form a large family of high-molecular weight glycoproteins that protect and hydrate the interface between tissues and the exterior environment [1]. The general mucin structure of non-glycosylated C- and N-termini and a highly glycosylated mid-part has inspired mucins to be paralleled with co-block polymers and this has led to a somewhat simplistic interpretation of mucin interactions with surfaces [2,3]. Biologically, however, mucins are not simple amphiphilic copolymers. Their conformation at the interface of water/hydrophobic surface is likely to be much more complex and heterogeneous than pictured in this simplistic view. There is therefore need for more refined understanding on the conformation of mucins on surfaces. We have in this study used ligand-specific biomolecular probes to study the surface interactions of bovine submaxillary mucin (BSM).

METHODS: Plate assays were performed on 96-well plates with hydrophobic surface (Brand, Wertheim, Germany). BSM (Sigma Aldrich, St. Louis, MO; purified as described in [4]) was let to spontaneously adsorb to the well surfaces. BSM conformation on the surface was analyzed with enzyme-linked immuno and lectin assays. A C-terminus specific Anti-MUC19 (Abcam, Cambridge, UK) was used in the immuno assay and wheat germ agglutinin (WGA; Sigma Aldrich) and peanut agglutinin (PNA; Sigma Aldrich) in the lectin assays. Protein concentration on the surface was tested with a BCA assay (Sigma Aldrich). Bulk conformation of BSM was studied using circular dichroism spectroscopy (Chirascan, Applied Photophysics Ltd, Surrey, UK) and size distribution using dynamic light scattering (Malvern Instruments Ltd, Worcestershire, UK).

RESULTS: While the amount of BSM on the well surfaces increased proportionally to the amount of BSM in the bulk solution, the anti-BSM (MUC19) showed a drastic variation in binding to BSM as a function of BSM concentration on the surface. Similar non-linear response to BSM concentration was also seen with WGA lectin assay but not with PNA lectin assay. Sodium chloride was found to influence the accessibility of WGA binding sites in BSM, but not PNA binding sites. Bulk BSM concentration had also an influence on BSM conformation; with an increasing concentration, a spectral shift towards more random conformation was observed.

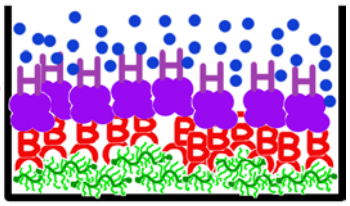

Fig. 1: Schematic presentation of the plate assays used for studying BSM on the microtiter well surface. Green: BSM, red: biotinylated lectin or antibody, streptavidin-conjugated HRP, blue: substrate for HRP.

DISCUSSION & CONCLUSIONS: The non-linear response of the antibody-based immuno assay suggests the C-termini of BSM to become less accessible for binding as the surface concentration of BSM is increased. Similarly, availability of WGA binding sites is decreasing by increasing BSM surface concentration, indicating concentration-dependent changes in BSM conformation on the surface. Effect of sodium chloride on availability of WGA but not PNA binding sites on surface-bound BSM indicates that electrostatic forces have an effect on concentration-conformation relationship of BSM. We suggest a model for concentration-dependent conformational changes of BSM both in bulk solution on a hydrophobic surface; in bulk, coiling of BSM molecules tightens as the concentration of BSM is increased. Similarly, at low surface concentrations BSM molecules are free to lie on the surface but at higher surface concentrations they are forced, due to steric and electrostatic repulsion, to curl up in loop-like conformations to facilitate adsorption of more BSM molecules.

REFERENCES: [1]R. Bansil and B.S. Turner. (2006) *Curr Opin Coll Interf Sci* **11**: 164-170. [2]I. M. Kesimer et al. Glycobiol. 18 (2008) 463-472 [3]P. Gniewek et al. (2012) *Biophys. J.* **102**: 195-200. [4]J.B. Madsen et al. (2013) *submitted,*.

ACKNOWLEDGEMENTS: M.A. Hachem and B. Svensson (Technical University of Denmark).

Bioactive and photoactive PEI hydrogels as platforms for biomolecule immobilization

A Paciello[1], AM Cusano[1], MG Santonicola[1,2]

[1] *Center for Advanced Biomaterials for Healthcare@CRIB, Istituto Italiano di Tecnologia, Italy*
[2] *Materials Science and Technology of Polymers, MESA+ Institute for Nanotechnology, University of Twente, The Netherlands*

INTRODUCTION: The objective of this research was to design a versatile hydrogel material for binding and release of plasmid DNA in a controlled manner. Because of their structural and mechanical properties, as well as the large flexibility in the functionalization of the polymer groups, hydrogels based on macromolecules are extensively applied in biomedical research, in particular for tissue engineering and drug delivery [1-2]. Polyethylenimine (PEI) is a cationic polyelectrolyte that contains a large number of secondary and tertiary amines, and has been predominantly used as a non-viral gene carrier due to its ability to form stable complexes with nucleic acids in solutions [3]. Here we investigate a pH-sensitive hydrogel based on PEI where plasmid DNA can bind in a reversible way.

METHODS: Hydrogels were prepared from partial methacrylation of branched PEI in dichloromethane at room temperature under inert atmosphere. After synthesis, the hydrogel material was purified by dialysis with several cycles against pure water and ethanol. The modified macromolecules were characterized by NMR spectroscopy using a Varian Unity INOVA 700-MHz spectrometer, and by FTIR spectroscopy in ATR mode using a Nicolet 6700 instrument (Thermo Scientific). The hydrogel morphology in liquid environment was investigated by small-angle X-ray scattering and confocal laser scanning microscopy (Leica TCS SP5). DNA entrapment and elution experiments were performed using a modified pUC18 plasmid.

RESULTS: Following hydration, the modified PEI macromolecules self-assemble to form a supramolecular network that can retain up to 95% of water. We investigated the micro-structure of the hydrogels prepared at different reaction conditions by several techniques, including fluorescence microscopy (*Fig. 1*), showing how the gel swelling and DNA binding properties can be controlled during synthesis by the amount of functional groups on the polymer backbone. The supramolecular PEI hydrogels could reversibly bind plasmid DNA up to 14 μg per mg of dry material. After elution from the hydrogel upon pH variation, the plasmid DNA maintained its integrity as assessed by agarose gel electrophoresis. As additional feature, during multi-photon microscopy experiments we found that the PEI-based hydrogels were easily activated by laser irradiation, and could be patterned when embedded in solutions with probes having free hydroxyl groups.

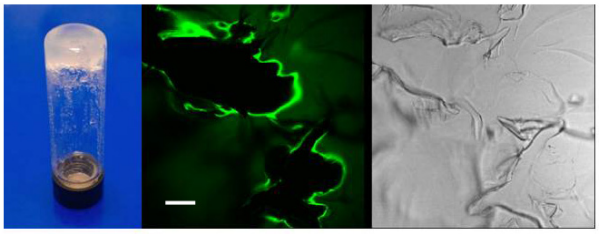

Fig. 1: PEI-based hydrogel after swelling in water overnight (left) and characterization of the porous hydrogel microstructure by confocal fluorescence microscopy and white light transmission (right). Scale bar is 100 μm.

DISCUSSION & CONCLUSIONS: In this work a supramolecular hydrogel based on the chemical modification of branched PEI with methacrylate groups is presented. The platform was successfully used for pH-sensitive binding and release of plasmid DNA. At the same time, the hydrogel platform showed interesting photoactive behavior in presence of selected molecular probes. Direct patterning of the hydrogel surface in solutions with hydroxyl-terminated probes was demonstrated in multi-photon microscopy experiments.

REFERENCES: [1]K. Deligkaris, T.S. Tadele, W. Olthuis, A. van den Berg (2010) *Sensors and Actuators B* **147**:765-774. [2]A. S. Hoffman (2002) *Advanced Drug Delivery Reviews* **54**:3-12. [3]D.N. Nguyen, J.J. Green, J.M. Chan, R. Langer, D.G. Anderson (2009) *Advanced Materials* **21**:847-867.

[*]Present address: Department of Chemical Engineering Materials and Environment, Sapienza University of Rome, Italy.

Polymers functionalization: when biomimetic peptides guide different biological effects.

F Boccafoschi, L Fusaro, M Botta, M Ramella, M Cannas

Laboratory of Human Anatomy, Department of Health Sciences, University of Piemonte Orientale "A. Avogadro", 28100 Novara, Italy

INTRODUCTION: In nature, cells respond to a variety of environmental cues, both mechanical or biochemical, leading to changes in cell function and phenotype. Tissues are normally formed by a complex, highly structured extracellular matrix (ECM) consisting largely of collagens, elastin, fibronectin and proteoglycans [1,2]. These molecules are fundamental in maintaining tissue structure (cell synthetic status) but also in guiding cell functions (phenotype expression). In tissue engineering, the biological substitutes can be developed with the help of natural or synthetic materials. In this case, polymeric materials are primarily used, because of the high variability in mechanical, physical and chemical properties. Biodegradable polymers (i.e. PLLA, PCL) are object of the majority of studies, because of the ability to be degraded by the host organism, avoiding late stent thrombosis unlike permanent grafts. In order to improve the material's bioactivity polymers surface was modified by grafted RGD, a fibronectin derived adhesion motif, and SIKVAV, a laminin derived motif [3,4]. Different cell lines have been used in order to verify cell behavior in presence of biomimetic peptides. The use of surface modified polymers should be interesting for different applications in tissue engineering.

METHODS: In order to verify the surface modification, XPS analysis was performed. After seeding, cells viability was confirmed by MTT assay and Proliferation Cell Nuclear Antigen (PCNA). Differentiation markers were analyzed by Western blot and cell morphology was observed by SEM.

RESULTS: Surface characterization, through contact angle measurement showed that water contact angle on hydrolysed and grafted surfaces is lower than control surface contact angle, meaning that modified surfaces are more hydrophilic than polymeric controls. XPS showed, as expected, nitrogen presence on grafted surfaces, due to the presence of grafted peptides. SEM images showed that cells morphology changes significantly in presence of different grafted peptides. These changes are confirmed by the evaluation of the expression of differentiation markers using western blot analyses.

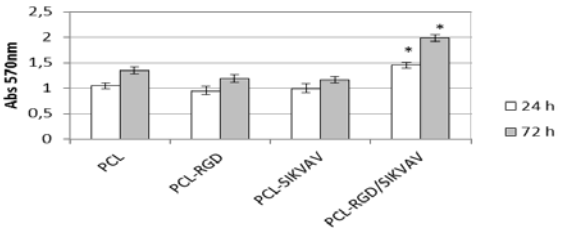

Fig. 1: SKNBE cells viability (MTT test).

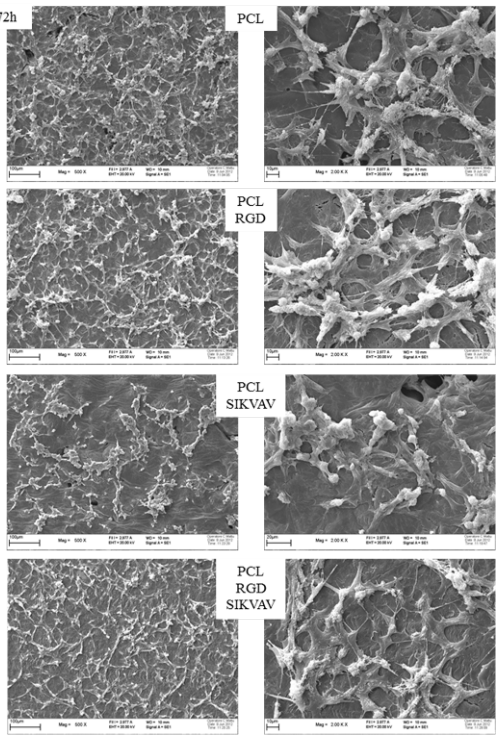

Fig. 2: SKNBE cells morphology (SEM)

DISCUSSION & CONCLUSIONS: These results suggest that bioactive molecules grafting could be useful on polymeric scaffolds for guiding cell phenotype expression, and, to ultimately maintain adequate biological characteristics suitable for the tissue functional regeneration.

REFERENCES: [1]Badylak SF, Freytes DO Gilbert TW (2009). *Acta Biomater. 5: 1-13.* [2]Stegemann JP, Hong H, Nerem RM. *(2005) J Appl Physiol.* 98: 2321-2327. [3]Hersel U, Dahmen C, Kessler H. (2003) *Biomaterials;* 24: 4385-4415. [4]Hill-Bator A, Opolski A. (2002) Postepy Hig Med Dosw. ; 56(5): 579-88.

Porous silicon as a scaffold for rat oral mucosal epithelial cells and transfer to the eye

Y Irani[2], SJP McInnes[1], HM Brereton[2], KA Williams[2], NH Voelcker[1]

[1] Mawson Institute, University of South Australia, Mawson Lakes, SA. [2] Department of Ophthalmology, Flinders University, Flinders Medical Centre, Bedford Park, SA.

INTRODUCTION: Dysfunction of adult corneal stem cells located in the limbus can lead to painful ocular surface disease (OSD) [1]. Transplantation of allogeneic limbal tissue has a poor prognosis. Stem cells expanded *ex vivo* from alternative sources such as autologous oral mucosa [1] require the use of a scaffold material for transfer to the eye. We hypothesised that nanostructured porous silicon (pSi) could be used as a scaffold to transfer oral mucosal epithelial cells (OMECs) to the eye. The biocompatibility of pSi in the eye has been confirmed previously [2]. We explored the ability of thermally oxidised, aminosilanised and collagen IV coated pSi to support rat OMECs. OMECs harvested from male Inbred Sprague-Dawley (ISD) rats were cultured on pSi membranes, characterised for epithelial and stem cell markers, and implanted subconjunctivally into the right eye of female ISD rats. Transplanted cells were detected in samples collected from the ocular surface using FTA paper by a PCR designed to amplify the male-specific *sry* gene.

METHODS: pSi membranes fabricated from n-type phosphorus-doped silicon were the gift of Dr Armando Loni (pSi Medica, UK). Membrane thickness was approximately 145 µm, with a porosity of approximately 70%. Pore sizes at the membrane surface were approximately 40-60 nm in diameter. Membranes were cut to size and thermally oxidised at 600 ^{o}C for 1 h, silanised with 50 mM 3-aminopropyltrimethoxysilane in toluene for 5 min, and washed in succession with methanol, acetone and dichloromethane before being dried in air. The collagen solution (10 µl, 5 mg/mL) was placed on the pSi (approx 1 cm^2) and spread over the surface using the pipette tip. It was then allowed to dry in the laminar flow. It was washed 2x with sterile PBS then allowed to dry completely. The coated pSi was left under UV overnight to sterilize.

RESULTS: The majority of OMECs expressed p63 and CK19 indicating a transient amplifying cell (TAC) phenotype. A population of cells expressed the putative stem cell marker ABCG2. A few differentiated cells expressing CK3 were observed. OMECs on pSi membranes were implanted into rat eyes, without excessive inflammation occurring. The implants remained visible at the operating microscope for 8 weeks. OMECs migrated on to the corneal surface, and were successfully detected by PCR up to 4 weeks post implantation.

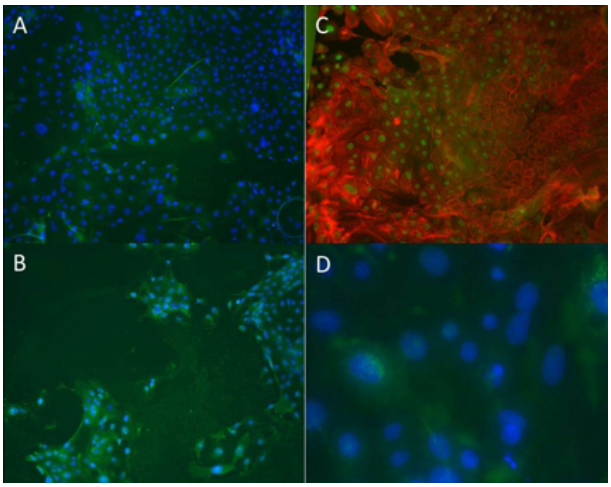

Fig. 1: Characterisation of oral mucosal epithelial cells grown on collagen IV coated pSi ***(A)*** *Superficial epithelial cell marker CK3 (green) cell nuclei (blue);* ***(B)*** *basal epithelial cell marker CK19 (green) cell nuclei (blue);* ***(C)*** *transient amplifying cell marker p63 (green) actin (red)* ***(D)*** *putative stem cells marker ABCG2 (green) cell nuclei (blue). Magnifications: A,B,C 10X & D 40X.*

DISCUSSION & CONCLUSIONS: pSi membranes supported the growth of a mixed population of rat OMECs including stem cells, TACs and terminally differentiated cells. OMECs migrated across the surface of the cornea, after subconjunctival implantation in rats, and were detected up to 4 weeks post implant. Further work is required to assess the ability to repair damage to the cornea in a rodent model of OSD.

REFERENCES: [1]T. Nakamura, T. Inatomi, C. Sotozono, et al (2004). *Br J Ophthalmol* **88**:1280-1284. [2]S.P. Low, N.H. Voelcker, L.T. Canham, et al (2009). *Biomaterials* **30**:2873-2880

Electric fields induced by electric polarization reduce proliferation rates of tumor cell through cell cycle modulation

A Nagai[1], T Hattori[1,2], K Nozaki[1], M Aizawa[2], K Yamashita[1]

[1] *Institute of Biomaterials and Bioengineering, Tokyo Medical and Dental University, Japan*
[2] *School of Science and Technology, Meiji University, Japan*

INTRODUCTION: The living body is subjected and adapted to a lot of stresses, such as environmental changes and physical or chemical stimulations. The electric signals are also utilized to facilitate many biological processes. However, it is difficult the electric stimulation applying on the living cells and evaluating the effects. We have shown that electric polarization treatment on some bioceramics produced electric fields around the material and induced surface charges, 1 and influenced on various cells and tissues.2,3 The polarized ceramic materials can be stored electric energy before examination and large-scale equipment was not needed at the point of use. In this study, we examined the effects of electric energy of polarized ceramics on the cell proliferation.

METHODS: Hydroxyapatite powders were synthesized by wet method, uniaxially pressed into pellets, and sintered. For the polarized specimens, electrical polarization in a d.c. field of 5 $kV \cdot cm^{-1}$ in air at 400 °C for 1 h was treated to the apatite pellets. The surface in contact with the anode and cathode was termed N-surface and P-surface, respectively. Characterization of the specimens was performed by SEM, XRD, FT-IR, and laser scanning microscope. Polarization energy was measured by thermally stimulated depolarization currents.

SK-LMS-1 (SK) cells, uterine leiomyosarcoma cells, were cultured on the specimens with or without polarization. For assessment of cell proliferation rate, MTT assay, TUNEL assay, and RT-PCR was performed. For cell cycle analysis, SK cells stably expressing a part of human Cdt1 fused to monomeric Kusabira-Orange2 (KO2) were prepared using pFucci-G1 Orange (SK-G1). The cells were fixed and stained with DAPI. After imaging, the number of the cells cultured on the specimens was quantified using a software.

RESULTS: The crystal structure, chemical composition, and surface roughness of each specimen did not alter before and after polarization. TSDC measurements revealed that the stored charges in polarized apatite were 3 $\mu C/cm^2$. Cells cultured on the polarized specimens reduced compared to non-polarized specimen in MTT assay. Apoptosis assessment using TUNEL assay and RT-PCR was shown that apoptosis did not cause the decrease of cell proliferation rates. Cdt1-KO2 protein in SK-G1 cells expressed during the G1 phase of the cell cycle. The Cdt1-KO2 expression cells increased on the P-surface and decreased on the N-surface, respectively, compared to the non-polarized surface.

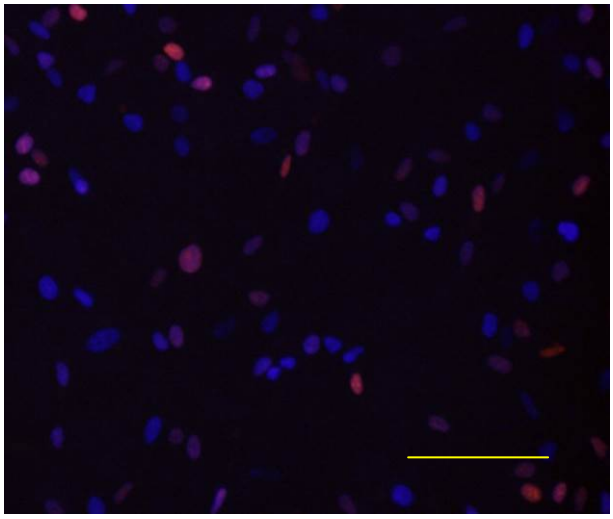

Fig. 1: Images of SK-G1 cells cultured on the non-polarized surface. The bar represents 200 μm.

DISCUSSION & CONCLUSIONS: Electric fields induced by electric polarization influenced to decrease proliferation rates of tumor cells. The decrease of the rates caused by more of change of cell cycle than apoptosis. Although both positive and negative surface charges suppressed cell proliferation, the mechanism seemed to be different.

REFERENCES: [1]K. Yamashita, N. Oikawa, T. Umegaki. (1996) *Chem Mater* **8**:2697-700. [2]S. Bodhak, S. Bose, A. Bandyopadhyay. (2009) *Acta Biomater* **5**:2178-88. [3]A. Nagai, M. Imamura, K. Yamashita, H. Azuma. (2008) *Life Sci* **82**:1162-68.

Enhanced cell response on zirconia by bio-inspired surface modification

YT Liu[1], KC Kung[1], TM Lee[2,3], TS Lui[1]

[1] *Department of Materials Science and Engineering, National Cheng Kung University, Taiwan*
[2] *Institute of Oral Medicine, National Cheng Kung University, Taiwan*
[3] *Medical Devices Innovation Center, National Cheng Kung University, Taiwan*

INTRODUCTION: Thanks to its high mechanical strength and excellent fracture toughness, zirconia is widely used in orthopedic and dental applications [1]. However, zirconia is categorized as a bio-inert material, which restricts its application in the field of biomedicine [2]. Therefore, developing a effective method to enhance its biocompatibility requires further study. The neurotransmitter, L-DOPA, is an important component in the adhesive structure of mussels. Previously, L-DOPA has inspired a versatile approach to surface coating [3]. This study applied an L-DOPA film on a zirconia surface and evaluated the physic-chemical properties and biocompatibility of the resulting film.

METHODS: The zirconia discs (10.6 mm diameter, 2 mm thickness) were immersed in a solution of L-DOPA (2 mg/ml) dissolved in 10 mM Tris-HCl (pH 8.5). Three kinds of experimental material were used in this study: (a) ZrO_2 substrate, (b) ZrO_2 coated with L-DOPA at 22°C (ZL22), and (c) at 37°C (ZL37). The surface chemistry of the specimens were determined through XPS. FBS was used as model proteins to simulate protein adsorption behavior. Human osteoblastic MG63 cells were cultured to evaluate material-cell responses.

RESULTS: The contact angle of the ZrO_2 specimen was 61°. In contrast, the contact angles of the ZL22 and ZL37 specimens were both less than 10°, which indicated that these specimens were hydrophilic and had a high surface energy. The zirconia substrates were successfully coated with a film of L-DOPA and that the N/Zr ratio increased significantly with an increase in temperature as the reaction proceeded (Table 1).

Table 1. Surface elemental compositions of L-DOPA coated surfaces determined by XPS.

	Atomic conc. (%)					
	O1s	N1s	C1s	Zr3d	N/Zr	N/C
ZrO_2	49.2	0.1	29.6	19.0	0.006	0.004
ZL22	29.8	5.2	55.3	9.0	0.579	0.094
ZL37	27.0	6.8	59.4	6.4	1.071	0.115

In Fig. 1(a), the accumulation of adsorbed serum protein corresponded to an increase in L-DOPA content, which implies that L-DOPA film has the ability to adsorb more proteins. Fig. 1(b) shows that L-DOPA film influenced the inceptive spreading of MG63 cells. Active cell-surface contact is sensitive to L-DOPA, which increases spreading and the formation of stable focal adhesions. After day 1-7 of culture, the cell numbers in the ZL22 and ZL37 specimens were significantly higher than that of the ZrO_2 specimen (Fig. 1(c)).

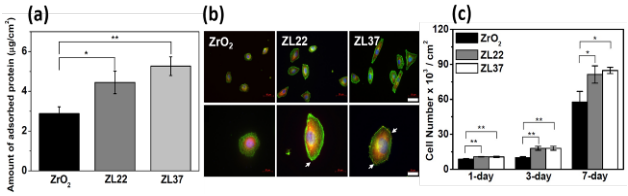

Fig. 1: (a) Serum adsorption onto various surface after 1 hours min incubation. (b) Cytoskeleton of MG63 cultured on various surfaces for 3 hours. (c) Cell proliferation results after 7 days of culture

DISCUSSION & CONCLUSIONS: The bio-inspired L-DOPA film altered the chemical properties of the zirconia surface considerably without affecting its topography. This technique involves the application of a film of L-DOPA via oxidative polymerization [4]. During the process, temperature could be used to control the properties of films. The presence of the preadsorbed proteins plays an important role in mediating cell response. Hence, a dopamine layer could be used to interconnect serum proteins and modulate cell attachment that greatly improves osteoblast responses.

REFERENCES: [1]ED. Rekow et al (2011) *J Dent Res* **90**:937-952. [2]L. Hao et al (2005) *J Mater Sci-Mater M* **16**:719-726. [3]H. Lee et al (2007) *Science* **318**:426-430. [4]D.R. Dreyer et al (2012) *Langmuir* **28**:6428-35.

ACKNOWLEDGEMENTS: This work was financially supported by the National Science Council, Taiwan (NSC 100-2221-E-006-263)

Electrospun scaffolds as a versatile controlled release platform to induce osteogenic differentiation of mesenchymal stem cells

K Göeken[1], C Ricci[2,] D D'Alessandro[2], L Trombi[3], S Berrettini[2], CA van Blitterswijk[1], S Danti[2], L Moroni[1]

[1] Tissue Regeneration Dept., University of Twente, Enschede, The Netherlands [2] Dept. of Surgical, Medical and Molecular Pathology and Emergency Medicine, University of Pisa, Pisa, Italy
[3]Dept. of Internal Medicine, University of Pisa, Pisa, Italy

INTRODUCTION: Electrospinning (ESP) is a fabrication technique that has gathered recent attention in the tissue engineering community. ESP fibers provide the scaffolds with a 3D filamentous architecture, hypothesized to mimic the natural extracellular matrix environment. ESP polymer processing occurs by solvent dissolution, facilitating the incorporation and release of active drugs [1]. In these settings, beaded fibers, which are normally considered as defects in the ESP scaffold fabrication process, could be used as drug reservoirs. Among active drugs, dexamethasone (Dex) is known to play a stimulatory effect on mesenchymal stem cell (MSC) differentiation (e.g., towards adipogenic, chondrogenic and osteogenic lineages) in a concentration-dependent manner [2]. In this study, ESP is used to create a tissue engineering platform for the controlled release of Dex.

METHODS: Polycaprolacton (PCL) and poly(lactic-co-glycolic acid) (PLGA) were used to fabricate scaffolds via ESP. Dex was added to the polymer/solvent solution at 0.1, 0.25 and 0.5% (w/w Dex/Polymer). Characterization of scaffold morphology was performed via scanning electron microscope (SEM). Dex-loaded scaffolds underwent release studies by spectrophotometry, intra-fiber distribution analysis by confocal microscope-assisted Raman spectroscopy, and energy dispersive X-ray spectroscopy. Bone marrow-derived human MSCs (hMSCs) were cultured in basic (α-MEM, 10% FBS, 0.2 mM ascorbic acid, 2 mM L-glutamin and antibiotics) or osteogenic (basic medium + 10 nM Dex) medium, on *(i)* polystyrene (PS) flasks, *(ii)* unloaded scaffolds, and *(iii)* loaded scaffolds. HMSC/scaffold interactions were evaluated by assessing cell proliferation (alamar Blue) and viability (Live/Dead), gene expression profiles (RT-PCR), Dex release (ELISA) and protein expression (histology).

RESULTS: Both PCL and PLGA were fabricated as fibrous and beaded scaffolds, depending on processing parameters (Fig. 1). Release rates were characterized for PCL and PLGA scaffolds. PCL showed short term (<1 day), while PLGA showed long term (>3 months) Dex release. Modification of Dex loading did not significantly alter release rates. Release profiles could be tailored by modifying fiber diameter and introducing beaded reservoirs. hMSCs cultured on Dex-loaded scaffolds showed proliferation rates comparable to cells grown on PS. Viable cells were detected covering large areas of both PCL and PLGA scaffolds. Fibrous scaffolds supported higher cell proliferation than beaded scaffolds. Enhanced ALP activity was observed for Dex-loaded PLGA fibers compared to the basic control. RT-PCR trends indicate that the loaded scaffolds had a slightly higher gene expression than the unloaded scaffolds in basic medium, suggesting a positive differentiation effect of Dex release.

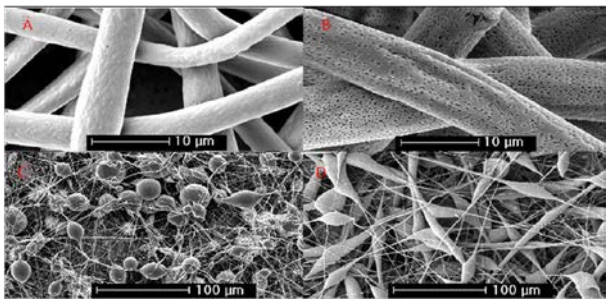

Fig. 1: SEM images of ESP scaffolds: (A, B) fibrous and (C, D) beaded (A, C) PCL and (B, D) PLGA scaffolds.

DISCUSSION & CONCLUSIONS: The ease of fabrication, simplicity of differentiating factors loading and release tailorability, and the support for cell growth suggest the potential use of this system to steer hMSCs differentiation for bone regeneration.

REFERENCES: [1]T.J. Sill, H.A. von Recum. *Biomaterials* (2008) **29**: 1989–2006. [2]H. Oshina, S. Sotome, T. Yoshii, I. Torigoe, Y. Sugata, H. Maehara, E. Marukawa, K. Omura, K. Shinomiya, *(2007) Bone* **41**: 575–583.

Evaluation of the biocompatibility of cholesterol-poly[2-(dimethylamino)ethyl methacrylate] synthesized by atom transfer radical polymerization

R Cordeiro[1], GL Santos[2], H Faneca[2], JP Mendes[1], AC Serra[1], JFJ Coelho[1]

[1] *CIEPQPF, Department of Chemical Engineering, University of Coimbra, PT.* [2] *Center for Neuroscience and Cell Biology and Department of Life Sciences, University of Coimbra, PT*

INTRODUCTION: The use of the Controlled/"Living" Radical Polymerization (CLRP) method to prepare tailor made polymers has been proved to be a powerful tool in the synthesis of polymeric structures to biological studies [1, 2]. In this work, we report the development of a CLRP method for poly[2-(dimethylamino)ethyl methacrylate)] (PDMAEMA) synthesis using mild conditions initiated with a cholesterol molecule. The viability for *in vitro* applications of the polymer was evaluated in two different cell lines.

METHODS: Cholesteryl-2-bromoisobutyrate and cholesterol-PDMAEMA (CHO-PDMAEMA) were synthesized according to a previously reported method [1]. The final product was characterized by proton nuclear magnetic resonance (^{1}H NMR), size exclusion chromatography (SEC) and in terms of their cytotoxicity, by a modified Alamar Blue assay [4] in 3T3-L1 and TSA cells, 48 hours after incubation with the polymer. Values of cell viability are expressed as a percentage of the untreated control cells (mean ± SD) obtained from three independent experiments with triplicates.

RESULTS: The ^{1}H NMR spectrum and SEC trace confirms the well controlled structure of the CHO-PDMAEMA polymer (Fig.1 and 2). The polymer also shows promising values of viability in both cell lines studied (Table 1).

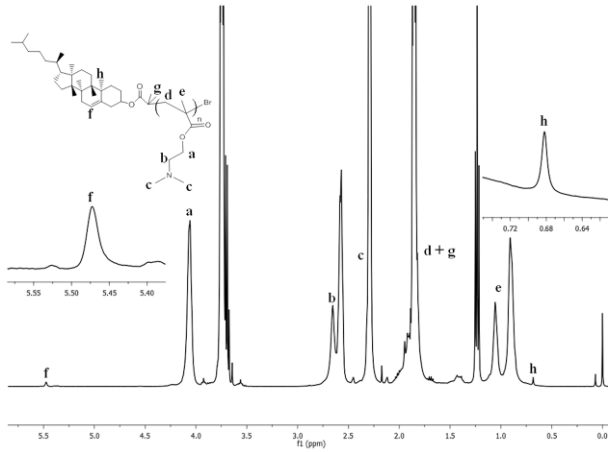

Fig. 1: ^{1}H NMR spectrum ($CDCl_3$, 400 MHz) of CHO-PDMAEMA.

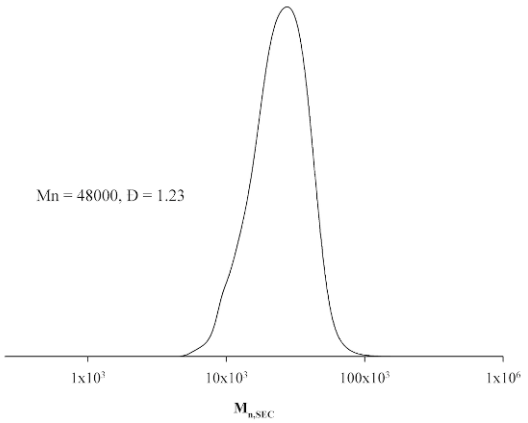

Fig. 2: SEC trace of CHO-PDMAEMA.

Table 1. Cell viability after 48 hours of incubation with the polymer. Values are expressed as a % of control cells and SD are given in brackets.

	Concentration (µg/mL)				
	0.1	0.5	2.5	5	10
3T3-L1	98.0 (5.3)	99.3 (5.3)	94.8 (6.7)	51.8 (7.9)	58.5 (6.4)
TSA	94.7 (5.9)	90.0 (8.2)	98.0 (6.0)	81.2 (15.7)	36.6 (23.5)

DISCUSSION & CONCLUSIONS: Results suggest a good control over of a CHO-PDMAEMA structure and good biocompatibility. In addition, the CLRP method used employs mild reaction conditions and sustainable GlaxoSmithKline (GSK)-based solvents[3]. The method developed for the polymer synthesis can be viewed an interesting and attractive solution for pharmaceutical industry.

REFERENCES: [1]RA Cordeiro et al (2013) *Polymer Chemistry* **4**(10):3088-3097. [2]J Coelho et al (2010) *EPMA Journal* **1**:164-209. [3]R Henderson et al (2011) *Green Chemistry* **13**:854-862. [4]H. Faneca et al (2004) *J. Gene Med.* **6**(6):681-692.

ACKNOWLEDGEMENTS: Rosemeyre Cordeiro acknowledges FCT-MCTES for her PhD fellowship (SFRH/BD/70336/2010).

Cell-Surface Interactions on Organic Thin Films: Chemistry or Electrostatics?

MR Wertheimer[1], A St-Georges-Robillard[1], JC Ruiz[1], S Lerouge[2], F Mwale[3], PL Girard-Lauriault[4] B Elkin[5], C Oehr[5], W Wirges[6], R Gerhard[6]

[1]*Dept. of Engineering Physics, École Polytechnique, Montréal, Canada* [2]*Dept. of Mechanical Engineering, École de Technologie Supérieure (ÉTS), and Centre de recherche du CHUM (CRCHUM), Montréal, Canada* [3]*Division of Orthopaedic Surgery, McGill University, and Lady Davis Institute for Medical Research, Montreal, Canada* [4]*Dept. of Chemical Engineering, McGill University, Montreal, Canada* [5]*Fraunhofer Institute for Interfacial Engineering and Biotechnology, Stuttgart, Germany* [6]*Applied Condensed Matter Physics, University of Potsdam, Germany*

INTRODUCTION: In recent communications from these laboratories, we have described observations that thin organic layers which are rich in primary amine (R-NH_2) groups are very efficient surfaces for the adhesion of mammalian cells, even for controlling the differentiation of stem cells. We prepare such deposits by plasma polymerization at low pressure (thin films designated "L-PPE:N", for "Low-pressure Plasma Polymerized Ethylene containing Nitrogen"), at atmospheric ("High") pressure ("H-PPE:N"), or by vacuum-ultraviolet photo-polymerization ("UV-PE:N"). More recently, we have also investigated a commercially available material, Parylene diX AM. In the present paper we shall, first, discuss the comparative results of physico-chemical characterizations of the various organic deposits mentioned above, which deliberately contain varying concentrations of nitrogen, [N], and amine groups, [NH_2]. Next, we briefly introduce literature relating to electrostatic interactions between cells, proteins, and charged surfaces. Finally, we present certain selected cell-response results that pertain mostly to applications in orthopedic medicine; we discuss the influence of surface properties on the observed behaviors of various cell lines, with particular emphasis on possible electrostatic attractive forces due to positively charged R-NH_3^+ groups and negatively charged proteins and cells, respectively.

RESULTS:

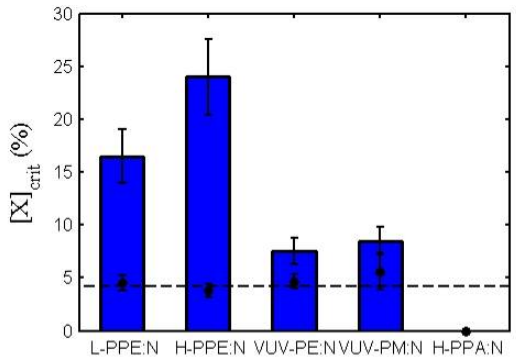

Fig. 1: Quantification of $[N]_{crit}$ in the adhesion experiments involving U937 cells. The "critical" nitrogen content, $[N]_{crit}$, required to stimulate adhesion of U937 monocytes to various substrates is shown in histogram-form. For each one of these coatings, the corresponding critical amino-group content, $[NH_2]_{crit}$ (o), is superimposed. The average value of $[NH_2]_{crit}$ is presented as a dashed, horizontal line. In the case of H-PPA:N, no adhesion of U937 was observed under any circumstances, in spite of high [N] values [1].

DISCUSSION & CONCLUSIONS: There exists a significant body of published literature, some going back several decades, that points to electrostatic (i.e. *physical*) adhesive forces between biomaterials surfaces and living cells, as opposed to *chemical* ones. Nevertheless, in view of the inherent complexity of biological phenomena, including cell biology, it is rarely simple to be able to separate them unambiguously; elsewhere [2] and here we show that under certain conditions there exists very strong support for an adhesive mechanism principally based on electrostatic attraction.

REFERENCES: [1]P.-L. Girard-Lauriault, F. Truica-Marasescu, A. Petit, H.T. Wang, et al. (2009), *Macromol. Biosci.* **9**: 911-921. [2]M. R. Wertheimer, A. St-Georges-Robillard, S. Lerouge, et al. (2012) Jpn. *J. Appl. Phys.* **51**: 11PJ04 (5 pp.)

ACKNOWLEDGEMENTS: The authors gratefully acknowledge financial support from the Natural Sciences and Engineering Research Council (NSERC) and the Canadian Institutes of Health Research (CIHR).

Study of the solid-liquid-solid mechanism through of the growth of nanowires as neuroprotection and excitotoxity model *in vitro*

JJ de S. Melo[1], LF Gomes[1], FHS Sales[1], RSB Melo[2]

[1]*Maranhão Federal Institute, São Luis, MA, Brazil.* [2] *Federal University of Maranhão, São Luis, MA, Brazil*

INTRODUCTION: The solid-liquid-solid (SLS) model is growth mechanism of nanowires having solid material as catalyst [1]. In this work, the growth nanowires was investigated as effect SLS mechanism caused by dewetting transition phenomenon, where gold thin film on silicon substrate were used as study samples in order to analyze the influence of the catalytic particle gold in the viability and cellular adhesion "in vitro" of silicon surfaces coated with SiO_2 nanowires.

METHODS: Gold thin films are vacuum thermally evaporated over (100) Si substrates pre-cleaned in HF solution for oxide removal, and submitted to a thermal treatment in Ar atmosphere in the sequence. The nanostructures are characterized via SEM/EDS and TEM images. The formation of the nanowires is observed at a heating temperature around 1050 °C for at least 30 minutes, with a large range of diameter (~10 nm to ~1 μm) and length sizes (to ~100 μm). How the metal layer deposited on the outside surface of balance "hydrophobic" semiconductor, when heated, and there are craters formed (which grow along the intake Si atomic planes with Miller indices h = 1, k = 1 l = 1) geometry triangle evolves into hexagon, similar to what occurs in the anisotropic corrosion of Si (100).

RESULTS: It was observed that the SLS mechanism occurs when the surface layer is submitted to thermal treatment high temperatures, but near the melting point of the solid material which constitutes it, resulting of square shaped holes, on gold surface, revealing the substrate surface, instead of isolated islands of Au [Fig 1]. The islands are not compact, featuring intricacies with straight edges, indicating the crystallization of Au along [111], as evidenced by X-ray diffraction. The Fig.2 shows that on samples treated at 1050 °C was observed the formation of nanowires [2].

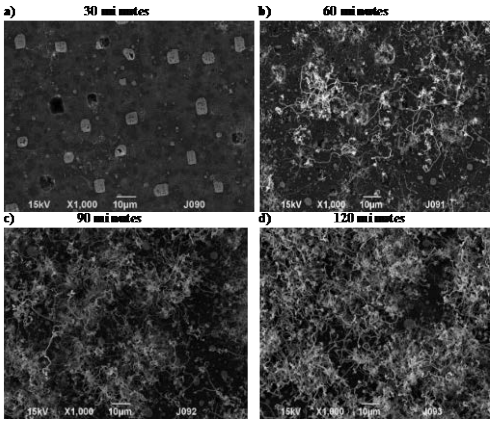

Fig 1: SEM images of the evolution of SLS mechanism on the film 50 nm gold deposited on Si after annealing at a temperature of 1050 °C under argon atmosphere: a)30 b)60 c)90 d)120 minutes.

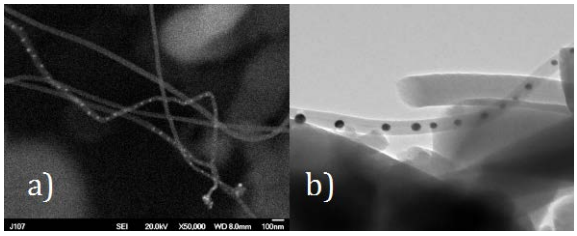

Fig 2: a) SEM image of nanowires with lengths exceeding 2μm and containing high number of nanospheres. b) TEM images of gold particles within the nanowire.

DISCUSSION & CONCLUSIONS: These nanowires can be used as a model system to study effects such as excitotoxicity or as study model of neuroprotection, in vitro, due the parameters its crystalline structure similarities to real systems. In this study we used the test by direct contact. The release of the toxic material can damage the cells or reduce the rate of cell growth in culture [3].

REFERENCES: [1]E. Jiran and C.V. Thompson (1992) *Thin Solid Films* **208:**23. [2]D.P. Yu; Y.J. Xing; Q.L. Hang; H.F. Yan, J. Xu; Z.H. Xi; S.Q. Feng (2001). *Physic E* **9:**305-309. [3]Robinson J.T, Jorgolli M, Shalek A.K, Yoon M.H, Gertner R.S, Park H. (2012). *Nat Nanotechnol*. 10,**7(3)**:180-4

ACKNOWLEDGEMENTS: The authors would acknowledge FAPEMA, CAPES and CNPq for financial support.

Cells and bacteria behaviour on micropatterned isotropic and anisotropic bioactive surfaces

A Carvalho[1, 2], A Pelaez-Vargas[3], D.Hansford[4], MH Fernandes[5], MP Ferraz[1, 6], FJ Monteiro[1, 2]

[1]INEB - Instituto Engenharia Biomédica, Porto, Portugal [2]DEMM, Faculdade de Engenharia, Universidade do Porto, Portugal [3]Universidad Cooperativa de Colombia, Medellín, Colombia [4]The Ohio State University, Dept. of BME, Columbus (OH), USA. [5]Faculdade de Medicina Dentária, Universidade do Porto, Portugal [6]Universidade Fernando Pessoa, Porto, Portugal

INTRODUCTION: It is well established that micron sized topography greatly affects cell-surface interactions [1]. Different types of surface topographies can influence behaviours such as adhesion, morphology, orientation, migration and differentiation depending on the scale and feature type of the substrate [2]. Understanding the mechanisms of cell-surface interaction is very important for the design of biomaterials and successful tissue engineering strategies [3]. The main goal of this work was to develop bioactive and micropatterned SiO_2 coatings to control cell attachment and spreading. Cells and bacteria behaviour on the isotropic and anisotropic coatings were evaluated with MSCs and *Staphylococcus aureus* respectively.

METHODS: Zirconia substrates were prepared in disc shape, by uniaxial pressing and sintered at 1400 ºC. A combined methodology of sol-gel and soft-lithography was used to produce micropatterned SiO_2 thin films. Anisotropic and isotropic patterns respectively as lines and pillars were applied to ZrO_2 substrates using a stamping method. Spin-coating was used to create a flat SiO_2 surface. Materials were characterized by SEM and contact angle. All the thin films were cultured with MSCs at three time-points (1, 7, 14 days). TCPS was used as control. Cells metabolic activity was measured at all time points and morphological analysis was carried out by fluorescence microscopy and SEM. The thin films were cultured with a *S. aureus* ATCC 25923 solution in the concentration of $1.5x10^8$ CFU/ml at 37ºC for 1 hour. After the incubation period, the adherent bacteria were analyzed by colony forming units (CFU), Live/Dead Staining and SEM.

RESULTS: Isotropic and anisotropic micropatterned silica thin films were successfully obtained. From day 1, MSCs showed an elongated morphology and orientation along the line patterns and a more random orientation on both the pillars and flat surfaces (Figure 1 A and B). Cell proliferation occurred over all surfaces throughout the culture time with increasing metabolic activity. At day 14, the flat SiO_2 group showed a statistically significant lower metabolic activity than the micropatterned thin films groups. Concerning bacterial adhesion, all the patterned materials showed significantly higher *S. aureus* adhesion than the flat SiO_2.

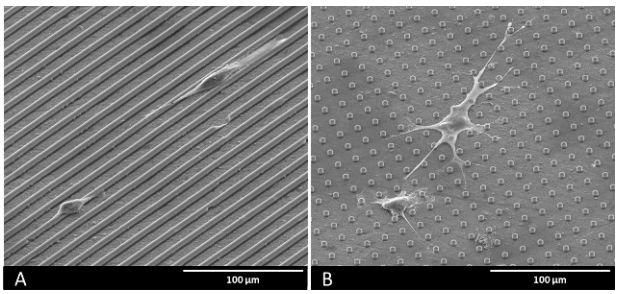

Fig. 1: SEM images of MSCs attachment and spreading on the micropatterned lines (a) and pillars (b) at day 1.

DISCUSSION & CONCLUSIONS: The micropatterned thin films were able to control cell attachment and alignment that was maintained, with increased proliferation, at all-time points. There was a significantly higher adhesion of *S. aureus* to the microtextured materials, where the surface area for contact is much higher. After implantation, a competition exists between integration of the material into the surrounding tissue and bacterial adhesion to the implant surface. With micropatterned materials this difficulty may be overcome, taking into account the higher cell proliferation observed.

REFERENCES: [1]M Bitar et al (2013) *J Mater Sci Mater Med* **24**: 1285-1292 .[2] P Roach, et al (2007) *J Mater Sci Mater Med* **18**: 1263-1277. [3] RG Flemming et al (1999) *Biomaterials* **20**:573-588.

ACKNOWLEDGEMENTS: The authors acknowledge financial support by FEDER.

Design of arrayed 3D architectures to induce and maintain cell patterns

T Saito, K Teraoka

National Institute of Advanced Industrial Science and Technology (AIST),Nagoya, Japan

INTRODUCTION: Cell microarrays have recently received considerable attention because of their important roles in fundamental cell biology, cell-based biosensors, and biomicroelectro-mechanical systems [1]. One effective method for creating cell microarrays is based on the micropatterning of protein-repellant chemicals such as polyethylene glycol on substrates to reduce the non-specific adsorption of cell-adhesive proteins from culture media. The problem resulting from using polyethylene glycol is that the formed cell patterns are temporary and break easily within several days. We previously showed another strategy for blocking the adhesion of cells using a perfluoroalkyl isocyanate layer on oxidized aluminum. However, the cells could not maintain their formed patterns for a long period [2].

METHODS: Glass slide-slips (76 × 26 mm) were sandblasted through mask patterns A and B to fabricate different 3D architectures on the surfaces. Images of the fabricated surfaces were observed by field emission scanning electron microscopy. The dimensions of the formed architectures were evaluated by confocal laser scanning microscopy. Mouse osteoblast-like MC3T3-E1 cells were seeded at about 5×10^3 cells/cm^2 onto the surfaces of samples #1, 2, and 3 and cultured in alpha-Minimum Essential Medium supplemented with 10% fetal bovine serum as previously described [3].

RESULTS: By sandblasting through mask patterns, 3 types of arrayed 3D architectures were fabricated on glass slide-slips just as designed; #1: pattern A with smoother surface grooves of greater width (300 µm), #2: pattern A with rougher surface grooves, and #3: pattern B with smoother surface grooves of smaller width (50 µm) (Fig.1). The depth of each groove was approximately 95 µm. Cell morphology, development of actin filaments, and cell proliferation of MC3T3-E1 cells were examined by field emission scanning electron microscopy observation, histochemical staining, and biological assays, respectively. From the results obtained so far, the cells that attached to the grooves, especially to those with smaller width (50 µm), tended to have cubic cell morphology with poorly developed actin filament and showed low cell proliferation.

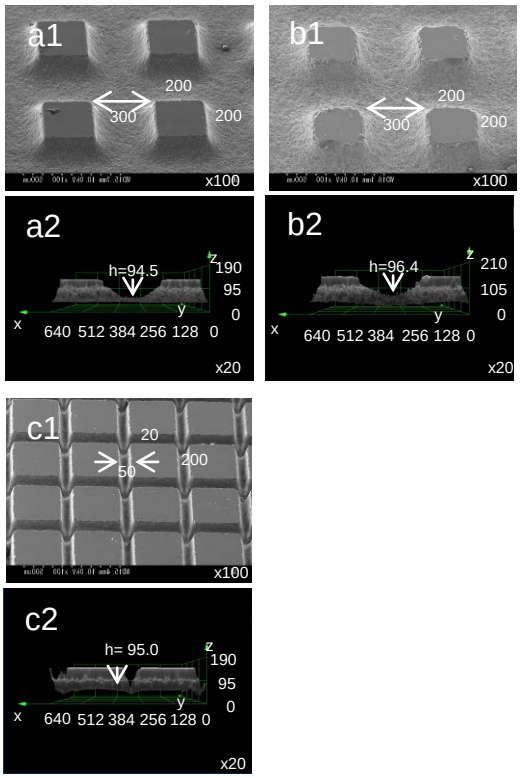

Fig.1: Field emission scanning electron microscopy (a1, b1, c1) and confocal laser scanning microscopy (a2, b2, c2) images of 3 types of designed 3D architectures fabricated on slide glasses by masked sandblasting. The dimensions in the images are presented in µm.

DISCUSSION & CONCLUSIONS: Among the tested samples, the arrayed 3D architectures in the prepared sample #3 is expected to be the most promising to fabricate more stable cell patterns. Compared to conventional methods, we propose here a completely different strategy to design arrayed 3D architectures on the surface to induce and maintain cell patterns applicable for creating stable cell microarrays.

REFERENCES: [1]M. Veiseh, B.T. Wickes, D.G. Castner, M. Zhang (2004) *Biomaterials* **25**, 3315-24. [2]T. Saito, H. Goto, M. Yagihashi, A. Hozumi (2010) Chem. Lett. **39**, 1048-49. [3]T. Saito, H. Hayashi, T. Kameyama, M. Hishida, K.Nagai, K. Teraoka et al. (2010) Mater. Sci. Eng. C 30, 1-7.

Surface modification of poly(L-lactic acid) electrospun scaffold by atmospheric plasma: scaffold properties and fibroblast morphological response

ML Focarete[1,2], LS Dolci[2], SD Quiroga[2], M Gherardi[3], R Laurita[3], A Liguori[3], E Ghedini[3,4], P Sanibondi[3], A Fiorani[1], L Calzà[2], V Colombo[3,4]

[1] Department of Chemistry "Ciamician", University of Bologna, Italy [2] Health Sciences and Technologies-Interdepartmental Center for Industrial Research (HST-ICIR), University of Bologna, Italy [3] Department of Industrial Engineering (DIN), University of Bologna, Italy [4] Advanced Mechanics and Materials - Interdepartmental Center for Industrial Research (AMM-ICIR), University of Bologna, Italy

INTRODUCTION: Surface functionalization of artificial polymeric biomaterials has been extensively studied as a useful strategy to improve material biointegration, promoting cell adhesion, proliferation and differentiation, without altering the main bulk properties of the material [1,2]. Electrospun nanofibrous scaffolds made of poly(L-lactic acid) (PLLA), mimicking the fibrillar arrangement of the extracellular matrix, have been widely used in tissue engineering applications. In this work the effect of atmospheric pressure non-thermal plasma surface functionalization of PLLA electrospun scaffold is investigated.

METHODS: Electrospun scaffolds were fabricated from a 12%w/v PLLA solution in dichloromethane:dimethylformamide (65:35), by means of an electrospinning apparatus made in house, composed by a high voltage power supply, a syringe pump, a glass syringe, a stainless-steel blunt-ended needle connected with the power supply electrode, and a rotating cylindrical collector. Scaffold surface functionalization was carried out by exposing the substrate to the plasma region generated by a non-thermal linear corona discharge (LC) plasma source operated at atmospheric pressure, using N2 as working gas. The plasma source was driven by a high voltage generator capable of producing pulses with a slew rate in the order of some kV/ns. PLLA scaffolds were characterized through morphological and thermo-mechanical analyses, and scaffold hydrophilicity was evaluated. The relative amount of carboxyl functional groups (COOH) generated by plasma treatment were assessed by means of a simple chemical conjugation reaction, functionalizing the surface of the scaffold with fluorescein isothiocyanate (FITC). Finally, mouse embryonic fibroblast cells were cultured on PLLA scaffolds to investigate how the plasma treatment affected cell morphology.

RESULTS: Scanning electron microscopy analysis showed that no morphological modification occurred after the exposure of the scaffold to the LC plasma source. Uniform, bead-free, sub-micrometer fibers (average fiber diameter 750 nm) were observed for both treated and unmodified PLLA scaffolds. Fiber wettability dramatically changed after the plasma treatment applied: treated scaffolds were instantaneously wetted by water while the unmodified PLLA scaffold was highly hydrophobic (water contact angle ~120°). Fluorescence intensity measured on the LC treated scaffold was 2 to 5 times higher than that measured on unmodified PLLA, indicating that a higher COOH concentration was generated on PLLA scaffold by the LC plasma treatment. Fibroblast cells growth and shape-factor were investigated. While fibroblast cells grown on pristine PLLA scaffold showed a small and star-like shape, those grown on plasma-treated PLLA scaffold assumed an highly elongated shape.

DISCUSSION & CONCLUSIONS: Surface functionalization of PLLA electrospun scaffolds was achieved using low temperature atmospheric plasma. A relevant increase of hydrophlicity and of COOH functional groups concentration was observed, without altering morphology and mechanical properties of the scaffold. Fibroblast cells on unmodified PLLA were smaller, rounded and "star-like", while those grown on treated PLLA were highly elongated and with "dendritic" morphology.

REFERENCES: [1] H.S. Yoo, et al (2009) *Adv. Drug Deliv. Rev.* **61**:1033–1042. [2] T. Desmet, et al (2009) *Biomacromolecules* **10**:2351-2378.

ACKNOWLEDGEMENTS: This work was supported by POR-FESR grant (Regione Emilia Romagna).

New strategies for developing cardiovascular stent surface with novel functions

N Huang, YX Leng, YJ Weng, J Wang, P Yang, JY Chen, H Sun, GJ Wan, AS Zhao, KQ Xiong

Key Lab. of Advanced Materials Technology, Ministry of Education, Southwest Jiaotong University, China

INTRODUCTION: Restenosis and late thrombus formation are the most challenge problems to stent intervention. Drug release from the surface is a very effective solution for suppressing restenosis, But increased late thrombus rate is even danger because of over 50% of death rate. This become a seirous problem in clinic for drug eluting stent(DES). Lack of abilities of anticoagulation and endothelialisation are the reasons for DES.

METHOD AND RESULTS: A stent consists of metal stent/titanium oxide film/drug eluting coating (mixture layer of the biodegradable polymer PLGA and rapamycin) produced by author's lab. has been obtained clinic approval. The drug eluting coating PLGA loaded with rapamycin is aimed for supressing restenosis. The titanium oxide film posses excellent blood compatibility. The two surface coating treated stent played multifunction anti-restenosis and thrombus resistance after stent intervention. At the acute stage the drug release plays the role to supress restenosis， and then the drug carrier PLGA is degraded and the Ti-O film surface with improved antithrombotic properties and supports the endothelialization is exposed to blood. In the long term stage the Ti-O film coating on the stent prevents the release of deleterious elements from the stent surface into the surrounding tissue and increased the long-term biocompatibility. Clinic trial data showed that restenosis rate of the developed stent was as lower as 1.1%, and no late thombus, however the restenosis and late thombus rate of the comparing commercial stent were 1.8% and 2.1% respectively during one year. And after two years 70% of the thombus formed patients in comparing group were die, however no late thombus was observed for the new stent even the intervention applied on over 3000 patients.

Another strategy by immobilization of selenocystamine on stents for catalytic generation of nitric oxide was performed. The selenocystamine immobilized surface possesses glutathione peroxidase (GPx) activity. Such selenocystamine immobilized surface showed the ability of catalytically decomposing endogenous S-nitrosothiols (RSNO), generating NO; thus the surface displayed the ability to inhibit platelet activation and aggregation. Furthermore smooth muscle cells were inhibited from adhering to the selenocystamine immobilized sample when RSNO was added to the culture media. It was revealed that cGMP in both platelets and smooth muscle cells significantly increased with NO release on selenocystamine immobilized samples. In vivo results showed that selenocystamine immobilized stents were endothelialized, and showed significant anti-proliferation properties, indicating that this is a favorable method for potential application in vascular stents.

DISCUSSION AND CONCLUSIONS: The stent surface posses novel multifunctions is very important because the interactions of stent materials with cardiovascular environment is very complicated and the anti-restenosis, anti-thrombus as well as prompt endothelialization all are the necessary abilities. This work revealed that the novel surface with multifunctions can be achieved and which should meet the clinic needs more ideally.

ACKNOWLEDGEMENTS: This research was supported by the NSFC 81271701 and Key Basic Research Program of China 2011CB606204

Degradation study of pure iron for applications as biodegradable cardiovascular devices in different simulated physiological fluids

J Harrison, R Tolouei, C Paternoster, S Turgeon, D Mantovani

Laboratory for Biomaterials and Bioengineering (CRC I), Dept. of Min-Met-Materials Eng., & University Hospital Research Center, Laval University, Quebec city, Canada.

INTRODUCTION: Biodegradable metals are designed to degrade in the body after having accomplished their function: this novel concept is the basis for the creation of biomedical devices that can be used for a variety of applications and eliminated after the tissues have healed without any additional surgery. One of these metals is pure iron, which has shown great promise in the development of cardiovascular devices, such as stents [1].

This work deals with the corrosion behavior of commercially pure iron substrates (ARMCO® iron) in different simulated physiological solutions. Although several works have been performed on magnesium and magnesium alloys [2,3], the mechanism of corrosion product formation on pure iron upon exposure in different static immersion tests is not yet well established. This study of in vitro corrosion is going to provide a basis for the understanding of the corrosion processes and ion release in physiological media.

METHODS: As received commercial pure (cp) iron foils (Figure 1) were cut and worked to obtain 20x10x0.5 mm^3 samples that were subsequently thermally homogenized. Microstructural evaluation before degradation was performed to investigate the microstructure-degradation behavior relationship of the studied materials. Samples were tested up to 14 days in 0.153 M NaCl, Hanks', modified Hanks' [1], phosphate buffered saline (PBS) and modified PBS solutions. Optical and scanning electron microscopy (SEM) was used for sample characterization, before and after corrosion tests, to assess the surface state and the morphology of the corrosion products; both surface and cross section of the samples were investigated. The chemical composition of the degradation layers was evaluated by energy dispersive X-ray spectrometry (EDX) and their structure by X-ray diffraction (XRD).

RESULTS & DISCUSSION: The degradation layer was found to be composed mainly of iron, oxygen, phosphorus, chlorine and calcium. A cohesive degradation layer is formed on the substrate surface, so that it prevents the contact of the material with the electrolytes. The formation of this corrosion product layer decreases the overall degradation rate; this effect was found for all the investigated samples. The morphology, composition and uniformity of the degradation layers were different for the different solutions investigated in this study. Some localized corrosion effects were found.

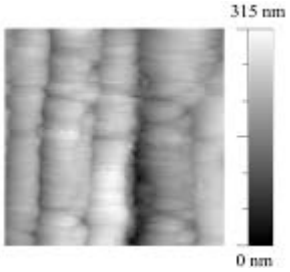

Figure 1: AFM image of surface of rolled iron sheet used in the experiments.

CONCLUSIONS: Degradation rate of rolled iron is lower than magnesium in all the considered solutions, but solution pH is less affected by Fe than by Mg [4]. The results of the present in vitro study indicate that ARMCO® iron is a suitable biomaterial for degradable implants, despite the formation of a layer of corrosion products impeding further dissolution of the material.

REFERENCES: [1] M. Moravej, S. Amira, F. Prima, A. Rahem, M. Fiset, D. Mantovani, Materials Science and Engineering: B, 176 (2011) 1812-1822; [2] Y. Xin, T. Hu, P.K. Chu, Acta Biomaterialia, 7 (2011) 1452-1459; [3] Y. Jang, B. Collins, J. Sankar, Y. Yun, Acta Biomater (2013), http://dx.doi.org/10.1016/j.actbio.2013.03.026; [4] Erlin Zhang, Haiyan Chen and Feng Shen, J. of Mat. Sci.: Mat. in Med., 21 (2010) 2151 – 2163.

ACKNOWLEDGEMENTS: The authors would like to thanks the Natural Sciences and Engineering Research Council of Canada for its financial support.

Anti-adhesive finishing of temporary implant surfaces by a plasma-fluorine-polymer

B Finke[1], H Rebl[2], B Nebe[2], R Bader[3], U Walschus[4], M Schlosser[4], KD Weltmann[1]

[1]Leibniz Institute for Plasma Science and Technology, Greifswald, DE. [2]Dept. of Cell Biology and [3]Dept. of Orthopedics, Rostock University Medical Center, Rostock, DE. [4]Medical Biochemistry & Molecular Biology, Ernst-Moritz-Arndt-University, Greifswald, DE.

INTRODUCTION: Metallic implants, especially made from titanium and its alloys, are state of the art in orthopedic and trauma surgery. Temporarily used implants such as intra-medullary nails, screws or external fixators for fractures support the mechanical stabilization of the bone consolidation but should not integrate into the bone because of their removal after fracture healing. An anti-adhesive coating could be very useful for these temporary implants to avoid protein and cell attachment as well as ingrowth into the surrounding tissue at last. Gas-discharge plasma processes are successfully applied for the modification of titanium surfaces and could be very valuable for the improvement of implant performance [1]. A new surface functiona-lization strategy was developed in close collabo-ration with cell biologists. The plasma polymeri-zation of octafluoropropane (C_3F_8) as precursor leads to the desired surface properties on Ti6Al4V. Here, we present an optimized plasma fluorine polymer (PFP) coating. Physico-chemical properties of the PFP-films were determined and the biological response *in vitro* and *in vivo* was tested.

METHODS: Discs (1 cm diameter) and platelets ($5\times5\times1$ mm^3) from polished, chemically pure titanium alloy Ti6Al4V were used as substrates. They were coated with ~300 nm thin films applying continuous wave low-pressure microwave discharge plasmas (10 Pa, 500 W, 600 s, 70/30 sccm C_3F_8/H_2). Film properties were analyzed by XPS, FT-IR, water contact angle measurements, SEM, as well as mechanically testing, e.g. the determination of total wear debris with artificial bone per 1 million cycles. Film stability was checked by sonication (10´) in distilled water. Human osteoblasts (MG-63 cells) were cultured on the samples. Adhesion and cell cycle phases were calculated by flow cytometry. *In vivo* biocompatibility was studied after intramuscular implantation of untreated Ti6Al4V and PFP-coated platelets in male LEWIS rats. The inflammatory tissue response was analysed after 7, 14, and 56 days.

RESULTS: A closed pinhole-free, strongly cross-linked (Fig.1), mechanical stable PFP film could be obtained. Sonication of these films showed good resistance against hydrolysis and delamination. Using XPS, an F/C ratio >1 was found and Ti6Al4V could not be detected by XPS. An advantageous medium hydrophobicity exists with a water contact angle of about 110°.

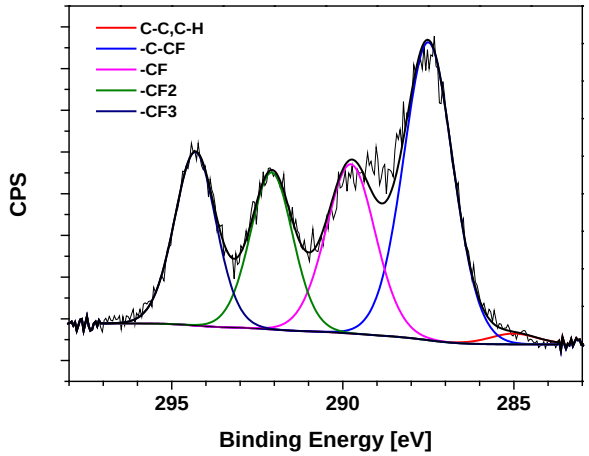

Fig. 1: C1s high resolution XPS spectrum of the PFP coating

Cell adhesion and cell spreading were drastically reduced on PFP coated Ti6Al4V *in vitro*. *In vivo* investigations revealed only a weak tissue reaction in comparison to untreated Ti6Al4V.

DISCUSSION & CONCLUSIONS: These optimized gas-discharge plasma-based PFP surface modification could be an option to improve the clinical handling of temporarily used Ti6Al4V implants

REFERENCES: [1]A. Quade, K. Schröder, et al (2011) *Plasma Process.Polym.* **8**:1165-73.

ACKNOWLEDGEMENTS: Thanks to U. Lindemann (INP), L. Middelborg for the excellent technical assistance. BF, HR, UW were supported by the BMBF (13N9779, 13N11188, Campus Plasma-Med).

Comparative biocompatibility evaluation of poly(β-amino ester) and poly[2-(dimethylamino)ethyl methacrylate]

R Cordeiro[1], GL Santos[2], H Faneca[2], AC Serra[1], JFJ Coelho[1]

[1] *Polymer Research Group - CIEPQPF, Department of Chemical Engineering, University of Coimbra, PT.* [2] *Center for Neuroscience and Cell Biology and Department of Life Sciences, University of Coimbra, PT.*

INTRODUCTION: Polycationic polymers have attracted increasing attention in the past decade for biomedical applications, mainly as nonviral vectors for gene delivery [1]. The optimal polymer structure for gene delivery carrier should combine low cytotoxicity with high transfection efficiency. In this work we compare the cell viability in two different cell lines (3T3-L1 and TSA) for two broadly used polycationic polymers in gene delivery: poly[2-(dimethylamino)ethyl methacrylate)] (PDMAEMA) and a poly(β-amino ester) (PβAE).

METHODS: PDMAEMA was synthesized and purified as previously described [2]. PβAE was synthesized through Michael addition reaction between 5-amino-1-pentanol (1.5g, 14.54 mmol) and 1,4-butanediol diacrylate (3.20 mL, 17.45 mmol) in dry acetone. After 24 h, the solution was dripped slowly and washed (3 times) into cold diethyl ether. PβAE was dried under reduced pressure and then dried overnight at 40ºC under vacuum. PβAE was stored at -20ºC until use. Cell viability was assessed by a modified Alamar Blue assay, as previously described [3] in two different cell lines (3T3-L1 (mouse embryonic fibroblast cell line) and TSA (BALB/c female mouse mammary adenocarcinoma cell line)). Cell viability (as a percentage of control cells) was calculated according to the equation:

$$Cell\ viability = (A_{570}–A_{600})/(A'_{570}–A'_{600})*100 \quad (1)$$

Where A_{570} and A_{600} are the absorbances of the samples and A'_{570} and A'_{600} those of control cells, at the indicated wavelengths. Values of cell viability measured by the Alamar Blue assay are expressed as a percentage of the untreated control cells (mean ± SD) obtained from three independent experiments with triplicates.

RESULTS: The cell viability assays reveal substantial differences between PDMAEMA and PβAE in both studied cell lines (Fig.1 and 2). The PβAE shows low cytotoxicity, being observed high levels of viability for both cell lines, even when incubated with high concentrations of PβAE.

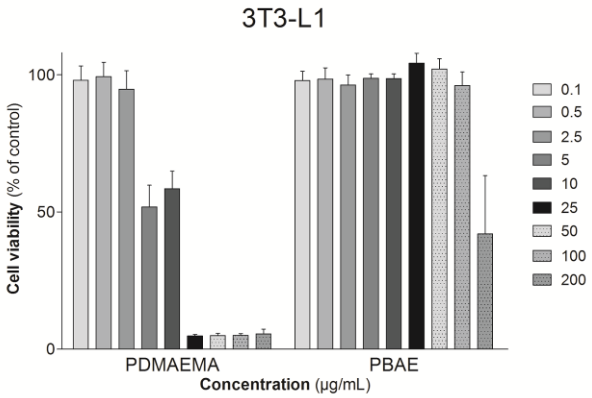

Fig. 1: Effect of PDMAEMA (left side) and PβAE (right side) concentrations on viability of 3T3-L1 cell line after 48h of incubation.

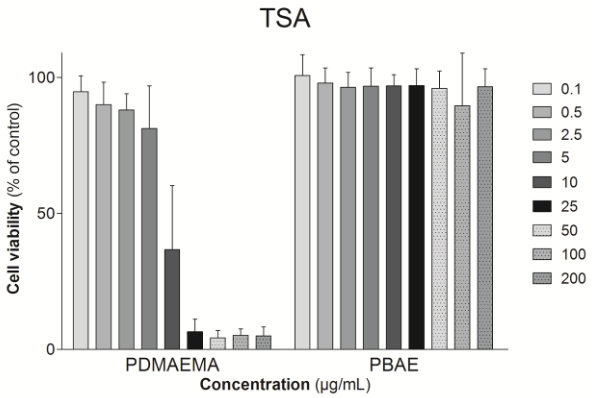

Fig. 2: Effect of PDMAEMA (left side) and PβAE (right side) concentrations on viability of TSA cell line after 48h of incubation. (1)

DISCUSSION & CONCLUSIONS: In this study we have shown that PβAE is much more biocompatible, even at high concentrations, than PDMAEMA as indicated by the viability assays.

REFERENCES: [1]J. Coelho et al (2010) *EPMA Journal* **1**:164-209. [2]R.A. Cordeiro et al (2013) *Polymer Chemistry* **4**(10):3088-3097. [3]H. Faneca et al (2004) *The Journal of Gene Medicine* **6**(6):681-692.

ACKNOWLEDGEMENTS: Rosemeyre Cordeiro acknowledges FCT-MCTES for her PhD fellowship (SFRH/BD/70336/2010).

Bioactive coating via layer-by-layer method to improve stent endothelialization

I Carmagnola[1], V Chiono[1], S Cabodi[2], F Boccafoschi[3], F Lograndi[2], G Tarone[2], G Ciardelli[1]

[1] *Department of Mechanical and Aerospace Engineering, Politecnico di Torino, Turin, Italy*
[2] *Department of Molecular Biotechnology and Health Science, Università di Torino, Turin, Italy*
[3] *Department of Experimental and Clinical Medicine, University of Piemonte Orientale, Novara, Italy*

INTRODUCTION: Stent re-endothelialization has been proven to prevent in-stent restenosis and very late thrombosis [1-3]. The specific ligand immobilisation onto stent surface can promote endothelial cells (ECs) adhesion. Wei et al. [4] demonstrated that the REDV peptide enhance the EC growth respect to smooth muscular cells (SMCs). In this work layer-by-layer coating was exploited for surface functionalization with CRETTAWAC [5] sequence to favour EC adhesion and hinder platelet attachment.

METHODS: Aminolysed films formed by (poly(L-lactide) and poly(DL-lactide-co-glycolide) (PLLA/PLGA) were dipped into alternate aqueous solutions (0.5 % w/v, pH: 4.5) of poly(sodium 4-styrene sulfonate) (PSS, M_w = 70 kDa) and poly(diallyldimethylammonium chloride) (PDDA, M_w = 200-350 kDa) for 15 min each, with intermediate washing steps in bi-distilled water (pH: 4.5) for 5 min. Heparin (HE≥180 USP) was deposited as the last layer of the coating. Surface composition was evaluated through XPS analysis The CRETTAWAC effect on endothelialization was evaluated in vitro using human umbilical vein endothelial cells (HUVECs). Cells were seeded onto three surfaces functionalised with CRETTAWAC, bovine serum albumin (BSA) and fibronectin (FN), respectively. The adhesion test was carried out at 2 and 4 hours.

RESULTS: After the deposition of 14 and 15 polylelectrolyte layers, surface nitrogen content was higher respect to aminolysed PLLA/PLGA due to the deposition of PDDA, whereas the presence of sulphur was attributable to both the deposition of PSS and HE (Table 1).

Table 1. Atomic percentage of chemical elements present on the first atomic layers of analyzed PLLA/PLGA samples by XPS analysis.

	C1s	O1s	N1s	S2p
Aminolyzed PLLA/PLGA	64.0	35.3	0,7	-
PLLA/PLGA + 14L	71.2	26.0	1.3	1.5
PLLA/PLGA + 15L	70.2	25.8	2.2	1.8

In vitro cell tests showed that after 2 hours the number of adhered cells on CRETTAWAC-functionalised surface was inferior respect to FN-functionalised substrate. After 4 hours HUVECs seeded on CRETTAWAC functionalised surface showed a spread morphology.

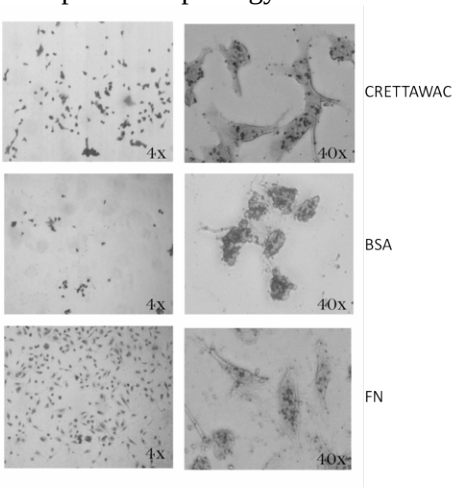

Fig. 1:Microscopy images of adhered HUVECs on different functionalised surface after 4hours.

DISCUSSION & CONCLUSIONS: LbL technique allowed the obtainment of functional coatings without altering the bulk properties. CRETTAWAC sequence was shown to bind the $\alpha_5\beta_1$ integrin that is present on the surface of ECs but lacking on platelets. LBL could be exploited for surface functionalisation with KKKKKKSGSSGKCRRETAWAC, able to electrostatically interact through KKKKKK sequence with HE and exposing selective bioactive recognition sequences for endothelial cell-surface interaction.

REFERENCES: [1] Q.K. Lin et al. (2010) *Biomaterials* **31**:4017-25. [2] A. Mel et al. (2008) *Biomacromolecules* **9**:2969-79. [3] S. Meng et al. (2009) *Biomaterials* **30**:2276-83. [4] Y. Wei et al, (2013) *Biomaterials* 34: 2588-99. [5] S.R. Meyers, et al. (2011) *Biomacromolecules* **12**:533-39.

ACKNOWLEDGEMENTS: NANOSTENT (Regional Project, Regione Piemonte).

Dynamic cell response behavior to various nanoparticles

F Watari[1,2], N Iwadera[1], S Ito[3], T Akasaka[1], Y Yawaka[1], R Ikhtiari[4], P Begum[4], B Fugetsu[4]

[1]Graduate School of Dental Medicine, [2]Creative Research Institution, [3]Center for Environmental and Health Sciences, [4]Graduate School of Environmental Science, Hokkaido University, Sapporo, Japan

INTRODUCTION: Materials are usually recognized by cells chemically with the form of dissolved ions for the macroscopic size. This effect is valid and enhanced due to the increase of surface area with downsizing to micro/nano size. In addition to chemical dissolution effect, cells also start to recognize materials as physical objects, when the size becomes smaller than a cell, about 10 μm in average. This physical size effect depends only on the size of materials. This induces the biological reaction such as phagocytosis for cells and inflammation in tissue. Through this biological process, materials show the functions different from those in macro. The examples of this conversion of functions [1-3] can be found in mesothelioma by acicular particles of asbestos and osteolysis by abraded particles produced from artificial joint. Thus to investigate the material nanosizing effect, it is necessary to observe cells in the living state and their dynamic behavior. Conventionally cell morphology has been observed after fixation where cells are mummified. In this study the dynamic behavior of cell reaction to nanoparticles were observed by time lapse method and analyzed [4,5].

METHODS: (1) Particles: TiO_2, CuO, In_2O_3, ITO (indium-tin oxide), Pt and carbon nanotubes (CNTs) in nano to micro range were used. (2) Cells: Mouse osteoblastic cells (MC3T3-E1) and human hepatocytes (Hc cells) were used. (3) Observation: The in situ successive time-lapse observation of cell behavior by optical microscopy was done by taking images every 2-5 min for up to 24 hrs at the Nikon Imaging Center of Hokkaido University.

RESULTS: The dynamic cell morphology could be visualized by the time lapse method which was different from the static one after fixation process. The feature of cell behaviour was largely classified as three modes: extension of pseudopods, approaching particles and engulf to phagocytosis, and scavenging effect to collect and wipe out particles from surrounding area. Depending on the species of nanoparticles, morphology looks different as shown in TiO_2 (Fig.1a) and Pt (b).

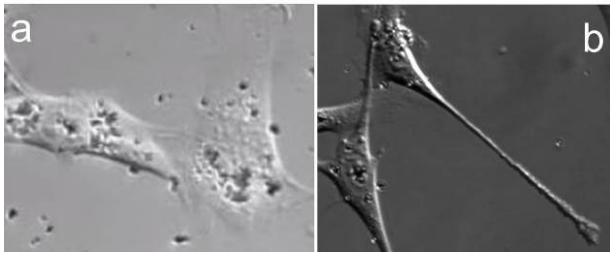

Fig. 1: Dynamic cell morphology reacted to TiO_2 (a) and Pt nanoparticles (b). Cell are osteoblastic cells (MC3T3-E1) .Width of each figure is about 100 μm.

DISCUSSION & CONCLUSIONS: Materials are inert to cells except for the chemical effect due to dissolved ions. Chemical effect appears usually strong as either acute toxicity or nutrition, whereas the stimulus of physical size effect is quite small and negligible which can be observed ideally for non-dissolved materials such as Ti. However it is significant since it induces the biological process of phagocytosis for cells and inflammation in tissue and this biological process leads to the conversion of functions specific to nano and different from those in macro. Nanoparticles are thus characterized as biointeractive since their size themselves induce the bioreaction of cells independently of material kinds. The bioreactive nature to work in either way of merit (bioactive) or demerit (toxic) also gives the basis for remodeling of hard tissue and carcinogenicity of asbestos.

REFERENCES: [1] F.Watari et al (2009) *J.Roy. Soc.Interface* **6**:S371-388. [2] F.Watari (2013) *Bio-Nanotechnology A Revolution in Food, Biomedical and Health Sciences, Chapter16* (edts D.Bagchi et al) Wiley-Blackwell, pp. 292–303. [3] F.Watari (2009) *Nano Biomedicine* **1**:2-8. [4] S.Itoh et al (2009) *Nano Biomedicine* **1**:95-108. [5] N.Iwadera et al (2012) *Nano Biomedicine* **4**: 57-65.

Thin films biomaterials: mechanical rigidity and bioactivity

D Chacon[1], C Wu[2], M Hindié[1], S Aslan[2], J Phelps[2], A Gand[1], P Van Tassel[2], E Pauthe[1,2]

[1] ERRMECe, Université de Cergy-Pontoise, 95302 Cergy-Pontoise cedex, France [2] Department of Chemical and Environmental Engineering, Yale University, New-Haven, CT 06520-8286, USA.

INTRODUCTION: Nanofilm materials formed via the layer-by-layer (LbL) assembly of oppositely charged macromolecular species are finding widespread application in energy, sensing, and biomedicine; particularly for applications involving contact with living cells / tissues – e.g. cell culture, tissue engineering, biomedical implants – since chemical, mechanical, and biological properties may be tailored to promote a desired cellular response. Initial cell attachment generally increases with film rigidity, itself enhanced through cross-links. Cell behavior may be further influenced through embedded biomolecules (e.g. growth factors), but chemical cross-linking – tending to promote cell / tissue integration – may act to suppress film bioactivity by diminishing biomolecular mobility and/or film degradation or by chemically altering the intra-film species. A key challenge is to simultaneously realize mechanical rigidity and bioactivity. Two different strategies to decouple mechanical rigidity and bioactivity are presented, with a goal of realizing nanofilm biomaterials that are both mechanically rigid and bioactive.

RESULTS & DISCUSSIONS: One strategy is to selectively cross-link the outer region of the film, resulting in a rigid outer skin to promote cell attachment, while leaving the film interior (with any embedded bioactive species) unaffected. We propose an approach whereby an N-hydroxysulfosuccinimide activated poly(L-glutamic acid) is added as the terminal layer of a multilayer film and forms (covalent) amide bonds with amino groups of poly(L-lysine) placed previously within the film.

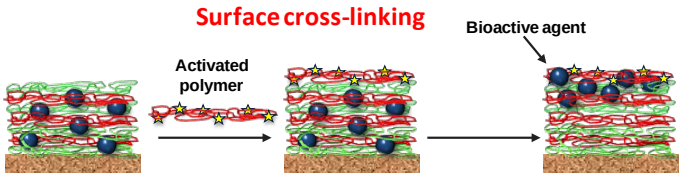

We characterize film assembly and cross-linking extent via quartz crystal microbalance with dissipation monitoring (QCMD), Fourier transform infrared spectroscopy in attenuated total reflection mode (FTIR-ATR), and laser scanning confocal microscopy (LSCM), and measure the attachment and metabolic activity of preosteoblastic MC3T3-E1 cells. We show cross-linking to occur primarily at the film surface and the subsequent cell attachment and metabolic activity to be enhanced compared to native films [1].

As a second strategy, we report nanoparticle templating toward porous, layer-by-layer assembled, thin polyelectrolyte films of high mechanical rigidity and significant bioactive species loading capacity. Functionalized latex nanoparticles are incorporated during layer-by-layer assembly, and following EDC-NHS cross-linking of the polyelectrolyte film, are removed *via* exposure to tetrahydrofuran.

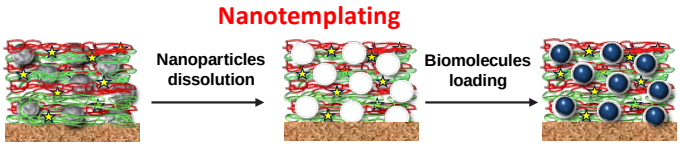

Film assembly, structure and organization are characterized via quartz crystal microbalance with dissipation monitoring (QCMD), scanning electronic microscopy (SEM) and ellipsometry. Nanoindentation analysis shows the resultant porous films to be of comparable mechanical rigidility to (non-templated) chemically cross-linked films, and laser scanning confocal miocroscopy confirms a high capacity for (fluorescently labeled) bioactive species loading (ca. 10% of film mass). Attachment, spreading, and metabolic activity of pre-osteoblastic MC3T3-E1 cells on templated, cross-linked films are statistically similar to that on non-tempated films, and much greater than that on (softer) non-cross-linked films [2]. Porous, rigid nanofilm biomaterials formed *via* layer-by-layer assembly are excellent candidates for a variety of cell-contacting applications.

CONCLUSION: These mechanically rigid and bioactive innovative nanobiomaterial systems are promising toward cell contacting applications, in particular when directing cellular behavior is desired.

REFERENCES: [1]J. Phelps, *et al.* (**2011**) *Langmuir*, 27, 1123-1130C. [2] C. Wu, *et al.* (**2013**) *Advanced Functional Materials*, 23, 66-74.

Biocompatibility and characterisation of a Kolsterised® medical grade cobalt-chromium-molybdenum alloy

M Caligari Conti[1], A Karl[2], P Schembri Wismayer[3], J Buhagiar[1]

[1] Department of Metallurgy and Materials Engineering, University of Malta, Malta [2] Bodycote Hardiff GmbH, Landsberg, Germany [3] Department of Anatomy, University of Malta, Malta

INTRODUCTION: Metal-on-metal prosthetic implants have been widely used by orthopaedic surgeons to perform total hip replacement. These prostheses replace the natural joint using biomedical cobalt-chromium alloys. Such materials exhibit biocompatibility whilst possessing the desired corrosion and wear resistance, strength, ductility and fatigue properties [1].

Several publications, such as the one recently published by Smith et al. in The Lancet [2] have raised concerns with regards to premature failure of metal-on-metal implants especially in large diameter heads. This research was based on the National Joint Registry of England and Wales for primary hip replacements (2003 - 2011) and results show that metal-on-metal implants have a lower survival rate when compared to ceramic-on-ceramic prostheses.

Following successful decrease in wear volume loss in austenitic stainless steels for biomedical applications, by the creation of a corrosion resistant diffused hardened layer know as expanded austenite or S-phase [3], interest has risen in inducing the same layer on cobalt-chromium-molybdenum alloys.

This will raise the hardness of these alloys, therefore making them more comparable to the hardness of ceramics whilst ideally keeping them both biocompatible and corrosion-wear resistant.

METHODS: A cobalt-chromium-molybdenum alloy abiding by the standard ASTM F1537-11 was Kolsterised® in order to create the S-phase layer. Kolsterising® is a low temperature diffusion process performed at a temperature below 500 °C for several days at a very high carbon potential.

The treated and untreated alloy were characterised by SEM, nano-indentation, depth profile chemical analysis, X-ray diffraction and electrochemically tested in Ringer's solution. Proliferation of a hFOB 1.14 human foetal osteoblast cell line was tested (XTT) on Kolsterised® Co-Cr-Mo and was compared to the untreated material together with positive and negative controls.

RESULTS: The presence of the S-phase layer (2.6 gm^{-2} of carbon) was confirmed using the afore mentioned characterisation techniques. Nano-indentation has shown that the value of hardness rose from 5.5 ± 0.1 GPa to 14.1 ± 0.4 GPa after treatment. The excellent corrosion resistance of the parent alloy was retained and improved. No pitting corrosion was observed and the corrosion current was reduced from 1.45 ± 0.01 X 10^{-8} Acm^{-2} to 0.86 ± 0.01 X 10^{-8} Acm^{-2}. Figure 1 shows that the biocompatibility of Kolsterised Co-Cr-Mo is similar to that of the untreated alloy.

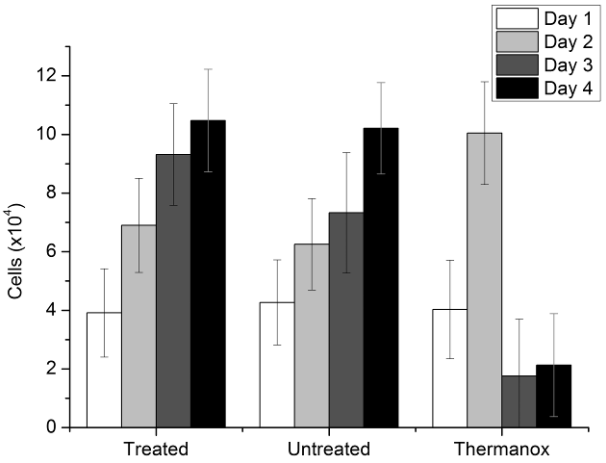

Fig. 1: hFOB 1.14 human foetal osteoblast cell proliferation kinetics (p>0.01) – ϕ9.5 mm coupons

DISCUSSION & CONCLUSIONS: The Kolsterising® treatment increases the hardness of the Co-Cr-Mo alloy without any detriment to corrosion resistance and biocompatibility. Increase in hardness is normally linked to an increase in wear resistance and therefore Kolsterising® makes a better bearing surface for artificial hip joints.

REFERENCES: [1] J. Cawley, J.E.P Metcalf, A.H. Jones, et al (2003) *Wear* **255**: 999-1006. [2] A.J. Smith, K. Vernon, M. Porter, A.W. Blom (2012) *The Lancet* **379**: 1199–1204. [3] J. Buhagiar, A. Jung, D. Gouriou et al (2013) *Wear* **301**: 280–89

ACKNOWLEDGEMENTS: The authors would like to thank Bodycote Hardiff GmbH and ERDF (Malta) for the financing of the testing equipment through the projects: ERDF No. 012 and 081.

Barrier membrane protected *in vivo* biosensors

S Anastasova, AM Spehar-Deleze, P Vadgama

Queen Mary, University of London, London, UK

INTRODUCTION: The primary requirements for biosensors for *in vivo* monitoring are selectivity, sensitivity and biocompatibility. These properties can be achieved by the appropriate choice of barrier membranes. An understanding of solute diffusion behavior to analytes and interfering substances at such membranes is key to optimized design and reliable performance in complex biological matrices. A general, needle-based, amperometric platform for continuous *in vivo* monitoring of glucose, lactate and O_2, respectively, has been developed and different sensor designs and membrane barriers established.

The biosensors are currently directed at monitoring during exercise to aid coaches in the training programs of elite athletes.

METHODS: A simplified two electrode system comprising a stainless steel tube as counter/reference electrode and an inner platinum wire working electrode was constructed [1]. As appropriate, an interferent rejecting inner ionomeric membrane was coated on the Pt wire prior to functionalizing with BSA crosslinked oxidase enzyme using glutaraldehyde. Finally, modified polyurethane layers were deposited sequentially from 20%, 30%, 40 % and 50 % (w/v) solutions in THF [1, 2]. Silicone barrier layers were used for O_2.

Sensors were evaluated in Sprague Dawley rats (300-350g) in accordance with authorized UK Home Office procedure. Rats were anesthesised using isoflurane inhalation. The output of the subcutaneously implanted sensors was recorded using an Apollo 4000 Free Radical Analyser (WPI, UK). Where possible, output was compared with independent blood assay, eg the Accu-Chek Glucometer (Roche Diagnostics, UK) for glucose. Sensors were tested in human subjects during exercise in accordance with the approved protocol of the Regional Ethical Committee following γ-sterilisation (ISO11137 2:2007 standard). Sensors were inserted into subcutaneous tissue *via* a trochar/cannula at 45 ± 10˚ to ~2 cm depth.

RESULTS: There was a short run-in period (~ 30 min) and a clear tissue response (~10 min) after systemic perturbation for glucose (Figs. 1a) in the rat model, but with apparent dampening of the tissue lactate response (Fig. 1b). Pre- and post-use calibration showed <10% change in lactate sensor response.

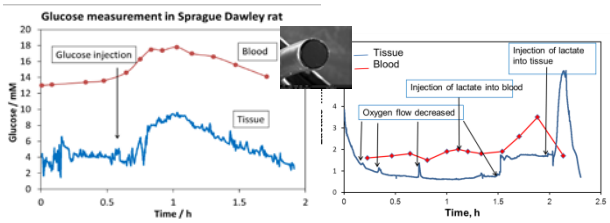

Fig. 1: Sensor based subcutaneous issue (a) glucose (b) lactate measurement in rat. (Inset shows sensor tip).

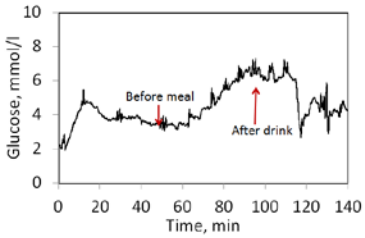

Fig. 2: Glucose measured in human subject after oral glucose load.

The glucose sensor followed tissue glucose after an oral glucose load in a human subject (Fig 2) with <10% drift over 2h.

DISCUSSION & CONCLUSIONS: Tissue is less well understood than blood as a compartment for assessing biochemical change. The membrane protected, biosensors developed here offer low drift measurement and the opportunity to make tissue/blood comparisons under dynamic conditions. This could provide new insights of relevance to exercise physiology and acute medicine.

REFERENCES: [1] S. Anastasova, A.M. Spehar-Deleze, D. Bickham, et al (2012) *Electroanalysis* **24**: 529-38. [2] A. Spehar-Délèze, S. Anastasova, Z. Rong et al (2012) General Platform for In vivo Sensors for Oxygen, Glucose and Lactate Monitoring *in* Portable Chemical Sensors - Weapons Against Bioterrorism *(ed D. Nikolelis)* NATO Science for Peace and Security Series A : Chemistry and Biology *pp* 287-303.

ACKNOWLEDGEMENTS: The authors wish to thank EPSRC for generous funding through Project EP/H009744/1 (ESPRIT).

Glycosaminoglycan sulfation of artificial extracellular matrix coatings enhances regenerative potential of bone cells

J Salbach-Hirsch[1], E Tsourdi[1], V Hintze[2], D Scharnweber[2,5], S Möller[3], M Schnabelrauch[3,4], M Rauner[1], LC Hofbauer[1,5]

[1]Division of Endocrinology, Diabetes and Bone Diseases, Dresden University Medical Center, Dresden, Germany [2]Max Bergmann Center for Biomaterials, Technische Universität Dresden, Germany [3]Biomaterials Department, INNOVENT e. V, Jena, Germany [4]Jena Center for Soft Matter, Jena, Germany [5]Center for Regenerative Therapies Dresden, Technische Universität Dresden, Germany

INTRODUCTION: In light of prolonged life expectancy, the need for biomaterials that govern bone regeneration increases. Improved bone regeneration and osseointegration can be achieved by functionalizing implant materials. The extracellular matrix (ECM) affects differentiation of bone cells and is critical for bone regeneration. Here we assessed the role of the natural occurring bone ECM glycosaminoglycans (GAGs) hyaluronan (HA) and chondroitin sulfate (CS), and their sulfated derivatives. In particular, their effects on differentiation and crosstalk of bone-resorbing osteoclasts, bone-forming osteoblasts and regulatory osteocytes involved in bone remodeling processes were assessed and evaluated for potential implant functionalization.

METHODS: The impact of native and sulfate-modified GAGs on viability, morphology, differentiation, gene expression and cell signaling was studied using murine bone marrow monocytes, mesenchymal stromal cells and the MLO-Y4/UMR-203 cell lines as a model for osteoblasts, osteoclasts and osteocytes, respectively. Cells were seeded on culture plates coated with artificial ECMs containing rat collagen type I (Coll)/hyaluronan (HA), Coll/chondroitin sulfate (CS) or Coll/high-sulfated GAGs (sHA3, sCS3). Coatings with Coll alone served as control. Using surface plasmon resonance, direct interactions of GAGs with the two main regulatory proteins in bone, receptor activator of nuclear factor kappa-B ligand (RANKL) and osteoprotegerin (OPG) were evaluated.

RESULTS: In response to native and high-sulfated GAGs profound effects on all stages of osteoclast differentiation were observed. GAG sulfate modification increased the viability of osteoclasts ($p<0.05$). However, tartrate resistant acid phosphatase (TRAP)-staining and immunofluorescence of regular sealing zone structures in osteoclasts were profoundly decreased ($p<0.05$). This was accompanied by a loss of resorptive activity up to 40% compared to cells exposed to native GAG ($p<0.01$) and decreased mRNA levels of osteoclastic marker genes, such as cathepsin K, osteoclast-associated receptor and TRAP ($p<0.05$). On the other hand, the proliferation and metabolic activity of osteoblasts and osteocyte-like cells treated with equal concentrations of GAGs was decreased ($p<0.05$) indicating a shift from the proliferative to matrix formation phase of osteogenic differentiation. And indeed, these cells showed altered matrix deposition and increased expression of gene products associated with differentiation, such as RANKL/OPG ratios, alkaline phosphatase-, osteocalcin, Runx2 and decreased SOST expression levels ($p<0.05$). Correspondingly, supernatants collected from these cells suppressed osteoclastogenesis ($p<0,05$) but did not affect their adhesion and viability. Using surface plasmon resonance, we demonstrated that GAGs can directly bind to OPG, but not RANKL, in a sulfation degree dependent manner resulting in modified OPG bioactivity.

DISCUSSION & CONCLUSIONS:

In summary, sulfation of GAGs increases osteogenesis and reduces osteoclastogenesis and pro-osteoclastogenic signaling from osteogenic cells and may represent a useful tool to control enhanced osteoclastic activity and bone loss adjacent to implant surfaces

ACKNOWLEDGEMENTS:

This study was supported by grants from Deutsche Forschungsgemeinschaft Transregio 67 subprojects A2, A3 and B2.

Effect of poly(vinylidene-trifluoroethylene)/barium titanate membrane on in vivo bone formation

HB Lopes[1], TS Santos[1], FS de Oliveira[1], GP Freitas[1], ALG de Almeida[1], R Gimenes[2], AL Rosa[1], MM Beloti[1]

[1] *Cell Culture Laboratory, School of Dentistry of Ribeirao Preto, University of Sao Paulo, Brazil* [2] *Institute of Physics and Chemistry, Federal University of Itajuba, Brazil*

INTRODUCTION: Guided bone regeneration (GBR) is a technique based on the use of barrier membranes to prevent soft tissue growth into bone defects and, consequently, to allow bone tissue regeneration. Although commercially available membranes display satisfactory results in terms of tissue regeneration, the development of novel biomaterials to be employed in GBR are of great interest in this research field. Here, we compare a new composite membrane comprised of poly(vinylidene fluoride-trifluoroethylene) and barium titanate (P(VDF-TrFE)/BT) with a polytetrafluoroethylene (PTFE) membrane.

METHODS: Wistar rats weighing 250-300 g were submitted to a surgical procedure to create 5-mm-diameter calvarial defects, which were randomly implanted with either P(VDF-TrFE)/BT or PTFE membranes. Four weeks post-implantation, the animals were euthanized, and the calvariae were harvested and processed for morphometric (n=4 for each membrane) and gene expression (n=4 for each membrane) analyses. Bone volume (BV), bone surface (BS), trabecular number (TN) and trabecular separation (TS) were evaluated using Micro-CT images obtained from a SkyScan 1172 System (SkyScan, Belgium). The gene expression of runt-related transcription factor 2 (Runx2), osterix (Osx), bone sialoprotein (Bsp) and osteocalcin (Oc) was evaluated by real-time PCR using a CFX96 Real-Time PCR Detection System (Bio-Rad Laboratories, USA) and a TaqMan System (Invitrogen-Life Technologies, USA). Data were compared using the Mann-Whitney U-test and the level of significance was established at $p \leq 0.05$.

RESULTS: The BS was larger (p=0.01) on the P(VDF-TrFE)/BT membrane compared with the PTFE membrane, and the TS was higher (p=0.04) on the PTFE membrane compared with the P(VDF-TrFE)/BT membrane (Table 1). The BV (p=0.07) and TN (p=0.11) were not affected by the membranes (Table 1). The gene expression of Osx (p=0.003), Bsp (p=0.001) and Oc (p=0.002) was higher on the P(VDF-TrFE)/BT membrane compared with the PTFE membrane, while that of Runx2 (p=0.29) was not affected by the membranes (Table 2).

Table 1. Morphometric parameters obtained from three-dimensional reconstructed micro-CT images of new bone formation on rat calvarial bone defects implanted with P(VDF-TrFE)/BT or PTFE membranes (n=4).

Parameter	P(VDF-TrFE)/BT	PTFE	p
BV (mm^3)	10.9±2.6	7.8±1.0	0.07
BS (mm^2)	286±46	194±16	0.01
TN (1/mm)	0.8±0.3	0.6±0.1	0.11
TS (mm)	0.6±0.1	0.7±0.1	0.04

Table 2. Gene expression of cells from new bone tissue formed on rat calvarial bone defects implanted with P(VDF-TrFE)/BT or PTFE (n=4).

Gene	P(VDF-TrFE)/BT	PTFE	p
Runx2	0.9±0.1	1.0±0.1	0.290
Osx	1.7±0.3	1.0±0.1	0.003
Bsp	2.4±0.3	1.0±0.2	0.001
Oc	3.1±0.8	1.0±0.1	0.002

DISCUSSION & CONCLUSIONS: Corroborating our previous in vitro results [1,2], we have shown, by histomorphometric and gene expression analyses, that the P(VDF-TrFE)/BT membrane enhances new bone formation compared with the PTFE membrane. Thus, this composite may be considered a promising alternative to be employed in GBR procedures.

REFERENCES: [1] M.M. Beloti et al (2006) *J Biomed Mater Res A* **79**:282-288. [2] L. N. Teixeira et al (2011) *J Mater Sci Mater Med* **22**:151-158.

ACKNOWLEDGEMENTS: Sao Paulo Research Foundation (FAPESP) and National Council for Scientific and Technological Development (CNPq).

Biomimetic tissue engineering approach using adipose mesenchymal stem cells

YM Elcin[1,2], YE Arslan[1,2], E Baykan[1,2], A Koc[1,2], T Ibsirlioglu[1,2], AE Elcin[1,2]

[1] Ankara University Stem Cell Institute, Ankara, Turkey [2] Ankara University Faculty of Science, TEBNL, Ankara, Turkey

INTRODUCTION: Adipose tissue has recently become a desirable alternative source of multipotent stem cells. Adipose mesenchymal stem cells (AdMSCs) can be collected in large quantities and can easily be propagated with stable population doublings and low senescence levels. Due to its multilineage differentiation potential, this cell source has shown to possess potential therapeutic applicability. Thus, the safety and efficacy of AdMSCs for regenerative therapies is currently under assessment. We have evaluated the osteogenic potential and mineralized bone-like tissue formation of AdMSCs on a biomimetic lamellar composite scaffold [1]. Secondly, we have evaluated the use of AdMSCs-derived cells together with a tubular compartmented tubular scaffold for the development of a biomimetic bioengineered vascular biograft with intima and media layers [2]. Here, some of the challenges of these two distinct biomimetic tissue engineering goals will be discussed.

METHODS: AdMSCs were isolated from human lipoaspirates, expanded upto the tenth passage, characterized immunophenotypically in all passages. While the AdMSCs were directly used in the bone tissue engineering experiments, cells were differentiated into either vascular endothelial-like cells or vascular smooth muscle cells for the vascular tissue engineering study using improved differentiation protocols. For the bone biograft study, AdMSCs were seeded on a nanofibrous multi-spiral composite scaffold and cultured under osteogenic conditions inside a perfusion bioreactor upto a month. For the vascular biograft study, AdMSCs-derived endothelial-like cells were seeded on the intima layer, while AdMSCs-derived vascular smooth muscle-like cells were seeded in the macroporous media layer of the tubular scaffold separately.

RESULTS: *Bone biograft study.* Histology, scanning electron microscopy, mitochondrial activity and calcium assays confirmed the formation of a bone-like tissue in parallel concentric layers producing a lamellar structure of viable osteogenic cells surrounded by a dense mineralized extracellular matrix starting from the second week of the dynamic culture. *Vascular biograft study.* On the other hand, in-vitro formation of a compartmented tubular construct was demonstrated by histochemistry, immuno-histochemistry, scanning electron microscopy, functional assays and quantitative PCR analysis.

DISCUSSION & CONCLUSIONS: Multispiral biomimetic composite scaffold and AdMSCs supported the formation of a lamellar bone-like tissue in-vitro. Secondly, the semi-permeable compartmented tubular scaffold together with AdMSCs-derived cells showed some of the major biological features of a blood vessel. The evaluated tissue types for in-vitro construction are mechanosensitive (either facing compressive loading or hemodynamic shear stress), thus mechanotransduction was necessary to acquire a positive outcome in both of the tissue engineering scenarios. Findings support the indicated potential of AdMSCs in tissue engineering and regenerative medicinal applications. Further studies are planned to reveal the appropriate timing of transplantation (or in-vivo conditioning) of both construct types with the goal to reach the ultimate biomechanical requirements.

REFERENCES: [1]Y.M. Elcin *et al.* Functional bone tissue engineering: generation of new bone tissue from adipose-derived stem cells under mechanotransduction (*in preparation*). [2] Y.M. Elcin *et al.* Mechanoactive vascular graft engineering with adipose mesenchymal stem cells (*in preparation*). Disclosures: Patent Application No.s TPE-2012/06370, TPE-2012/01600.

ACKNOWLEDGEMENTS: The support of The Scientific and Technological Research Council of Turkey is acknowledged (project no.s 108M501, and 111M336).

Bio-inspired surface modification of PET for haemocompatibility enhancement

ED Giol, S Van Vlierberghe, P Dubruel

Polymer Chemistry and Biomaterials Research (PBM) Group, Ghent University, Krijgslaan 281 (S4 bis), B-9000 Ghent. E-mail:peter.dubruel@ugent.be

INTRODUCTION: An increasing demand for synthetic grafts emerged in recent years, as approximately half of the annual human deaths, both in Europe and USA, are related to cardiovascular diseases [1]. Nowadays, large-caliber synthetic vascular grafts are manufactured from poly(ethylene terephthalate) (PET, trade name Dacron®). However, a major drawback of PET is its poor haemocompatibility. Generally, pristine PET presents a hydrophobic surface which allows platelet adhesion and activation, subsequently resulting in graft occlusion (due to thrombosis formation) and ultimately in prosthesis failure.

MARTERIALS & METHODS: Commercially available PET foils (Goodfellow, biaxially oriented) were used as substrates to perform the surface modification. Pristine PET is an inert material lacking functional groups on its surface and thus disabling the possibility of direct grafting of biopolymers. Hence, a two-step surface modification strategy was applied, with an intermediate "coupling agent" inspired from nature. Briefly, a prime layer was initially grafted onto the substrate via an aqueous wet-chemistry procedure enabling, in a subsequent step, the covalent attachment of a biopolymer coating (e.g. gelatin). Gelatin has been selected due to its non-toxic nature, biodegradability and cell-interactive properties, as a protein derived from the extracellular matrix (ECM) [2].

An in depth characterization of thus modified-PET was performed using static contact angle measurements, atomic force microscopy and X-ray photoelectron spectroscopy. In addition, preliminary blood tests, such as platelet adhesion and haemolysis assays were applied on all modified samples.

RESULTS: Variations of the applied surface modification protocol and substrate preparation prior to modification were investigated (see Figure 1). Interestingly, a positive correlation between the nature of layers deposition (cfr. prime layer and gelatine layer) and blood compatibility behaviour was observed. As anticipated, the cumulated effect of the surface roughness and free surface energy influenced the platelet activation.

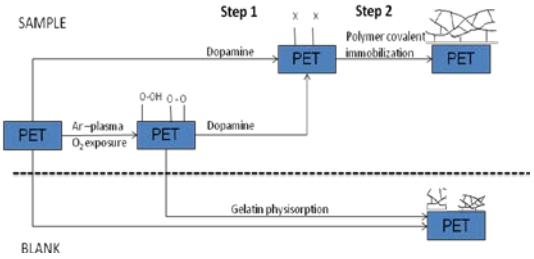

Fig. 1: Schematic representation of the general surface modification strategy.

DISCUSSION & CONCLUSIONS: Up to now, most PET surface modifications were based on physical adsorption of proteins accompanied or not by protein crosslinking reactions. Unfortunately, long-time stability and toxicity issues upon leaching out of the crosslinking agents (e.g. formaldehyde, glutaraldehyde) have been frequently reported [3]. As an alternative, several approaches of chemical surface modification of PET were also reported in literature. But, most of them presented complex, time-consuming and sometimes questionable (regarding bulk properties preservation) procedures. As a result, the successful development of a novel facile chemical approach to couple gelatin onto PET is reported herein. Moreover, a clear improvement of substrate anti-thrombogenicity, after surface modification, was observed.

REFERENCES: [1]European Cardiovascular Disease Statistics (2005 edition), Dept. of Public Health, University of Oxford. [2] S. Van Vlierberghe, et al., (2011) *Polymers* **3**(1): 114-130. [3] Y. Noishiki, et al., (1998) *Artificial Organs* **22**(8): 672-680.

ACKNOWLEDGEMENT: The authors would like to thank Ghent University for the financial support under the form of the GOA project Biomedical Engineering for Improved Diagnosis and Patient-Tailored Treatment of Aortic Aneurysms and Dissection (BOF10/GOA/005). Sandra Van Vlierberghe acknowledges the FWO for the awarded post-doctoral fellowship.

Interaction of human pancreatic ductal adenocarcinoma cells with polymeric scaffolds to develop tissue-engineered cancer models.

C Ricci[1,2], D D'Alessandro[2], S Ugel[1], S Sartoris[1], V Bronte[1], L Moroni[3], S Danti[2]

[1] Dept. of Pathology and Diagnostics Immunology Section, University of Verona, Verona, Italy [2] Dept. of Surgical, Medical and Molecular Pathology and Emergency Medicine, University of Pisa, Pisa, Italy [3] Tissue Regeneration Dept., University of Twente, Enschede, The Netherlands

INTRODUCTION: Pancreatic Ductal Adenocarcinoma (PDAC) is a fatal neoplasia of the exocrine pancreas with a high mortality rate. PDAC microenvironment is heterogeneous and has been found to play a crucial role in carcinogenesis and negative response to treatments. Moreover, early biomarkers are missing [1]. Biomimetic models of PDAC are thus desirable to understand the underlying molecular mechanisms and to approach new therapies. In this view, the development of 3D tumor models via tissue engineering can offer valuable opportunities [2]. The aim of this study was to investigate the interactions between PDAC cells and different scaffolds to generate new 3D *in vitro* models for the study of tumor growth and development.

METHODS: Polymeric scaffolds were fabricated with different techniques: three-dimensional fibre deposition (3DF) and electrospinning (ESP). The polymers employed were PolyActive™ and polycaprolactone (PCL), respectively. Scaffold morphology was characterized via scanning electron microscopy (SEM). After pre-wetting with 2% bovine gelatin, top surfaces of sterile scaffolds were seeded with 150,000 human PDAC cells (seeding volume 50 µl) and cultured in RMPI complete medium for 7 days. At the endpoint, the samples were incubated with Neutral Red (NR) (50 µg/ml) for 3 h and observed under light microscopy to assess cell colonization and viability. Specimens were dehydrated and treated for SEM observation to evaluate cell infiltration and morphology.

RESULTS: 3DF scaffolds were produced with aligned fibers: fibre diameter (d_1) = 260 µm, fibre spacing (d_2) = 800 µm and layer thickness (d_3) = 225 µm. ESP scaffolds showed randomly oriented fibers with diameters ranging in the rage of 1-10 µm. After 1 week, PDAC cells were viable on both scaffolds. However, the NR uptake showed different level of intensity (Fig. 1), denoting diverse viability of the cells grown on the two scaffolds (Table 1). Specifically, PDAC cells on 3DF scaffolds displayed the highest viability. Maximum depth allowing cell infiltration from the top surface was detected at 2 mm for 3DF, while at 1 mm for ESP scaffold (Table 1).

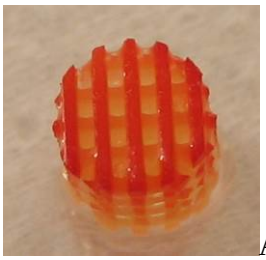
A


B

Fig. 1: Photographs of PDAC cell/scaffold constructs showing localization of viable cells (red) in: (A) 3DF and (B) ESP scaffolds.

Table 1. PDAC cell interaction with 3DF and ESP scaffolds: comparative evaluation.

	3DF scaffold	ESP scaffold
Cell viability	high	mild
3D infiltration	2 mm	1mm

DISCUSSION & CONCLUSIONS: Human PDAC cells were able to colonize both types of scaffolds; however, they showed higher affinity (i.e., viability and infiltration) for 3DF PolyActive™-based scaffolds than for ESP PCL-based scaffolds. Tissue engineering can be exploited to gain knowledge in cancer mechanisms creating 3D *in vitro* biomimetic models with higher complexity and reliability than spheroids or traditional cell culture.

REFERENCES: [1]C. Feig, A. Gopinathan, A. Neesse, D. S. Chan, N. Cook, D.A. Tuveson (2012) *Clin Cancer Res* **18** (16) 4266-4276. [2]E. Burdett, F. K. Kasper, A.G. Mikos, J.A. Ludwig (2010) *Tissue Eng B* **16**: (3) 351-359

Interaction of MSCs with biomimetically-functionalized PU substrates for meniscal tissue engineering

D Cilli[1,2], S Bertoldi[1,3], S Farè[1,3], MC Tanzi[1,3], JJ Cooper-White[2]

[1]BioMatLab, Dept. of Chemistry, Materials and Chemical Engineering "G. Natta", Politecnico di Milano, Milan, Italy [2]Tissue Engineering and Microfluidics Lab (TEaM Lab), Australian Institute for Bioengineering and Nanotechnology (AIBN), University of Queensland, Brisbane, Australia [3]Milano Politecnico Local Unit, INSTM, Firenze, Italy

INTRODUCTION: The meniscus plays a crucial role in load bearing, shock absorption, joint lubrication and stability. The meniscus ECM is mainly composed of Type I-II Collagens (COLI, COLII) and GAGs, in particular Chondroitin-6-sulfate (C6S) [1]. Synthetic polymers, hydrogels and ECM components have been investigated as possible scaffolds for meniscal tissue regeneration [2]. The final aim of our work is to develop biomimetic 3D polyurethane (PU) scaffolds with surface-engineered pores for meniscus regeneration. In this work, we assessed the application of a new surface modification method to 2D PU substrates (of identical chemical composition as the 3D PU scaffolds). The *in vitro* performance of these surfaces, in terms of adhesion, morphology and proliferation, was assessed using human bone marrow-derived mesenchymal stem cells (hBM-MSCs).

METHODS: The PU films were obtained by a previously set up gas foaming process [3]. An appropriate amount of reaction mixture (MDI prepolymer, a polyether-polyol mixture and water as expanding agent) was spread on a glass plate to obtain a thin and compact film. The PU film was then coated with a thin layer of a novel cross-linked gelatin hydrogel system (GEL, with concentrations varying from 3 to 15%) [4]. The gelatin was subsequently modified with biomolecules (COLII and C6S), covalently bound with EDAC/NHS chemistry [5]. At each step of modification, the surfaces were characterized using ATR-FTIR, XPS, BCA protein assay, DMMB Assay and antibody staining. Culture of hBM-MSCs was performed on the modified PU films for 6, 24 hours and 7 days. Cell adhesion, morphology and proliferation were investigated using Cristal Violet, Hoechst and Phalloidin staining.

RESULTS: The IR spectra of the surfaces after each modification step confirmed the presence of the multi-layered biofunctional coating on the PU film, with typical fingerprints regions of both PU and gelatin, and peaks related to the presence of COLII covalently bound to the gelatin and of sulfate groups (i.e. C6S). The XPS survey scan showed an important increase in nitrogen for the coated PU films, due to the binding of proteins, and the presence of sulphur, related to the addition of the sulfate of C6S. By DMMB assay, the adsorption of C6S onto the 15%GEL/COLII was double than that of the 3%GEL/COLII, was detected (56.65±10.56% *vs.* 27.77±12.29%, respectively).

Differences in cell morphology, with more spread cells, between the coated and non-coated surface were visible after 24 hours and 7 days, while no significant differences in cell adhesion between all the modified surfaces were observed, also compared to modified or unmodified TCP controls (Fig. 1a). Stress fibers on the coated PU films were observed after 7 days of culture (Fig. 1b).

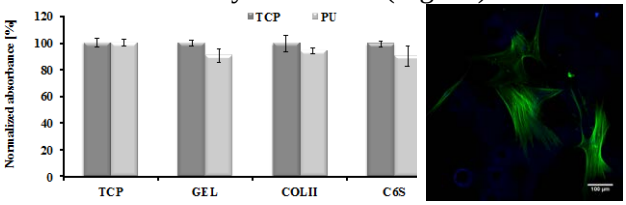

a) b)

Fig. 1: a) Normalized absorbance values by Crystal Violet staining of hBM-MSCs cultured for 6 hours on modified or not TCP and PU films; b) Phalloidin and Hoechst staining of hBM-MSCs cultured for 7 days on GEL-COLII-C6S PU films.

DISCUSSION & CONCLUSIONS: Using the developed coating procedure, multi-layered biofunctional 2D substrates offering specific cell binding sites were produced, thus allowing for adequate hMSCs adhesion and spreading. These promising results suggest that these biomimetically-functionalized surfaces may prove useful in promoting hBM-MSCs differentiation into a chondrocyte phenotype. This critical step will be further investigated, both on 2D and in 3D PU-GEL scaffolds.

REFERENCES: [1]M.A. Sweigart, et al (2001) *Tissue Eng* **7**:111-29; [2]E.A. Makris, et al (2011) *Biomaterials* **32**:7411-31; [3]S. Bertoldi, et al (2010) *J Mater Sci Mater Med* **21**:1005-11; [4]M.C. Tanzi, et al (2012) Patent PCT/EP2012/660277; [5]G.K. Tan, et al. (2011) *Biomaterials* **32**:5600-14.

Using a co-culture model to vascularize a natural cardiac patch from porcine extracellular matrix

Y Wang[1], U Sarig[1], T Bronshtein[2], FYC Boey[1], SS Venkatraman[1], M Marchluf[1,2]

[1] NTU-Technion Biomedical Lab, School of Materials Science and Engineering, Nanyang Technological University, Singapore [2] The Lab for Cancer Drug Delivery & Cell Based Technologies, Faculty of Biotechnology and Food Engineering, Technion-Israel Institute of Technology, Haifa, Israel

INTRODUCTION: Vascularization remains a critical requirement for long term survival of thick engineered tissue construct, such as regenerated cardiac patch. Due to the lack of oxygen and nutrient, cells in native tissue do not survive more than 100 μm away from the nearest blood vessels. Acellular extracellular matrix (ECM), has been intensively studied in recent years owing to its chemical and mechanical properties resembling those of the native cardiac tissue.

METHODS: In this study, a co-culture system of human mesenchymal stem cells (MSC) and human umbilical vein endothelial cells (HUVEC) was employed to analyze and predict the population dynamics of the two species using the Lotka-Volterra model and given culturing conditions [1]. Thick (10-15 mm) acellular cardiac ECM patch was derived from porcine left ventricle with a patented decellularization process [2] with preserved inherent vascular structure. DiI labelled HUVECs singly or co-cultured with MSCs were applied to re-cellularize the vasculature and a perfusion bioreactor was employed to supply medium through the vasculature to the entire tissue slab (*Fig. 1*) over 21 days. AlamarBlue™ assay, histology, and confocal microscopy were used to monitor the cell viability and proliferation overtime.

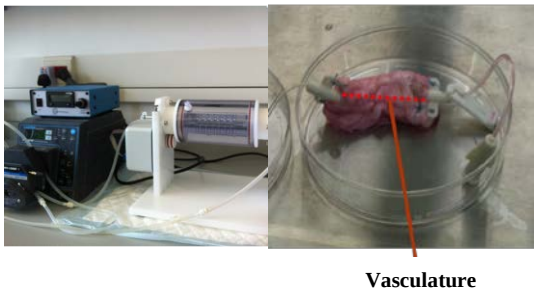

Fig. 1: Perfusion bioreactor system (left) for dynamic culture of thick acellular porcine ECM patch with preserved vasculature (right).

RESULTS: The two species in co-culture system demonstrated a "prey and predator" interaction pattern, in which MSCs exhibited inhibiting "self effect" and enhancing "other effect" on HUVECs. A monolayer of HUVECs lining the vasculature after dynamic culture for 21 days is shown in *Fig. 2*. Improvement of cell coverage and viability was observed with a co-culture dynamic model.

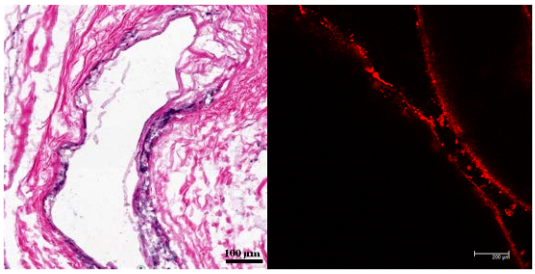

Fig. 2: Cross-sectional image from H&E staining (left) and longitudinal image from confocal microscopy (right) for HUVEC seeded vasculature embedded in the ECM slab.

DISCUSSION & CONCLUSIONS: In this study, we demonstrated that using a mathematical model, the interaction between MSC and HUVEC in co-culture environment can be quantified and predicted. The pre-existing vasculature-like paths embedded in acellular ECM patch supported the subsequent re-endothelialization process. By combining the co-culture approach, accellular ECM scaffold, and dynamic culturing system, growth and stability of cells lining the ECM vasculature were achieved.

REFERENCES: [1] Y. Wang, T. Bronshtein, et al (2013) *Tissue Eng Part A* **19**:1155-64. [2] Y. Eitan, U. Sarig, et al (2010) *Tissue Eng Part C Methods***16**:671-83.

ACKNOWLEDGEMENTS: This research is supported by the Singapore National Research Foundation under the CREATE programme.

Droplets and other things made by microfluidic technology

P Tabeling

MMN, ESPCI, 10 rue Vauquelin, Paris (France)

Microfluidic technology is about handling fluids, under control, in micrometric systems. This technology is entering a new phase of development, in which the number of applications is increasing at an unprecedented rate. Still, the technology has not reached a mature stage.

I will illustrate the situation by commenting on microfluidic droplet technology, in which MMN lab has developed some effort over the last few years.

Droplet based microfluidics is now an important branch of microfluidics. Droplets can be used as chemical reservoirs. They are produced at fast rates in microfluidic chips, and, if their contents can be varied at the droplet level, can be used as screening systems. The current sizes of microfluidic droplets range from 30 to 100 µm. In MMN lab, we have shown that, on using the same microfabrication materials (PDMS), placing ourselves in the same soft lithographic paradigm, one can decrease their sizes by a factor of ten, still keeping an excellent control level. Examples of droplets we currently synthesize are shown on Fig 1. One can see a micrometric photocured particle, a Janus droplet, double droplets. The figure shows that microfluidic technology penetrates into the colloidal domain, by synthesizing objects of colloidal size.

Applications of droplet based technology in the field of droplet material synthesis, drug delivery, biotechnology will be shown. They will illustrate, with other examples, the dynamical stage in which microfluidic technology is experiencing at the moment.

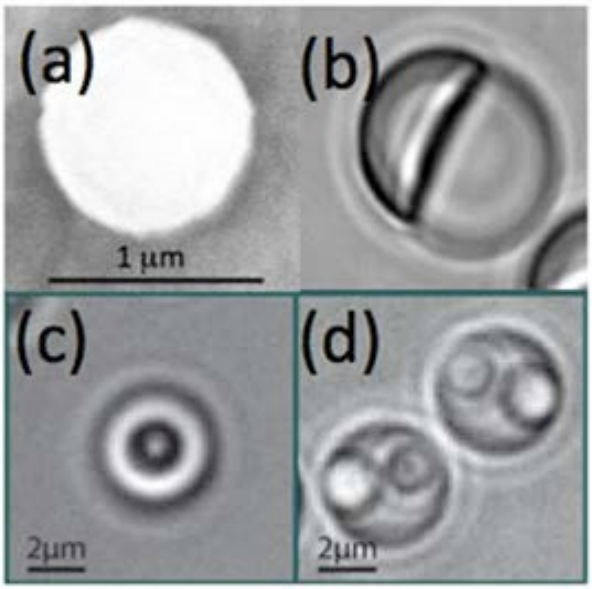

Fig. 1:Examples of colloidal droplets synthesized in MMN Lab.

ACKNOWLEDGEMENTS: We acknowledge ESPCI, CNRS, IPGG for their support.

New microfluidic reactors for Raman imaging of catalytic biomaterials

F Paquet-Mercier, NB Aznaveh, M Safdar, J Greener

Microfluidics and Spectroscopy Labs, Département Chimie, Université Laval, Québec, Canada

INTRODUCTION: Microfluidics (MFs) is growing as a general platform for synthesis and discovery of functional biomaterials due reduced material consumption and the high degree of control over chemical, thermal and hydrodynamic conditions. However, to sustain the growth of new applications, there is a need for sensitive and versatile *in situ* characterisation. For example, new biofilm-based catalysts in flow-through reactors are particularly challenging to monitor spectroscopically because they are low density materials and they consume reagents and produce products at low concentrations. To address this, our group has developed highly functional next-generation MF reactors, which support multi-modal *in situ* spectroscopic imaging. The platform consists of nanostructured metal layers for surface enhanced Raman spectroscopy (SERS). In addition, a novel, two-level reactor architecture enables flow confinement against the SERS surface. Liquid confinement at the SERS surface conserves material, enables localized surface reactions and biofilm growth, and is critical for spectroscopic imaging of the biofilm/surface interface. This system opens the way for sensitive chemical and thermal imaging of biofilms and the related biochemical catalysis they facilitate.

METHODS: A MF channel in polydimethyl siloxane (PDMS) was formed by casting against a mould. A layer of Ag or Au was electrolessly deposited to the bottom of the channel. The metal layer was then transformed into a SERS surface by exposure to air plasma, forming nano structures *via* sputtering. A second PDMS layer was aligned and bonded to the first to introduce a second flow stream, which confined inoculant, growth media and the biofilm and against the SERS surface.

RESULTS: Evidence of the effect of the plasma in forming nanostructured SERS surface was demonstrated with absorption spectroscopy in the UV-visible range. After an initial decrease in absorbance, due to the removal of organic impurities from the metal surface, an increase in absorbance of the Ag plasmon band at 430 nm was observed for plasma treatment times $1 \leq t \leq 19$ mins (Fig 1a). Further optimisation could be achieved by increasing exposure time. Nanoscale surface roughness was confirmed by SEM. A slight increase in the electrical resistance with the plasma treatment time was also observed. Without special optimization of the surface or the analytes, detection at the SERS surface reduced the limit of detection by 100 times while enabling a reduction in the acquisition time by 10 times (Fig. 1b). In addition, the use of special optics allows the monitoring of both Stokes and anti-Stokes scattering bands, for thermal imaging.

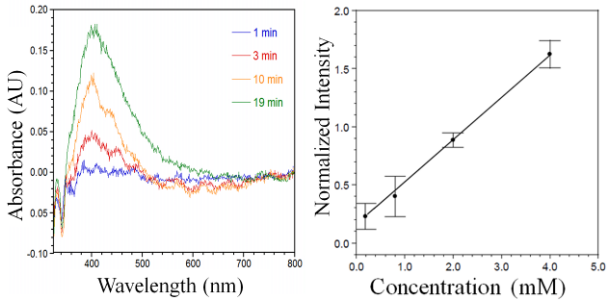

Fig. 1: (a) Diffuse reflectance of the silver surface after different exposures to air plasma (30W, 600 MPa). (b) Calibration of the vC-COO citrate band normalised using vOH band of water (3420 cm^{-1}).

DISCUSSION & CONCLUSIONS: The development of a SERS-based imaging system opens the way for rapid, highly sensitive chemical and thermal imaging of adsorbed biomaterial species and their liquid environments (Fig. 2). In this paper we demonstrate the utilisation of the SERS substrate in MF channels for probing chemical species close to the surface under simple flow as well as in flow patterning conditions. The SERS layer is also investigated as a multipurpose surface, enabling resistive heating and heterogeneous catalysis inside the MF channel.[1]

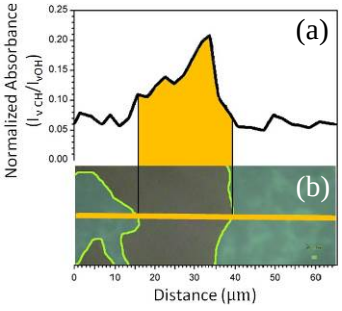

Fig. 2: (a) SERS linear spectral image showing of the CH absorbance intensity from the biofilm, normalized to water OH band. (b) A microscope image of a biofilm segment in a MF channel with edge enhancement (green) to show the biofilm boundary. Spectral image in (a) is acquired along the orange line in (b)

REFERENCES: [1]Xu, B.-B., et al., (2012) *Chemical Comm.* **48:**1680-1682.

Surface patterning for wetting and liquid flow control

A Giacomello[1], M Chinappi[2], S Meloni[3], CM Casciola[1]

[1] *Dipartimento di Ingengeria Meccanica e Aerospaziale, Sapienza Università di Roma, Rome, Italy*
[2] *Center for Life Nano Science@Sapienza, Istituto Italiano di Tecnologia, Rome, Italy,* [3] *CINECA Consortium, Rome, Italy*

INTRODUCTION: Wetting on rough surfaces is a conundrum that challenges both the scientific and the technological communities. The increasing interest for the development of biomimetic material with tailored wetting properties is in fact accompanied by the need of a deeper understanding of interfacial phenomena. The wetting properties of rough surfaces is ruled by the combination of surface morphology and chemistry. A paradigmatic example is provided by the Lotus leave where the multiscale rough surface structure coated by a hydrophobic wax, promotes the entrapment of air or vapour within asperities, resulting in macroscopic properties, such as high contact angle and self-cleaning, that are collectively indicated as superhydrophobicity. Superhydrophobic surfaces are useful in several biomedical-related areas. e.g. as substrates for particle production as support for cell response studies and for anti-bioadhesion applications [1]. In spite of the recent technological advancements, the stability of the entrained air bubbles and the mechanism of wetting remain largely elusive, making it difficult to predict how long a superhydrophobic state will last and to design effectively synthetic material. In this contribution we employed theoretical and simulation method to analyze the stabilty of superhydrophobic state and its effect on liquid flow.

METHODS: Molecular dynamics (MD) simulation have been used to explore the metastable states associated to the wetting of an hydrophobic system at nanoscale [2]. At microscale a generic theoretical approach based on contrained minimization of the system free-energy [3] at different value of liquid filling is employed for different surface patterns. The fluid dynamics of a liquid for different wetting state is characterized via both non-equilibrium MD [4] (at nanoscale) and continuum fluid dynamics approach (at microscale).

RESULTS: The main results of the present research activity are: I) The characterization in term of free-energy barrier and transition pathway of the wetting on regularly patterned surfaces. In particular a novel asymmetric transition mechanism is found for grooved surfaces. II) The application of an innovative generic continuum approach [3] to analyse wetting as a function of the surface morphology and chemistry and of the thermodynamics state. Comparison between MD and continuum results provides evidence of the applicability of the proposed continuum approach also at nanoscale. III) The determination of the drag reduction associated with different wetting states for a realistic system coated by an organic hydrophobic layer. The crucial role of meniscus curvature and triple line position is highlighted.

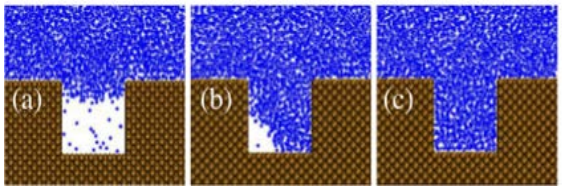

Fig. 1: Snapshot of asymmetric transition pathway of a liquid (blue atoms) filling a hydrophobic groove (brown atoms) obtained via Molecular Dynamics Simulation

DISCUSSION & CONCLUSIONS: State of the art of MD techniques for metastable states analysis and a novel theoretical approach recently developed by our group [3] have been applied to analyse the wetting of regularly patterned surfaces. The emerged phenomenology is significantly richer than expected from existing literature. Our findings potentially open the way to new design criteria for new superhydrophobic materials (potentially inspired by natural organisms) for wetting and friction control.

REFERENCES: [1]B. N. Lourenco et al. (2012) *Biointerphases* **7**:46. [2]A. Giacomello, S. Meloni, M. Chinappi, C.M. Casciola (2012) *Langmuir* **28**:10764–10772. [3]A. Giacomello, M. Chinappi, S. Meloni, C.M. Casciola (2012) *Phys Rev Lett.* **109**:226102. [4]M. Chinappi, C.M. Casciola (2010) *Phys of Fluids* **22**:042003.

ACKNOWLEDGEMENTS: Computational resources for MD simulation were made available by ICHEC (grant ndphy022a) and CINECA (HPC grant 2012)

Nanoparticulated calcium phosphate ceramic for diagnostic: physico-chemical characterization and microbiological properties

A Gala-García[1], T Lobaina[2], R Zhurbenko[2] , I Alfonso[2], DS Peñaranda[3], ADM Gomes[3], SML Gontijo[1], RD Sinisterra[3], C Rodriguez[2], ME Cortes[1]

[1]Department of Restorative Dentistry, Universidade Federal de Minas Gerais – Brazil. [2]Department of Medium Culture Research, Centro Nacional de Biopreparados – Cuba. [3]Chemistry Department, ICEX – UFMG – Brazil.

INTRODUCTION: The search for more rapid diagnostic methods and effective for early detection of microorganisms responsible for infections in humans as well as to control water quality, food and industrial environment of biopharmaceuticals, is coupled to the use of the exceptional tools offered today nanoscience [1]. Nano-funtionalized surfaces have promising biological properties that can be employed for the development of diagnostic systems capable for the faster identification of pathogens microorganism's presents in clinical samples. The aim of this study was to develop nanoparticulated calcium phosphate ceramic devices of rapid diagnosis for detection of micro-organisms [2].

METHODS: Ceramic calcium phosphate synthetic (OSDG) or oyster ceramic derivate (CFN) were characterized physico-chemically by Scanning Electron Microscopy, X-ray diffraction, thermo gravimetric analysis, differential thermal analysis and Potential Z. The microbiological properties were evaluated by incorporating 0,2 ml culture medium and fluorogenic substrate for bacteria. After 3h was added a bacterial culture at $3x10^8$ UFC/ml de *E. coli* and *E. faecalis*, and their detection was performed by UV visible emission ($\lambda = 366$).

RESULTS: The results show that the OSDG nanoparticulated ceramics had polycrystalline structure, higher thermal stability and lower particle size than the CFN and the ratio of calcium / phosphate was 1:6. Nanoparticulated CFN ceramics showed the crystal structure and its ratio of calcium / phosphate was 1:7. The microbiological results showed that the OSDG nanoparticulates ceramics and CFC ceramics reacted fluorogenic effective for rapid detection of *E. coli* and *E. faecalis* after 1:30 h 1:00 h, respectively (Fig. 1).

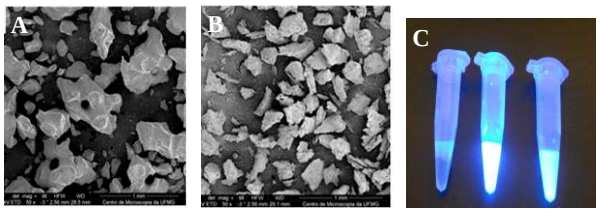

Fig. 1: SEM images of CFN (A) and OSDG (B). Fluorescence detection (C), from left to right: Control, OSDG and CFN.

DISCUSSION & CONCLUSIONS: The characterization of CFN and OSDG showed similar crystal structure, thermal stability and chemical elemental composition, according to the Ca/P ratio of hydroxyapatites. CFN and OSDG ceramics differ among themselves, as regards morphology, structural topography, particle size distribution and capacity of water absorption. These properties influence the rate of microbiological response. Although both materials can be employed as nanostructured supports in microbial diagnostic systems, showing correlation between the enzyme activity of the microorganisms tested and enzyme markers of each composition. The OSDG showed better response than CFN with fluorogenic signal emission in a shorter time.

REFERENCES: [1] K. Riehemann et al., (2009) *Angew Chem Int Ed*, **48(5)**:872-97. [2]M. Cantin et al., (2010). *Int J Odontostomat*, **4(2)**:127-32.

ACKNOWLEDGEMENTS: This work was financed by CNPq, CAPES NanoBiofar, Biocen and FAPEMIG.

Investigation on the influence of grain size on strength, ductility, and corrosion properties in Mg and Mg-Zn based alloys for biodegradable stents

E Mostaed[1], Q Ge[1], M Vedani[1], PA De Oliveira Botelho[2], C Zanella[2], F Deflorian[2]

[1] *Department of Mechanical Engineering, Politecnico di Milano, Milan, Italy*
[2] *Department of Industrial Engineering, University of Trento, Trento, Italy*

INTRODUCTION: Magnesium alloys have been considered as promising candidates for biodegradable stents due to their low corrosion resistance in human-body fluids and good biocompatibility[1]. However, studies also indicated that high degradation rate of magnesium alloys causes the premature loss of stent mechanical integrities in vessels. Thus, before usage, their mechanical and electrochemical behaviour should be considered and possibly improved. From a mechanical point of view, high strength and ductility are required to provide a mechanical support and avoid the recoil of the vessel. [2]. It is proven that adding alloying elements and grain refinement improve both the mechanical and corrosion properties of Mg [1,3]. In this study, Equal Channel Angular Pressing (ECAP) was used to improve mechanical and corrosion properties of pure Mg, ZK21, and ZK60 alloys through achieving an ultra-fine grain (UFG) structure. The mechanical, microstructural, and corrosion behaviour characterization before and after ECAP are reported.

METHODS: wrought ZM21, AK60, and hot extruded pure Mg were selected for investigation. The ECAP for each material was carried out at different initial temperature. That is, three steps at which 4 passes were done, for ZK60 at 250°C, 200°C, and 150°C, two steps for ZM21 at 250°C and 200°C and two for pure Mg at 275°C, 250°C. Microstructural observation was performed by optical and electron microscopy after ECAP. Mechanical properties were assessed on tensile test specimens, and micro hardness tests on the samples. The corrosion behaviour of ECAP processed alloy was compared to that of as received coarse-grained materials by performing open circuit potential (OCP) tests in phosphate buffered solution (PBS) of pH 7.4 and controlled temperature of 37°C.

RESULTS: Fig. 1 shows the microstructure of all the materials after ECAP. It is demonstrated that the processed materials feature equiaxed grains throughout the sample volume for both alloys (the average grain size for ZM21 and ZK60 were 520 and 700 nm, respectively). However, the final grain size ~ 20µm induced by ECAP was achieved for pure Mg. All mechanical features and their values for three different materials are listed in table 1.

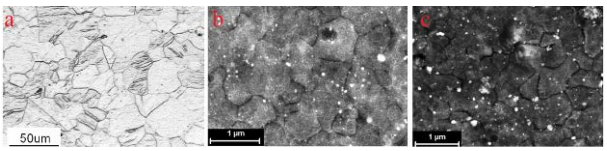

Fig. 1: microstructural of different samples after ECAP processing: pure Mg(a), ZM21 (b), and ZK60(c)

Table 1: mechanical properties of the alloys before and after ECAP

Samples	YS(Mpa)	UTS (MPa)	Elongation to failure (%)	Hardness (HV)
Coarse grain ZM21	180	259	20	50
ECAP ZM21	340	353	11.5	74.3
Coarse grain ZK60	117	340	18.8	67.4
ECAP ZK60	200	285	33.7	80.1

According to the OCP results, in the unprocessed samples a nobler electrochemical behavior of the alloys were observed compared to pure Mg due to the alloying elements, after the ECAP a shift toward more positive potentials can be realized for three samples.

DISCUSSION & CONCLUSIONS: ECAP processing promoted the achievement of ultra-fine grain structure. During the procedure the strength, as well as the ductility of the alloys considerably increased. The corrosion tests revealed a nobler electrochemical behavior of the alloys with respect to pure Mg due to the alloying elements. Furthermore, the OCP measurements showed a meaningful shift toward more positive potentials for both pure and alloys after ECAP process.

REFERENCES: [1] Gu XN, Zheng YF. (2010) *Front of Mater Sci in China* **4**:111–5. [2] H. Hermawan, et al. (2010) *Acta Biomaterialia* **6**:1693–1697.[3] A. Yamashita, et al (2001) *Mater. Sci. Eng. A.* **300**:142-147

Sandwich material systems: A solution for medical applications?

A Carradò[1], G Pourroy[1], L Rimondini[2], H Palkowski[3],

[1] IPCMS UMR 7504 UDS-CNRS, Strasbourg, France [2] Università del Piemonte Orientale, Laboratory of Biomedical and Dental Materials, Novara, Italy [3] IMET, Clausthal University of Technology, Clausthal-Zellerfeld, Germany

INTRODUCTION: Sandwich systems are hybrid materials offering interesting perspectives for the enhancement of biomaterials in terms of e.g. strength or stiffness combined with low density. A tailored biomedical application of such designed systems (BioSMS) can be used to solve the mismatch between bone and implants under load leading to failure of implants, with strong consequences in terms of biological and economical costs. Some examples are given for BioSMS and their mechanical behaviour as well as the cell growth and viability on their surfaces.

METHODS: BioSMS are used as a combination of 316L/PP-PE/316L and Ti/PP-PE/Ti [1], where PP-PE (polypropylene copolymer) and austenitic stainless steel (316L) or Titanium (Ti) represent the core and the skins, respectively. To adapt the BioSMS mechanical properties to the specific needs, the thickness of the layers can be varied. Tensile tests were performed.

For biocompatibility studies, the mono-materials were cleaned with acetone, ethanol and double distilled (dd) water. The specimens were immersed in 10 M NaOH solution, washed with dd water and dried. After that, they were immersed in an acidic bath (Ac) for calcium-phosphate (Ca–P) coating. The composition and the operating conditions of the Ac bath are indicated in [2]. After seeding cells onto the samples' surfaces, the cells proliferation evaluation was assessed by the trypan blue assay [2]. Osteoblasts morphology was investigated by immunofluorescence staining (IF). Cells viability was evaluated by MTT assay.

RESULTS: Table 1 shows the effect of using different skin materials on the resulting mechanical data, e.g. using Ti instead of 316L in the thickness combination 0.5/0.6/0.5 mm reduces the Young's modulus E approx. 50%, coming much closer to the bone condition. Following the rule of mixture [1], one can design the mechanical properties of BioSMS.

Cell viability is much higher in samples with Ca–P layer than in the uncoated ones (Fig. 1). Furthermore, Ca–P coating produced by Ac bath acts as promoter for osteoblasts proliferation. Osteoblasts morphology investigated by IF proves that they are attached and well spread [2].

Table 1. Mechanical properties of mono-materials and selected BioSMS. StSMS and TiSMS are the BioSMS with steel skin and Ti, respectively. UTS: Ultimate Tensile Strength and YS: Yield Strength

	Thickn [mm]	YS [MPa]	UTS [MPa]	E [GPa]
316L	0.5	293±8	641±20	198±10
Ti	0.5	170±3	321±2	93±1
PP-PE	0.6	27±1	31±1	1.5±0.2
Bone (cort.)		30-100	70-150	15-30
StSMS	1.6	193±8	398±13	99±4
TiSMS	1.6	114±2	211±2	52±2

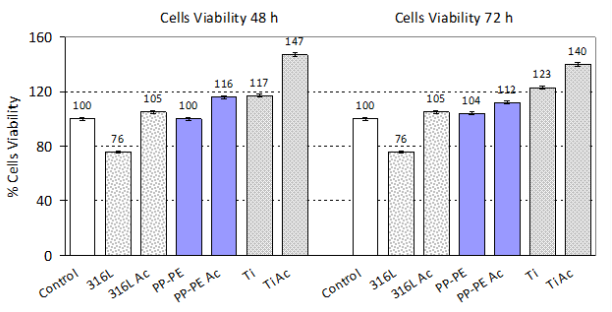

Fig. 1: Osteoblasts viability onto untreated and treated (– Ac) mono-materials after 48 h and 72 h of cells-biomaterials direct contact.

DISCUSSION & CONCLUSIONS: It can be stated that: (i) Changing the thickness of the layers allows the mechanical properties to be adjusted to the needs; (ii) Ca-P coatings increase the cytocompatibility of all surfaces so to be a promising treatment to improve the biocompatibility of BioSMS and (iii) Ca-P layers improve the osteoblasts proliferation as well as their density in respect to the uncoated surfaces of PP-PE and 316L.

REFERENCES: [1] A Carradò et al (2011), *Compos Struct* **93**:715-721. [2] VQ Le et al, (2013) *RSC Adv* DOI: 10.1039/C3RA23385E.

ACKNOWLEDGEMENTS: The authors thank DFG, DAAD, EGIDE, and APIC-DEU-PICS for funding this research.

Nanowire silk fibroin/hyaluronic acid scaffolds via a novel process

SQ Yan[1], WL Xu[1], MZ Li[2], Q Zhang[1]*

[1] *College of Textile Science and Engineering, Wuhan Textile University, Wuhan, China.* [2] *National Engineering Laboratory for Modern Silk, Soochow University, Suzhou, China*

INTRODUCTION: The design of biodegradable, biofunctional and biocompatible nanostructured materials is a major goal of recent work in the world of biomaterials research [1]. We sought to develop nanostructure scaffolds using a novel method to produce a stable and controllable nanowire by degradation of silk fibroin (SF) in silk fibroin/hyaluronic acid (HA) scaffolds with collagenase IA, while avoiding wild organic solvents.

METHODS: SF, SF/HA scaffolds were prepared following a procedure described previously [2]. Collagenase IA (2.7 U/mg, Sigma) was employed to degrade the silk based scaffolds. The changes in the SF, SF/HA scaffolds were investigated by scanning electron microscopy (SEM) and energy-dispersive X-ray spectrometer (EDS).

RESULTS & DISCUSSIONS

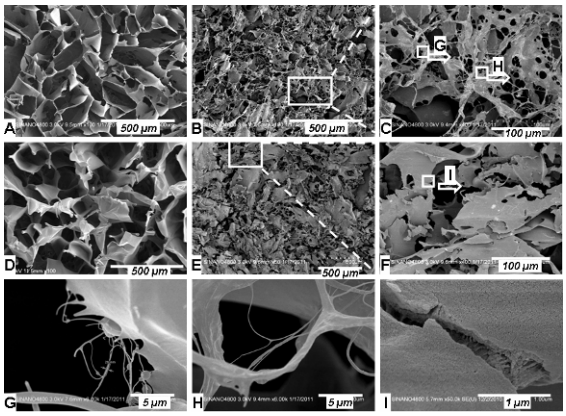

Fig. 1 Morphological changes of SF based scaffolds degraded at different time points. (A, B, C, G, H) SF/HA scaffolds, (D, E, F, I) SF scaffolds, (A, D) 0 d, (B, E) 12 d.

SEM photographs showed that their pore morphologies were intact and uniform and the pore size was large before incubation (Fig. 1). After incubation the two kinds of scaffolds did not keep their original form and had collapsed. After 12 days immersion in enzyme solution, the SF scaffold was fragmented and discontinuous (Fig. 1(E, F)) and some SF crystals were exposed (Fig. 1I). While the SF/HA scaffold remained porous, a network structure and many fiber-like wires were also observed (Fig. 1(B, C, G and H)). HA contains 59.61% C, 2.42% N, and 30.57%, O [3].

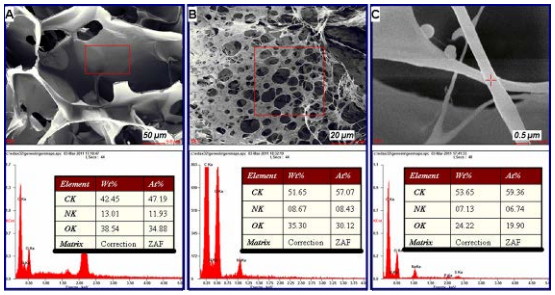

Fig. 2 EDS analysis SF based scaffolds degraded. (A) SF scaffolds before degradation, (B, C) SF/HA scaffolds degraded for 12 d.

The C content of the degraded SF/HA scaffolds was higher than that of pure SF scaffolds, and the N and O contents were diminished. The elements C, N, O percentages of the nanowire (53.65%, 7.13%, 24.22%) also confirmed that the predominant component of the nanowires was HA. These suggests that a small amount of HA degraded during incubation with the collagenase IA solution. The collagenase IA enzyme molecules easily penetrated into the random coil structure of the scaffolds, broke peptide bonds, and released free soluble peptides or free amino acids [4]. HA molecules with large molecular weights were many times larger than that of SF and could be cross-linked with SF by EDC [5]. When part of SF was degraded and digested, the HA and a few SF were left to compose the degraded scaffold skeleton and form nanowires after freeze-drying.

CONCLUSIONS: Nanowires were obtained by a novel approach of enzyme degradation. Silk scaffolds with nanowires, along with the robust material properties of HA, increase the degradation lifetime of scaffolds from days to months or longer.

REFERENCES: [1] Zhang Q, Zhao Y, Yan S, et al (2012) *Acta Biomater* **8**:2628-38. [2] Yan S, Zhang Q, Wang J, et al (2013) *Acta Biomater* **9**:6771-82 [3] Ren Y, Zhou Z, Liu B, et al (2009) *Int J Biol Macromol* **44**:372-8. [4] Zhao C, Wu X, Zhang Q, et al (2011) *Int J Biol Macromol* **48**:249-55. [5] Yan S, Li M, Zhang Q, et al (2013) *Fiber Polym* **14**:188-94.

ACKNOWLEDGEMENTS: This work was supported by Introduction Funding of Wuhan Textile University (125010, 125018).

Chitosan scaffolds with hierarchical porosity

L Altomare[1], E Guglielmo[1], EM Varoni[2], L Rimondini[2], L De Nardo[1]

[1]*Dipartimento di Chimica, Materiali, Ing. Chimica 'G. Natta', Politecnico di Milano. Italy*
[2]*Dipartimento Scienze della Salute, Lab Odontostomatologia, Università del Piemonte Orientale, Italy* *lina.altomare@polimi.it*

INTRODUCTION: Chitosan (CH) is a versatile biopolymer whose morphological and chemico-physical properties can be modified for a variety of biomedical applications [1]. By exploiting the CH electrolytic nature, cathodic polarization allows its deposition on electrically conductive substrates [2], resulting in tunable thin porous structures [3]. Here we propose an easy method to obtain CH scaffolds with highly oriented microchannels for tissue engineering application via a simple control of the process parameters.

METHODS: Cathodic deposition on patterned metallic substrates has been performed in galvanostatic conditions (j =15-40 mA cm^{-2}) starting from CH solution [1g/L] in acetic acid (pH 3.5). Morphological and structural analysis of the coatings have been performed after rinsing in deionized water and drying overnight. Self-standing scaffolds have been detached from the cathode after freeze drying the coatings. Specimens have been weighted and observed by optical and Scanning Electron Microscopy

RESULTS: Obtained porous structures showed a morphology and weight dependence on apparent current density, time, and substrate patterns. A progressively increase in mass deposition have been observed (Fig 1) as a consequence of the total amount of the charge passed during the electrochemical process.

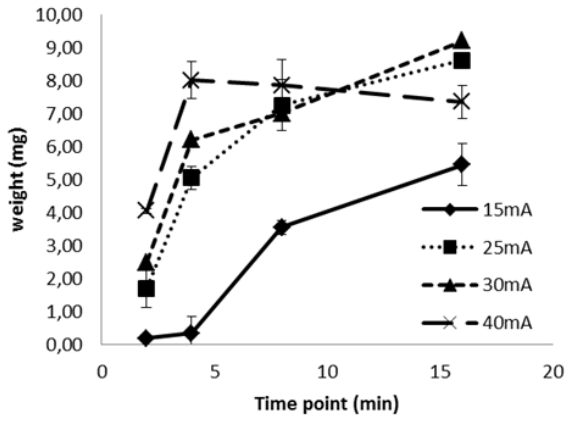

Fig. 1: Deposition on 500µm grid at different currents and time points.

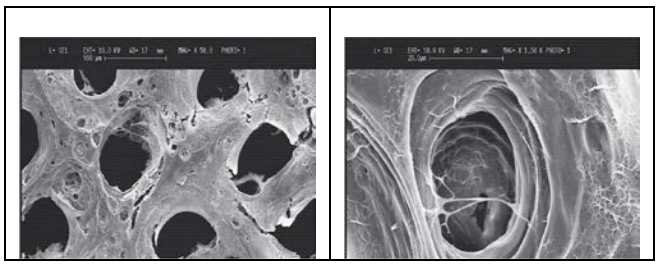

Fig. 2: SEM image of oriented pore structure. The electrodeposited CH net displays an oriented macro-porosity, (A), a random micro-porosity (B).

Figure 2 shows the typical morphology of the obtained structures. It is possible to notice macro-pores (micro-channels), due to the substrate patterning, and micro-pores, due to H_2 bubble evolution [2]. Both levels of porosity can be controlled in order to design scaffolds with a hierarchical organization. Dimensions of microchannels strongly depends on substrate patterns and total charge passed, decreasing in diameter by increasing the polarization time and currents.

DISCUSSION & CONCLUSIONS: Cathodic polarization is an easy technique to realize scaffold with different porosity and highly oriented microchannels. The oriented channels can improve cells and tissue orientation while the microporosity support nutrient diffusion and could promote vascularization; in vivo tests with promising results are under investigation. The properties of these scaffold such as porosity, channel dimensions, thickness and swelling ability, can be easily tuned and target depending on the tissue to be regenerated.

REFERENCES: [1] A. Francesko and T. Tzanov (2011) *Adv Biochem Eng Biotechnol* **125**:1-27 [2] J. Redepenning et al. (2003) *JBMR*; **66A**:411-6 [3] L. Altomare et al (2012) *Materials Letters* **78**, 18–21.

ACKNOWLEDGEMENTS: LA and LD thank MIUR - FIRB Futuro in ricerca (Surface-associated selective transfection - SAST, RBFR08XH0H) for the economic support.

Effect of dialysis and freezing on the properties of silk fibroin hydrogels

MR Ribeiro[1, 2*], MA de Moraes[3], MM Beppu[3], FJ Monteiro[1, 2], MP Ferraz[1, 4]

*[1] Instituto de Engenharia Biomédica, Universidade do Porto, Porto, Portugal [2] Departamento de Engenharia Metalúrgica e Materiais, Faculdade de Engenharia (FEUP), Universidade do Porto, Porto, Portugal [3] Faculdade de Engenharia Química, Universidade Estadual de Campinas (UNICAMP), Campinas-SP, Brasil [4] Centro de Estudos em Biomedicina, Universidade Fernando Pessoa, Porto, Portugal. * ribeiro_marta88@hotmail.com*

INTRODUCTION: Silk fibroin (SF) is a natural fibrous protein spun from *Bombyx mori* silkworm. The cocoon of the silkworm is mainly constituted by two protein components, fibroin and sericin. Sericin is a glue-like protein that holds SF fibers together in the cocoon case [1-3]. SF has two types of molecular conformation of the secondary structure, called silk I and silk II. Silk I is a metastable form of SF that is soluble in water and non-crystalline; random coil and α-helix conformations are usually called silk I. On the other hand, silk II is a highly stable and organized structure that is insoluble in water; the β-sheet conformation is called silk II [3]. The aim of this work was to verify the influence of dialysis and freezing on the properties of silk fibroin hydrogels.

METHODS: Cocoons of *Bombyx mori* silkworm were supplied by Bratac (São Paulo, Brazil). The cocoons were degummed three times by soaking in 1 g/L of Na_2CO_3 solution at 85 °C for 30 min to remove the sericin. The SF fibers were dried and dissolved in a ternary solvent of $CaCl_2$:CH_3CH_2OH:H_2O, in a molar ratio of 1:2:8, at 85 °C, to a SF solution of 10% (w/v). SF gels were prepared after 3 and 7 days of dialysis and the influence of freezing process was analyzed. Thus, a part of the SF gels underwent a slow freezing at -20 ºC for 24 h, followed by lyophilization and the other part of SF gels were kept at 8 ºC for 24 h, with further lyophilization. The samples were characterized by X-ray diffraction (XRD), Fourier transformed infrared spectroscopy (FTIR), thermogravimetric analysis (TGA) and scanning electron microscopy (SEM).

RESULTS: XRD results showed that all SF hydrogels had a distinct halo at 2θ=20-21°, indicating that the secondary structure conformation of the hydrogels is β-sheet. Gels formed after 7 days of dialysis showed another halo at around 2θ=45º. FTIR-ATR results indicated that silk I and silk II structures are presented simultaneously in all SF gels. TGA analysis showed that all samples presented similar trends with a peak of thermal degradation at around 330 ºC. SEM results showed that the SF gels subjected to freezing presented a pore size much larger (Fig. 1a and c) than the gels kept at 8 ºC (Fig. 1b and d).

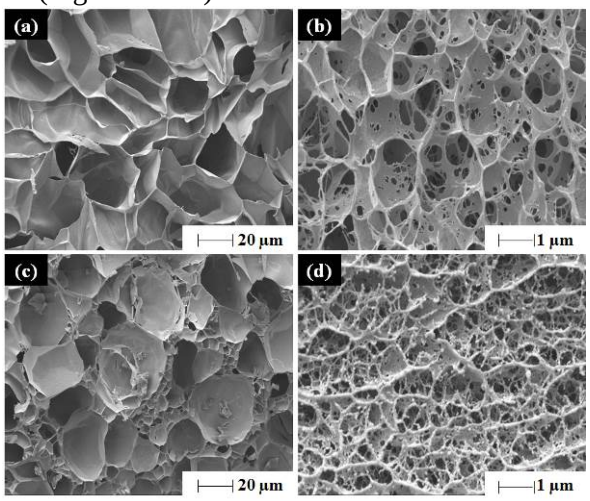

Fig. 1: SEM images of the porous structure of (a) SF gel formed at 37ºC after 3 days of dialysis and subjected to freezing, (b) gel formed at 37 ºC after 3 days of dialysis and kept at 8 ºC, (c) gel formed after 7 days of dialysis subjected to freezing and (d) gel formed after 7 days of dialysis kept at 8 ºC.

DISCUSSION & CONCLUSIONS: Both silk I and silk II are present in all SF gels. Freezing did not alter the material crystallinity; however, dialysis time affected it. Dialysis time and freezing did not alter the thermal behavior of gels. The effect of freezing was visible on the porous structure of SF gels considerably increasing pore size. Freezing will probably increase the mechanical strength of the gel and this is subject of ongoing work.

REFERENCES: [1]G.H. Altman, et al (2003) *Biomaterials* **24**:401-16. [2]N. Bhardwaj, et al (2011) *Int J Biol Macromol* **49**:260-67. [3]M.A. Moraes, et al (2010) *Polymers* **2**:719-27.

ACKNOWLEDGEMENTS: This work was financed by FEDER (COMPETE) and by FCT in the framework of the NaNOBiofilm project (PTDC/SAUBMA/111233/2009) and PhD grant (SFRH/BD/90400/2012), whose support is acknowledged. The support of CAPES-FCT, CNPq e FAPESP is acknowledged.

Chitosan/apatite composite bulk materials by low temperature processing techniques and its mechanical properties

T Onoki[1], T Tago[1], Y Naganuma[1], A Nakahira[1,2]

[1]Department of Materials Science, Graduate School of Enginnering, Osaka Prefecture University, Japan. [2]Kansai Center for industrial Materials Research, Institute of Materials Research, Tohoku University, Japan.

INTRODUCTION: Composite materials based on hydroxyapatite (HA) [$Ca_{10}(PO_4)_6(OH)_2$] and natural or synthetic polymers have been developed. The advantages of these kinds of systems lie, in general, in combining the functional properties of single phase materials. Natural polymer-based composites obtained from collagen, alginate, gelatine, and chitosan (CHI) play a significant role in many tissue engineering applications due to their tailor-made physical, chemical, mechanical, and biological characteristics [1]. In this study, we aimed at the synthesis of a material with better biocompatibility and mechanical properties by composed chitosan and HA. CHI and calcium hydrogen phosphate dehydrate (DCPD), which is well known as precursor of HA were mixed via a co-precipitation method. CHI/HAp bulk ceramics was prepared by a hydrothermal hot-pressing method (HHP) [2-5] that prepare bulk ceramics as low temperature as 150˚C and its flexural strength were estimated.

METHODS: A co-precipitation method was employed for processing CHI/DCPD hybrid material in nano-meter scale. CHI powder (LLWP, Kimika, Japan) was selected for preparing composites. The CHI powder was dissolved in aqueous acetic acid until a homogeneous 5 mass % CHI solution was attained. Then, the CHI solution was mixed into a 1.0-*M* calcium nitrate solution. CHI/DCPD hybrid material was prepared by the above explained addition of CHI and Ca ion source to 1.0-*M* diammonium hydrogen phosphate solution. The synthetic CHI/DCPD hybrid material and calcium hydroxide were mixed in a mortar for 90 min with a Ca/P stoichiometric ratio of HA (1.67). The mixed precursors were solidified in 2h at 150˚C with 10-40 MPa presser conditions via the HHP [2-5]. And then composite bulk materials with different densities were obtained. Mechanical strength of the CHI/HA composite was evaluated by 3-point bending tests.

RESULTS: Fig. 1 shows relationship between bending strength and chitosan content with HAp in various pressure conditions. Under pressure conditions of 10, 20, 40 MPa, bending strength of 3.5 wt% additive amount was improved about twice the additive-free CHI.

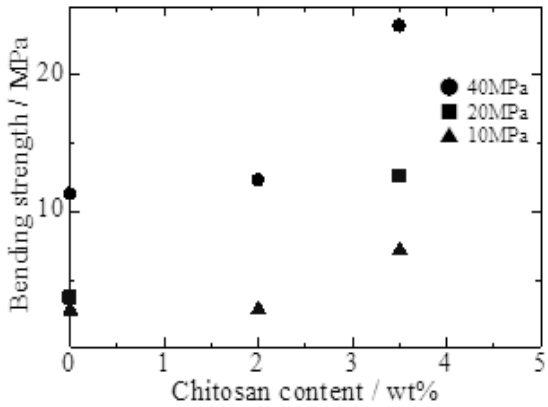

Fig. 1: Relationship between bending strength and chitosan content in various HHP pressure.

DISCUSSION & CONCLUSIONS: Compared with the HA only material, The density and bending strength of the prepared composite bulk materials were close to values of human cortical bone by above shown low temperature techniques. The composite bulk materials have possibilities for new biomaterials with good strength and density. CHI and DCPD in submicron meter scale, was useful for improving for mechanical properties of CHI/HA bulk material in processing CHI/DCPD hybrid material.

REFERENCES: [1] N.Davidenko *et al., Acta Biomaterialia*, **6** (2010) 466–476. [2] N. Yamasaki *et al., J. Mater.Sci. Lett.*, **5** (1986) 355-365. [3] T.Onoki *et al*., *Scripta Mater.*, **52** (2005)767-770. [4] S. Ishihara *et al., Mater. Sci. Eng. C*, **29** (2009) 1885-1888. [5] T. Onoki *et al., Appl. Surf. Sci*., **262** (2012) 263-266.

ACKNOWLEDGEMENTS: This work was partly supported by a "Grant-in Aid, 23760702 and 25390043" from the Ministry of Education, Culture, Sports, Science and Technology of Japan.

Entrapment of Cells within Core-shell Electrospun Scaffold Fibers

A Hui Ying[1], SA Irvine[1], R Avrahami[2], U Sarig[3], T Bronshtein[3], E Zussman[2], F Boey[1], M Machluf[3], S Venkatraman[1]

[1]NTU-Technion Biomedical Lab, School of Material Science and Engineering, Nanyang Technological University, Singapore [2]Faculty of Mechanical Engineering, Technion – Israel Institute of technology, Haifa, Israel [3]Faculty of Biotechnology and Food Engineering, Technion – Israel Institute of technology, Haifa, Israel

INTRODUCTION: Co-axial electrospinning has been used to produce core-shell fibers. This structure is useful in many applications including drug delivery and material encapsulation. Proteins, genes and growth factors are common biomolecules that have been entrapped in core-shell fibers. Prokaryotic cells such as *E coli.* and *Z. mobilis* have been reported to be entrapped within the electrospun scaffolds.[1-3] However it remains a challenge to produce a fiber containing a sufficient density of viable and quantifiably proliferative mammalian cells. Such a cell bearing fiber can form the basis of a bioactive scaffold with the physical support for cellular growth and can express biological signals to modulate tissue regeneration. Here, we assess the use of a PCL shell and a novel core solution containing 2%PEO in 50%FBS to produce a robust electrospinning system for fabricating cell bearing scaffolds for 293 cell line and primary Human Umbilical Endothelial cells (HUVECs).

METHODS: Core-shell fibers were electrospun using a PCL (shell) and PEO:FBS (core) polymer system. Mammalian cells, HEK 293 cells and HUVECs were stained with an appropriate dye (please specify which one) and resuspended in the PEO:FBS core solution prior to coaxial electrospinning at a voltage of 12kV. After the collection of the fibers, the entrapped cells were visualized using fluorescence microscopy using DiI stain. Cell viability was evaluated using Fluorescein diacetate (FDA) and AlamarBlue® assays.

RESULTS: The 293 cells and HUVECs were successfully entrapped in the core-shell electrospinning system. Intact entrapped cells were observed using DiI. FDA positive viable cells were detectable for up to 48 hrs post spinning. For an extended viability studies, the rezasurin-based AlamarBlue® assay was performed. The results showed that cells were viable and proliferative within the fibers for at least two weeks. This demonstrates that cells can be viably entrapped within electrospun scaffolds with the potential of controllable cell deposition for even distribution of cells within a bioengineered scaffold.

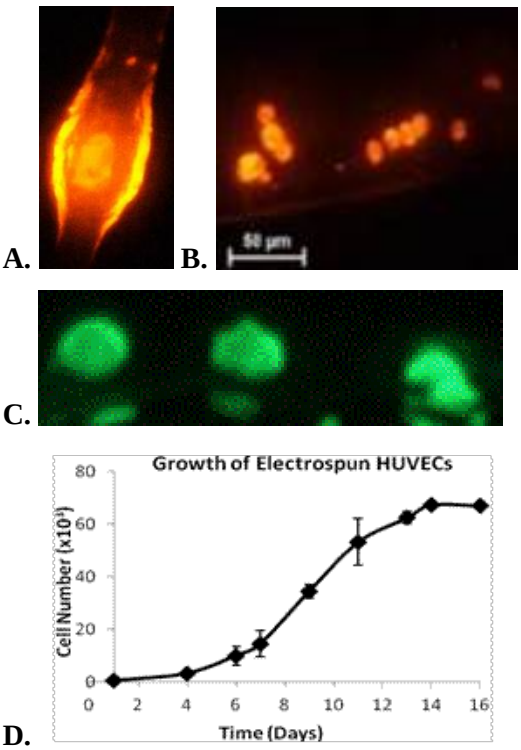

Fig. 1: DII stained 293 cells (A) and HUVECs in PCL fiber (B), FDA stained HUVECs in PCL fibers(C) Growth assay of electrospun HUVECs using Alamar blue (D).

CONCLUSION: Eukaryotic cells can be successfully entrapped within PEO:FBS core and PCL shell fibers. The entrapped cells are viable and are shown to be proliferative within fibers as seen from the microscopic images and AlamarBlue assay.

REFERENCES: [1] Liu, M. H. Rafailovich, R. Malal, D. Cohn, D. Chidambaram (2009) *PNAS* **106**:14201-6 [2] J. S. Klein, R. Avrahami, S. Tarre, M. Beliavski, M. Green, E. Zussman (2009) *Biomacromolecules* **10**:1751-56. [3]Townsend-Nicholson, S. N. Yayasinghe (2006) *Biomacromolecules* **7**:3364-69

ACKNOWLEDGEMENTS: This research is supported by the Singapore National Research Foundation under CREATE programme (NRF-Technion): The Regenerative Medicine Initiative in Cardiac Restoration Therapy Research Program.

Mesoporous titanium surfaces limit bacterial adhesion

F Variola[1], S Francis Zalzal[2], A Leduc[2], J Barbeau[2], A Nanci[2]

[1]*Faculty of Engineering, University of Ottawa, Faculty of Dentistry* [2]*Université de Montréal, Canada*

INTRODUCTION: Contamination of surfaces, fomites and medical instruments by opportunistic pathogens is the main culprit for hospital-acquired infections. The costs in human lives, extended hospital stay and antibiotic therapies add considerable burden on healthcare. The problem extends to implantable materials, where infection can jeopardize the success of prosthetic devices. While rigorous cleaning, disinfection and sterilization protocols are there to remain, the search is still on for materials that will inherently discourage the spread of microorganisms. Adhesion is the initial step in the invasion of surfaces by microorganisms. It therefore becomes evident that interfering with it holds the key to preventing the subsequent cascade of events that leads to colonization and biofilm formation. In this work, we have evaluated the capacity of a simple oxidative chemical treatment to control the adhesion of microorganisms on titanium. The adhesion of *E. coli*, *S. aureus* and *C. albicans* was tested because together they are responsible for a large proportion of nosocomial infections in hospitals and biomedical applications.[1] Our results show that the adhesion of two of these microorganisms was significantly hampered by the mesoporous surface, and suggest that it can also affect the integrity and invasive potential of *C. albicans*.

METHODS: A 50:50 mixture of H_2SO_4 (37N)/H_2O_2 (30%) was used to generate mesoporous surfaces. These are characterized by a network of nanosized pits with a diameter of about 20 nm and the presence of a 40-50 nm thick amorphous TiO_2 layer, which exhibits a greater wettability as compared to the naturally occurring passive titanium dioxide.[2]

RESULTS: There was much less binding of *S. aureus* on the mesoporous Ti as compared to polished control Ti. More than 80% of the scanning electron microscope (SEM) images taken on mesoporous surfaces showed less than 25 bacteria and 11% of them showed no bacteria at all. Only 5% of images contained more than 100. For control samples, the percentage of images with less than 25 bacteria was 26%, and 58% of regions examined were colonized by more than 100 bacteria. In the case of the *E. coli* strain, SEM imaging of side-by-side smooth/mesoporous surfaces displayed a visually and readily evident reduction in adhesion on the treated half of the titanium discs. Quantitative experiments with *C. albicans* were more complex to interpret because of the filamentous nature of this microorganism. However, SEM images overall showed less long filaments on the mesoporous surface suggesting a reduction in pathogenic capacity. In addition, the overall structural integrity of the microorganism appeared affected compared to controls.

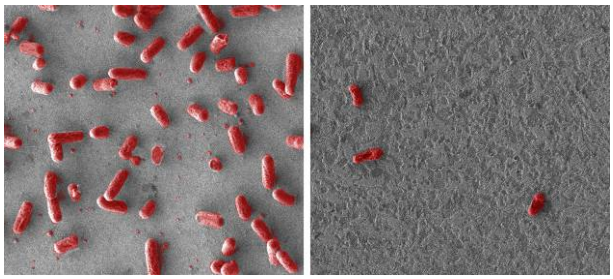

Fig. 1: Bacterial adhesion (S. Aureus) on smooth (left) and mesoporous (right) titanium.

DISCUSSION & CONCLUSIONS: We demonstrate that oxidative nanopatterning can be applied to titanium to reduce adhesion of *E. coli*, *S. aureus*, and the aggregation capacity and integrity of *C. albicans*, microorganisms responsible for implant-related and hospital-acquired infections. Based on these results, it can be inferred that the physicochemical cueing exerted by the mesoporosity is a determinant factor in the observed antimicrobial effects.

REFERENCES:

[1]D.P. Calfee (2012) *Annu. Rev. Med.* **63**:359–371.
[2]F. Variola, J. Brunski, G. Orsini, et al (2011) *Nanoscale* **3**:335-353.

ACKNOWLEDGEMENTS: Support from the Canada Foundation for Innovation (CFI), the Canadian Institutes of Health Research (CIHR) and the Natural Sciences and Engineering Research Council of Canada (NSERC).

Nanoporous titanium surfaces for sustained drug elution

K Komm, M Miles-Rossouw, A Ketabchi, F Variola

Faculty of Engineering, University of Ottawa, Canada.

INTRODUCTION: The development of nanostructured surfaces that effectively promote biological events at the material- tissue interface has emerged as an efficient strategy to improve current biomedical implants by securing a faster and more stable tissue integration [1]. The next generation of implantable devices should also feature the capacity to prevent the onset and spreading of bacterial infection. Approximately 5% of the orthopedic prostheses require in fact replacement because of bacterial infection [2]. Therefore, the creation of implantable metals capable of simultaneously serving multiple purposes has quickly become a priority. Oxidative nanopatterning (i.e. etching with solutions of an acid, or base, and an oxidant) is an effective tool to improve the biological response to titanium. This results in the creation of characteristic nanoporous surfaces capable of direct physicochemical cueing to cells [3]. In this work, we have quantified for the first time the loading capacity and elution kinetics provided by the nanoporosity without the use of linking agents. To this end, bovine serum albumin (BSA, a large globular protein) and vancomycin (i.e. one of the most effective antibiotics against gram-positive bacteria) were selectively chosen to reflect commonly used model compounds.

METHODS: A 50:50 mixture of H_2SO_4/H_2O_2 was used to generate nanoporous surfaces on grade 2 titanium disks. To investigate elution profiles, BSA- and Vancomycin-loaded disks were immersed in custom-made holders containing distilled water at 37 °C to mimic body temperature, and placed on a horizontal shaker. Aliquots were collected at various time points and analyzed by UV-VIS spectroscopy. Scanning electron microscopy (SEM) was used to image samples before and after elution.

RESULTS: Scanning electron imaging of treated surfaces revealed the characteristic nanometric 3-dimensional sponge-like structure on titanium surfaces (Figure 1). This is composed by nanosized pits of about 20 nm in diameter. At the chosen concentration, smooth controls did not provide any significant direct effects on retaining the compounds onto the surface. Nanoporous surfaces, however, offer a 3-dimensional porosity with nanoconfined volumes that provided physical entrapment and/or additional adsorption sites for the bioactive agents, ultimately allowing loading them onto titanium surfaces. The 3-dimensional nanoporosity also contributed to control their dissolution kinetics, ultimately providing an extended elution. The linear portion of the curve was used to extrapolate the dissolution rate (i.e. initial burst). We are now extending these studies to Raman spectroscopy and imaging to validate their application to the quantification of elution profiles and molecule-surface interactions.

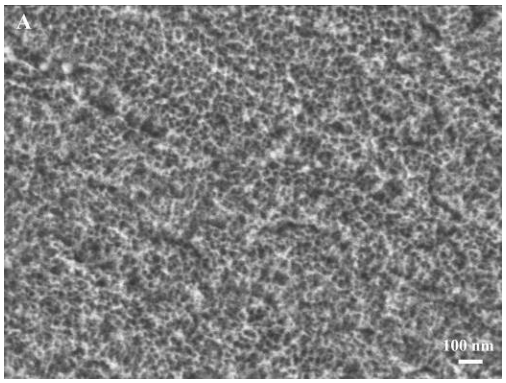

Fig. 1: Nanoporous titanium surface generated by oxidative nanopatterning.

DISCUSSION & CONCLUSIONS: Our study shows that, compared to smooth controls, nanoporous surfaces enable to load significantly greater amounts of BSA and Vancomycin, and provide their extended release over relatively longer periods of time. Taken together, these results demonstrate that, similarly to anodization, oxidative nanopatterning is an efficient strategy to engender nanostructured titanium surfaces that synergistically integrate enhanced bioactivity and sustained drug-delivery capabilities.

REFERENCES: [1]F. Variola, J. Brunski, G. Orsini, et al (2011) *Nanoscale* **3**:335-353. [2]B. Ercan, E. Taylor, E. Alpaslan et al (2011) *Nanotechnology* **22**:295102-295113. [3]F. Vetrone, F. Variola, P. T. de Oliveira, et al (2009) *Nano Letters* **9**:659-665

ACKNOWLEDGEMENTS: F. Variola acknowledges funding from the uOttawa Faculty of Engineering, the Canada Foundation for Innovation, Ontario Ministry of Research and Innovation and the Natural Sciences and Engineering Research Council of Canada (NSERC).

HELP-based matrices for stimuli-responsive controlled release of bioactive compounds

A Markulin, L Corich, V Borelli, F Vita, A Bandiera

Dipartimento di Scienze della Vita, Università di Trieste, Trieste, IT.

INTRODUCTION: Direct delivery of bioactive substances to the sites of injury represents a key issue for therapies based on regenerative medicine and tissue repair [1]. Protein derived hydrogels represent an interesting system for this purpose because they possess several features that make them suitable to this purpose. A method for preparation of hydrogel matrices based on Human Elastin-like Polypeptide (HELP) has been set up [2]. HELPs are a family of elastin-like recombinant biopolymers modeled after the most regularly repeated domain in human tropoelastin, retaining peculiar properties as self-assembling and thermoresponsive behavior [3]. In this study we assayed two elastolytic activities from different sources to test their potential to specifically degrade the HELP matrix.

METHODS: Proteolytic activities were obtained from *P. aeruginosa* PAO1 strain and activated human polymorphonuclear neutrophils (PMN). HELP and HELP1 biopolymers degradation by elastolytic activities was analyzed by 10% SDS-PAGE. HELP matrices were prepared as already detailed [2]. A method to follow HELP matrix degradation was set up adding Coomassie blue dye before crosslinking. Matrix degradation was followed monitoring the release of the dye in the supernatant.

RESULTS: First we tested our HELP and HELP1 biopolymers against the two elastolytic activities to assess their susceptibility to proteolysis. (Fig.1).

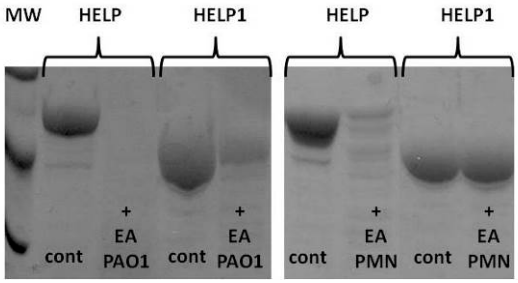

Fig. 1: SDS-PAGE analysis of HELP and HELP1 biopolymers treated with elastolytic activities (EA) derived from P. aeruginosa PAO1 strain and from PMN

The analysis evidenced that HELP biopolymer is more susceptible to degradation that HELP1 This is suggestive of a prominent degradation at the level of the crosslinking domains that are present only in the HELP biopolymer and confirming the presence of elastolytic activity in the samples.
Then we tested the same proteolytic activities against the HELP derived matrices. Both elastolytic activities have been shown to be able to degrade the matrix since it was entirely dissolved within 48 hours while the control counterparts remained intact (Fig. 2).

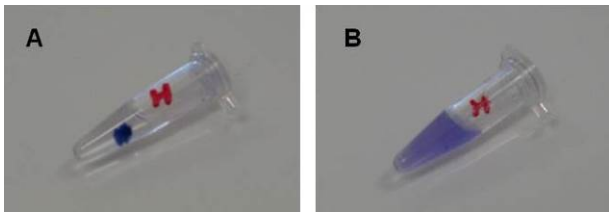

Fig. 2: HELP matrix after 48 hours incubation at 37°C in the absence (A) and in the presence (B) of P. aeruginosa proteolytic activity

DISCUSSION & CONCLUSIONS: The procedure to prepare stable hydrogels from HELP biopolymer exploited the reaction catalyzed by the microbial enzyme transglutaminase. This method can be employed for entrapment of proteic bioactive substances and can be used to realize smart devices for the delivery of biological products. In particular, pathologic conditions that involve an abnormally increased elastolytic activity like for example cystic fibrosis and chronic wounds could represent interesting models to assay the potential therapeutic use of our matrices. Our results show that HELP hydrogels represent a promising tool to realize loadable delivery devices to elicit drug release by a specific stimulus.

REFERENCES: [1]R. Censi, P. Di Martino, T. Vermonden, et al (2012) *J. Control Release* **161**:680-92. [2]A. Bandiera (2011) *Enzyme Microb Technol* **49**:347-52. [3]A. Bandiera, P. Sist, R. Urbani (2010) *Biomacromolecules* **11**:3256-65.

Recombinant human elastin-like magnetic microparticles for drug delivery and targeting

G Ciofani[1], GG Genchi[1,2], B Mazzolai[1], V Mattoli[1], A Bandiera[3]

[1] *Center for Micro-BioRoboti cs, Istituto Italiano di Tecnologia, Italy* [2]*The BioRobotics Institute, Scuola Superiore Sant'Anna, Italy.* [3]*Department DSV, University of Trieste, Italy*

INTRODUCTION: Recombinant proteins represent a new and promising class of polymeric materials in the field of biomaterials research. Human elastin-like polypeptides (HELPs) have been developed as recombinant versions of elastin, with the purpose of enhancing some peculiar characteristics of the native protein, like self-assemby [1-2]. Here, we report on the production of magnetic HELP microparticles prepared through a water-in-oil emulsion process for drug delivery and targeting.

METHODS: HELP microparticles were prepared with an emulsion/reticulation approach. Briefly, 50 µl of the protein solution (50 mg/ml in TRIS/HCl 10 mM, pH 8) were mixed with 5 µl of magnetic nanoparticles (25 mg/ml, Fe_3O_4 100 nm, stabilized with oleic acid), 50 µl of Tween 85 (a surfactant) and 5 µl of transglutaminase (120 U/ml), an enzyme that allows HELP reticulation to occur. This aqueous phase has been mixed in 400 µl of isoctane (the oil phase) and stirred under vigorous magnetic agitation (1,200 rpm) for 2 hours at room temperature. Thereafter, microparticles were collected and washed through several centrifuge steps in bi-distilled water.

The obtained microparticles were characterized with optical microscopy, scanning transmission electron microscopy (STEM) and dynamic light scattering (DLS).

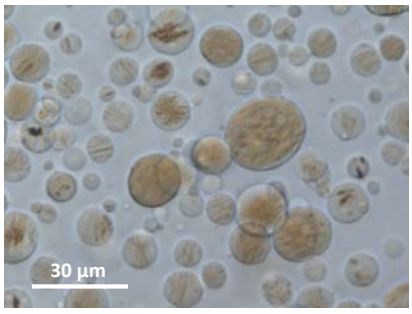

Fig. 1: Optical microscope image of the prepared microspheres.

RESULTS: The presence of lysine and glutamine residues within the alanine rich domains of HELP allows the specific enzymatic cross-linking by transglutaminase to occur [3]. Thus, solid polymeric microparticles through the water in oil emulsion process could be obtained.

The obtained microspheres (Fig. 1) own a perfectly regular and round shape, having an average size of about 11 ± 5 µm. STEM imaging and microanalysis, moreover, revealed an even distribution of magnetite inside the particles, that confers them magnetic properties, thus allowing their manipulation through an external magnetic field (Fig. 2).

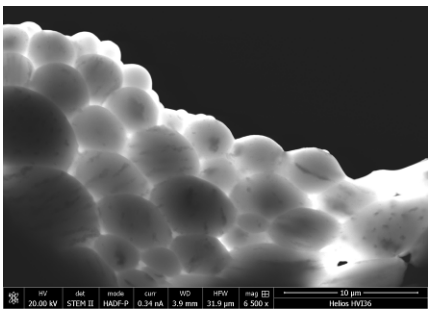

Fig. 2: STEM image of the microspheres, showing magnetite nanoparticles inside the polymeric structure.

DISCUSSION & CONCLUSIONS: Magnetic, recombinant human elastin based microparticles were prepared. Current studies are focused on the characterization of their magnetic properties and on the assessment of their drug delivery and targeting abilities. This system represents an interesting multifunctional platform: the developed microparticles could be in fact exploited as drug delivery and targeting system, but applications in hyperthermia could also be envisaged, making HELP-based systems intriguing and innovative "smart" materials.

REFERENCES: [1] A. Bandiera, A. Taglienti, F. Micali, et al (2005) *Biotechnol. Appl. Biochem.* **42**:247-56. [2] G. Ciofani, G.G. Genchi, I. Liakos, et al (2013) *Acta Biomater.* **9**:5111-21. [3] A. Bandiera (2011) *Enzyme Microb. Techn.* **49**:347–52.

ACKNOWLEDGEMENTS: Authors would like to thank Mr. Carlo Filippeschi (Istituto Italiano di Tecnologia) for electron microscopy technical assistance.

Scaffold-free tissue engineering based on surface-modified magnetic human cells

MR Dzamukova, EA Naumenko, NI Lannik, RF Fakhrullin

Kazan (Idel buye/Volga region) Federal University, Institute of fundamental medicine and biology, Kreml uramı 18, Kazan, Republic of Tatarstan, 420008, RF.

INTRODUCTION: Tissue engineering aims at the fabrication of human tissues *de novo*, the using cells as building blocks. Typically, cells are placed on artificial scaffolds to reconstitute the native tissue [1]. Magnetic tissue engineering allows for creating tissue prototypes with elaborate structure without using scaffolds. In addition, magnetically-labelled tissues could be easily visualized using magnetic resonance imaging. Thus, the application of magnetic nanoparticles (MNPs) in human tissue engineering methodology is currently regarded as an advanced technique.

The method of magnetization, which we earlier described [2] as alternative strategy for magnetic labelling of human cells, is based on employing the cationic polyelectrolyte-stabilized MNPs for the direct one-step surface modification of human cell membranes without compromising the viability of the cells.

RESULTS AND DISCUSSION: At the first stage we prepared (poly)allylamine hydro-chloride (PAH) stabilized positively charged MNPs as reported elsewhere [2]. We apply our technique for magnetic labeling of adenocarcinomic human alveolar epithelial cells (A549) and human skin fibroblasts (HSF) used here as the model cells for prototype lung tissue engineering. The influence of magnetic functionalization on different physiological features of cells has been carefully examined. We investigated the enzyme activity, apoptosis induction, cell index, membrane and DNA integrity and zeta-potential. The lung-tissue mimicking multicellular clusters were created using the viable MNPs-coated A549 and HSF cells and permanent magnetic field. As shown in Scheme 1, the first layer of the cells was assembled from the MNPs-coated HSF above the 3 mm NdFeB cylindrical magnets positioned under the wells, and 2 days later the second layer was formed likewise using the MNPs-coated A549 cells.

After 2 days of co-incubation we observed the formation of alveoli-mimicking emerging and mature pores in the multilayered clusters (Figure 1). In addition, we found that the MNPs do not penetrate in cytoplasm and do not affect the viability of the cells. This technique is a new effective application of surface-functionalized magnetic human cells for the fabrication of lung-tissue mimicking assemblies [3].

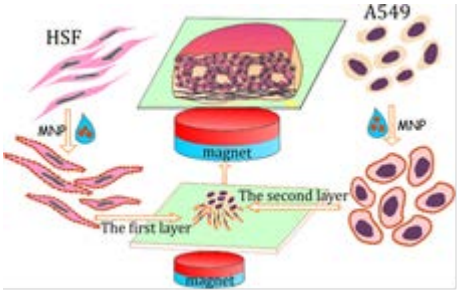

Scheme 1. A sketch illustrating the lung-mimicking tissue fabrication employing magnetically-facilitated assembly of MNPs-functionalized HSF (first layer) and A549 (second layer) cells.

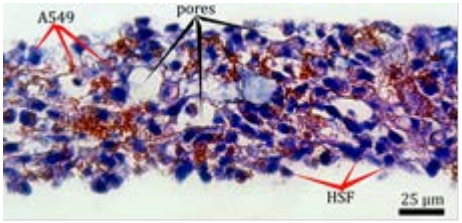

Fig. 1 Optical microscopy images of thin sectioned paraffin-embedded hematoxylin–eosin stained magnetically-facilitated lung-mimicking multicellular clusters fabricated from MNPs-functionalized A549 and HSF cells.

REFERENCES: [1] M. Horst, S. Madduri, V. Milleret, T. Sulser, R. Gobet and D. Eberli, *Biomaterials* (2013) **34**: 1537-45. [2] M.R. Dzamukova, A.I. Zamaleeva, D.G. Ishmuchametova, Y.N. Osin, D.N. Nurgaliev, A.P. Kiyasov, O.N. Ilinskaya and R.F. Fakhrullin, *Langmuir* (2011) **27**: 14386-93. [3] M.R. Dzamukova, E.A. Naumenko, N.I. Lannik, R.F. Fakhrullin, *Biomater. Sci*. (2013) DOI:10.1039/C3BM60054H.

ACKNOWLEDGEMENTS: This study was supported by RFBR 12-04-33290 (Leading young scientists support) grant.

Engineered nanocarbon surfaces for nanomedicine

S Orlanducci[1], S Gay[1], G Reina[1,2], V Guglielmotti[1,2], E Tamburri[1], T Lavecchia[1], ML Terranova[1], M Rossi[3]

[1] Minimalab, Dip. di Scienze e Tecnologie Chimiche, University of Rome Tor Vergata, Via della Ricerca Scientifica 00133 Roma, Italy. [2] Nanoshare s.r.l.Via G. Peroni 386, 00131 Roma, Italy [3] Electron Microscopies and Nanoscopies (EMiNa) Lab, Department of Basic and Applied Sciences for Engineering, and Sapienza Nanotechnologies and Nanosciences (SNN) Lab, CNIS, University of Rome Sapienza, Rome Italy

INTRODUCTION: The research of new materials and multimodal architectures for nanomedicine is today a rapidly developing research area and functional systems engineered at the nanoscale are finding wide application for prevention, diagnosis and treatment of diseases. These systems provide promising alternatives to conventional biosensors, and open completely new routes to imaging/labeling, to drug delivery, to fabrication of micro- and nano-scale scaffolds for tissue growth.

However, for biomedical applications, composition and structure of the surfaces contacting biological systems must meet strict requirements in terms of biocompatibility and long-time reliability.

Recent researches demonstrated that, among the inorganic materials used in nanomedicine, the sp^2 and the sp^3 hybridized nanocarbons have the primacy.

It has been proven that nanodiamond is excellent substrate for the adhesion and growth of several types of cells in vitro, and that its surface can selectively bind various biological molecules. In this context, nanodiamond can be considered a good candidate for bio-implants, for controlled administration of therapeutic agents, as well as an ideal surface for site-specific targeting/labeling and for sensing/detecting biological systems[1,2] .

As regards sp^2 carbon, fullerenes, graphite nanoplatelets, carbon nanofibers and nanotubes have been tested as drug delivery platforms, as sensing elements and reinforcing agents for bio-devices, as tools for separating and purifying biological systems.

RESULTS: In our labs a variety of different strategies are being explored to prepare specifically shaped surfaces enabling nanocarbon-based bioapplications. In particular, graphitic dendrimers with various size, shape, branching and surface functionality and nanodiamond systems formed by elongated structures (nanorods, nanowhiskers, nanopillars nanocones) are proposed as attractive scaffolds for tissue growth, for selective attachment of targeting groups and for bioanalytical applications.

This presentation will illustrate some relevant synthetic strategies for the engineering of nanocarbon-based platforms and some examples of multivalent architectures for bio-related applications.

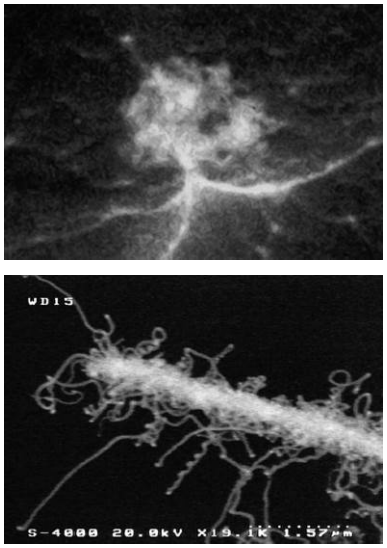

Fig. 1: Examples of dendridic carbon structures.

REFERENCES: [1]Xiao X, Wang J, Liu C, Carlisle JA, Mech B, Greenberg R, Guven D, Freda R, Humayun MS, Weiland J, Auciello O (2006) *J Biomed Mater Res B Appl Biomater.* **77(2)**: 273-81. [2]Yang W, Auciello O, Butler JE, Cai W, Carlisle JA, Gerbi JE, Gruen DM, Knickerbocker T, Lasseter TL, Russell JN Jr, Smith LM, Hamers RJ. (2002) *Nature Material* **1(4)**: 253-7. [3] S. Orlanducci, V. Guglielmotti, V. Sessa, E. Tamburri, M.L. Terranova, F. Toschi, M. Rossi, (2012) *Mater. Res. Soc. Symp. Proc.* **1395**, 93-98.

Nanocarbon-based biomaterials: present and future

OS Shenderova[1,2], S Hens[1], I Vlasov[3], JM Rosenholm[4]

[1] *International Technology Center, Raleigh, NC.* [2] *Adámas Nanotechnologies, Raleigh, NC.*
[3]*General Physics Institute, Moscow* [4] *Abo Akademi University, Turku, Finland*

INTRODUCTION: Being made from the major element of life, carbon nanostructures represent a special class of nanomaterials which raise minimum concern on biocompatibility when integrated with biological systems. All major representatives of the nanocarbon family, carbon nanotubes, graphene, fullerenes and nanodiamonds have unique properties rendering their use in different niche biomedical applications. After a brief survey of major classes of nanocarbons and their potential medical use, we will focus on two nanocarbons, nanodiamond (ND) particles and nano-graphene\graphite oxide (nGO), which recently emerged as multifunctional non-toxic alternatives to semiconductor quantum dots for biomedical imaging and carriers for drug delivery.

RESULTS: ND particles with the smallest crystal size of just a few nanometers (Fig.1a,b) are produced by detonation of carbon-containing explosives or by grinding microdiamond powders manufactured by static high-pressure, high-temperature synthesis [1]. Diamond particles have remarkable optical and mechanical properties in combination with biocompatibility, high specific surface area, and tunable surface structure. They are the least toxic of all carbon nanoparticles [1]. Foreign atoms can be incorporated into the lattice of ND particles, providing unique photoluminescent (PL) and spin properties. Particularly, the nitrogen-vacancy (NV) center in diamond has photostable red\NIR emission without blinking and long life time (~20ns) appealing for the time-gated imaging. The spin state of the negatively charged NV center in ND particles is highly sensitive to a surrounding magnetic field so that ND-NV can be used to probe the nanoscale intracellular environment of cells. NDs containing radiation defects were used in cathodoluminescent and photoacoustic imaging. Using the ND as a drug carrier, improved therapeutic efficiency and safety were demonstrated and applications have included gene delivery and cancer therapy [1].

Multifunctional composites of PL ND and porous silica shell used for theranostic applications [2] as well as PL carbon dot-decorated NDs will be also discussed demonstrating synergistic advantages of combining nanostructured materials. *In vivo* multiphoton imaging using nGO (Fig.1c,d) produced by oxidation of nanographite structures using graphite intercalated acids [3] will be also demonstrated.

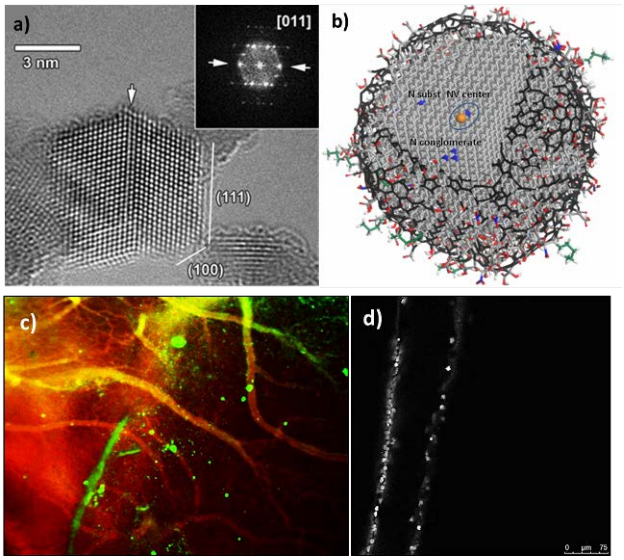

Fig. 1: HRTEM of detonation ND particles demonstrating highly ordered diamond core (a) and schematic model illustrating the structure of a single ~5-nm ND (b). (c) Metastasized cancer cells (green) moving toward blood vessels (red) imaged with stereo microscope. (d) High resolution multiphoton imaging of nGO-labeled cancerous HeLa cells (grey) decorating blood vessels.

Development of multimodal imaging probes based on 5nm ND and doping of ND with new functional elements are future directions for this field. The key issues that impact the nanodiamond market with a particular emphasis on research and development, manufacturing and cost implications will be discussed.

REFERENCES: [1] V. Mochalin, O. Shenderova, et al. (2012) *Nature Nanotech.*, **7 (1)**: 11-23. [2] N. Prabhakar et al., (2013) *Nanoscale* **5**: 3713-22 [3] Hens et al.(2012) *J.Phys.Chem.C* **116**: 20015-22.

ACKNOWLEDGEMENTS: N. Prabhakar and T. Näreoja are acknowledged for *in vivo* imaging,

Porous silicon films and microparticles as a vehicle for the loading and extended release of Infliximab to the eye

SJP McInnes[1], Y Irani[2], HR Lad[1], KA Williams[2], NH Voelcker[1]

[1] Mawson Institute, University of South Australia, Mawson Lakes, SA. [2] Department of Ophthalmology, Flinders University, Flinders Medical Centre, Bedford Park, SA.

INTRODUCTION: Infliximab is a chimeric IgG1 monoclonal antibody against tumour necrosis factor-alpha (TNFα), which is used systemically for the treatment of uveitis, (prevalence of 17 people per 100,000). Porous silicon (pSi) is a highly porous inorganic material, which completely degrades in the body to non-toxic orthosilicic acid[1]. The material's pore size and degradation kinetics can be easily tuned via the fabrication parameters and the surface chemistry. pSi has the ability to load large amounts of drug [1]. Here, we use porous silicon (pSi) films and microparticles (MP's) as carriers for the localized release of Infliximab to the tissues of the eye. The biocompatibility of pSi in the eye has been confirmed previously in our laboratory (Fig. 1) [2].

METHODS: pSi films (Fig. 2 A and B) p^{++} type Si wafers (resistivity 0.55-1 mΩcm) are produced by electrochemical etching in a Teflon anodization cell and at 226 $mAcm^{-2}$ in a 3:1 v/v HF:EtOH mix for 20 sec. pSi MP's (Fig 2 C and D) are produced by etching for 4 min and subsequently electropolished for 10 sec at 500 $mAcm^{-2}$. pSi was then sonicated for 20 min in ethanol and dried under vacuum. pSi films and MP's were thermally oxidised for 1 h. pSi films and MP's were immersed in 1 mg/mL Infliximab solution for 16 h.

RESULTS: SEM micrographs of pSi film and MP are shown in Fig 2. The pSi films were found to load a maximum of 1.69 mg Infliximab per mg of pSi, quantified via interferometric reflectance spectroscopy, while the MP's were able to load approximately 0.117 mg/mg, quantified by thermogravimetric analysis. Release of Infliximab from pSi MP's was monitored over 9 days via ELISA at a rate of 19.3 pg/mg per day, with more or less zero order release profile (Fig. 3). Our results demonstrate the potential for extended antibody release over several weeks.

DISCUSSION & CONCLUSIONS: The higher loading of Infliximab onto films is proposed to be due to the more efficient trapping of the substrate bound pSi films compared to the pSi MP's which are open on both sides and cannot trap the payload as easily. We envisage that the Infliximab loaded pSi can be implanted or injected in a single administration and would degrade in the body. This would be a significant advance over the current antibody therapy, requiring regular intraocular injections which are painful and bear the risk of infection.

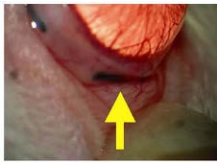

Fig. 1: pSi surgically implanted under the subconjunctiva of a rat.

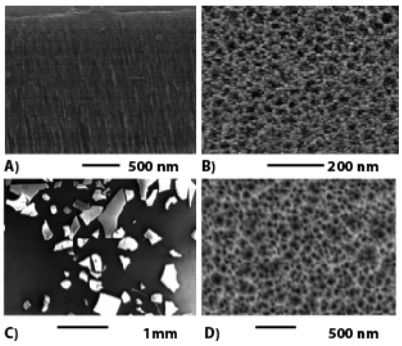

Fig. 2: Characterisation of pSi films and MP's. A) pSi film cross section, B) top down view of the porous structure showing pores of 30 - 80 nm, C) pSi MP's showing a size distribution of 195.8 ± 88.9 μm and thickness of 30 μm and D) pSi MP pore structure with pores ranging from 30 - 40 nm.

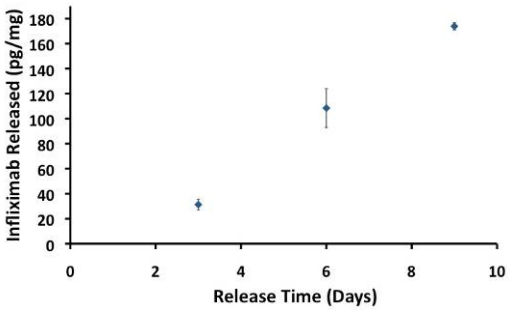

Fig. 3: Release of Infliximab from pSi MP's quantified by means of ELISA.

REFERENCES: [1] S.J.P. McInnes, N.H. Voelcker (2009) *Future Med. Chem.* **1**(6):1051-1074. [2] S.P. Low, N.H. Voelcker, L.T. Canham, et al (2009) *Biomaterials* **30**:2873-2880.

Novel thermo-responsive poly (N-vinyl caprolactam)-g-chitosan sponges as an on-demand drug delivery system for pain management

S Indulekha, P Arunkumar, R Srivastava, D Bahadur

Indian Institute of Technology, Bombay, Mumbai-400076, India

INTRODUCTION: Orthopaedic surgeries which include Total knee replacement and surgeries for Joint injuries, Osteoarthritis, are mostly accompanied by pain and discomfort in the affected region. Several strategies have been followed to manage the pain and swelling caused, but still remains ineffective. Current regimes of the pain management include administration of Non-steroidal anti-inflammatory drugs (NSAIDs) and opioids and in combination of both. However these NSAIDs can possibly cause side effects such as gastro-intestinal problems and drowsiness. An effective drug delivery system has been developed in order to control pain and swelling caused due to the post-surgical implications especially for the orthopaedic surgeries in knee and joints. Hence the drug delivery systems has to be designed in such a way that when they are placed at the surgical site, can deliver the drug on application of heat locally. The application of heat is by means of a heat pad which can be used by the patient whenever they experience the pain. To achieve this, a novel thermo-responsive sponge has been developed which is made up of thermo-responsive polymer Poly (N-Vinyl Caprolactam) grafted onto Chitosan (PNVCL-g-CS) loaded with a NSAID, Etoricoxib (COX-2 inhibitor) for the pain management application.

METHODS: PNVCL is a water soluble, biocompatible polymer which exhibits phase transition at ~ 33° C and synthesized using free radical polymerization of the monomer, N-vinyl caprolactam. However the phase transition temperature of the polymer has to be increased to around 40°C for the desired application of controlled drug release on application of heat locally. In order to achieve this, PNVCL is grafted by EDC-NHS coupling onto the chitosan [1], which is also a hydrophilic, biodegradable and biocompatible polymer and optimized to the desired phase transition temperature by varying its grafting ratio. PNVCL-*g*-CS sponges are synthesized by crosslinking with glutardehyde followed by neutralizing and washing procedures [2].

RESULTS: The sponges are characterized for Scanning Electron Microscopy (SEM) to analyse the surface morphology of the sponges, Fourier Transform Infra Red Spectroscopy (FT-IR) to confirm the grafting and formation of the crosslinked sponges and Differential Scanning Calorimetry (DSC) studies to determine the phase transition temperature which is 40°C. Porosity, swelling and in vitro degradation of the prepared sponges also have been studied for the prepared sponges. Drug loading at room temperature and *in vitro* drug release at desired temperature (40°C) with Etoricoxib has been measured. Cell viability (MTT assay) has been done for these thermo-responsive sponges with L929 mouse fibroblast cell lines and proven its biocompatibility *in vitro.*

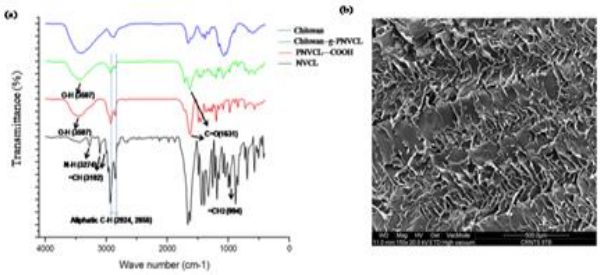

Fig. 1(a): FTIR representing the grafting of PNVCL and chitosan. Fig.1(b) SEM morphology of PNVCL-g-chitosan sponges.

DISCUSSION & CONCLUSIONS: The drug release profile clearly shows a significant increase in drug release at 40°C than at room temperature. Hence the thermo-responsive PNVCL-g-CS sponges can be a promising on-demand smart drug delivery system for the pain management especially for orthopaedic post-operative application. It can be easily delivered by application of local heat when required by the patient to reduce the pain.

REFERENCES: [1] M. Prabaharan, J.J. Grailer, D.A. Steeber, S. Gong (2008) *Macromol. Biosci.* **8**: 843-51. [2] R. Jayakumar, R. Ramachandran, V.V. Divyarani, K.P. Chennazhi, H. Tamura, S.V. Nair (2011) *Int. J. Biol. Macromol.* **48**: 336-44.

In situ PCL micro particles loaded chitosan composite gels as an intra articular drug delivery system for the treatment of osteoarthritis

P Arunkumar, S Indulekha, R Srivastava, P Sharma, S Vijayalakshmi

Indian Institute of Technology, Bombay. Mumbai-400076. India

Email id: kumar.arun205@gmail.com

INTRODUCTION: With the increase in the understanding of the pathogenesis of Osteoarthritis (OA), there has been an introduction of wide variety of drugs including DMOADs, NSAIDs and biological agents. However, current therapy of OA is still challenged by several issues. These include lack of specificity, limited half-life, toxicity, high cost, and lack of efficacy. Currently the delivery of the drugs is usually systemic which comes with severe adverse effects like gastrointestinal toxicity. In addition, the pharmacokinetics of systemic and oral delivery is mostly not desirable. Taking these problems together, an ideal treatment for OA would give maximal efficacy at a minimal dosage; accumulate preferentially at the sites of inflammation and joint destruction.

One way of increasing the effective dose and reducing the total dosage is by means of intra-articular drug delivery systems. The main goal of the current work is to develop an in situ thermo-gelling composite system for intra articular delivery of drugs for OA. In this work, we have prepared a composite in situ thermo-gelling Chitosan system (CIG) which comprise of Etoricoxib (a COX-2 inhibitor) loaded PCL (Poly Caprolactone) microparticles embedded in an in situ forming chitosan gel, which becomes gel at physiological temperature (37°C). There can be two advantages of having in situ gelling system. Firstly, to prevent the escape of the drug loaded microparticles from the intra-articular (IA) region. Secondly, Chitosan, a glucosamine derived from chitin and has a similar structure as that of hyaluronan is found to prevent chondrocytic apoptosis, which is found to happen in OA.

METHODS: Etoricoxib loaded PCL microparticles is prepared by Oil/Water (O/W) emulsion solvent evaporation method. SEM, FTIR and DSC studies are done for the microparticles. In situ chitosan thermogelling system is prepared by mixing 1.6% chitosan solution with 60% Ammonium Hydrogen Phosphate (AHP) followed by incubation at 37°C. The composite in situ gels (CIG) is prepared by dispersing PCL microparticles in the chitosan-AHP solution and incubated at 37°C. . In vitro drug release studies are done using dialysis method. The biocompatibility of the CIG system is studied using MTT assay in L929 cell lines.

RESULTS & DISCUSSION: The particles are found to be smooth and spherical using SEM.

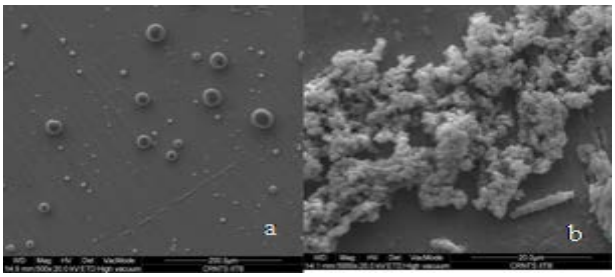

Fig. 1(a). SEM Images of Etoricoxib loaded PCL micro particles. 1(b) SEM image of chitosan in situ gel.

FTIR studies confirm the absence of any chemical interaction between PCL and Etoricoxib. The drug loading and entrapment efficiency are also determined. The drug entrapment efficiency was found to be around 70% for 1:40 drug:polymer ratio. *In vitro* drug release studies done by dialysis-membrane method using 900ml PBS, pH7.4 is found to have controlled release around 20 days. Gellation time of CIG is determined to be around 11 minutes. The *in vitro* drug release study of CIG is compared with release kinetics of PCL microparticles. The drug is found to be released in a much more controlled manner from CIG when compared to PCL microparticles alone. The biocompatibility of the system is confirmed by performing in vitro cytotoxicity studies using MTT Assay in L929 cell lines.

CONCLUSIONS: Thus to conclude, this novel composite in situ system can be a good, non-invasive intra-articular drug delivery system for the controlled delivery of drugs and proteins to the diseased joints.

REFERENCES: [1] H. Ingo, (2008) *Expert Opin. Drug Deliv* **5**: 1027. [2] D.H.P Ossa et al. (2012*) J Control Release* **161**: 927-932. [3]S. Lakshmi et al (2007) *Biomacromolecules* **8**: 3779–3785.

Non-equilibrium plasma applications to advanced surface and interface engineering of biomaterials

A Sarkissian, C Côté, SW Wolfe

Plasmionique Inc, 171B-1650 boulevard Lionel-Boulet, Varennes, QC Canada J3X 1S2

INTRODUCTION: Medical prosthesis or devices in addition to addressing bio- and haemocompatibility issues must also possess the specific mechanical, electrical or tribological properties. Selecting materials that could simultaneously satisfy a multiple of physical, chemical, electrical, biological and/or tribological properties constitutes a significant challenge to biomaterial engineering community. Given that the interaction of biological cells with implanted devices takes place at the interface of the material and that of living cells, and that the cell response is determined by chemical and morphological properties of the surfaces they interact, the surface engineering of implantable medical devices becomes a critical step for assuring desirable outcome.

PLASMA PROCESS: Plasma state is a gaseous state of mater, which includes neutral molecules, atoms, radicals, photons and sufficient number of electrons and ions such that the electrical property of the gaseous state is changed significantly. Listed below are the plasma-based processes used for surface engineering applications. They are categorized based on the outcome of interaction of plasma species with material surfaces, which are determined by the energy of interacting particles and their chemical affinity.

- Ion Implantation (E_k>10 keV)
- Sputtering
  - Cleaning (E_k<2 keV)
  - Deposition (E_k<1 keV)
- Etching (E_k ~ few eV)
- Deposition
  - Physical (E_k ~ 0.5 to 50 eV)
  - Chemical
- Surface Activation (E_k ~ few eV)
  - Particles (electrons, ions or neutrals)
  - Photons

TECHNIQUES: There are several organic, inorganic and composite materials that are fair candidates as bio- or haemocompatible materials; however, not all satisfy the required conditions in order to be considered for implantation in human body. Nevertheless, these materials in thin film coatings could act as a buffer layer.

Amongst various surface engineering methods, plasma-based techniques offer the most versatile approach, since they allow surface modifications with monolayer precision. Plasma techniques, in general, could significantly reduce the required heat load for deposition or modification of surfaces; therefore, they allow independent control of the thermal effects. An important group of biomaterials is biopolymers, which have low tolerance to heat load. Pulsed plasma application furthermore reduces the required heat load on the surface. The main advantage of pulsed plasma is that it produces significant quantities of ions, electrons and radicals, which are required for the process of deposition or surface modification, at low average energy cost.

APPLICATIONS: Among numerous applications include the implantation of beta emitting radioisotopes [1], which allow local treatment of aneurysm [2]. One could also contemplate its application to local treatment of cancer. Deposition of nanostructured silver coating for antibacterial applications is another active area of R&D [3]. Plasma functionalization of surfaces with receptors for various pharmaceutical or biological molecules is another common application [4]. An important class of biomaterial coatings are plasma synthesized polymer coatings [5], which offer superior stability because of their higher crosslinking.

CONCLUSIONS: Plasma-based techniques allow precision engineering of biomaterial surfaces and interfaces with monolayer accuracy. In addition, plasma allows synthesis of new materials. Above examples, along with numerous other examples, highlight the extent of plasma-based applications related to biomaterial surface and interface engineering.

REFERENCES: [1]Fortin M.A., et al (2006) *Applied Radiation and Isotopes* **64**: 556, [2]Raymond J., et al (2003) *Stroke* **34**: 2801, [3]Sant S.B. et al (2000) *Phil. Mag. Lett.* **80**: 249, [4]Siaow K.S. et al (2006) *Plasma Processes and Polymers* **3:** 392; [5]Yasuda H., et al (1982) *Biomaterials* **3**: 68.

Correlation between plasma physicochemical characteristics and treated surface chemistry

M Mavadat[1,2], S Turgeon[2], G Laroche[1,2]

[1]*Dept of Materials Engineering. Université Laval, Québec, Canada* [2] *Centre de recherche du CHU de Québec, Québec, Canada*

INTRODUCTION: Non-equilibrium plasmas have a great impact on polymeric material science, in that they allow modifying the outermost surface layer, in 'cold' processes, conferring materials a tailored surface composition and properties such as adhesion, wettability, and biocompatibility. Different plasma external parameters (pressure, input power and gas flow) affect the characteristics of the plasma and consequently the surface chemistry of plasma modified polymers. Hence, the knowledge of fundamental processes occurring in the plasma is a prerequisite for further process control. Accordingly, the aim of this work was to correlate the plasma experimental parameters and physicochemical characteristics with the resulting chemistry (as quantified from XPS) of treated PTFE through multivariate analysis.

METHODS: The microwave reactor for the experiments was purchased from Plasmionique Inc. (Varennes, QC, Canada). The feed gases used for the plasma treatments were N_2 gas (99.998% purity), H_2 gas (99.999% purity) and Ar gas (99.999% purity) purchased from Linde Canada. Commercial flat sheets of poly(tetrafluoroethylene) (PTFE) 250µm in thickness to be treated through plasma were purchased from Goodfellow Corp (Devon, USA) and cut as square with the side of 20 mm. The plasma-treated surface chemistry was ascertained through XPS. Plasma physicochemical characteristics were determined from emission spectroscopy that allowed quantifying rotational and vibrational temperatures as well as atom densities within the plasma. On one hand, near infrared spectra were recorded with a FTLA2000 FTIR (770-3300 nm) spectrometer purchased from ABB-Bomem (Québec, QC, Canada). On the other hand, UV–VIS (300–800 nm) emission spectra were recorded using a HR4000 apparatus from Ocean Optics (Dunedin, FL, USA). Correlation between the process condition and plasma parameters as the predictor (X) to the surface characteristics as the response (Y) was established by applying a partial least square (PLS) algorithm.

RESULTS: Figure 1 shows the variable importance on the projection as determined from the PLS calculations. As can be seen, the relative amount of N_2 and H_2 within the plasma chamber has a major influence on the resulting plasma chemistry. In addition, parameters such as rotational and vibrational temperatures, and nitrogen atomic density also play a major role in the surface modification process.

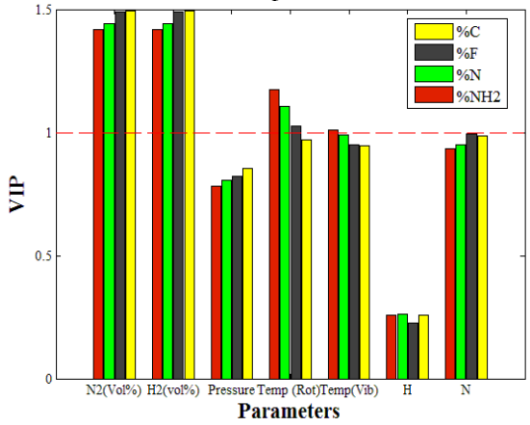

Fig. 1: VIP histogram showing the relative importance of plasma parameters and physicochemical characteristics on the chemistry of plasma-treated PTFE .

DISCUSSION & CONCLUSIONS: This work demonstrates the great potential of both UV-visible and IR emission spectroscopy to monitor plasma processes and better understand the plasma surface modification mechanisms. In addition to plasma process conditions, the plasma characteristics, measured through the so-called spectroscopy methods, can be used as powerful tools to predict the treated surface chemistry and highlight the mechanisms responsible for the surface modification. The approach consisted in generating a mathematical model through the partial least square method that correlates an input matrix containing both experimental plasma conditions and plasma characteristics, with an output matrix built with XPS surface chemistry data. The correlation coefficient obtained using this mathematical model showed a very good fit between predicted and actual surface chemistry data and therefore confirmed the predictive ability of the model.

ACKNOWLEDGEMENTS: The authors thank NSERC for financial support.

RF-plasma and UVC pretreatment increasing the metal and semiconductor nanoparticles bacterial inactivation in the dark and under light irradiation

S Rtimi, C Pulgarin, J Kiwi

Ecole Polytechnique Fédérale de Lausanne, EPFL-SB-ISIC-GPAO, Station 6, CH-1015, Lausanne, Switzerland

INTRODUCTION: In presence of residual O_2 gas RF-pretreatment generates anions and cations (O^-, O^+), radicals, excited O* sates, molecular-ions and high-energy electrons in a system that is not in equilibrium. These O-generated species interact with the textile surface introducing functional groups C–O^-, COO^-, –O-O^- in the presence of O_2 (air). UVC activation with a lower energy than the RF-plasma, does not lead to cationic or anionic oxygen species and only atomic (O) and excited oxygen (O*) species are formed (185 nm light) with an energy < 495 kJ/mol necessary to split $O_2 \rightarrow 2O^*$ [1]. The absence of cationic or anionic oxygen leads to more uniform distribution in the activated sites on the pretreated surfaces leading to more uniform deposits of Ag, TiO_2 and Cu-oxides. RF-plasma power of 100 W and UVC treatments at 185 nm (25 W) are able to break the intermolecular bonds (H-bonds) due to the high local heating segmenting the cotton, polyester and polyamides fibers leading to an increase in the O-surface functionalities [3].

METHODS: Pretreated samples either by RF-plasma or UVC were subsequently exchanged–impregnated, dried and sonicated to remove the loosely colloidal particles of Ag^o/Ag^+, CuO/Cu^+ and TiO_2/Ti^{4+} attached trough electrostatic attraction/chelation with the negative O-functionalized groups. Bacterial inactivation of *E. coli* was carried out following the ISO-Standards [3]. Characterization of the surfaces was carried out by EM, XPS, diffuse reflection spectroscopy (DRS) and XRD in the case of the TiO_2 textile.

RESULTS & DISCUSSION: The bacterial inactivation by RF-plasma and UVC pretreated Ag-loaded textiles pads used in wound healing was investigated. RF-plasma pretreated Ag-pads inactivated bacteria within 24 h while UVC was able to completely suppress *E. coli* within 30 min due to the more even distribution of Ag^o/Ag^+ clusters on the pads induced by O*/O-atomic produced by UVC. Ag-clusters were 3-8 nm as detected by EM [1].

TiO_2 bondability of particles produced by sol-gel was seen to increase on Nylon surfaces when pretreated by RF-plasma and UVC. These particles led to a rapid inactivation of bacteria and organic compounds as detected by the lack of C, N, S, O continuing residues on the TiO_2 -Nylon surface by XPS at the end of the photocatalysis. The mineralization of the *E. coli* proceeds: $CxHyNzSw + H_2Ov + O_2(air) \rightarrow CO_2 + SO_p + NO_q + H_2O$.

Bacterial inactivation of *E. coli* by RF-plasma pretreated cotton with high surface area CuO 65 m^2/g powders [3]. The effect the RF-plasma pretreatment of the cotton on the binding of CuO, is shown in Figure 1.

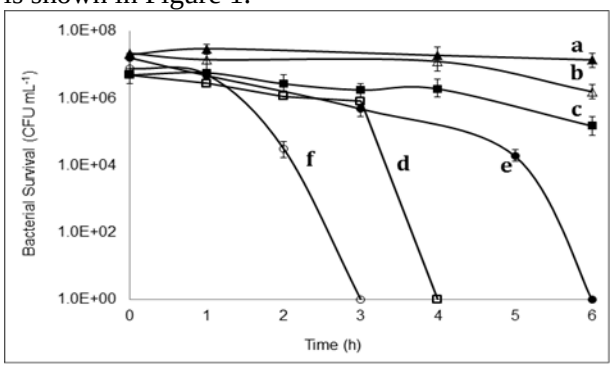

Fig. 1: E. coli inactivation, a) cotton alone, dark b) cotton under visible light (4.7 mW/cm^2) c) cotton/CuO (65m^2/g), (0.71 %wt/wt), dark d) cotton/CuO (65m^2/g), (0.71% wt/wt), under visible light (4.7 mW/cm^2) e) RF-plasma cotton/CuO (65m^2/g), (071% wt/wt), dark f) RF-plasma cotton/CuO (65m^2/g), (0.71% wt/wt), under visible light (4.7 mW/cm^2 or 1% of full solar AM1 light)).

RF leads in Fig 1 to a significant increase in the bacterial inactivation in the dark or under light.

REFERENCES: [1] T. Yuranova el al (2003) *J. Photochem. Photobiol. A* **161**:27-34. [2] M.I. Mejia et al (2010) *ACS Appl. Mater & Interf.* **1**:2190-98. [3] A. Torres et al (2010) *ACS Appl. Mater & Interf.* **2**:2547-52.

ACKNOWLEDGMENTS: We thank the EPFL, the Limpid FEP-7 collaborative European Project NMP 2012.2.2.2-6 and the COST Action TD 0906 for support of this work.

Tribocorrosion Behavior of Anodic Titanium Oxide Films and Assessment of Cell-Materials Interactions

SA Alves[1], R Bayón[2], V Saénz de Viteri[2], MP Garcia[3], A Igartua[2], MH Fernandes[3], LA Rocha[1,4]

[1]*Centre for Mechanical and Materials Technologies, University of Minho 4800-058 Guimarães, Portugal* [2] *Fundación IK4-Tekniker, 20600 Eibar, Spain* [3] *Faculdade de Medicina Dentária da Universidade do Porto, 4200-392 Porto, Portugal* [4] *Department of Mechanical Engineering, University of Minho 4800-058 Guimarães, Portugal *e-mail: sofialves@dem.uminho.pt*

INTRODUCTION: Titanium (Ti) has been widely used for implant applications due its excellent biocompatibility and high corrosion resistance. However, Ti presents poor wear resistance. Dental implants are often subjected both to a corrosive environment and cyclic micro-movements at implant/bone interface, becoming part of a tribocorrosion system. Tribocorrosion is characterized by the liberation of wear debris and corrosion products to peri-implant sites, inducing to inflammatory responses and implant loosening. Further, the lack of osseointegration is also one of the most frequent causes of implants failure. [1] Hence, the main goal of this work was to modify the surface features of Ti in order to produce bio-multifunctional surfaces able to display improved tribocorrosion and biological performances.

METHODS: Square samples of commercially pure (cp)-Ti grade 2 (Goodfellow Cambridge Ltd., UK) were treated by Plasma Electrolytic Oxidation (PEO). A commercial electrolyte (CE) containing NaF and a Ca- and P-based solution (Cβ) were used for PEO treatments (Table 1).

Table 1. Parameters used for PEO treatments

Group of samples	Current density (A/dm^2)	Process duration (minutes)	Electrolyte
PEO_CE,8,5	8	5	CE
PEO_CE,8,10	8	10	CE
PEO_Cβ,8,5	8	5	Cβ
PEO_Cβ,25,10	25	10	Cβ

After treatments, the surface features of the anodic films were investigated. Afterwards, reciprocating sliding tests were performed in artificial saliva at 37ºC. The tribocorrosion behavior was analyzed by Open Circuit Potential (OCP) measurements and the coefficient of friction was monitored during sliding. The morphology of the wear scars was evaluated by SEM and wear volume measurements were also carried out. The samples presenting the best tribocorrosion performances were submitted to biological assays in order to assess their interactions with MG63 bone cells. The osteoblastic cells morphology and viability were evaluated for 1, 3 and 7 days of culture.

RESULTS: Micro-porous anodic oxide films were produced on Ti by PEO. The tribocorrosion behavior of Ti was enhanced after PEO treatments in both electrolytes. However, the wear/corrosion behavior of Cβ-treated samples was greatly enhanced, as it can be observed by OCP evolutions depicted in Fig. 1. Moreover, the wear volume of Cβ-treated samples was significantly lower than both on reference and CE-treated specimens.

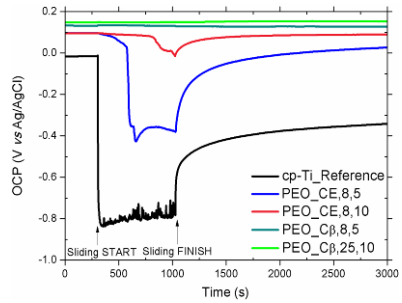

Fig. 1. OCP of treated and untreated Ti samples prior, during and after sliding tests.

The cells were able to adhere and spread on all the surfaces. In agreement with SEM observations, MTT assay revealed that cell proliferation increased throughout the culture time, with Cβ-treated samples exhibiting the best performance.

DISCUSSION & CONCLUSIONS: Porous anodic oxide films were produced on Ti by PEO and the anodizing conditions influenced the features of the films. PEO treatments greatly improved the tribocorrosion performance of Ti and the electrolyte composition appears to play a crucial effect by decreasing the tendency to corrosion and mechanical damage. PEO_Cβ,25,10 surface features significantly improved the tribocorrosion and biological performances of Ti. The major highlight of this study relies on the production of the Cβ-treated samples as very attractive candidates for implant applications.

REFERENCES: [1] M.T. Mathew, V.A. Barão, J.C-C. Yuan, W.G. Assunção, C. Sukotjo, M.A. Wimmer (2012) *Journal of the Mechanical Behavior of Biomedical Materials*. **8**: 71-85.

Plasma surface modification of a new family of microfluidic chips for biological applications

B Da Silva[1], G Schelcher[1], L Winter[1], C Guyon[1], P Tabeling[2], D Bonn[3], M Tatoulian[1]

[1]*Laboratoire de Génie des Procédés Plasmas et Traitements de Surface, ENSCP, Paris*
[2]*Microfluidique, MEMS, Nanostructure, ESPCI, Paris* [3]*Institut Moissan, ENSCP, Paris*

INTRODUCTION: Microfluidic devices have become increasingly attractive for sundry biological applications due to their reduced size and high surface area-to-volume ratio, enabling fast analysis, short reaction times and potential for patterning. Robust application of microfluidics to biology requires surfaces that can be hydrophilic, patterned, optically transparent and charged. As a result, surface properties play a major role in determining the microfluidic chip characteristics. Currently, the most commonly used microfluidics material is polydimethylsiloxane (PDMS). Despite exhibiting several advantageous properties, this material is extremely hydrophobic and difficult to modify. Although many studies have shown that PDMS surfaces can be modified using various techniques, a major concern is the stability of coatings necessary for fabricating biologically-functional microfluidics. To overcome this challenge, a new family of thermoplastic polymers such as COC (Cyclic Olefin Copolymers), NOA (Norland Optical Adhesive®) and THV (Dyneon®) were investigated using plasma-enhanced chemical vapour deposition (PECVD) in order to produce well-adhered, thin coatings with wide ranges of surface functionalities.

METHODS: Polymers such as PDMS, COC, NOA and THV were evaluated as surface-modified microfluidic materials, including investigating the incorporation of different functional groups onto these surfaces. Starting from various precursors such as acrylic acid, allylamine and hexamethyldisiloxane, the functionalization of these novel materials was performed using a bell-jar plasma reactor, a hybrid reactor equipped with magnetron sputtering, and a PECVD apparatus incorporating a remote ICP plasma source. Coated microfluidic surfaces were then evaluated in terms of wettability, stability, composition, and structure using water contact angle (WCA), scanning electron microscope (SEM), X-ray electron spectroscopy (XPS), and Fourier-transform infrared spectroscopy (FTIR) measurements.

RESULTS: Under optimal conditions, we have demonstrated that Teflon-like film deposition by plasma treatment allowed incorporation of fluorinated groups on suitable microfluidic material. COC, NOA and THV microreactors exhibited stable and hydrophobic surfaces with a high ratio of incorporated fluorine groups, confirmed by XPS analysis. In addition, these surfaces were successfully rendered hydrophilic (and remained thus for several months) by means of a silica layer deposition, confirmed by FTIR and XPS. Water and air aging revealed the instability of such coatings on PDMS surfaces due to the hydrophobic recovery of this material. Finally, for all materials studied (including PDMS), we also demonstrated the incorporation of both amine and carboxylic groups by plasma polymerization of allylamine and acrylic acid, respectively.

DISCUSSION & CONCLUSIONS: Plasma surface modification of thermoplastic polymers such as COC, NOA and THV produced material with surface properties suitable for biological applications, including hydrophilicity and patterning. Although PDMS remained hydrophilic in air and water for only a few days, we managed to confer stable surface properties on COC, NOA and THV microreactors. These promising results open opportunities to further developments in microfluidics and biotechnology for diverse challenges including biosensors, tissue engineering and cell-surface interactions.

REFERENCES: [1] E Sollier et al (2011) *Lab Chip* **11**: 3752. [2] A Duboin et al (2012) *Surface and Coatings Technology* **206** (19-20): 4303-4309

ACKNOWLEDGEMENTS: The authors would like to thank Jean-Louis Viovy's team (MMBM, UMR CNRS 168, Institut Curie, Paris) for providing THV and COC substrates.

Plasma modification of porous scaffolds by means of plasma assisted processes

E Sardella[1,*], M Garzia Trulli[2], R Gristina [1], JC Shearer[3], ER Fisher[3], P Favia [2]

[1] *CNR-Institute for Inorganic Methodologies and Plasmas (CNR-IMIP), Bari, Italy*

[2] *Department of Chemistry, University "A. Moro"; Bari, Italy*

[3] *Department of Chemistry, Colorado State University, Fort Collins, Colorado, USA.*

INTRODUCTION: Polymers are commonly used in biomedical applications because of their excellent bulk properties, such as strength and good resistance to chemicals. However, their surface properties are for most biomedical applications inadequate due to their low surface energy. A surface modification is often needed, and plasma surface modification has been used with success in the past decades. A recent application of plasma processing is devoted to 3D scaffolds for tissue engineering [1,2]. In this field, the surface properties of porous scaffolds need to be altered to promote a good cell adhesion, growth and proliferation in order to make them suitable for implants and tissue regeneration. In this study, we utilized N_2 and H_2O vapor plasmas to modify PCL porous scaffolds and looked at their interaction with cells.

METHODS: Poly ε-caprolactone (PCL) scaffolds, having a pore size ranging from 150μm to 300μm, fabricated by solvent casting/particulate leaching, were treated in a low pressure plasma reactor. Plasma processes fed with N_2 and H_2O vapors have been performed by changing the gas feed composition from 100% of water (100_H_2O) to 100% of nitrogen (100_N_2) to a mixture containing both N_2 and H_2O (50:50_N_2/H_2O). Plasma surface modification was performed in borosilicate glass chamber and the plasma discharge was initiated with three external, capacitively-coupled copper band ring-electrodes connected to a 13.56 MHz radio frequency (rf) power source through a matching unit. The total gas flow was maintained at 15 sccm, at 150 mTorr and 30 W for 4 min treatment time. Saos2 cell were grown in DMEM medium supplemented with 10% FBS. Samples were placed in 48 well plates and $5*10^4$ were seeded on each scaffolds.

RESULTS: Chemical/physical characterization was performed on the tops, cross-sections, and bottoms of plasma treated scaffolds. Plasma treatment imparted immediate hydrophilicity and ability to absorb water on the top and bottoms of the scaffolds regardless the used gas feed. Water drops of 4ul were completely absorbed into 50:50_N_2/H_2O scaffolds in < 6 ms, making measurements of WCA and drop volume challenging. For comparison, it should be noted that untreated PCL scaffolds do not absorb water. Plasma treatments performed in this work are able to effectively change the chemical characteristics of both the external and internal surface of the scaffolds. The position of the N_{1s} signal for 50:50_N_2/H_2O samples shows the presence of amide functionalities that should be that not only add the polar groups necessary for increasing hydrophilicity, but also should enhance Saos2 osteoblast cell growth. Saos2 osteoblast cells were incubated for 18, 42, and 114 hours to observe the cells metabolic activity by MTT colorimetric assay. Cells viability strongly increase on samples in the time lapse from 42 to 114h. After 114h cells seeded on 50:50_N_2/H_2O scaffolds were the most viable ($p<0.05$ against the other ones) among plasma modified samples. Fluorescence microscopy characterization of actin cells cytoskeleton shows that cells on plasma treated scaffolds clearly exhibit the presence of stress fibers and were well spread. Furthermore, cells on water containing surfaces show a strong clusterization, respect to nitrogen-containing surfaces.

DISCUSSION & CONCLUSIONS: Plasma modification was shown to have a significant impact on the wettability, surface functionality, and cell growth capabilities of PCL scaffolds. Low pressure plasmas are able to effectively modify the external and internal surface of the scaffolds improving the ability of such materials to support cell ingrowth.

REFERENCES: [1] F. Intranuovo, E. Sardella, R. Gristina, M. Nardulli, L. White, D. Howard, K.M. Shakesheff, M.R. Alexander, P. Favia (2011) *Surf. Coat. Tech.* **205-2**: S548-S551. [2] J. J. A. Barry, D. Howard, K. M. Shakesheff, S. M. Howdle, M. R. Alexander (2005) *Adv. Funct. Mat.*; 15, 1134.

ACKNOWLEDGEMENTS: S. Cosmai is acknowledged for his technical support.

Surface treatments of SS316L substrates for plasma-based Diamond Like Carbon coatings: study of the surface properties

L Angeloni[1,2], R Tolouei[1], C Paternoster[1], L Lévesque[1], S Turgeon[1], M Rossi[2], D Mantovani[1]

[1] Lab. for Biomaterials and Bioengineering (CRC-I), Dept. Min-Met-Materials Eng. & University Hospital Research Center, Laval University, Quebec City, Canada [2] Department of Basic and Applied Sciences for Engineering, University of Rome Sapienza, Rome, Italy

INTRODUCTION: In biomedical devices, such as prostheses, the bulk material plays a key role in the achievement of structural and mechanical properties, but the surface state deeply influences the interaction phenomena with the biological environment. For this reason many surface modification techniques are often used to effectively modulate the interface properties while bulk ones are preserved. Stainless steel is the gold standard bulk material to realize a great deal of medical devices, while Diamond Like Carbon (DLC) coating represent a promising surface material because of its proved biocompatibility, chemical inertness and stability in corrosive environment [1]. There are evidences that, besides the chemical reactivity, other surface properties, such as roughness and surface energy, can control cells adhesion and tissue growth on the implants [2, 3]. The influence of roughness on the surface energy and the effect of these two combined properties on the biological response is, currently, matter of investigation. Surface energy can be modulated by modifying the roughness, the surface chemistry, for example applying a coating, or by a combination of both these modification techniques. Accordingly, the aim of this work is to evaluate the effects of roughness modification treatments and DLC coatings on the surface properties of stainless steel substrates.

METHODS: Different surface morphologies were obtained on 316L stainless steel (SS316L) substrates by two different industrial finishing methods: electropolishing and sand blasting.
The electropolishing process was performed using an electrolyte composed of a mixture of glycerol, phosphoric acid and D.I. water. The sand blasting was carried out using particles of silica and pressured air flow directed normally to the surface. DLC coatings were obtained by Plasma Enhanced Chemical Vapour Deposition (PE-CVD) on the treated stainless steel substrates. The chemical composition changes of the surfaces were evaluated by X-ray Photoelectron Spectroscopy (XPS). The micro and nano-roughness was measured by a Dektak profilometer and by Atomic Force Microscopy (AFM), respectively. The surface energy evolution was evaluated by static contact angle measurements, carried out with D.I. water at room temperature. Bacterial adhesion tests were performed in order to evaluate the effects of the surface modifications on biological behaviour.

RESULTS & DISCUSSION: Different surface roughness on stainless steel substrates were obtained by different surface finishing treatments as shown in Fig. 1.

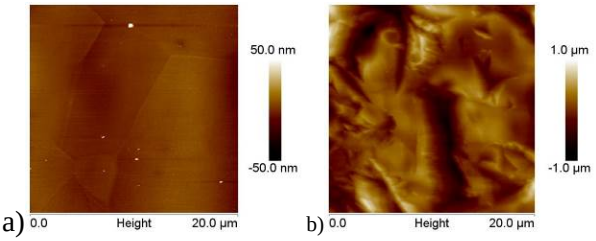

Fig. 1: AFM images of SS316L substrates after (a) electropolishing and (b) sand blasting treatment.

Contact angle measurements showed that different roughness does not affect in a significant way the surface wettability of the stainless steel substrates. Surface modification of SS316L substrates by DLC coating has a significant effect on the wettability of the surface resulting in a considerable increasing of the surface hydrophobicity. Results on bacterial adhesion will be discussed.

CONCLUSIONS: The results indicate that the roughness of SS316L can be engineered by electropolishing and sand blasting processes without influencing the surface energy in a significant way. Moreover, the wettability of surfaces with different roughness can be modulated by DLC coating.

REFERENCES: [1] G. Dearnaley, J.H. Arps (2005) *Surf. Coat. Technol.* **200**:2518-2524. [2]R.G. Flemming, C.J. Murphy, G.A. Abrams, et al (1999) *Biomaterials* **20**:573-588.[3] M. Nikkhah, F. Edalat, S. Manoucheri et al, (2012) *Biomaterials* **33**: 5230-5246.

Study of cell proliferation on modified diamond-like carbon films prepared by plasma enhanced CVD

A Stoica[1], V Buršíková[1,2], T Novotný[2] , L Zajíčková[1], A Manakhov[1], J Procházková[3]

[1] *Central European Institute for Technology (CEITEC), Masaryk University, Brno, Czech Republic* [2] *Department of Physical Electronics, Masaryk University, Brno, Czech Republic* [3] *Department of Animal Physiology and Immunology, Masaryk University, Brno, Czech Republic*

INTRODUCTION: In the last decade carbon based thin films prepared by plasma enhanced chemical vapour deposition (PECVD) have attracted research interest for medical applications. The unique properties of diamond-like carbon (DLC) such as chemical inertness, high wear, and corrosion resistance, etc. [1] make it a prospective material that can be used in medical devices such as implants, stents, and lenses. DLC properties can be further improved by incorporating other chemical elements [2]. Reactive groups can be created by plasma functionalisation or PECVD for the immobilisation of biomolecules at surfaces. Control of surface mechanical properties can influence cell interaction with the material [3].

METHODS: Modified DLC coatings that incorporate H, N, Si, and O were prepared from different gas mixtures of methane (CH_4), hexamethyldisiloxane (HMDSO), hydrogen (H_2) or nitrogen (N_2) by low pressure radio frequency PECVD on several different substrates, such as polycarbonate (PC), glass, and silicon. Thin film composition was analysed by Rutherford Backscattering Spectrometry (RBS), Elastic Recoil Detection Analysis (ERDA) and X-ray Photoelectron Spectroscopy (XPS). Mechanical properties of the coatings were studied by the instrumented indentation technique. Surface free energy (SFE) was evaluated on the basis of the interaction between the sample surface and different liquids by contact angle measurements using acid-base regression model [4]. Surface roughness was calculated using Gwyddion software by evaluating the results obtained from AFM and confocal microscope. The assays of proliferation and detachment of cells from plasma coatings were performed using the evaluation of cell number (Accuri C6, B.D). C2C12 mouse myoblasts were seeded ($4 \cdot 10^5$/ml) on UV sterilized plasma treated coverslips and cultivated for 2 days. The number of cells floating in the media (detached and dying) and attached to the coverslip was evaluated separately. The cell compatibility and the effects between the discharge conditions, precursor gas mixture composition, film structure, and film properties will be investigated.

RESULTS: Regardless of the type of the prepared coatings, the surface roughness of the deposited thin films is essentially influenced by the topography of the substrate. After comparing different DLC films deposited on smooth substrates such as glass, no significant change was observed regarding cell proliferation. The content of HMDSO in the precursor gas mixture had limited effect on the proliferation of the attached cells. However, on the rougher PC substrates an influence of surface energy on cell proliferation was observed. The dependence was found between cell attachment and proliferation and the surface free energy of tested samples, more exactly its polar component. The basic component of the surface energy (γ^-) was found higher on the coated PC and increased with the decrease of the relative flow rate of HMDSO in the deposition chamber. Overall, cell proliferation was increased on the coated substrates compared to the untreated PC surfaces.

REFERENCES: [1] A. Grill (2003). *Diamond and Related Materials* **12**:166-70. [2] M.C. Vasudev, K.D. Anderson, T.J. Bunning, et al (2013). *ACS Applied Materials and Interfaces* **5**:3983-94. [3] I. Hopp, A. Michelmore, L.E. Smith, et al (2013). *Biomaterials* **34**:5070-77. [4] V. Buršíková, P. Sťahel, Z. Navrátil, J. Buršík, and J. Janča (2004) *Surface Energy Evaluation of Plasma Treated Materials by Contact Angle Measurement*, Masaryk University Brno.

ACKNOWLEDGEMENTS: This work was supported by the projects CZ.1.05/1.1/00/02.0068 'CEITEC – Central European Institute of Technology', and CZ.1.05/2.1.00/03.0086 'R&D center for low-cost plasma and nanotechnology surface modifications' funded by European Regional Development Fund.

Hygroscopic swelling in single trabeculæ from human femur head

F Marinozzi [1], F Bini [1], A Marinozzi [2]

[1] *Mechanical and Thermal Measurements Laboratory, Department of Mechanical and Aerospace Engineering, "Sapienza" University of Rome, Via Eudossiana, 18 – 00184 Rome – Italy.*
[2] *Orthopaedics and Traumatology Unit, University "Campus Bio-Medico", Via Emilio Longoni, 83 –00155 Rome – Italy.*

INTRODUCTION: Bone is a composite material whose mechanical properties are determined by the intimate relationships among the constituent phases, that is the collagen fibers and the apatite nanocrystals [1-2]. Given the macro and microstructure of these phases and their specific physical-chemical properties, the bone results a porous and hygroscopic medium. Its porosity is evident on many distinct scales, namely those of intertrabecular, vascular, lacuno-canalicolar, collagen-apatite. The characteristic length of this latter is imposed by the intermolecular collagen bonds (cross-links), the water content and by the degree of mineralization [3-6]. Re-hydrating the specimens causes a consistent large increase of the lateral spacing of the collagen molecules and thus produces a measurable swelling [7-8].

METHODS: Thirteen specimens of cancellous bone were extracted from human femur heads withdrawn from five donors (female: age 67, 62 and 61; male: age 65, 60) suffering by moderate coxo-arthritis (CA). Their capita were substituted by hip arthroplasty surgery. Trabeculae were dissected from slices of about 10 mm corresponding to the frontal plane in the middle of the femur capita. The free hygroexpansion of single trabeculae along their main axis (length, width and thickness was then measured by a custom-made high resolution dilatometer by sudden immersion of the specimen in distilled water.

RESULTS: The measured dimensional changes of single trabeculae are listed in Table 1. Percent mean and standard deviation of measured values averaged over all the specimens were 0.26±0.15 (length), 0.45±0.25 (width) and 1.86±0.97 (thickness).

DISCUSSION & CONCLUSIONS: The amounts of dimensional changes (Table 1) were appreciably lower than those reported for bovine cortical bone reported by [5] and [9] but in good agreement with those at single osteon level [10] for equine bone. The analysis of these discrepancies is beyond the scope of this work and should be investigated considering the different arrangement of the lamellae in trabecular or in osteonal cortical bone. Also different initial and final water content are likely to affect the measured swelling. These informations are crucial, since the growth of Hydroxyapatite crystals is driven by ions diffusing from systemic extracellular fluid, and the degree of mineralization does progress according to the water content of the tissue

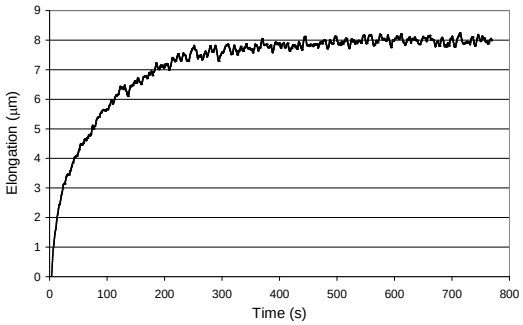

Fig. 1: Example of measured hygroscopic swelling of a trabecula over time.

Table 1. Mean percent dimensional changes

Length	Width	Thickness
0.26%	0.45%	1.86%

REFERENCES: [1]Weiner S, Traub W (1992) *FASEB journal* **6**:879-885. [2]Weiner S and Wagner H D, (1998) *Annu. Rev. Mater. Sci*. **28**:271–98. [3]Lees S, (1981) Calcif. *Tissue Int*. **33**:591-602. [4]Lees S, (1987) *Connect Tissue Res* **16**:281-303. [5]Lees S, Heeley J D, Cleary P F (1981) *Calcified Tissue International* **33**:83-86. [6]Lees S, Pineri M, Escoube M (1984) *Int. J. Biol. Macromol.* **6**:133–136. [7]Pineri M H, Escoubes M and Roche G (1978) **17**: 2799-2815. [8]Nomura S, Hiltner A, Lando J B, Baer E (1977) *Biopolymers* **16**: 231-246. [9]Finlay J B, Hardie W R, (1994) *Journal of Engineering and Medicine* **208**: 27–32. [10] Utku F S, Klein E, Saybasili H, Yucesoy C A, Weiner S, (2008) *Journal of Structural Biology* **162**: 361–367

Description of mechanical and biological factors affecting the bone-biomaterial(β tricalcium phosphate and chitosan), implanted in animal model

S Arce[1], CH Valencia[2]

[1] Research Group New Solid with Industrial Application (GINSAI), Universidad Autónoma de Occidente. Facultad de Ingenieria, Cali, Colombia [2] Universidad del Valle, Escuela de Odontologia. Cali

INTRODUCTION:When designing a biomaterial, it is necessary to take into account both biological and mechanical factors that could affect its proper performance. From the biological point of view, when a biomaterial is implanted in bone tissues, it generates two interfaces: one between the foreign implanted material and the tissue surrounding it, and another one between inner parts of the material and the undegraded cells surrounding it. Cells neighboring bone surfaces, will try to invade the material to regenerate and reabsorb the defect created. This process is requires the production of type I and III collagen fibers, blood vessel growth, cell differentiation osteogenic and osteoclastogenesis which is the connection between the bone and the implanted material. However, these biological factors have a direct relationship with the mechanical factors involved in the healing process of injured tissues. The objective of this research is to obtain a synthetic, biocompatible and bioresorbable biomaterial. It is also easy to handle for the surgeon, and has a hardening time and moldability that facilitate its application. On the other hand, it has shown ability to stimulate bone formation at sites of non - union without adding other components.

METHODS: The biocomposite consisted of a solid phase (calcium phosphate and zinc oxide) and a liquid phase (chitosan), in an optimal combination that keeps physiological pH and temperature ranges, and a work hardening and time appropriate for clinical needs. The biomaterial of 5 mm in diameter was implanted bilaterally in the right parietal bones of 12 rats. The left sides were left without biomaterial and acted as controls. After 20, 40 and 60 days rats were sacrificed. Samples were prepared for histochemical studies with hematoxylin and eosin, Masson's trichrome, Gomori, Von Kossa; besides immunohistochemistry with actin and tartrate-resistant acid phosphatase (TRAP).

RESULTS: The obtained biomaterial had a pH between 6.5 and 8.5. The temperature was 20°C and the hardening time 7 mm. These parameters gave plasticity allowing handling "in situ" in a convenient time for intraoperative work. In all the studied periods, control defects remained unregenerated, showing only a thin layer of soft tissue covering them. The parietal bones with the biomaterial exhibit a strong inflammatory reaction (leukocytes and monocytes), which decreases over time, and simultaneously the material is incorporated in dense connective tissue continuous with the periosteum of neighboring bone surfaces. There is evidence of blood vessels growth, the presence of collagen fibers, reticular fibers, bone cells and TRAP-positive cells involved in phagocytosis of the biomaterial (see Figure 1).

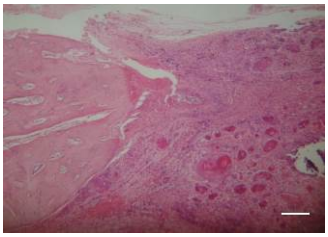

Fig. 1: The biomaterial (Bio), is including in connective tissue. At left border bone (B) and periostic tissue (P) are in close contact (20 xs). Haematoxylin-eosin. Scale bar= 50 micra.

DISCUSSION & CONCLUSIONS: A material withrecognized biocompatibility, osteoconduction, bioactivity, and complete reabsorption was obtained. The developed model behaved as critical defect size. The expected results are in accordance with those reported in the literature for the healing of critical size defects. Lack of regeneration in the defect control was observed. In the healing process, bone neoformation was evidenced in the defect implanted: resetting a vascular network, bone cells, forming a fibrillar network of collagen type I and type III, and initial deposit of material osteoid followed by the subsequent replacement by tissue bone. The biomaterial resorption seems to start on day 20 and is mediated by multinucleated giant cells similar to osteoclasts.

REFERENCES: [1] JO Hollinger, JC Kleinschmidt (1990) *J Craniofacial Surgery* **1**:60–68. [2] Geris L, Gerisch A, Vander-Sloten J, Weiner R, Van-Oosterwyck H (2008) *Journal of Theoretical Biology*.**251**:137-58.

Biotribological properties of bovine submaxillary mucin (BSM) at the hydrophobic interface

JB Madsen[1], N Nikogeorgos[1], MA Hachem[2], B Svensson[2], S Lee[1]

[1] Department of Mechanical Engineering, Technical University of Denmark, DK-2800, Kgs. Lyngby, Denmark [2] Department of Systems Biology, Enzyme and Protein Chemistry, Technical University of Denmark, DK-2800, Kgs. Lyngby, Denmark. [*]Corresponding author: seele@mek.dtu.dk

INTRODUCTION: The macromolecule mucin is the major constituent of the mucous secretions that coat epithelial surfaces exposed to the outside in animals. The primary function of mucins and mucous gels is to provide protection to epithelial surfaces from invasive microbes and physical insults by forming a lubricating layer [1]. 50-80% of the molecular weight of mucin consists of post-translational N- and O-linked glycosidic modifications. The ability of the glycosylations to retain water at the epithelial surface facilitates lubrication [2,3]. N- and C-terminal interactions and also entanglement of the glycosidic modifications lead to a viscoelastic material that offers excellent lubrication properties. In this work, the influence of purification on the tribological properties of commercially available Bovine Submaxillary Mucin (BSM) was investigated. Furthermore, chemical and enzymatic decomposition of BSM was performed so as to assess the impact on lubricity by overall structural degradation or removal of specific molecular species from the macromolecule.

METHODS: Anion exchange chromatography was employed to purify BSM. A full description can be found in J.B. Madsen et al. (2013, in press) [4]. Purified BSM was proteolytically degraded by select proteases. Deglycosylation was carried out either enzymatically or via β-elimination. Adsorption behavior was investigated by optical waveguide lightmode spectroscopy (OWLS). Biotribological properties of the various states of BSM were investigated by pin-on-disc tribometry (PoD) and atomic force microscopy (AFM) on PDMS surfaces.

RESULTS: OWLS studies have shown the adsorbed masses of ar-BSM and ae-BSM on PDMS surface are 161 and 46 ng/cm^2, respectively. PoD revealed slight, yet consistently higher COF for ar-BSM (in the range of 0.04 to 0.09) than ae-BSM (0.004 to 0.01) at the sliding contact of PDMS within the speed range of 1 to 100 mm/s (1 Newton load) in neutral aqueous solution.

DISCUSSION & CONCLUSIONS: Superior lubricity of ae-BSM compared to ar-BSM, despite inferior adsorbed mass can be caused by competitive adsorption of non-mucinous, less slippery components in ar-BSM. Further, it is also possible that non-mucinous components in ar-BSM might have altered the conformation of ae-BSM at the surface. Biotribological properties of chemically and enzymatically decomposed BSM were also studied in parallel with surface adsorption studies, which were not simply correlated with each other. Statistical validation is firstly required, and a further understanding on the compositional and conformational changes of BSM both in bulk and at the surface is required. This study confirms the current understanding of BSM as an amphiphilic macromolecule with regards to surface adsorption and its lubrication properties in relation to a hydrophobic surface. The surface adsorption behavior of BSM could be assigned mainly to the unglycosylated N- and C-terminal regions, while the lubricity could be ascribed to the glycosylated region of the macromolecule.

REFERENCES: [1]Coles, J.M., D.P. Chang, and S. Zauscher, *Molecular mechanisms of aqueous boundary lubrication by mucinous glycoproteins.* Current Opinion in Colloid & Interface Science, 2010. **15**(6): p. 406-416. [2]Roussel, P. and P. Delmotte, *The diversity of epithelial secreted mucins.* Current Organic Chemistry, 2004. **8**(5): p. 413-437. [3]Tian, E. and K.G. Ten Hagen, *Recent insights into the biological roles of mucin-type O-glycosylation.* Glycoconjugate journal, 2009. **26**(3): p. 325-334. [4] J. B. Madsen et al., submitted (2013)

Fibrinogen and albumin adsorption on sol-gel calcium phosphate substrates measured by FTIR-ATR

M Boix[1], S Eslava[2], G Machado[2], E Saiz[2], J de Coninck[1]

[1] *Université de Mons-UMONS, Laboratoire de Physique des Surface et des Interface, Mons, Belgium* [2] *Centre for Advanced Structural Ceramics, Department of Materials, Imperial College, London, UK.*

INTRODUCTION: There is a growing concern about bone diseases such as osteoporosis or arthritis, as a result of the increase in life expectancy. When the bone fails to heal properly, a surgery is required to replace the diseased bone, using own patient's or a donor's bone graft. But, the use of natural bone grafts involves certain risks such as infection or insufficient quantity [1]. The most studied synthetic bone grafts are calcium phosphate phases, since they represent the 50%wt. of natural bone.

In the first hours, a layer of proteins will be formed on the implant. This layer is crucial in the interaction with cells [2].

METHODS: Coatings of hydroxyapatite (HA) and a mix of tricalcium phosphate and hydroxyapatite (BCP) are synthesized using a sol-gel process and deposited on silicon prisms. Then, the adsorption of human serum albumin (HSA) and fibrinogen from bovine plasma is studied by attenuated total reflectance Fourier transform infrared (FTIR-ATR) spectroscopy. We reveal in-situ the protein adsorption amount and its secondary structure.

RESULTS: Fig. 1 shows the protein adsorption with time. The measured signal is larger for HA and fibrinogen. For HSA, we deconvolute amide I (1600-1700 cm^{-1}) in 3 peaks. 1636 cm^{-1} peak for random coils, representing a 57±3% for HA and 42±6 for BCP. 1656 cm^{-1} for α-helix, representing 36±4% for HA 43±9% for BCP. 1675 cm^{-1} for turns, representing 7±1% for HA and 15±4% for BCP.

For fibrinogen, we deconvolute amide I band in 5 peaks. 1628 cm^{-1} for beta sheets, representing 24±1% for HA and 20.0±0.7% for BCP. 1644 cm^{-1} for random coils, representing 34±3% for HA 62±8% for BCP. 1660 cm^{-1} for α-helix, taking 26±2% for HA and 23±2% for BCP.1670 cm^{-1} for turns, taking 13±1% for HA and 9±1% for TCP. 1689 cm^{-1} for beta sheets, taking 3.0±0.4% for HA and 4±1% for BCP.

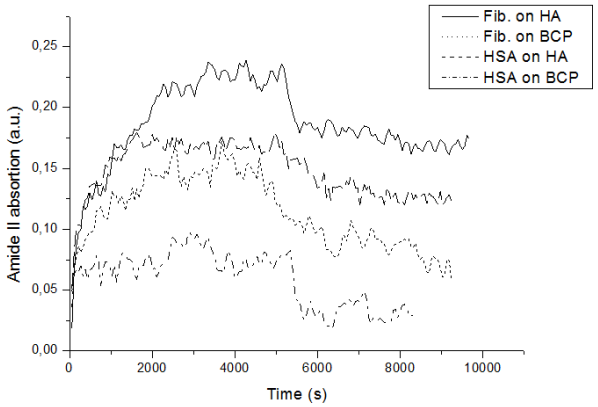

Fig. 1: Evolution of Amide II total IR absorption of adsorbed HSA and fibrinogen on HA and BCP. The mean is presented for each substrate.

DISCUSSION & CONCLUSIONS: Electrostatic force plays a key role in the protein adsorption process. HA exhibits a larger negative ζ-potential than BCP [3] that could cause an increase in protein adsorption. In addition HSA and fibrinogen present negative surface charges at a pH of 7.4. Then, the proteins have to change its shape to expose the inner positive charges. The larger decrease of α-helix of HSA on HA could be caused by its larger negative surface charge.

For fibrinogen, the proportion on beta sheets is decreased by 22% on BCP. This large change could affect its biological function, closely related with inflammation [4].

REFERENCES: [1] J.O. Eniwumide, H. Yuan, S.H. Cartmell,et al (2007) *European Cells and Materials* **14**:30-39. [2] Kefeng Wang, Changchun Zhou, Youliang Hong, et al (2012) *Interface Focus* **2:**259-277. [3] X. D. Zhu, H. S. Fan, C. Y. Zhao et al (2007*) J Mater Sci: Mater Med* **18:**2243-49. [4] Dimitrios Davalo, Katerina Akassoglou (2012) *Semin Immunopathol* **34**:43–62

ACKNOWLEDGEMENTS This work takes place inside Biobone ITN, funded by the European Framework Programme 7.

Chromatographic techniques in surface characteristic of ceramic biomaterials

K Adamska [1], M Szubert [1], K Szymański [1], A Voelkel [1]

[1] *Poznan University of Technology, Poznan, Poland*

INTRODUCTION: Examination of the properties of the biomaterial surface layer is essential when adsorptive or adhesive properties should be estimated. In order to improve currently available materials different modification are carried out to trigger a specific biological response in vivo, e.g., attracting or rejecting specific proteins, promoting or preventing cell growth. Modification influences energy properties of biomaterial surface (e.g. ability to donor-acceptor interactions) and, consequently, the ability to protein adsorption [1, 2]. The aim of this work was the application of Inverse Gas Chromatographic (IGC) to determine the dispersive (γ_s^d) and the specific component (γ_s^{sp}) of the free surface energy, the acidic γ_s^+ and basic γ_s^- parameters of hydroxyapatite and β-tricalcium phosphate and estimate the influence of its modification on these parameters [3]. Inverse Liquid Chromatography (ILC) technique was used in studies of adsorption behavior of protein on unmodified and modified biomaterials.

METHODS: Materials used were - hydroxyapatite (HA) and β-tricalcium phosphate (β-TCP), unmodified and modified by poly(3-hydroxybutyrate) (PHB) and polyethylene glycol (PEG, Mw=2000). Biomaterials were used as stationary phase in chromatographic experiments. In IGC measurements volatile test compounds, with known physicochemical properties were injected and transported by carrier gas over the surface of examined material. Obtained retention data were used to calculate the components of the surface energy. The bovine serum albumin (BSA) was used as the adsorbed protein in ILC experiments (HPLC Ultimate 3000, Dionex). All solutions of BSA were prepared in SBF. Adsorption isotherms were determined by the peak maximum method and amount of adsorbed BSA (q) was calculated.

RESULTS: Modifications influence the increase of the total surface energy of materials, but for modified HA lower data were obtained in comparison with modified β-TCP. The highest ability to dispersive interactions shows HA-PEG (γ_s^d=81.6 mJ/m^2), other materials characterizes higher ability to specific interactions (higher values of γ_s^{sp}). HA modification by PHB induced an increase of γ_s^+ component. This material can act as the strongest electron acceptor fm all examined materials (γ_s^+=144.6mJ/m^2).

Table 1. Components and total free surface energy values for unmodified and modified biomaterials.

	γ_s^d mJ/m^2	γ_s^{sp} mJ/m^2	γ_{total} mJ/m^2
HA	48.3±0.2	8.8±0.5	56.1
HA PEG	81.6±0.8	7.5±0.9	89.1
HA PHB	52.1±0.5	144.6±1.5	186.6
TCP	43.09±1.0	111.0±1.2	154.9
TCP PEG	41.0±0.3	215.8±0.7	230.2
TCP PHB	47.67±05	213.0±0.3	257.7

DISCUSSION & CONCLUSIONS: Surface energy parameters influence BSA adsorption. HA-PEG with small surface activity shows the weakest capacity to BSA adsorption (low q value). For TCP-PHB having the highest total surface energy the strongest adsorption of BSA was observed - it starts at the lowest values of albumin concentration in the mobile phase, reaching the highest q values of adsorbed BSA among all examined materials. The chromatographic techniques are useful tool for characterization of the physicochemical properties of the biomaterial surface and also estimation of the influence these parameters on adsorption process.

REFERENCES: [1]E.M. Harnett, J. Alderman, T. Wood (2007) , *Colloid Surface B* **55**: 90-97. [2]E.A. dos Santos, M. Farina, G.A. Soares, K. Anselme (2008) *J Mater Sci: Mater Med.* **19**: 2307–16. [3]A.Voelkel, B. Strzemiecka, K. Adamska, K. Milczewska (2009) *J Chromatogr A.* **1216**: 1551–66.

ACKNOWLEDGEMENTS: This paper was supported by N N204 137638 grant of Ministry of Science and Higher Education what is gratefully acknowledged.

Oleic acid surfactant in polycaprolactone (PCL)-based composites for bone tissue engineering

GBC Cardoso[1-2], D Maniglio[3], FZ Volpato[3], A Tondon[4], C Migliaresi[3], R Kaunas[4] and CAC Zavaglia[1-2]

[1] State University of Campinas, Materials Engineering Department, Campinas, Brazil [2] Biofabris, Campinas, Brazil [3]University of Trento, Department of Industrial Engineering and Biotech Research Center, Trento, Italy [4]Texas A&M University, Department of Biomedical Engineering, College Station, Texas, USA.

INTRODUCTION: Bone defects and diseases are a major cause of disabilities in the world. Autologous bone grafting is typically used to bridge bone defects, but the available graft material is limited and involves additional surgery causing chronic donor-site pain in many patients [1]. Tissue engineering approaches are being investigated as viable alternatives. Biodegradable 3-dimensional scaffolds in combination with induction factors, e.g. bioactive molecules and inorganic phases, are the most common and efficient tissue engineering approaches. Calcium phosphates, e.g. hydroxyapatite (HAp), are regularly applied as induction factors due to their chemical similarities with the natural bone. HAp mixes poorly with hydrophobic polymers, e.g. PCL, thus contributing to poor particle distribution and reduced integration into bone tissue. The use amphiphilic molecules acting as surfactants, e.g. oleic acid (OA), has been reported to enhance ceramic dispersion into hydrophobic polymeric matrixes. In this study, we investigated the potential of using oleic acid to improve PCL/HAp integration for composites intended for bone tissue engineering.

METHODS: PCL (80 kDa MW), oleic acid and hydroxyapatite whiskers were synthesized as previously described [2]. Films were casted by dissolving oleic acid in chloroform (10:1 v/w) for 30 minutes, addition of hydroxyapatite (15 %v/v) and stirring at room temperature for 2 hours. PCL was then added and stirred for 24 hours. Pure PCL, PCL/OA and PCL/OA/HAp samples were prepared and characterized by contact angle, differential scanning calorimetry (DSC), atomic force microscopy and scanning electron microscopy. Cell adhesion was characterized with human osteosarcoma cell line (U2OS) expressing GFP-actin with laser scanning confocal images captured at 1, 3 and 7 days. Cell and actin stress fiber morphology was analyzed with ImageJ software as described previously [3].

RESULTS: SEM images confirmed the improved dispersion of hydroxyapatite within the polymeric matrix. Furthermore, the addition of OA increased the surface roughness from 89 nm for pure PCL to 117 nm for PCL/OA and 200 nm when HAp was added. Oleic acid increased the wettability of the samples as indicated by a change in static contact angle from 104º (+ 4,8) for pure PCL to 61º (+4,4) for PCL/OA. DSC results indicated that the addition of HAp reduces the crystallinity to 33% as compared to 39% for pure PCL, which leads to an increase in the degradation rate of the matrix. To investigate how surface properties may affect cell behavior, samples were cultured with human osteosarcoma cells. The incorporation of HAp into PCL did not affect cell viability, meanwhile the presence of the surfactant increase the cell surface contact to the substrate.

DISCUSSION & CONCLUSIONS: This experimental approach demonstrates that oleic acid enhances HAp dispersion in PCL and introduces significant surface modifications that improve cell adhesion.

REFERENCES: [1]Kao, ST, Scott, DD. (2007) *Oral Maxillofac Surg Clin North Am* **19**:513-21.[2] Cardoso, GBC, Ramos, SLF, Rodas, ACD, Higa, OZ, Zavaglia, CAC, Arruda, ACF. (2010) *Journal of Materials Science* **45:** 4990-93. [3]Tondon, A, Hsu, HJ, Kaunas R. (2012) *Journal of Biomechanics* **45**:728-35.

Corresponding author:
guicardoso@fem.unicamp.br;
maniglio@ing.unitn.it; fabiozomer@gmail.com;
a.tondon@neo.ta; claudio.migliaresi@ing.unitn.it
rkaunas@bme.tamu.edu; zavagl@fem.unicamp.br

Characterization of Dental Interfaces with Electron Tomography

K Grandfield[1], H Engqvist[2]

[1] *Department of Materials Science and Engineering, McMaster University, Hamilton, ON, Canada.*
[2] *Applied Materials Science, Department of Engineering Sciences, Uppsala University, Uppsala, Sweden.*

INTRODUCTION: Understanding the interface between dental materials and tooth is critical in the prevention of secondary caries. Assessing this interface with high-resolution clarity has traditionally been challenging. This work highlights electron tomography as a novel technique to obtain both three-dimensional and nanometre scale information on dental materials in contact with dentin. The versatility of this technique can be extended to applications in other biointerfaces, including dental and orthopaedic implant interfaces to bone. [1]

METHODS: Dental cements Ceramir® C&B (Doxa AB, Sweden) and Fuji I (GC Europe, Belgium) were applied to extracted teeth according to manufacturer's guidelines. Samples were sectioned longitudinally with a slow-speed saw to reveal the dentin–cement interface in cross-section. Focused ion beam (FIB) was used to create thin lamellae (<100 nm) of this interface for subsequent transmission electron microscopy (TEM) study. Z-contrast electron tomography was performed on a Titan 80-300 (FEI Company) operated at 300 kV. High-angle annular dark-field (HAADF) images were recorded over a ± 60° angular range with FEI's Explore3D software. Reconstructions were performed using weighted-back projection in IMOD[1], while 3D volumes were visualized in Amira® (VSG, an FEI Company).

RESULTS: SEM analysis of cement-dentin provides an overview of cement attachment, yet clearly lacks sufficient resolution to draw further conclusion about degree of integration, Fig. 1.

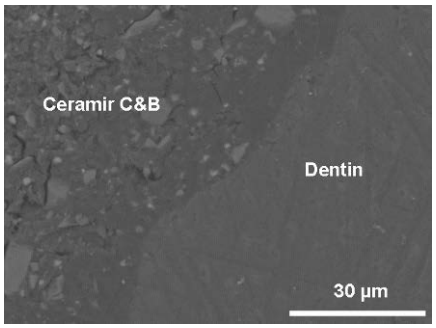

Fig. 1: SEM image of the dentin–Ceramir® interface of interest.

FIB preparation successfully maintained interface integrity for further TEM study, Fig. 2. Tomography reconstructions, Fig. 3, enabled high-resolution visualization of the attachment zone of dentin with commercial glass ionomer (Fuji I) and calcium aluminate (Ceramir) cements.

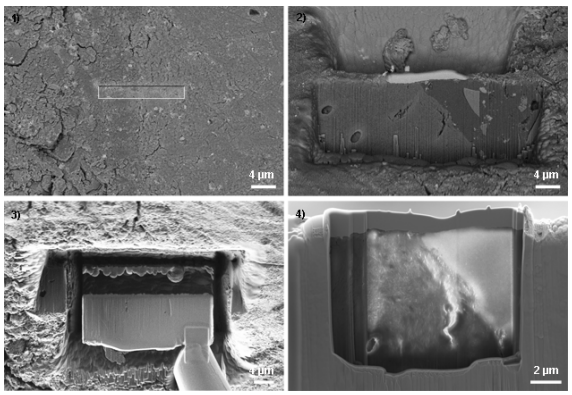

Fig. 2: FIB in-situ sample preparation technique for TEM lamellae production.

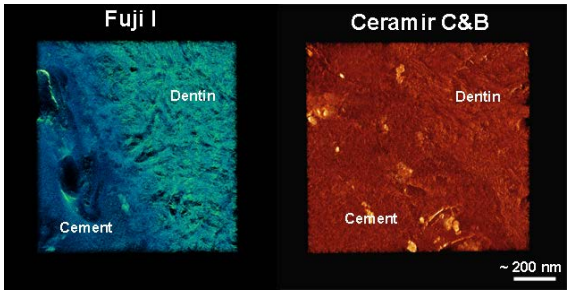

Fig. 3: 3D volume renderings of the dentin–cement interface.

DISCUSSION & CONCLUSIONS: Results demonstrate a clear difference in the attachment zones between glass ionomer and calcium aluminate cements, easily visualized via electron tomography. Z-contrast electron tomography has presented itself as a promising technique for interfacial dental material studies.

REFERENCES: [1]K. Grandfield, A Palmquist, H. Engqvist (2012) *Phil. Trans. R. Soc. A* **370**:1337-51. [2]J.R. Kremer, D.N. Mastronarde, J.R. McIntosh (1996) *J. Struct. Biol.* **116**:71-6.

ACKNOWLEDGEMENTS: The tomography work was carried out at the Canadian Centre for Electron Microscopy, a National Facility supported by NSERC and McMaster University.

Cryogenic X-ray Photoelectron Spectroscopy enables studies of unaltered biological and biomedical surfaces and interfaces

A Shchukarev, M Ramstedt

Department of Chemistry, Umeå University, Umeå SE-901 87 Sweden

X-ray photoelectron spectroscopy (XPS) is one of the most widely used principal techniques for surface and interface analysis of materials. Routinely, XPS applications are limited by ultra-high vacuum conditions inside the electron spectrometer which are necessary to obtain spectra. In the case of hydrated samples, this limitation can be avoided in two general ways recently discussed [1]. In particular, cryogenic XPS with fast-frozen samples was shown to be a very promising technique to reveal important phenomena at the mineral-aqueous solution interface, and it can be applied to any suspension, slurry, gel, etc. including hydrated microbial samples and biomaterials in biologically relevant media.

The fast-freezing sample preparation protocol is discussed in detail and compared with traditional freeze-drying procedure that has been applied to study the chemical composition of bacterial cell walls. For the Gram-positive bacterium *Bacillus subtilis*, cryogenic XPS allowed identification and quantification of surface functional groups (carboxylate, amide and phosphate) responsible for the acid-base properties of the cell wall [2]. Moreover, it was possible to follow the protonation of amide groups and the metabolic activity of the cells (excretion of proteins and/or peptides) caused by changes in pH of the bacterial suspension. Contrary to freeze-dried bacteria, samples with fast-frozen cells reveal interface processes such as local pH/cell charge regulation at the surface. This can be observed by following changes in Na/Cl atomic ratio at the bacterial cell surface, as a function of suspension pH.

Surface chemical changes in the bacterial cell wall that are caused by mutations or by external factors, such as growth conditions, can be monitored by applying multivariate analysis of cryogenic XPS data (C 1s spectra) as demonstrated for a range of Gram-negative *Escherichia coli* mutants [3]. The approach is easy to use and predicts the content of lipids, carbohydrates, and proteins/peptidoglycans at the surface of any microbial sample.

The development of surface charge and rapid protein adsorption are two major phenomena experimentally observed at the surface of three bone graft substitute materials (Algipore®, Bio-Oss®, and bioactive glass 45S5) that were treated in α-MEM cell culture medium with and without an addition of fetal bovine serum [4]. The formation of positively charged interface with a continuous layer of adsorbed protein covering the surface was common for all three biomaterials in the protein containing medium. These two phenomena seem to be necessary prerequisites to facilitate osteoblast attachment, recognition, and subsequent biomineralization. The immediate protein adsorption on these surfaces raises a question regarding the applicability of simulated body fluid and pure α-MEM for testing bioactivity of artificial materials.

REFERENCES: [1] A. Shchukarev (2006) *Adv. Colloid Interface Sci.* **122**:149-157. [2] L. Leone, J. Loring, S. Sjöberg, et al (2006) *Surf. Interface Anal.* **38**:202-205. [3] M. Ramstedt, R. Nakao, S.N. Wai, et al (2011) *J. Biol. Chem.* **286**: 12389-12396. [4] A. Shchukarev, Z. Mladenovic, M. Ransjö (2012) *Surf. Interface Anal.* **44**: 919-923.

Electrochemical and XPS studies of AISI 316L stainless steel after ethylene oxide sterylization

W Walke[1], J Przondziono[2], J Szade[3]

[1] *Department of Biomaterials and Medical Engineering Devices, Silesian University of Technology, Zabrze, Poland* [2] *Department of Technology Materials, Silesian University of Technology, Katowice, Poland* [3] *A. Chełkowski Institute of Physics, University of Silesia, Katowice, Poland*

INTRODUCTION: Usability of a respective way of surface modification requires performance of a number of tests, under both laboratory as well as clinic conditions. The initial stage includes corrosion tests performed under in vitro conditions, simulating specific environment of the tissue to which certain product is to be inserted. Therefore, this study analyses the impact of the way of surface preparation and sterilisation process in ethylene oxide on corrosion characteristics of AISI 316L steel [1-4].

METHODS: Wires made of AISI 316L steel with differentiated way of surface preparation were used for the tests. Proper surface roughness (R_a = 0.12 μm) was obtained through application of mechanical polishing. Samples were then subject to chemical passivation in 40 % HNO_3. The last stage included sterilisation of samples in ethylene oxide at the temperature of T = 55 °C in sterilisation device Steri-Vac 5XL. In order to obtain information regarding physical and chemical properties of modified surface of AISI 316L steel, potentiodynamic tests were carried out as well as EIS and XPS. Anodic polarisation curves were registered with application of potentiostat PGP-201 by Radiometer Analytical SAS. Impedance measurement was made with application of measurement system AutoLab PGSTAT 302N equipped with FRA2 (Frequency Response Analyser) module. Analysis of chemical composition of the upper layer was made with application of a multifunctional electron spectrometer by Physical Electronics PHI 5700/660.

RESULTS: Application of sterilisation in ethylene oxide caused increase of mean value of corrosion potential, irrespective of the way of surface modification. Favourable increase of polarisation resistance was also proved, and therefore - decrease of corrosion current density. Next, Nyquist diagrams, determined for various modifications of the surface of samples, present fragments of large, incomplete semicircles that are a typical impedance response of thin oxide layers. Maximum values of phase angles, presented in Bode diagrams, in a wide range of frequencies, irrespective of the way of surface modification, are similar and do not exceed $\theta \approx 85°$. $\mathrm{Log}|Z|$ inclinations in the whole scope of frequency changes are close to -1, which proves capacitive character of the passive layer. Next, large values of impedance $|Z| > 10^6\ \Omega cm^2$ in the range of the smallest frequencies prove good dielectric and protective properties of passive layers created on the surface of samples made of AISI 316L steel after sterilisation in ethylene oxide. The following elements were identified in the passive layer: N, O, S, Cr, Fe, Ni, Mo. Obtained spectra of the respective elements showed that passivation process caused increase of concentration of oxygen connected mainly with chromium and iron. Concentration of the respective alloy elements (Fe, Cr, Ni, Mo) in relation to chemical composition of the substrate was substantially decreased, which should be seen favourable for bio-tolerance.

DISCUSSION & CONCLUSIONS: On the ground of performed potentiodynamic and impedance tests and evaluation of chemical composition it was explicitly proved that employment of chemical passivation process of 316L steel used for cardiological implants is reasonable and entirely useful in order to improve safety of their application. Then, application of ethylene oxide as a sterilising agent for, among other things, stents or heart valves did not have negative impact on physical and chemical properties of created passive layer.

REFERENCES: [1] N.D. Nam, S.H. Lee, J.G. Kim et all (2009) *Diamond & Related Mat.* **18**:1145–1151. [2] W. Walke, J. Przondziono (2012) *Przegląd Elektrotechniczny* **88**:144-147. [3] W. Walke, J. Przondziono (2012) *Metalurgija* **51**:237-240. [4] Z. Paszenda (2008) *Advances in Soft Computing* **47**:15-27.

ACKNOWLEDGEMENTS: This project was financed from the funds of the National Science Centre in Cracow, Poland.

Electrochemical behavior and XPS studies of X10CrNi 18-8 steel after steam sterilization

J Przondziono[1], W Walke[2]

[1] *Department of Technology Materials, Silesian University of Technology, Katowice, Poland*
[2] *Department of Biomaterials and Medical Engineering Devices, Silesian University of Technology, Zabrze, Poland*

INTRODUCTION: Stainless steel X10CrNi 18-8 is popular in medicine, among other things for production of surgical instruments used for the improvement of implementation techniques of electrotherapy devices. Endocavital electrodes implantation would not be possible without guide wires – in the form of a thin wire, which enable to insert electrodes inside blood vessels and control their location. Quality of applied guide wires conditions the course of treatment and its success to a great extent [1-4].

METHODS: Wires made of X10CrNi 18-8 steel with diameter of d = 1.5 mm were used for the tests. Samples surface was differentiated by means of mechanical working – grinding (R_a = 0.40 μm) and polishing (R_a = 0.12 μm). Steam sterilisation process was carried out at the temperature of T = 121 ^{o}C, pressure p = 1.1 bar for t = 30 min. In order to simulate conditions that can be found in blood vascular system samples were exposed to artificial blood plasma (T = 37±1 ^{o}C) for the time of 8 h. In order to obtain information regarding physical and chemical properties of modified surface of wire made of X10CrNi 18-8 steel, EIS test and tests of chemical composition of the surface layer XPS were made.

RESULTS: Characteristics of impedance of phase boundary: steel X10CrNi 18-8 – surface layer – artificial blood plasma was made through approximation of experimental data with application of electrical equivalent circuits – fig. 1. Next, obtained spectra of the respective elements showed that passivation process caused increase of oxygen concentration connected with mainly with chromium and iron. Concentration of the respective alloy elements (Fe, Cr, Ni) in relations to chemical composition of the substrate was substantially decreased, which must be seen as a favourable factor for bio-tolerance. It was proved that chemical passivation process had a favourable impact on characteristics of the surface layer after sterilisation in pressurised water steam. Whereas, in addition, on the surface of the samples exposed to blood (8 h), the following elements were identified: Na, Cl, K, Mg, O, C, H and Ca.

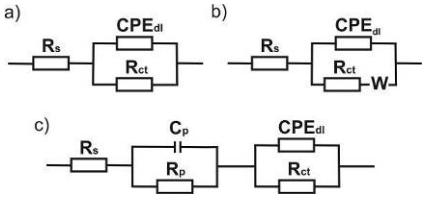

Fig. 1: Electrical equivalent diagrams for steel with surface that was: a) polished, pasivated, passivated and sterilised and passivated, sterilised (exposure 8h – blood), b) polished and sterilised, c) polished, sterilised (exposure 8h – blood).

DISCUSSION & CONCLUSIONS: On the ground of performed EIS and XPS tests, favourable impact of steam sterilisation process on corrosion resistance of X10CrNi 18-8 steel was observed only for the case when chemical passivation was applied prior to sterilisation. Exposure to the solution simulating blood and vascular system (artificial blood plasma) did not influence physical and chemical properties of created passive layer in a negative way. Employment of chemical passivation process of X10CrNi 18-8 steel used for cardiological instruments is reasonable and entirely useful in order to improve safety of its application.

REFERENCES: [1] W. Kargul, R. Młynarski, E. Piłat (2005) *Chirurgia Polska* **7**:267-279. [2] W. Walke, J. Przondziono (2013) *Metalurgija* **52**:371-374. [3] W. Walke, J. Przondziono (2012) *Lecture Notes in Computer Science* 7339: 389-397. [4] P.A. Schneider (2009) *Endovascular skills. Guidewire and catheter skills for endovascular surgery.* Informa Healthcare.

ACKNOWLEDGEMENTS: This project was financed from the funds of the National Science Centre in Cracow, Poland.

Spectroscopic and morphological studies on interaction between gold nanoparticles and liposome constructed with phosphatidylcholine(PC)

C Tsukada[1], T Tsuji[1], K Matsuo[2], G Kutluk[2], H Nameki[3], T Yoshida[4], S Yagi[4]

[1]Graduate School of Engineering, Nagoya University, Japan [2]Synchrotron Radiation Center, Hiroshima University, Japan [3]Aichi Center for Industry and Science Technology, Japan [4]EcoTopia Science Institute, Nagoya University, Japan

INTRODUCTION: Gold nanoparticles(Au NPs) are paid attention to use of the hyperthermia for cancer cells in the medical field, and the many investigations for the hyperthermia using Au NPs and cells have been carried out[1]. However, the adsorption reaction between biomolecule constructing our body and Au NPs has not been reported. Thus, we have selected the reaction under water environment as one of the reaction conditions in our body, and revealed the adsorption reaction between L-cysteine and Au NPs with clean surface under water environment in our previous study[2]. The L-cysteine has adsorbed on Au NPs surface at thiol group and in addition those Au NPs have been aggregated by hydrogen bonding between the amino and carboxyl groups assigned to the adsorbates. Subsequently, we focus on the interaction between liposome constructed by phosphatidylcholine(PC) and the Au NPs. The liposome is generally utilized as the cell membrane model. The purpose in this study is to reveal the adsorption reaction between PC liposome and Au NPs surface by spectroscopic and morphological studies.

METHODS: The Au NPs colloidal solution was prepared by solution plasma method[2]. The PC liposome was fabricated by means of extrusion procedure[3]. The PC powder(Egg, >99 %) was dissolved into distilled water and the PC suspension solution was extruded through a polycarbonate membrane with pore diameter of 400 nm. The solution with PC liposome is called in this paper as “PC liposome solution”. The fabricated Au NPs colloidal solution and PC liposome solution were mixed. To clear the adsorption chemical states for several functional groups of PC molecules adsorbed on Au, Au sheet was reacted in PC suspension solution, which did not includes liposome, and was dried in air after rinsing with distilled water. This sample is described as “PC/Au”. TEM observation using H-7600(Hitachi) and Phosphorous(P) K-edge Near-Edge X-ray Absorption Fine Structure(NEXAFS) measurement at HiSOR BL-3 were carried out.

RESULTS: Fig.1 shows TEM image after mixing PC liposome solution and Au NPs colloidal solution. The Au NPs are observed on the PC liposome. The Au NPs look like covered with membrane molecule. The peak position of P K-edge NEXAFS spectrum for the PC/Au varies in comparison with that for PC, which does not react with Au.

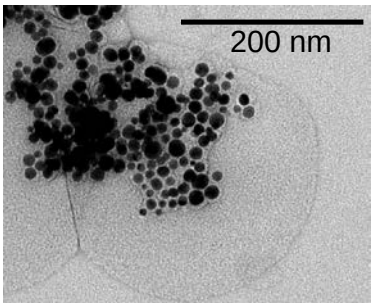

Fig. 1 TEM image after mixing PC liposome solution and Au NPs colloidal solution.

DISCUSSION & CONCLUSIONS: We think the membrane molecule around the Au NPs has been generated by the adsorption of PC molecules, which do not construct liposome. Moreover, because the obtained P K-edge NEXAFS spectra possess the difference, it is speculated that the NPs interact with a phosphate group of PC. The details of the reaction including the chemical states of other functional groups for PC molecule will be discussed in this conference.

REFERENCES: [1] H.-C. Huang et al. (2010) *J. Am. Chem. Soc.* **4**:2892-2900. [2] C. Tsukada et al. (2013) *e-J. Surf. Sci. Nanotech.* **11**:18-24. [3] R.C. MacDonald et al. (1991) *Biochim. Biophys. Acta* **1061**:297-303.

ACKNOWLEDGEMENTS: This work was supported by JSPS Research Fellow, and performed under the approval of HSRC Program Advisory Committee (No. 13-A-26). We thank Prof. J. Usukura for useful discussions.

On the surplus of combinatorial surface analysis of biomaterials: The case of degradation in Zirconia ceramics at body temperature

KG Nickel[1], M Keuper[1], C Berthold[1]

[1]*University Tuebingen, Applied Mineralogy, Wilhelmstr. 56, D-72074 Tuebingen, Germany*
klaus.nickel@uni-tuebingen.de

INTRODUCTION: The surficial degradation of Zirconia dental and orthopedic bioceramics is a threat to the longevity of the implants. The common surface analysis by XRD techniques is prone to yield ambiguous interpretations unless boundary conditions are known. We will show that only a calibration of the equipment at the specific setting on the material of interest provides the basis to correctly infer kinetics of surface processes from XRD and the simultaneous application of further analytical techniques.

METHODS: Our case study is on Zirconia stabilized by 3 mol% Y_2O_3 (3Y-TZP), which is a common material in dental and orthopedic applications. Degradation occurs by surficial phase transformation due to water-ceramic interaction. In experiments running for several years it can be shown that this process is slow, but active at body temperatures and comparatively fast at steam sterilization [1]. The analytical techniques used next to Micro-XRD is Micro-Raman Spectroscopy, the calibration investigation is done by FIB/SEM.

RESULTS: Surface XRD yields data, which are quantified by Rietfeld-type calculations. However, the results obtained hereby are not merely averages from a zone penetrated by X-rays. The exponential increase of absorption of X-rays with depths (law of Lambert-Beer) distorts results for all cases, where no statistical distribution of phases is present (Fig. 1). Sections and lamellae cut by FIB and observed by SEM, EBSD and Raman spectroscopy allow to infer a simple layer-growth type situation and provide fix points for a calibration of XRD interpretations. However, the point in time, at which the degradation starts at body temperature is somewhat variable. Our results indicate a variation as a function of water content in the atmosphere, temperature and subtle microstructural differences.

DISCUSSION & CONCLUSIONS: Only after the calibration utilizing FIB-sections we can recalculate the XRD data as a reflection of an advancing front of a largely transformed layer. The fact of a maximum of transformability in Zirconia from low-temperature degradation is the reason for earlier misinterpretations, claiming a stopping or retardation of the degradation with time.

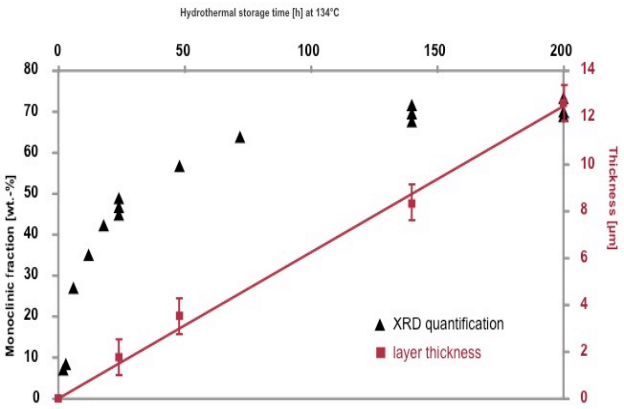

Fig. 1: Linear low-temperature degradation from FIB and exponential increase of calculated monoclinic fraction from XRD (after[1])

The transformation of ambiguous calculations into information about the kinetics of a corrosive attack provides an example for the necessity to apply more than one method of analysis to evaluate bioceramics surface behavior. Consequently it is now possible to quantify the kinetics of low temperature degradation of Zirconia and provide figures of merit for improvements.

REFERENCES: [1]M. Keuper et al., (2013) *Acta Biomaterialia* **9(1)**:4826-35.

ACKNOWLEDGEMENTS: Funding by DFG (Ni299-23/1) and support by VITA Zahnfabrik, Bad Säckingen, Germany is greatfully acknowledged

Biocompatibility, bio-degradation and mechanical properties of Mg-0.5Sr alloy for use as temporary cardiovascular implants: The formation of Sr-substituted hydroxyapatite

M Bornapour[1], M Cerruti[1], D Shum-Tim[2], M Pekguleryuz[1]

[1] *Department of Mining & Materials Engineering, McGill University, Montreal, Canada*
[2] *Department of Cardiac Surgery, McGill University, Montreal, Canada*

INTRODUCTION: Magnesium (Mg) is a potential material to use in biodegradable implants due to its light weight and biocompatibility which make it appropriate for a wide range of applications varying from bone implants to cardiovascular stents [l-2]. The main shortcoming of Mg alloys is its high corrosion rate in physiological conditions. It was found that the addition of low levels of strontium (Sr) to Mg (~0.5wt%) improves the mechanical properties and increases the corrosion resistance [3-4] but the corrosion mechanism of Mg-Sr alloys has not been well understood to-date. In our study, the degradation behavior and the biocompatibility of Mg-0.5Sr are studied via *in-vitro* and *in-vivo* tests; the corrosion mechanism and the evolution of the surface in physiological conditions are elucidated.

METHODS: Mg-0.5Sr alloy was synthesized using pure Mg (99.9wt%,) and pure Sr (99.99wt%) in a Lindberg/Blue M Crucible Furnace and cast into thin plates. Mg-0.5Sr samples were immersed in simulated body fluid (SBF) and the degradation behavior and mechanism were studied via X-ray diffraction (XRD) and scanning electron microscopy (SEM) equipped with energy-disperse spectrometry (EDS). The corroded surface was characterized by X-ray photoelectron spectroscopy (XPS). Mechanical properties of Mg-0.5Sr were investigated via tensile and three-point bending tests. The cytotoxicity of the alloy was evaluated by an indirect cell viability assay. Samples were incubated in 10 ml of F-12K medium for 72 hrs to obtain the extraction medium. HuVEC cells were exposed to the Mg-0.5Sr extraction medium in a humidified atmosphere with 5% CO_2 at 37°C for 1, 4 and 7 days. Also, a tubular Mg-0.5Sr stent sample was implanted into the right femoral artery of a dog for three weeks to investigate its in-vivo biocompatibility.

RESULTS: XRD characterization revealed the formation of hydroxyapatite (HA) and $Mg(OH)_2$ on the surface of Mg-0.5Sr after 3 days of immersion in SBF. SEM and EDS analysis on both surfaces indicated the presence of Ca and P, and a Ca/P ratio ~1.6, corresponding to the formation of HA. ***XPS showed the formation of a Sr-substituted HA layer on the alloy surface, which is deemed responsible for the lower degradation rate of the alloy.*** Mg-0.5Sr demonstrates higher strength but less ductility than pure Mg. Cytotoxicity assays showed that the viability of HuVEC cells cultured in Mg-0.5Sr extraction medium is close to the control after 24h of exposure and the viability increases with longer exposure to the alloy extract. Mg-0.5Sr alloy stent implanted in femoral artery did not trombose after 3 weeks. The retrieved sample was degraded to almost half of its initial volume.

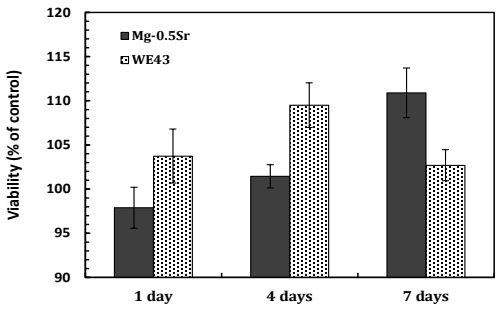

Fig. 1: Cell viability expressed as a percentage of the viability of cells in the control (F-12K) after 1, 4 and 7 days of exposure to the extraction of Mg-0.5Sr and WE43 alloys.

DISCUSSION & CONCLUSIONS: In vitro and in vivo tests show that Mg-0.5Sr has the potential to be used as temporary vascular implant: its released ions were not toxic to HuVEC cells and a stent made with this alloy did not lead to thrombosis. A crucial finding of this study is the formation of a Sr-substituted HA layer on Mg-0.5Sr during bio-corrosion in SBF. The formation of this modified layer stabilizes the surface and reduces the degradation rate of this alloy in physiological conditions. However, further alloy development is needed to optimize mechanical properties.

REFERENCES: [1] M.P. Staiger, et al (2006) *Biomaterials* **27**:1728-1734. [2] B. Heublein, et al (2003) *Heart* **89**:651-656. [3] X.N. Gu, et al (2012) *Acta Biomater* **8**:2360-2374. M.Bornapour, et al (2013) *Acta Biomater* **9**:5319-5330.

Surface characteristic and *in vitro* biocompatibility of HPT-deformed NiTi alloys

DN Awang Shri[1,2], K Tsuchiya[1,2], A Yamamoto [2]

[1] *Graduate School of Pure and Applied Sciences, University of Tsukuba, Tsukuba, Ibaraki 305-8577, Japan* [2] *National Institute for Materials Science, Tsukuba, Ibaraki 305-0047, Japan*

INTRODUCTION: Nickel titanium (NiTi) shape memory alloys are used widely in medical device applications due to its unique properties such as shape memory effect and superelasticity. Bulk nanostructured NiTi can be obtained by using high pressure torsion (HPT) in which the sample is subjected to a compressive force and concurrent torsional straining [1]. The biocompatibility of the NiTi alloys has been attributed to the formation of protective passive film that forms spontaneously upon contact with air [2]. In biological environment, this natural oxide films acts as interface between material-cell interactions. However, the changes in NiTi structure due to HPT deformation may affect the behavior of this oxide film. In this present study, the effect of phase composition and structural changes on the biocompatibilities and surface characteristics of the NiTi alloys were investigated.

METHODS: Two different NiTi alloys, martensitic Ti-50%Ni and austenitic Ti-50.9%Ni, were subjected to HPT at number of rotation (N), N=0.25, 1 and 10 rotations. The phase and hardness of the samples were analyzed using X-ray diffractometer and micro Vickers hardness tester. The cytocompatibility of the samples was investigated using colony formation assay of murine fibroblast L929 cells. The surface compositions of the sample before and after immersion in the medium were analyzed using X-ray photoelectron spectroscopy while the surface potential was measure using Kelvin force microscopy. Ni ion release was quantified using inductively coupled plasma mass spectrometry.

RESULTS AND DISCUSSION: Phase analysis shows both alloys turns into nanocrystalline/ amorphous structure with increased hardness after subjected to HPT. Cytocompatibility test shows the plating efficiency of the cell colonies on the surface of the sample increases after the HPT, indicating no cytotoxic effect. Fig. 1 shows the difference in cell colony morphology formed on before HPT (BHPT) and N=1 of Ti-50Ni samples after 7 day inoculation in cell culture medium. Before HPT, the colony formed was loose with larger cell size. However, in HPT deformed NiTi, the formed colony has clear defined edges with high cell density indicating faster cell growth and better cell-cell interaction [3].

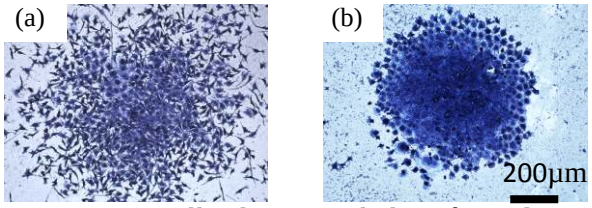

Fig. 1: L929 cell colony morphology formed on (a) BHPT and (b) N=1 sample surface.

XPS results reveals passive film formed on BHPT was enriched with metallic Ni. However, after HPT, Ni enrichment on the sample surface decreases for both alloys. KFM results also shows HPT deformed NiTi have higher surface potential corresponds to better corrosion resistance. This behavior may influenced the Ni ion release suppression of HPT deformed NiTi into the cell culture medium as shown in Fig.2.

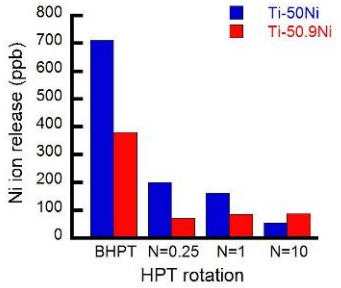

Fig. 2: Ni ion release into cell culture medium over 7day period.

CONCLUSIONS: This study has shown that bulk nanostructuring of NiTi via HPT improves its mechanical and surface properties. Passive films with no Ni enrichment formed on NiTi after HPT deformation has led to suppression of Ni ion release and better cell response in vitro.

REFERENCES:

[1]K. Tsuchiya, et al (2007) *Mater. Sci. Forum.* **539-543**:505–510. [2]Shabalovskaya, S., et al (2008) *Acta Biomater.* ***4*(3)**:447-467.[3]Furuhashi, A.,et al. (2012) *Odontology* ***100*(2)**:199-205.

Nano-thick amorphous oxide layer grown on SS316L to improve corrosion characteristics in biological environment

M Dorri[1], M Cloutier[1], S Turgeon[1], N Brodusch[2], R Gauvin[2], D Mantovani[1]

[1] *Lab. for Biomaterials and Bioengineering (CRC-I), Dept. Min-Met-Materials Eng. & University Hospital Research Center, Laval University, Quebec City, Canada*

[2] *Dep. of Mining and Materials Engineering, McGill University, Montreal, Canada*

INTRODUCTION: Localized corrosion, the main source of failure in stainless steel medical grade (SS316L) devices, can be decreased effectively by converting the micro-scale grain structure of the oxide layer to an amorphous structure [1]. In previous works, the native oxide layer of SS316L, which is inhomogeneous and mechanically unstable, was removed in a Glow Discharge Radio Frequency (GDRF) plasma, and then replaced by a newly grown oxide layer via plasma oxidizing (PO) treatment. Results showed that this process increased the corrosion resistance [2, 3]. To optimize the uniformity and the thickness of the oxide layer, the first step is to find an appropriate characterization method to validate the existence of the amorphous oxide layer and to measure its thickness. The microstructural characterization of the nano-thick oxide layer was not possible with common surface characterization methods. Finally, for the first time, a combination of Electron Backscatter Diffraction (EBSD) and Electron Channeling Contrast Image (ECCI) was able to successfully assess the amorphous oxide layer.

METHODS: The samples were cleaned and electropolished (EP) before entering the GDRF reactor. Plasma surface modification was done in two steps: 1) removal of the native oxide layer 2) growing the new oxide layer by PO [2]. For microstructural characterization the idea was to use EBSD patterns and ECCI at different electron beam energies in order to deduce the crystalline/amorphous state of the surface layer. Monte-Carlo simulations estimated the thickness of the oxide layer. Potentiodynamic test and X-ray Photoelectron Spectroscopy (XPS) were applied to evaluate the corrosion rate and the chemical composition. The results were compared with the EP sample as the control.

RESULTS: XPS depth profiles of PO samples revealed the formation of a thicker oxide layer in comparison with the EP, along with a significant decrease of the nickel content from the surface. Tafel analysis from potentiodynamic curves showed significant improvement of the corrosion properties after PO (corrosion rate decreased from 0.30±0.02 µm/year for EP to 0.09±0.06 µm/year for PO). ECCIs of PO samples obtained with a decreasing energy (5keV, 2keV and 1keV) showed progressive contrast extinction. It denotes the presence of a thin (6-11 nm from Monte-Carlo simulations) amorphous layer that extinguish the diffraction signal from the underneath substrate. EP interfaces did not show the same tendency, with grain contrast still easily visible at 1keV. EBSD patterns showed a similar behavior, with a marked decrease of Kikuchi bands contrast and sharpness at decreasing energy, for the PO treated samples (some of the results, Fig. 1).

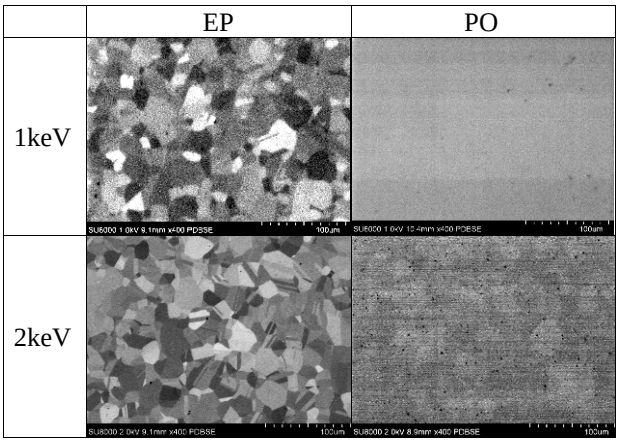

Fig. 1: ECCI of EP and PO samples with 1 and 2 keV electron beam energies.

DISCUSSION & CONCLUSIONS: The oxide layer produced after PO has amorphous structure which explains significant improvement of the corrosion rate. These characteristics of the new oxide layer on SS316L made it more resistant to leaching of potentially toxic materials in biological environment.

REFERENCES: [1] R. Cottis, L. L. Shreir (2010) Corrosion of amorphous and nanograined alloys. 4th ed. **3**:2192-2202. [2] M. Cloutier, et al (2011) *Adv Mat Res* **409**:117-122. [3] J. Okado, et al (2008) *Surf Coat Tech* **202**(22–23):5595-5598.

ACKNOWLEDGEMENTS: The authors acknowledge Pascale Chevallier scientific support.

Interface implant – bone cement : Damage mechanism of thin film coating on TiAl6V4- alloy

P Choungthong, S Sribuddthinipon, C Dumkum

Department of Production Engineering, King Mongkut's University of Technology Thonburi, Bangkok, Thailand

INTRODUCTION: The premature failure of the cemented hip endoprosthesis from Titanium-based alloy is caused by aseptic loosening. This mode of failure can be associated with the generation of so called wear debris [1-3]. These particles are generated because of the surface damage at the interfacial contact between implant and bone cement even though the hip implant was coated with hard thin film layer e.g. TiN, TiAlN and TiAlCN. However, there is no study about coating by Titanium Aluminium Vanadium Carbonitride ($TiAlVC_xN_y$). This study will be investigated the effect of methane flow rate during Titanium Aluminium Vanadium Carbonitride coating on Titanium Alloy (Ti-6Al-4V) which will affected to improve the coating surface properties. In addition, the damage mechanism regarding to the thickness coating layer on Titanium specimens should be consider as well.

METHODS: Blasting Process: TiAl6V4 (Dimension: 30 mm x 12 mm x 6 mm) specimens were blasted by apply various blasting media (Alumina Grit or Steel Ball) in order to modify the different surface roughnesses of the specimens.

Coating Process: To compare the effects of coating layer on the damage mechanisms, Titanium Nitride and Titanium Aluminium Vanadium Carbonitride ($TiAlVC_xN_y$) were selected as coating layer in DC unbalance magnetron sputtering physical vapor deposition. Before coating process, the substrate was cleaned with trichloroethylene and acetone in ultrasonic cleaning device for 10 minutes. Then, the substrate was brought into the coating chamber.

Wear Testing: the coated TiAl6V4 specimens were set to run against the bone cement (cranioplastic: methylmethacrylate resin) incrementally in the oscillating wear testing device with a linear constant amplitude of 100 µm. The nominal contact pressure was held at 6 MPa and the frequency of 10 Hz. The maximum running time was limited at 1 million cycles. After wear testing, the surfaces of TiAl6V4-specimens were investigated by SEM, EDX and XRD.

RESULTS: The surface morphology and cross sectional image of coating layer as can be seen in Figure 1. It was found that thickness layer of $TiAlVC_xN_y$ is 0.615 µm.

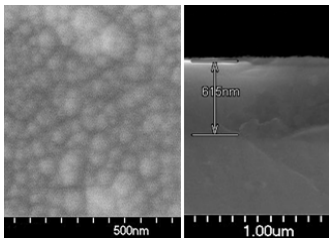

Fig. 1: (Left) coating morphology (Right) cross sectional image of coating thickness.

Fig. 2 represents the abrasive wear mode (left) and the surface delamination (right) of coating layer.

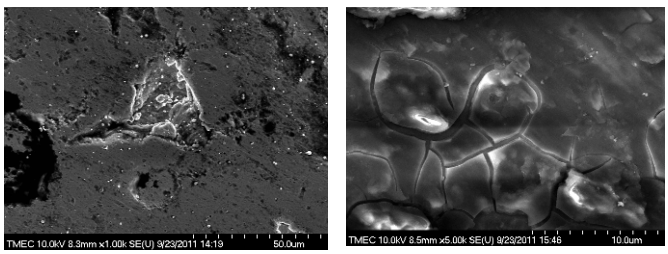

Fig. 2: Mode of surface damages left) abrasive wear right) surface delamination of thin film coating after wear test 1,000,000 cycles at wet condition.

DISCUSSION & CONCLUSIONS: The experimental outcomes demonstrate the effects of methane gas flow rate on the tribological effects of the $TiAlVC_xN_y$ layer and the thickness of coating layers determine the surface damage mechanisms which can be explained by Hertzian contact theory.

REFERENCES: [1] A.V. Lombardi, et al (1989) *J Bone Joint Surg* **71-A** 1337- 1342. [2] H.J. Agins, et al (1988) J Bone Joint Surg **70-A** 347-356. [3]P. Choungthong et al (2004) BIOmaterialien **4 (4)** 305-313.

ACKNOWLEDGEMENTS: The study was financial supported by the Thailand Research Fund (TRF).

Characteristics and biological responses of strontium-substituted hydroxyapatite coatings on titanium by electrochemical deposition

KC Kung[1], YT Liu[1], HL Chang[2], YC Li[2], TM Lee[3,4], TS Lui[1]

[1] *Department of Materials Science and Engineering, National Cheng Kung University, Taiwan*

[2] *Institute of Manufacturing Information and Systems, National Cheng Kung University, Taiwan*

[3] *Institute of Oral Medicine, National Cheng Kung University, Taiwan*

[4] *Medical Devices Innovation Center, National Cheng Kung University, Taiwan*

INTRODUCTION: The titanium and its alloys are widely used in orthopedic and dental field. Calcium phosphate, especially hydroxyapatite (HA), coated on titanium could improve the titanium property [1]. Strontium-substituted calcium of calcium phosphates has been developed, because strontium (Sr) could increase bone formation and decrease bone resorption [2]. The electrolytic deposition is an attractive process for coating calcium phosphate on titanium surface. The aim of this study is to investigate the characteristics and biological responses of Sr-HA coatings by the electrolytic deposition.

METHODS: Disks of medical grade titanium, measuring 12.7 mm in diameter and 2 mm in thickness, were selected as substrate. The electrolyte was prepared by dissolving $Ca(NO_3)_2$, $Sr(NO_3)_2$, and $NH_4H_2PO_4$ in di-ionized water. The specimen was used as the cathode, and a Pt plate was used as the anode. The samples were treated with an applied current of 60 mA/cm^2 for 30 min. For heat treatment, the specimens were heated at temperature of 700°C with a heating rate of 2°C/min and then held for 4 h. The physicochemical properties were evaluated by SEM, EDS, and XRD equipments. The biological properties were evaluated by *in vitro* tests, in term of the cell morphology and cell proliferation.

RESULTS: Figure 1 shows the microstructures of the coatings morphology. The Sr-HA was uniformly coated on the titanium. The EDS analysis indicated that the strontium element can incorporate into coatings during process of electrolytic deposition. The XRD results showed that HA phase was observed in the pattern. Besides, the deposited Sr-HA coatings exhibited the excellent bioactivity properties. The surfaces of Sr-HA coatings were covered with apatite after immersion in the SBF. Cell morphologies were shown in the Figure 2 after 0.5 and 12 h of cell culture. At 0.5-h of culture, the cell shape was observed with filopodia extensions. At 12-h of culture, the cells were flattened on the specimens. Moreover, the cell proliferation on the Sr-HA coatings was indicated that cell number was significant increase.

Figure 1 Figure 2

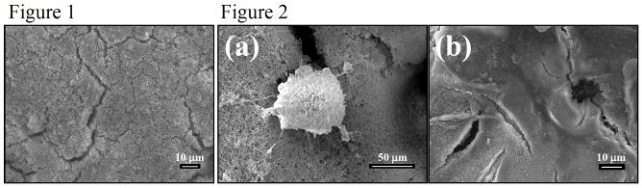

Fig. 1: SEM micrograph of deposited Sr-HA coatings.
Fig. 2: Cell morphologies on the Sr-HA coatings. (a) 0.5 h, and (b) 12 h.

DISCUSSION & CONCLUSIONS: The structures with open pores were observed which corresponds with Capuccini study [3]. In XRD pattern, the Sr-HA peak is left shift. Because the ionic radius of Sr is larger than that of calcium, the c-axis of lattice constant is increased. With the incorporation of Sr into HA coatings, it is possible to change the ability of apatite formation. As the HA contains Sr, solubility increased with increasing Sr content. The Sr-HA coatings exhibited the excellent biological responses. A study indicated that Sr-doped in calcium polyphosphate presented good biocompatibility and enhanced osteogenesis [4]. Hence, the Sr-HA coatings by electrochemical deposition can be designed to support cell functions on the implant.

REFERENCES: [1] T.M. Lee et al (2001) *JBMR* **55**:360-367. [2] P.J. Meunier et al (2004) *N Engl J Med* **350**:459-68. [3] C. Capuccini et al (2008) *Acta Biomater* **4**:1885-93. [4] M. Tian et al (2009) *J Mater Sci Mater Med* **20**:1505-12.

ACKNOWLEDGEMENTS: The authors would like to thank Medical Devices Innovation Center of National Cheng Kung University (Grant D101-21008).

Osmotically conditioned superporous hydrogels: assessment of pore network topography

S. Laurencin[1], K Roelofs[2], K Spiller[3], G Palmese[1], A Lowman[4]

[1]*Department of Chemical and Biological Engineering, Drexel University, 3141 Chestnut Street, Philadelphia, PA 19104, USA,* [*]*SJL22@drexel.edu*

[2]*Department of Materials Science and Engineering, Stanford University*

[3]*School of Biomedical Engineering, Drexel University*

[4]*College of Engineering, Office of the Dean, Rowan University*

INTRODUCTION: The use of a novel liquid-liquid phase separation technique for the synthesis of superporous physically crosslinked hydrogels as a biomaterial for knee joint articular cartilage focal defect repair is being investigated [1]. The superporosity is expected to facilitate integration with the native tissue through internal pore network topography conducive for cellular migration without sacrificing mechanical integrity. Hydrogels swell or shrink in response to the osmotic pressure of their environment. The goal of this research is to determine the influence of an osmotically pressured environment mimicking the knee joint on hydrogel internal pore network topography using a nondestructive imaging approach.

METHODS: Polyvinyl alcohol (PVA) and polyvinyl pyrrolidone (PVP) in a ratio of 99:1 (v/v) was added to distilled water forming a 10% (w/w) solution and autoclaved at 121^{o}C for 1hr. The organic solvent, Ethyl acetate (EA), was added drop-wise to the PVA-PVP solution while mixing at 300rpm for 10min. Solvent concentrations of 0%, 10%, and 25% (v/v) were evaluated. Solutions underwent 6 cycles of 21hr freezing at -20^{o}C and 3hr thawing at room temperature to form a crosslinked polymer scaffold. Hydrogels were exposed to an osmotic pressurized environment following a previously established protocol [2]. Hydrogel pore network was imaged in the hydrated state using a scanning electron microscope (Model: FEI/Phillips XL30) in environmental (nondestructive) mode. Hydrogels (n=4) were cut while frozen in the midsection transverse plane and the cut surface was imaged while hydrated. The percent area of void space and the average diameter of the pores of the imaged surface of the hydrogel was determined using ImageJ software.

RESULTS: The internal pore network of a hydrogel prepared with 10% EA is shown below (Figure 1). The use of organic solvent to increase the inherent porosity of freeze-thawed hydrogels was assessed by changing the concentration of organic solvent used in hydrogel synthesis. The mean total pore surface area increased from 4.0% to 9.8% when organic solvent increased from 10% to 25%. There was no statistically significant difference in average pore diameter when comparing the same organic solvent concentrations. The swelling behavior of the hydrogels was assessed over four weeks. Both 10% and 25% EA hydrogels showed no statistically significant change in total pore surface area over the course of four weeks. Changing the solvent concentration had no impact on average pore diameter at each swelling time point. However, the average pore diameter decreased significantly from the one day to the two week time points, after which there is no significant change in average pore diameter.

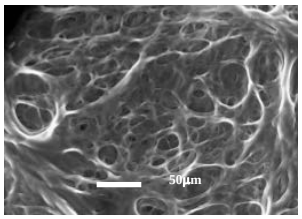

Fig. 1: Pore network of 10% EA hydrogel

DISCUSSION & CONCLUSIONS: Pore diameter larger than chondrocyte size is expected to be required for cell migration, which is evident in non-osmotically conditioned hydrogels. By two weeks of swelling, the average pore diameter reaches sizes likely to hinder cell migration. This study shows hydrogel pore network diameter and topography is significantly affected by its osmotic environment.

REFERENCES: [1] K. Spiller et al. (2008) *Acta Biomaterialia.* **4**:17–25. [2] J. Holloway et al.(2011) *Acta Biomaterialia*. **7(6)**:2477-2482.

New photoactive surfaces based on poly(ethylene glycol)-graphene composite hydrogels for MALDI-TOF analysis of biomolecular interactions

L Sánchez-Abella, V Ruiz, I Loinaz, G Cabañero, H-J Grande

IK4-Cidetec, Fundación Cidetec, New Materials Division, San Sebastián, SP.

INTRODUCTION: Matrix-assisted laser desorption/ionization (MALDI) mass spectrometry (MS) became popular in the late 80s and has become a powerful analytical tool in chemical and biological research. MALDI-TOF MS has been used to analyze biomolecular interactions [1] that do not usually require labelling, providing structural information on the binding partners. One major obstacle remains its poorer detection limits compared to label-based techniques.

The analysis of "small molecules" (Mw < 1500 Da) is limited by the interference between the matrix and the analyte signals, dependent on the chosen matrix, and low reproducibility of the analyte cocrystallization with the matrix. Such obstacles restrict the discovery of many pharmaceutical drugs that target proteins.

In the current work, a new photoactive coating for MALDI plates based on a polyethylene glycol (PEG) hydrogel and graphene oxide (GO) was developed to be used in LDI analysis.

METHODS: PEG coatings were synthesized directly on the MALDI plate using the "sandwich method" after surface activation by acid treatment. Organic matrix (CHCA, *α*-Cyano-4-hydroxycinnamic acid) and graphene oxides (GO) produced by different methods (top-down, TD and bottom-up, BU) or graphene quantum dots (GQD) were covalently attached by basic peptide coupling. MALDI-TOF MS was performed using a Microflex mass spectrometer (Bruker Co.) on photoactive hydrogel-coated MALDI plates and compared to uncoated ones.

RESULTS: LDI-TOF MS analysis of an aqueous solution (1 µL) of biotin (1mg/mL and lower) was performed for each modified surface. Mass spectra with low background signals were obtained in positive ionization mode, showing mass peaks corresponding to sodium and potassium adducts. The LOD (limit of detection) of the modified surfaces were compared (*Fig. 1*). A remarkable LOD of 4 pmol was obtained for the coating prepared with the top-down GO.

One-step synthesis of the coating based on PEG and GO TD was optimized. XPS, SEM and contact angle were used to characterize the coating. N-Acetyl-Cysteine (NAC) and BSA were analyzed by LDI-TOF MS using the modified plate.

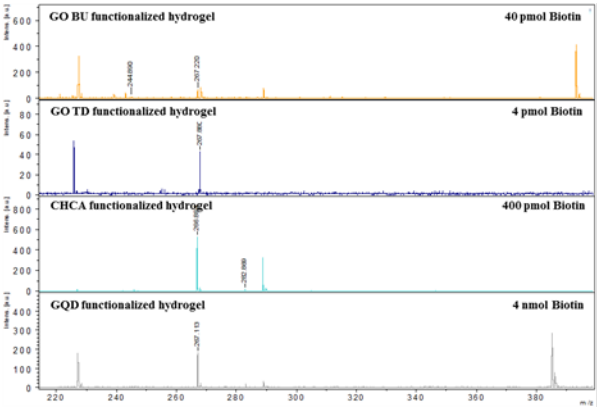

Fig. 1: Mass spectra of biotin with different substrates comparing their LOD in positive mode.

LOD of NAC at 60 pmol could not be reduced but cleaner spectra were obtained compared to conventional MALDI analysis. In the case of BSA conventional organic matrices were required but a synergic effect with the photoactive hydrogel allowed lowering LOD 50 times.

Further covalent functionalization of the coating with biotin enabled the targeted analysis of neutravidin and *viceversa* using MALDI-TOF MS.

DISCUSSION & CONCLUSIONS: This work has demonstrated that MALDI targets modified with a non-fouling surface functionalized with different GO or conventional organic matrices as CHCA are useful for (MA)LDI-TOF MS and can lead to better LODs. The GO TD/PEG hydrogel with an optimized synthesis gave great results (two orders of magnitude lower than conventional analysis). Low LOD obtained with GO TD might be due to its larger lateral size (> 1 µm) allowing a good energy transfer (higher electronic delocalization) to assist desorption/ionization compared to GO BU and GQD modified surfaces. These coatings could also be functionalized for targeted detection of biochemical interaction/processes without interfering.

REFERENCES: [1] P.L. Urban, A. Amantonico, and R. Zenobi (2011) *Mass Spectrom Rev* **30**:435-478.

ACKNOWLEDGEMENTS: The authors want to thank Dr. Antonio Sánchez for helpful discussions.

Interfacial design of conjugated polymer hybrid sensor probes for enhanced-and-suppressed optical and spectral signals in PL and Raman scattering

C Cui[1], DJ Ahn[1,2,3]

[1]Department of Chemical & Biological Engineering, Korea University, Republic of Korea
[2]Department of Biomicro System Technology, Korea University, Republic of Korea, [3]KU-KIST Graduate School of Converging Science & Technology, Korea University, Republic of Korea

INTRODUCTION: Nanobio sensing materials are quite important in developing novel ultra sensitive and high-throughput assay methods for analysing chemical and biological targets. Among promising materials, conjugated polymer hybrids with inorganic nanoparticles are of much interest owing to their signal functions in response to surrounding conditions. The sensory conjugated polymers [l-2] have been known to generate optical and/or electronic signals upon molecular recognition event. In this present study, we report a novel hybrid core-shell nanoarchitecture generating enhanced photoluminescence (PL) and Raman signals at the same time upon sensing. We will discuss a method of assay based upon these hybrid probe materials.

METHODS: The hybrid structure consists of silver nanoparticle with the diameter of ca. 150 nm as a core and polydiacetylene with the thickness of ca. 20 nm as a shell. Diacetylene monomers dissolved in THF were reprecipitated in aqueous solution containing silver nanoparticles. The repricipitated samples were consecutively aged under hydrothermal condition at 100 ^{o}C. Then the photopolymerization was executed under 254 nm UV light to generate the shell in the form of conjugated state, i.e. the polydiacetylene.

RESULTS: Fig. 1. shows the structure of the Ag/conjugated polymer hybrid core shell particles.

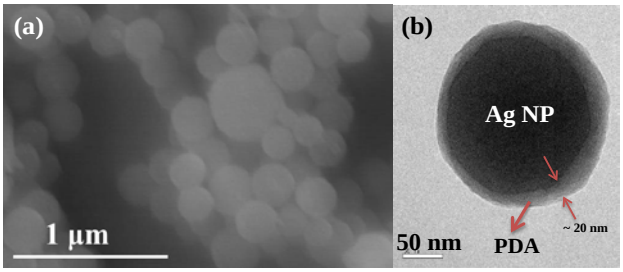

Fig. 1: Structure of Ag/polydiacetylene hybrid particles in SEM (a) and TEM (b).

The hybrid particles are in blue-phase upon photopolymerization of diacetylene shell and turn into red-phase as external stimuli imposed.[3] Along with colorimetric transition, the photoluminescence was observed to become enhanced by ca. 50 times in the red-phase as compared to the blue phase. On contrary to the enhanced photoluminescence, it is quite striking to observe Raman spectral signals showing a sudden suppression in intensities by ca. 90 times in the red-phase compared to the blue-phase.

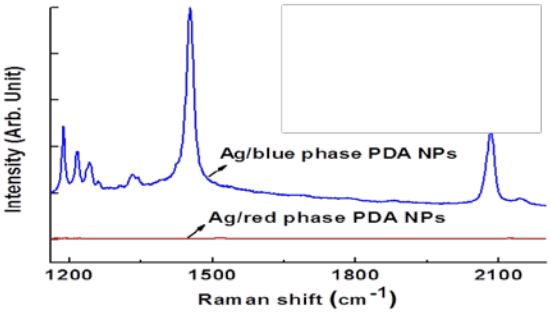

Fig. 2: Raman spectral variation per phase change of the hybrid sensor materials upon external thermal stimuli. The intensity of Raman scattering was suppressed whereas that of PL was enhanced.

DISCUSSION & CONCLUSIONS: The new sensor materials developed in this study by designing the polydiacetylene shell covered on Ag showed unique optical and spectral variations, which have not been observed yet. Interactions of surface plasmons on Ag with conjugated polymers would result in versatile optical and spectral sensor probes in response to physicochemical and/or biochemical conditions.

REFERENCES: [1] D. Ahn, E. Chae, G. Lee, H. Shim, H., T. Chang, K. Ahn, J. Kim (2003) *J. Am. Chem. Soc.* ***125***: 8976. [2] D. Ahn, J. Kim (2008) *Acc. Chem. Res.* ***41***: 805. [3] D. Charych, J. Nagy, W. Spevak, M. Bednarski (1993) *Science* **261**: 585.

ACKNOWLEDGEMENTS: This work was supported by the Korean government (NRF and MKE).

Preparation and characterization of polymeric nanoparticle as carrier for pulmonary administration

P Patel [1], T Soni[2], V Thakkar[3], T Gandhi [3]

[1]Dept of Pharmaceutical science, Saurashtra Unv., Rajkot, India [2] Dharmsinh desai university, Nadiad, India [3] Anand Pharmacy college, Anand, India

INTRODUCTION: The lungs are an attractive route for drug delivery due to their high epithelial surface area available for absorption. Nanoparticles on the other hand have gained increasing interest in drug delivery due to the wide variety of advantages they possess that allow for temporal, spatial and targeted delivery of therapeutics that can be fine tuned for various applications. Further, the pulmonary administration of polymeric nanoparticle based drug delivery systems is of great interest for both systemic and localized therapies. However, little is understood about the relationship between nanoparticle size and its effect on pulmonary absorption from a drug delivery perspective. Therefore the aim of this study was fabricate FP loaded polymeric nanoparticle for COPD and to investigate the effect of nanoparticle size on their biodistribution from lungs after pulmonary administration by histopathology study along with thoroughly evaluate their feasibility for the pulmonary drug delivery.

METHODS: In this research, spray dried nanoparticles were synthesized of chitosan suspensions using a deaggregating agent mannitol along with L-leucine. The effects of various experimental parameters were optimized by means of experimental box-behnken design. The properties of Spray dried powders containing chitosan, mannitol and L-leucine were studied in terms of their production yield, encapsulation efficiency and dissolution study along with characterization by scanning electron microscopy, X-ray diffraction, DSC, IR. Particle size and zeta potential were evaluated by using zetatrac particle size analyzer, cascade impactor using investigated aerodynamic properties. Histopathology of lung were also examined for the normal group, cigarette smoke exposed group, treatment group and was compared with marketed group.

RESULTS: Chitosan loaded nanoparticle having appropriate size range for deep part of the lung. Experimental design it was evaluated that inlet temperature and polymer concentration influence on the production yield. Feed flow rate impact on particle size. Results showed that spray drying technique yield 985 to 4060nm indicate nanosize range. However lowest value of PI was found in particles i.e. 0.168 demonstrate uniform particle size distribution. Zeta potential shows good stability index of nanoparticle formulation. Prepared polymeric nanoparticles emit 36 to 45% investigated by cascade impactor indicate deep targeting of FP to alveoli. L-leucine gives a powder a better flowability and produce smaller particles, also have an improved aerodynamic behaviour. Indicates the high aerosol performance of nanoparticles. Diffusion kinetic was found to be predominant as mechanism follow higuchi. Histopathology revealed that MDI protects the lungs against the chronic inflammation and airspace enlargement reducing.

CONCLUSIONS: Chitosan loaded polymeric nanoparticle shows the optimum size for deposition beyond the narrow airway into the alveoli. That is suitable for respiratory deposition. Polymeric nanoparticles open up a wide range of treatment applications of pulmonary and systemic diseases using targeted delivery strategies.

REFERENCES: [1] Severine JP, Pascal BH, Geraldine PL, Micheldogne LD and Brigitte ED, (2007) *European Journal of Pharmaceutics and Biopharmaceutics*, **65**: 47–56.

ACKNOWLEDGEMENTS: The authors are grateful to Sun pharmaceuticals ltd., Halol, Gujarat and CognisGmbh,Germany for providing giftsamples of fluticasone propionate and chitosan.

Metal oxide nanotubular layers loaded with Ag and ZnO nanoparticles intended for antibacterial coatings

A Roguska[1], M Pisarek[1], M Lewandowska[2], KJ Kurzydłowski[2]

[1] *Institute of Physical Chemistry, Polish Academy of Science, Warsaw, PL.* [2] *Faculty of Materials Science and Engineering, Warsaw University of Technology, PL.*

INTRODUCTION: To date, studies of modified metal surfaces for biomedical purposes have focused on their morphology and physicochemical properties which influence the cellular response. However, for implant materials, also an antibacterial property is of high importance. TiO_2 is commonly known for its photocatalytic properties under strong UV light and wide use in disinfection [1]. However, to obtain the bactericidal activity under dark conditions or very weak UV intensity such as indoor UV light, TiO_2 needs to be modified. It was reported that the addition of Ag to TiO_2 may enhance the overall photocatalytic efficiency and the damage to bacterial cells [2]. In this work, we present a simple preparation method of nanotubular oxide layers on Ti and Zr loaded with Ag and/or ZnO nanoparticles. As such composite coatings are expected to provide both biocompatibility and antibacterial properties, they are discussed here in terms of possible biomedical applications.

METHODS: The nanotubular (NT) layers were fabricated on Ti or Zr substrate via electrochemical anodization at constant voltage in a glycerol based electrolyte containing fluoride ions. Silver and ZnO nanoparticles were deposited onto the nanotubes surface using sputter deposition technique or cathodic electrodeposition technique. In order to reveal the morphological and chemical features, the composite coating fabricated were studied with the aid of scanning electron microscopy (SEM) combined with energy dispersive X-ray spectroscopy (EDX) and surface analytical techniques: Auger electron spectroscopy (AES), X-ray photoelectron spectroscopy (XPS). To evaluate the potential use of the composite layers as biomedical coatings we compared their ability to adsorb protein (bovine serum albumin) and to induce apatite nucleation in simulated body fluid with reference Ti and Zr samples.

RESULTS: SEM images of typical nanotube layers grown by anodization of Ti loaded with ZnO and Ag nanoparticles are shown in Fig. 1. It has been found that both silver and ZnO nanoparticles are distributed homogeneously in the coating, which is promising to maintain a steady antibacterial effect. The fabrication strategy applied allowed to precisely control the nanotube length and diameter, thus enabling to load different amounts of nanoparticles and control the release rates.

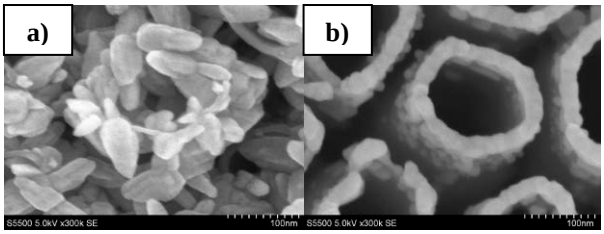

Fig. 1: SEM images of TiO_2 nanotubes loaded with a) ZnO, b) Ag nanoparticles.

The titania and zirconia nanotubular layers have been shown to significantly enhance apatite formation in simulated body fluid. In addition, composite coating surfaces have adsorbed higher amount of protein (bovine serum albumin) than the reference surfaces.

DISCUSSION & CONCLUSIONS: A serious problem common to all biomaterials, the risk of infection, can be alleviated by incorporating Ag or ZnO nanoparticles into the biomaterial surface. Our results have shown that those nanoparticles can be incorporated in a simple and economic manner, suitable for fabrication of new types of bactericidal materials. The highly ordered Ag and ZnO-loaded metal oxide nanotube arrays offer unique surface features of biomedical implants that may assure both biocompatibility and antibacterial properties.

REFERENCES: [1] H.A. Foster, I.B. Ditta, S.Varghese, et al (2011) *Appl Microbiol Biotechnol* **90**:1847–1868. [2] S. Lee, J.A. Scott, K.K. Chiang, et al. (2009) *J Nanopart Res* **11**: 209–219.

ACKNOWLEDGEMENTS: This work was financially supported by the National Science Center (DEC-2011/03/N/ST5/04388). A.R. gratefully acknowledges financial support received from the Foundation for Polish Science (START Program).

Wettability patterns prepared on superhydrophobic TiO_2 photocatalyst films

S Nishimoto, M Becchaku, Y Kameshima, M Miyake

Okayama University, 3-1-1 Tsushima-Naka,Okayama, Japan

INTRODUCTION: Relatively rough TiO_2 surfaces can be readily made superhydrophobic with water contact angles (CAs) of over 150° by depositing self-assembled monolayers (SAMs) of hydrophobic compounds such as octadecylphosphonic acid (ODP). On ultraviolet (UV) irradiation, these superhydrophobic TiO_2 undergo dramatic wettability conversion to become superhydrophilic with water CAs of less than 5° due to a photocatalytic reaction. This convenient technique for photostimulated wettability conversion can be used to prepared superhydrophobic–superhydrophilic patterns. The superhydrophobic-superhydrophilic patterns with the high wettability contrast of the surface with a water CA difference of over 150° can be used in many applications including cell growth, spotting of biomolecules, and fluidic microchips. To further develop such functional materials, it is important to enhance the wettability contrast of such surfaces. However, in contrast with the numerous reports on conventional superhydrophobic surfaces (water CA: 150–170°), there are few reports on super water-repellent (water CA: 170–180°) solid surfaces. This paper reports the preparation of superhydrophobic–superhydrophilic patterns with an extremely high wettability contrast (~170°) by using hydrothermally treated Ti plates.

METHODS: Ti plates were sonicated in acetone for 5 min, dried in air, and heated at 400°C for 1 h to form TiO_2 layers on their surfaces. The Ti plates were immersed in a 10 M NaOH solution in autoclaves. The autoclaves were placed in an oven and heated at 110°C for 6 h. After hydrothermal treatment, the samples on the Ti substrates were washed with deionized water and 0.1 M HCl solution and then heated at 500°C for 1 h. The thus-prepared TiO_2 surfaces were modified with an ODP monolayer by immersion in a 0.5 mM (10^{-3} mol/dm^3) 2-propanol solution of ODP for 20 h. The substrates were then removed from the solution and rinsed thoroughly with 2-propanol before being heat treated at 110°C for 2 h. The samples were characterized by SEM, contact angle meters etc. In addition, the wettability patterns were obtained by area-selective UV irradiation onto the ODP-modified TiO_2 surfaces by using a photomask.

RESULTS: The sample surface contained many pores with diameters ranging from about 100 nm to 1 μm (Fig. 1(a)). The ODP-modified surface exhibited a static water CA of 173.6 ± 1.7° (volume of water droplets: 8.3 μL). A wettability pattern was produced by area-selective UV irradiation using a striped photomask (Fig. 1(b)).

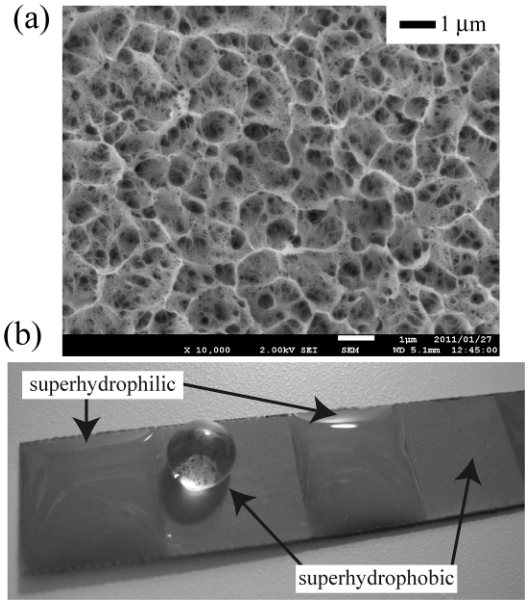

Fig. 1: (a) SEM image of TiO_2 film prepared by hydrothermal treatment and (b) images of a spherical water droplet placed on an ODP-modified TiO_2 film exhibiting superhydrophobicity and a water layer on a UV-irradiated ODP-modified TiO_2 film exhibiting superhydrophilicity.

DISCUSSION & CONCLUSIONS: The remarkable superhydrophobicity was believed to result from the special surface morphology of the film. The superhydrophobic TiO_2 films could be conveniently patterned with UV light to produce superhydrophobic –superhydrophilic patterns with an extremely high wettability contrast (~170°). This functional interface has the potential to be used in a wide range of applications.

Surface characterization of chitosan/PEO/levan ternary blend films

M Sennaroglu Bostan[1], E Mutlu[2], H Kazak[2], SS Keskin[3], E Toksoy Oner [2], MS Eroglu[1,4]

[1] *Department of Chemical Engineering, Marmara University, Istanbul, Turkey* [2] *Department of Bioengineering, Marmara University, Istanbul, Turkey* [3] *Department of Environmental Engineering, Istanbul, Marmara University, Turkey* [4] *TUBITAK-UME, Chemistry Group Laboratories, Kocaeli, Turkey*

INTRODUCTION: Binary blend films of chitosan, PEO and levan have been attracting a considerable interest in biomedical and food applications [l, 2]. Therefore, ternary blend films are expected to have a higher potential since chitosan and levan may enhance mechanical and thermal stability of PEO films while reducing the water solubility and minimizing the crystallinity via intermolecular hydrogen bonding. Considering these facts, this study focused on preparation of ternary blend films of chitosan, PEO and levan to establish their surface and biological properties.

METHODS: Chitosan was prepared by deacetylation of chitin of shrimp shell. Levan was produced by microbial fermentation of *Halomonas smyrnensis* AAD6^T cultures [3]. Poly(ethylene oxide), PEO (300.000) was supplied from Sigma Aldrich and used as received. Films were prepared by solution casting with the compositions detailed in Table 1.

Table 1. Composition of blend films

Sample code	Chitosan/PEO/Levan (w/w/w)
CPL1	78.3/8.7/13
CPL2	69.6/17.4/13
CPL3	60.9/26.1/13
CPL4	52.2/34.8/13

Static contact angle (CA) measurements were recorded using Krüss GmbH DSA-100 model instrument equipped with a single direct dosing system consisting of a High Performance Frame Grabber Camera T1C (25 frames per second). Atomic Force Microscope (Park systems XE70 SPM Controller LSF-100 HS) was used for recording the surface topography and phase separation morphology of the films at ambient temperature. To assess the biocompatibility of the blend films, WST-1 cell proliferation and viability assay (Roche, Germany) were performed with the mouse fibroblast cell line L929.

RESULTS: Surface energy and morphology of the films were characterized by one liquid CA measurements and atomic force microscopy (AFM) (Fig 1). CA measurements showed a surface enrichment of PEO at the film surfaces having more than 30% of PEO. At lower concentrations, chitosan and levan were enriched on the surfaces leading to more amorphous and homogenous surfaces. This result was further confirmed by AFM images. For all the four blends, more than 80% of the cells were found to retain their viability (Fig 2).

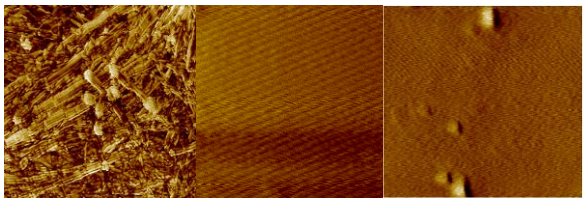

Fig. 1. AFM phase images (5x5 µm) of A:PEO (rms:22.64nm), B:CPL3 (rms:0.48 nm) and C: CPL4 (rms:0.58nm)

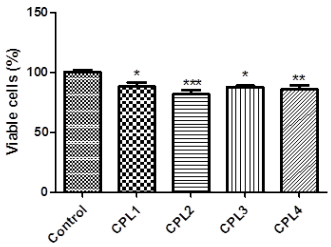

Fig. 2. Cell viability of L929 cells after being cultured with the blend samples (CPL1, CPL2, CPL3, CPL4) for a period of 24 h.

DISCUSSION & CONCLUSIONS: These biocompatible ternary blend films are expected to have high potential to find uses as active food packaging, hemodialysis membrane and artificial skin materials.

REFERENCES: [1] J. Li et al. (2010) *Carbohydr Polym.*, **79**:786–791. [2] JR Barone and M Medynets (2007) *Carbohydr Polym.***69**:554–561. [3] A. Poli et al. (2009) *Carbohydr Polym*, **78**:651.

ACKNOWLEDGEMENTS: This study was supported by TUBITAK (111M232) and Marmara Univ. Research Fund (FEN-C-DRP-030912-0306).

Nanomechanical characterization of soft materials and nanocomposites by atomic force microscopy

D Passeri[1], M Reggente[1], L Angeloni[1], E Tamburri[2], V Guglielmotti[2], G Reina[2], ML Terranova[2], M Rossi[1,3]

[1] *Electron Microscopies and Nanoscopies (EMiNa) Lab, Department of Basic and Applied Sciences for Engineering, University of Rome Sapienza, Rome, Italy* [2] *Micro and Nano-structured Systems (MINAS) Lab, Department of Chemical Sciences and Technologies, University of Rome Tor Vergata, Rome, Italy* [3] *Sapienza Nanotechnologies and Nanosciences (SNN) Lab, CNIS, University of Rome Sapienza, Rome Italy*

INTRODUCTION: Atomic force microscopy (AFM) has been extensively used as a platform to develop techniques for the mechanical characterization of materials at the nanoscale. Through them the mechanical properties of a wide range of samples, from stiff materials to compliant polymers, biomaterials and biological samples, can be qualitatively and/or quantitatively measured in a single point or mapped on a selected area on the sample surface. Moreover, nanomechanical imaging may be employed to image stiff nanomaterials included in soft matrices. In this work, we review some of these techniques. As examples, AFM quasi-static indentation (I-AFM) has been used for year to study the mechanical properties of soft matter [1]. More recently, such properties have been mapped by contact resonance AFM (CR-AFM) and other ultrasound based AFM techniques [2]. Such techniques, in particular those based on nonlinear effects, have been demonstrated to enable the detection of nanoparticles buried in polymers [2,3] or internalized in biological structures [2]. Explicitly developed for soft matter, torsional harmonics AFM (TH-AFM) has been used to measure and map the elastic modulus of polymers and biological samples [1,2]. We report here also some results on polymeric nanocomposites and biomaterials and biological samples.

METHODS: I-AFM and CR-AFM have been performed using a Solver AFM apparatus (NT-MDT, Russia) equipped with standard Si cantilevers. TH-AFM has been performed using an Icon AFM apparatus (Bruker Inc.), equipped with T-shaped cantilevers.

RESULTS & DISCUSSION: I-AFM, CR-AFM and TH-AFM have been used to characterize the indentation modulus of a number of different polymer-nanodiamond (ND) composites. As an example, Fig. 1a and 1b show the topography and the elastic modulus map, respectively, obtained through TH-AFM, of a fibre of polyaniline (PANI) doped with ND, surrounded by nanofibrils, on a Si substrate. Similar characterization has been performed on poly-aminopropyltriethoxysilane doped with ND, which revealed the stiffening of the polymer induced by the ND. Results retrieved through different techniques have been compared, showing their substantial agreement. Increase of the elastic modulus of fluorocarbon ultrathin films has been studied as a function of exposition time to methanol plasma, which increases also the biocompatibility and proliferation of endothelial cells. Finally, nanomechanical characterization of some biological samples (collagen fibres and bacteria) has been reported.

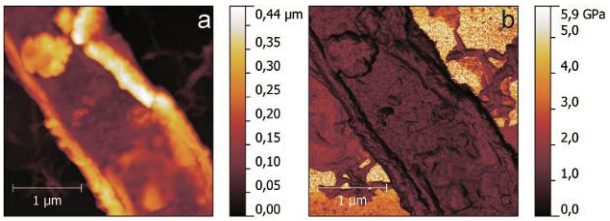

Fig. 1: Topography (a) and indentation modulus map (b) of a PANI-ND fibre and nanofibrils.

CONCLUSIONS: AFM has been described as a powerful platform to develop techniques for the nanomechanical characterization of soft matter. Comparison among results obtained on some polymers through different techniques demonstrates the reliability of the techniques. While polymers represent well established samples to be characterized though these techniques, efforts are still required to the complete extension of our techniques to biological materials.

REFERENCES: [1] D. Passeri, et al (2013) *Anal Bioanal Chem* **405**:1463-78. [2] F. Marinello, D. Passeri, E. Savio eds (2012) *Acoustic scanning probe microscopy*, Springer Berlin Heidelberg (2012). [3] K. Kimura, et al (2013) *Ultramicroscopy* **133**:41-9.

Characterization of VPS coated CFR PEEK interface and substrate

M Regis[1, 2], S Fusi[1], F Sbaiz[1], P Bracco[2]

[1]*R&D Dept., Limacorporate S.p.A., Villanova di San Daniele (UD), Italy* [2] *Chemistry Dept., Turin University, Italy*

INTRODUCTION: The use of carbon fibre reinforced (CFR) PEEK in orthopaedics has been increasingly growing in the last few years. Its application as a long term bearing component looks promising, especially considering its wear resistance properties [1]. In order to reach a good level of bone integration though, porous coating interfaces have to be realized on the material surface [2]. Since PEEK has shown to undergo significant changes in crystallinity and microstructure due to thermal and stress history [3], investigating the evolution of those properties after thermo-mechanical coating processes is of great interest. This work is aimed to characterize the crystallinity of injection moulded vacuum plasma sprayed (VPS) coated CFR PEEK samples, and to study the evolution of the crystal phase during all the coating process steps.

METHODS: PAN based CFR PEEK samples have been injection moulded starting from granules, and have been sandblasted and VPS coated with Titanium beads. Crystallinity measurements have been performed by DSC analysis (heat cycle from 30°C to 400°C at 20°C/min) on granules and injection moulded material, in order to provide information on crystallinity evolution during the injection moulding and after each coating process step. A detailed electron microscope image analysis has been performed, in order to assess the reliability of the coating and the substrate morphology. Sample sections have been examined with SEM-EDX to evaluate coating appearance; focused ion beam (FIB) was employed to etch the surface and look at the substrate morphology before and after coating operations

RESULTS: Crystallinity changes from granules to the injection moulded material, as well as after sandblasting and coating process (Table 1), demonstrating that thermal and stress history affect the microstructural properties of the composite. Coating morphology is acceptable, and substrate appearance in terms of fibre orientation and integrity seems to be unaffected by coating procedures (Figure 1).

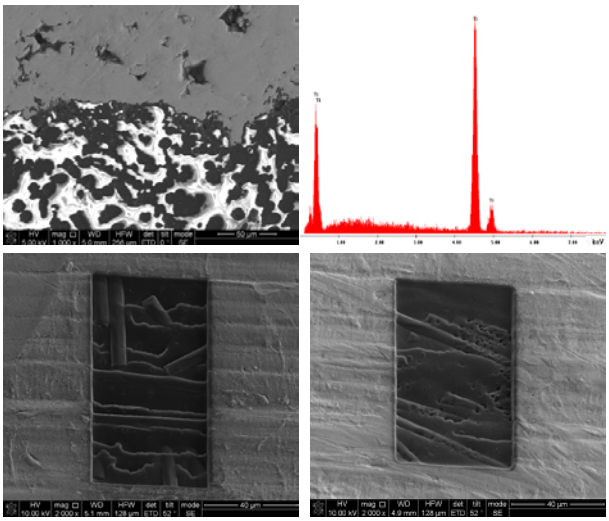

Fig. 1: Top: interface between coating and substrate (left), and EDX spectrum of VPS coating (right); down: fibre orientation after sandblasting (left) and coating (right).

Table 1. Crystallinity at different coating stages.

Sample (CFR PEEK)	Crystallinity [%]
Granule	31,9
Injection moulded	32,5
Sandblasted	38,5
Coated	29,4

DISCUSSION & CONCLUSIONS: Although it is demonstrated that good adhesion properties and coating morphology can be achieved, stress and thermal history at the basis of the VPS coating process may play a role in changing the CFR PEEK final properties. In fact, mechanical properties can be affected either by differences in fibre matrix adhesion or by a modified polymeric matrix, both induced by changes PEEK crystallinity. An optimal choice and/or tailoring of the coating process has therefore to be taken into consideration for the realization of highly durable orthopaedic components.

REFERENCES: [1] C.L. Brockett et al (2012) J Biomed Mater Res B **100**:1459-1465. [2] S.M. Kurtz (2012) *PEEK biomaterials handbook*, Elsevier Inc., pp. 131-143. [3] M. Buggy, A. Carew (1994) J Mat Sci **29**:1925-1929.

Studying surface interaction with proteins using advanced surface characterization techniques

G. Diaconu[1], T. Schäfer[1,2]

[1] *POLYMAT, NanoBioSeparations Group, University of the Basque Country, San Sebastian, Spain*
[2] *Ikerbasque, Basque Foundation for Science, Bilbao, Spain*

INTRODUCTION: Studying the interactions of proteins with a solid surface has promoted a widespread interest in many research areas. There is no doubt that protein adsorption is a common phenomenon that plays a key role in many natural and synthetic processes including biotechnology, biomedicine and separation processes. The protein adsorption is influenced by several parameters including protein structural stability, surface polarity and charge, pH, ionic strength and temperature[l]. However, the understanding of protein adsorption is highly dependent on reliable techniques which should be capable of providing information on adsorbed mass, adsorption rate, conformation and/or orientation of the adsorbed protein layer.

In this study surface plasmon resonance (SPR) and quartz crystal microbalance with dissipation monitoring (QCM-D) were used as *in situ* sensing techniques to follow *in situ* interfacial interaction quantitatively and in *real time*. Polysulfone (PSU) was used as a surface as it is the most common material used for UF membranes. Membrane fouling is the main constraints in separation processes. Thus, to elucidate and control the membrane fouling phenomenon requires knowledge on foulant-surface interactions which are not completely understood yet. This work aims at *real time* characterization of protein adsorption on PSU surface using advanced characterization techniques like SPR and QCM-D.

METHODS: QCM-D and SPR techniques were used to characterize the adsorption of the model protein, bovine serum albumin (BSA) on PSU surface. QCM-D is a mass sensitive technique that simultaneously monitors the resonant frequency, *F*, and the energy dissipation, *D*, changes caused by the formation of a BSA layer during the adsorption process. Thus, in addition to quantitative information on the adsorbed mass on the surface measured as changes in frequency, it provides information on the viscoelasticity of the adsorbed layer monitoring the dissipation. SPR is complementary optical method which, based on changes in refractive index, allow determining the amount of adsorbed protein per unit surface area.

RESULTS: PSU coated quartz crystal surface was scanned in tapping mode and its topography is shown in Fig.1A. Time-resolved QCM-D measurement parameter shifts are presented in Fig. 1B, revealing the characteristic *F* and *D* profiles in response to interactions between the BSA (1mg/ml, ionic strength 10mM, pH 5.8) and PSU surface.

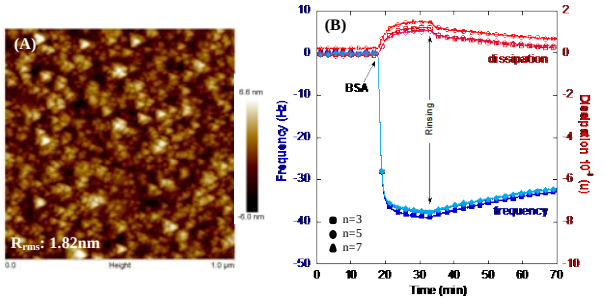

Fig. 1: (A) Tapping mode AFM image (1x1μm) of PSU-coated crystal surface. (B) Frequency and dissipation responses induced by the adsorption of BSA on PSU surface. Frequency and dissipation data are presented of 3rd, 5th and 7th overtones.

DISCUSSION & CONCLUSIONS: BSA was irreversibly adsorbed on PSU surface as low desorption was observed with rinsing, and caused a shift in SPR resonance angle, frequency and dissipation of 0.48º, 39Hz and $1.2x10^{-6}$, respectively. The combination of these two techniques allowed determining the "dry" and "wet" masses of BSA adsorbed on PSU surface, yielding in this way information on the "softness" of the layers adsorbed. Thus, adsorbed "dry" and "wet" masses of BSA on PSU after rinsing step were found to be 299 and 583ng/cm^2, respectively, indicating that the adsorbed BSA layer contained more than 48% of water. Consequently, BSA was irreversibly adsorbed in a flat rigid layer on PSU surface.

It could be shown that QCM-D and SPR are powerful and complementary techniques which provide information in a non-invasive way on *real-time* adsorption of protein on polymeric surface for elucidating early stage adsorption phenomena leading to membrane fouling.

REFERENCES: [1] M. Rabe, D. Verdes, S. Seeger (2011) *Adv. Colloid Interface Sci* **162**:87-106.

Low temperature plasma-based process for surface functionalization of cotton textiles

R Tolouei, C Paternoster, S Turgeon, D Mantovani

Lab. for Biomaterials and Bioengineering (CRC-I), Dept. Min-Met-Materials Eng. & University Hospital Research Center, Laval University, Quebec City, Canada

INTRODUCTION: The use of plasma processes to functionalize surfaces is growing at a tremendous rate in all fields of science and technology. The textile industry is also experiencing the benefits of plasma technologies in its diverse field of applications [1]. Amongst interesting plasma-deposited materials, amorphous carbon based thin films exhibited excellent properties such as high hardness, low friction, high corrosion resistance and chemical inertness to most environments. The huge potential to use amorphous carbon thin film lies in the fact that the characteristics of the films can be governed by changing the plasma parameters [2]. Modifications in the pre-treatment and deposition conditions provides a direct method to control the formation of free radicals and ions in the plasma and on the surface of samples in addition changes the topography which, in turn, can affect adhesion and wettability in addition to thin film growth. The micro/nano roughness of materials is the key to control the wettability behaviour of the surfaces. Cotton textiles with high hydrophobicity behaviour would constitute an attractive option in many applications as water proof, easy-to-clean or even bacteria anti-adhesion apparel. To date, many different methods have been studied using approaches such as polymeric grafting or polymeric coating [3]. However, the current methods are hampered by their lack of stability of the hydrophobic state. Hence, in this study the effect of plasma-based modification on stability of hydrophobicity properties of cotton cords were investigated.

METHODS: Cotton cords (Darice, USA) were cut into size of 20 mm. Surface modifications were performed using a hybrid plasma enhanced chemical vapor deposition (PE-CVD) reactor, operating at 13.56 MHz at room temperature. Argon and methane were used as gas precursors for plasma pre-treatment and deposition of the amorphous carbon film on the cotton cords, respectively. The evolution of surface morphology and film adhesion properties were investigated by FEG-SEM. the thickness of the film deposited on silicon substrates was measured by SEM. XPS and FTIR were used to study the structure and chemistry of the modified samples. The wettability of the surfaces before and after treatment has been measured using static water contact angle (WCA).

RESULTS: Surface chemical composition analysis of untreated samples indicated the presence of carbon, oxygen and nitrogen. XPS graphs of samples after plasma treatments revealed that the surfaces were completely covered by amorous carbon, with no presence of nitrogen. The morphological changes due to plasma treatments were investigated by SEM as shown in Fig. 1. It reveals a fairly smooth surface for untreated samples, whereas plasma pre-treatment and deposition caused a significant morphological change.

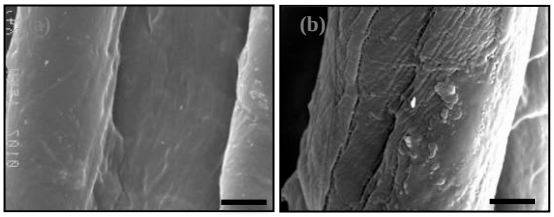

Fig. 1: SEM micrographs of the cotton samples (a) as received an7 (b) after treatments. scale bar 2 µm.

The comparison of the water contact angle measurements of untreated and treated samples displayed a significant increase in hydrophobicity, with a contact angle of coated cotton cords around 145º.

DISCUSSION & CONCLUSIONS: Our results clearly show that it is possible to use plasma based processes to functionalize the surface of textiles towards lower wettability and easy-to-clean applications. Plasma pre-treatments could increase adhesion of deposited film and modify the wettability of fibers and fabrics. With the deposition of amorphous carbon based thin films, the cotton cords achieved a controlled chemical stability and a higher hydrophobic state.

REFERENCES: [1]Dastjerdi, R. et al. (2010) *Colloid Surf B Biointer* **79**:5-18. [2]Robertson, J. (2010) *Industrial Plasma Technology: Applications from Environmental to Energy Technologies*, 277-299. [3]Liu, Y. et al. (2008) *Bioinspir Biomim* **3**(4):046007.

Physicochemical properties of collagen/silk fibroin films

I Ghaeli[1,2], MA Moraes[4], M Beppu[4], FJ Monteiro[1,2], MP Ferraz[1,3]

[1] INEB, Instituto Nacional de Engenharia Biomédica, Porto,Portugal [2] FEUP, Faculdade de Engenharia, Universidade do Porto, Departamento de Engenharia Metalurgia e Materiais, Porto, Portugal [3] Universidade Fernando Pessoa, Porto, Portugal [4]Faculdade de Engenharia Química, UNICAMP,Campinas (SP), Brazil

INTRODUCTION: Both silk fibroin (SF) and collagen are promising biocompatible materials used in scaffolds for tissue engineering. Due to the exclusive limitations of pure SF and collagen, blending of both materials was suggested with proven miscibility between collagen and SF blend films [1, 2].

Several studies obtained films and scaffolds by blending these two biomaterials with altering pH and raising temperature to induce collagen denaturation [3, 4]. Indeed, solubilizing collagen in SF solution occurs due to the breakage of the collagen triple helix chains.

This study prepared collagen/SF blend films whilst respecting the native structures of the two biomaterials.

METHODS: Silk fibroin and collagen are prepared as follows: Briefly, the degummed cocoons of *B. mori* were dissolved in a concentration of 1% in the ternary solvent of $CaCl_2$:ethanol:water with the molar ratio of 1:2:8 at 85 °C and the pH is adjusted to 9 with NaOH. The 0.5% concentrated collagen solution is prepared by dissolving bovine type I collagen in acetic acid 0.5M at 4 °C.

The collagen/SF blends are prepared by mixing different ratios of 100:0, 25:75, 50:50, 75:25 and 0:100. Afterwards, the blending solutions are dialysed against distilled water for 3 days and cast to form films. At the end, physicochemical properties of the films are analysed by different analysis methods such as differential scanning calorimetry (DSC), Fourier transformed infrared spectroscopy (FTIR), and scanning electron microscopy (SEM).

RESULTS: Figure 1 shows the thermodynamic properties of collagen, SF and collagen/SF blends (50/50 v/v) using DSC. DSC analysis of the blend film shows no transition temperature in the region of 39-51 °C. It suggests that the collagen native structure of triple helix is preserved in the blending film of collagen/SF because there is no thermal transition in the denaturation region of collagen.

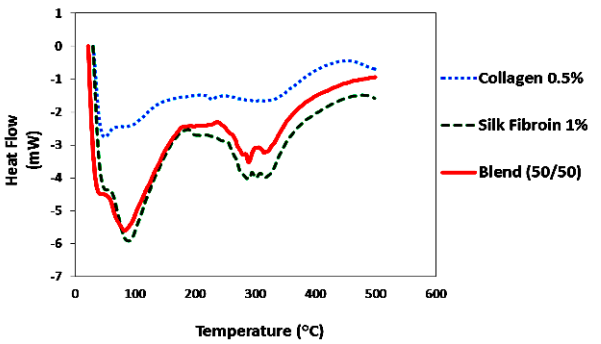

Fig. 1: DSC curves of Collagen (0.5%), SF (1%) and SF/Collagen blend with ratio of 50/50

DISCUSSION & CONCLUSIONS: According to the native collagen and SF structures, the blending is not possible without the interference of other parameters, such as T or pH. Collagen alpha helix structure is so stable that there is no tendency to bind physically or chemically with SF structure. However, native SF has random coil structures and stirring transforms its structure to beta sheets which influences on the blending with collagen. So, in this study, the binding of the two biopolymers has been done with electrostatic forces by altering pH and using the dialysis bath trying to retain the biomaterials native structures in solution. By DSC tests it was possible to conclude that the blend film is more stable than the collagen film, due to the presence of SF which is thermally more resistant than collagen. The main functional groups of collagen and SF and morphology of the films was observed by FTIR and SEM.

REFERENCES: [1] C. H. Lee, A. Singla, and Y. Lee (2001), *Int. J. Pharm*, **221**: 1-22. [2] N. Minoura, M. Tsukada, M. Nagura (1990), *Biomaterials*, **11**: 430-434. [3] Qiang Lu et. al. (2008), *J. Appl Polym Sci*, **109**: 1577-1584. [4] Qiang Lu et. al., (2007), *J. Mater Sci*, 19: 629-634.

ACKNOWLEDGEMENTS: The support from FEUP and INEB institution in Portugal and CAPES-FCT from Brazil are gratefully acknowledged.

Micro-topographic patterns direct endothelial and smooth muscle cell fates for cardiovascular devices

Y Ding[1], P Huang[2], X Lu[3], N Huang[3], Y Leng[1]

[1]*Department of Mechanical Engineering,* [2]*Division of Life Science, The Hong Kong University of Science and Technology, Hong Kong*

[3]*Key Lab. of Advanced Materials, Ministry of Education, Southwest Jiaotong University, Chengdu, China*

INTRODUCTION: The risk of restenosis and in-stent thrombosis, which are caused by endothelial cell (EC) dysfunction and smooth muscle cell (SMC) proliferation, limits the ultimate success of cardiovascular devices. Thus, an ideal device should selectively favour EC growth while inhibiting SMC proliferation. It has been well documented that the fates of cells can be influenced by surface topography. However, optimal parameters of micro-topographic patterns for cardiovascular application have not been clearly identified. Here, we show a high-throughput platform with an array of micropatterns (anisotropic grooves and isotropic pillars, two commonly studied pattern types) for screening optimal parameters directing both EC and SMC fates. This approach can help mitigate errors introduced by inter-sample variation and increase experimental processing.

METHODS: We designed and fabricated an array of six micropattern areas (3mm × 3.8mm) on a silicon wafer by photolithography and dry etching. There were two types of micropatterns: grooves and pillars. Each type had six feature sizes (width equal to spacing) ranging from 0.5 to 50μm with constant depth of 3.5μm. All patterned surfaces were coated with TiO_2 thin films (50nm) by RF sputtering process. Both EC and SMC responses to varied micropatterns were studied.

RESULTS: Grooves induced much more favorable EC responses than pillars having feature sizes smaller than 10μm. Especially, EC on 1μm grooves showed significant enhancement in cell adhesion, spreading, elongation, proliferation and endothelial cell marker (CD31) expression. As shown in Figure 1, after 3 days, 1μm grooves induced a confluent endothelium monolayer formation with in vivo-like morphology. In contrast, 1μm pillars showed the most adverse influence on EC spreading and proliferation. Notably, the EC density and proliferation showed a significant drop as the pillar size decreased from 20 to 1μm. As the pillar size further decreased to sub-micron scale, EC proliferation increased. This result suggests that there is a critical size, around 1μm, at which the pattern affects the EC fate reaching its maximum level. Interestingly, in contrast to higher EC density on grooves, SMCs were more isolated, having a lower density on the same grooves. Analogous to EC behaviour, SMC growth on pillars with sizes from 0.5 to 10μm was strongly inhibited, as shown in Figure 1.

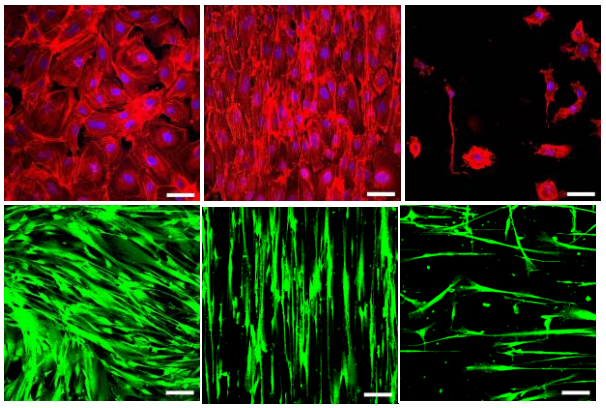

Fig. 1: Images of EC (upper, red, scale bar: 50μm) and SMC (lower, green, scale bar: 100μm) on flat (left), 1μm grooves (middle) and 1μm pillars (right) after 72 h culture.

CONCLUDING REMARKS: Using micro-fabrication techniques, we are able to achieve high-throughput screening of a set of micro-topographic patterns with varied feature sizes and shapes for studying vascular compatibility. We propose an optimized pattern of 1μm grooves for selectively favouring EC fates but inhibiting SMC growth, which may be applied to design and development of vascular devices where rapid endothelialization is required.

ACKNOWLEDGEMENTS: This work was supported by Research Grants Council of Hong Kong FSGRF13EG58.

Microfluidic Lab on-a-Chip devices for high throughput rare cell sorting

T Fatanat-Didar[1], K Li[3], T Veres[3], M Tabrizian[1,2]

[1] *Biomedical Engineering Dept. and* [2]*Faculty of Dentistry, McGill University, Montreal, Canada*
[2] *Heath Science Division, National Research Council of Canada, Boucherville, Canada*

INTRODUCTION: Biomedical devices developed for detection, sorting and *in vitro* culture of cells are important tools in both clinical diagnostics and fundamental research. Recently, with the advances in miniaturization, Lab-on-Chip (LOC) devices have started to play an important role in detection and enrichment of rare cells[1]. Combined with label-free methods that do not alter the properties of target cell, LOCs provide a suitable option for cell separation. We developed two main label-free approaches exploring the difference in size or adhesion properties of cell to sort them. The first device was a multilayered, fully thermoplastic-based microfluidic chip that was designed and fabricated for high throughput size-based separation of rare cells[2]. The second microchip was employing a well–designed biointerface that could separate the cells based on their affinity towards the microfabricated surface[3].

METHODS: The first microfluidic device was composed of a bottom layer, commercially polycarbonate porous membrane layer, top layer and a pneumatic air control layer, fabricated on thermoplastic elastomers, all by hot embossing. Top layer had three access holes that could be used as inlets or outlets depending on the peristaltic micro-pumping configuration. These layers were connected through the membrane in a circular channel area where liquid exchange could occur. The microfluidic device was then connected to a homemade 12-channels pneumatic control manifold using silastic laboratory tubing.
For the second platform microcontact printing was used to print aminopropyltriethoxysilane (APTES) onto the glass surface to provide region specific patterns of amine groups which were later activated through EDC-NHS chemistry. Microfluidic patterning was then used to create highly resistant protein patterns. This achieved by forming the PDMS-Glass microfluidic platform and flowing biomolecules of choice into the device to covalently attach them to the patterned amine groups on the surface.

RESULTS: Separation of rare oligodendrocyte progenitor cells (OPCs) from rat brain primary cultures was used as the proof on concept. Using multilayered microfluidic chip with a 5 µm pores membrane and micropumping system, a separation efficiency of 99% was achieved. This microchip was able to operate at flow rates up to 100 µl/min, capable of separating OPCs from a confluent 75 cm^2 cell culture flask in less than 10 min.

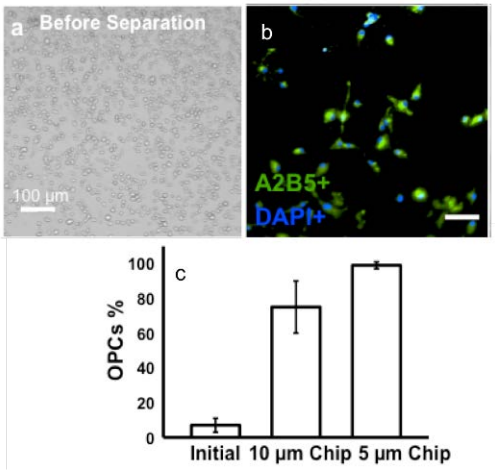

Fig. 1. (a) Image of initial cell mixture (b) OPCs population after separation using 5 µm pore size (c) % of OPCs in the initial cell mixture and after separation using chips with 10 µm and 5 µm membrane pore sizes.

Similar separation efficiency of OPCs, were obtained with the second platform. In addition, target cell attachment and single cell spreading could be precisely controlled. Isolated OPCs could proliferate and differentiate into mature oligodendrocytes on the separation platform.

DISCUSSION & CONCLUSIONS: The traditional macroscale techniques for OPCs separation require pre-processing of cells and/or multiple time consuming steps with low efficiency leading very often to alteration of their properties. The proposed label-free methodologies could separate OPCs, either based on their smaller size compared to other glial cells based on their affinity towards the developed biointerface, with a separation efficiency greater than 95%.

REFERENCES: [1]K. Sun Min et al. (2008). *Lab on a Chip* **8**:1015-23. [2]T. Fatanat Didar et al. (2013) *Biomaterials* **34(22)**:5588-93. [3] T. Fatanat Didar et al. (2011) *Anal Chem* **84(2)**:1012-8.

ACKNOWLEDGEMENTS: Genome Quebec, Nano Quebec, NSERC, Fac. Medicine, Drs G. Almazan, D. Junker, M. Mekhail and M. Dipaula.

Stepwise cell patterning using a near-infrared-responsive gel

H Koga[1], T Sada[2], T Fujigaya[2], N Nakashima[2,3], K Nakazawa[1,3]

[1] *Department of Life and Environment Engineering, The University of Kitakyushu, Japan*
[2] *Department of Applied Chemistry, Kyushu University, Japan* [3] *JST-CREST*

INTRODUCTION: Cell patterning technique is a useful approach for controlling cellular micro-environment and cell behaviour. Therefore, it has been used for cell-based assay, tissue engineering, and fundamental study of cell biology. Generally, lithography or inkjet printing techniques are used for the cell patterning [1]. However, when stamping or masking techniques are used, the formation of a cell-adhesive area depends on the mold structure; therefore, alteration and/or addition of cell patterns during the culture period is limited. On the other hand, we have developed a live pattering technique, which enables the formation of stepwise and/or complex cell patterns, using near-infrared (NIR)-responsive gel composed of agarose and carbon nanotubes (CNTs) [2]. Agarose gel has non-cell adhesion property and causes gel-sol transition by heat. CNTs have a capacity for photo-thermal conversion upon NIR laser irradiation. Therefore, NIR irradiation is absorbed by CNTs in the composite gel to cause local heating, which leads to local solation of the agarose gel and consequent formation of a selective cell-adhesive area on the tissue culture surface (Fig. 1). In this study, we evaluated the properties of CNT/agarose gel and investigated the formation of stepwise cell patterns.

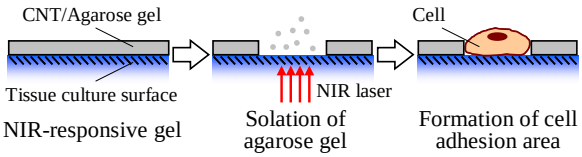

Fig. 1: Cell patterning using CNT/agarose gel.

METHODS: A single-walled CNT aqueous dispersion (1 mg/mL) containing 0.1% (w/v) carboxymethyl cellulose as the dispersant was prepared by sonication, and then 2% (w/v) agarose (melting temperature, <65°C) was blended into the CNT aqueous dispersion. After the CNT/agarose was dissolved at 70 ◦C, it was applied to the tissue culture dish and spread using a spin-coater. The CNT/agarose-coated dish was placed at 4°C for gelation. The NIR laser irradiated the bottom of dish, and the location of irradiation was controlled by the electric stage of the microscope system.

RESULTS & DISCUSSION: An agarose gel without CNTs was no response to NIR irradiation. In contrast, the CNT/agarose gel was rapidly solated by NIR irradiation, and selective cell-adhesive area was exposed on the dish. The solation area was positively correlated with the NIR intensity and magnification of the object lens, indicating that we can factitiously control the solation area by the parameters of NIR irradiation.

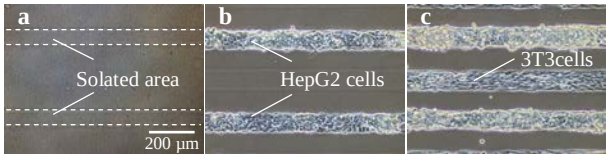

Fig. 2: Stepwise cell patterning. (a) Formation of primary solated patterns, (b) adhesion of HepG2 cells, and (c) formation of stripe patterns of HepG2 and 3T3 cells.

Co-culture patterns of HepG2 and 3T3 cells were established by selective and stepwise NIR irradiation of the CNT/agarose gel. Primary linear solated patterns were generated on the dish by NIR irradiation (Fig. 2a), and then the seeded HepG2 cells formed linear cell patterns (Fig. 2b). Next, secondary linear solated patterns were prepared between the HepG2 cell patterns. The seeded 3T3 cells preferentially adhered to the second cell solated area and formed linear cell patterns, and consequently, the uniform stripe patterns of HepG2 and 3T3 cells were formed (Fig. 2c). The liver functions of HepG2 cells in the patterned co-culture were well maintained during the culture period.

CONCLUSIONS: We established the technique of stepwise co-culture using the NIR-responsive gel. This technique is promising for formation of stepwise and/or complex cell patterns.

REFERENCES: [1] D. Falconnet, G. Csucs, H.M. Grandin, et al (2006) *Biomaterials* **27**: 3044-63. [2] H. Koga, T. Sada, T. Fujigaya, et al (2013) *Biofabrication* **5**: 015010.

Staphylococcus aureus and *Streptococcus sobrinus* adhesion in microfluidic device under dynamic conditions

M Pinto[1,2], JM Miranda[2,3], FJ Monteiro[1,2]

[1] *INEB-Instituto de Engenharia Biomédica, Porto, Portugal* [2] *FEUP-Faculdade de Engenharia, Universidade do Porto, Portugal* [3] *CEFT-Centro de Estudos de Fenómenos de Transporte, Universidade do Porto, Portugal*

INTRODUCTION: Bacterial Adhesion to surfaces is the onset of biofilm formation, being considered a public health problem [1]. So, in the last decade, microfluidic technology applied to microbiologic research, has gained considerable interest to mimic physiological conditions and to develop strategies to prevent bacterial adhesion to biomaterials and obtain more accurate results [2,3]. Therefore, the aim of this work is to develop and set-up a microfluidics system, which allows studying the initial adhesion of *Staphylococcus aureus* and Streptococcus *sobrinus* under continuous flow.

METHODS: The micro-channels are fabricated in Polydimethylsiloxane (PDMS) by soft lithography. The material was characterized by EDS, zeta potential, AFM and contact angle measurement, providing the composition, the charge, the roughness and hydrophobicity, respectively, of the material surface.
The behaviour of *S. aureus* (ATCC 25923) and *S. sobrinus* (clinical isolate) in a concentration of 1.5×10^8 CFU/ml, at different flow rates (1, 5, 10 and 15 µl/min) was visualized in a light microscope during 1 hour in a 100 µm high and 300 µm wide micro-channel. The bacteria adhered to the surface were analyzed by Live/Dead staining and SEM.

RESULTS: The bacterial adhesion in the channel was observed over time for different flow rates, showing that the material has suitable properties for this purpose, being the material surface characterization represented in Table 1.
Adhesion of *S.aureus* and *S.sobrinus* in the presence of the flow rate that leads to a higher adhesion, 5 µl/min (2.78×10^{-3} m/s, wall shear stress of 0.056 N/m^2), is represented in Fig. 1, having an adhesion rate of 118 cell/(cm^{2}s) and 109 cell/(cm^{2}s) respectively. The adhesion rate decreases for velocities above 2.78×10^{-3} m/s due to the increased of the wall shear stress.

DISCUSSION & CONCLUSIONS: The results indicate that the adopted techniques for materials production were effective and successfully performed. Also a strong bonding was obtained between PDMS and the substrate, avoiding leakage. Regarding the bacterial adhesion, both of them have a better attachment in the presence of a flow rate of 5 µl/min in the conditions mentioned above.

Table 1. Material surface characterization of glass coated by PDMS.

	Contact angle (°)	Zeta potential (mV)	Ra (nm)
Surface	122.90 ±1.193	-26.28 ±0.776	0.156 ±0.07

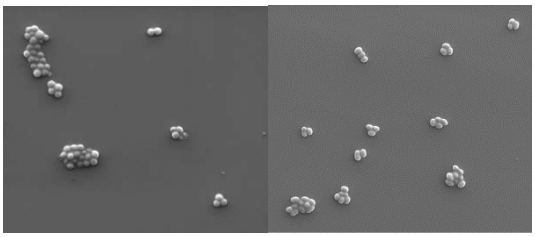

Fig. 1: SEM images of bacterial attachment in the channel for a flow rate of 5 µl/min with a magnification of 10000× – Left- S. aureus; right- S.sobrinus.

REFERENCES: [1]H. C. Busscher, Henk J. and Van der Mei (2006) *Clinical Microbiology Reviews*, **19(1)**: 127–141. [2]M. Binz, A. P. Lee, C. Edwards, and D. V. Nicolau (2010) *Microelectronic Engineering* **87(5–8)**:810–813. [3]J.-H. Lee, J. B. Kaplan, and W. Y. Lee (2008) *Biomedical microdevices* **10(4)**:489–98.

ACKNOWLEDGEMENTS: This work was financed by FEDER funds through the Programa Operacional Factores de Competitividade – COMPETE and by Portuguese funds through FCT – Fundação para a Ciência e a Tecnologia in the framework of the projects BONAMIDI PTDC/CTM/100120/2008 and PTDC/EQU-FTT/105535/2008.

CHO cell adhesion on modified surfaces of different materials.

WW Araújo[1], MC Salvadori[1], FS Teixeira[1], HJM Amorim[1], GN Silva[2], DMF Salvadori[2],IG Brown[3]

[1]Institute of Physics, University of São Paulo, São Paulo S.P., Brazil [2]Department of Pathology, Center for Genotoxins and Carcinogens Evaluation, TOXICAN, Botucatu Medical School, UNESP, SP Brazil [3]Lawrence Berkeley National Laboratory, Berkeley, California 94720, USA.

INTRODUCTION: Epithelial cells are mainly responsible for the formation of tissues that cover the external and internal surfaces of organs like skin, lining of the lungs and intestines. The cells must adhere to substrates and to each other in compliance with certain stimulus. In this way, adhesion properties can be regulated by the cell which simultaneously senses the chemical and mechanical properties of its environment. Their adhesion and growth on biomaterials depends on substrate properties such as surface wettability, topography and chemistry. The aim of this study is to investigate cell-surface interactions using several materials and different surfaces.

METHODS: We have used several materials with different surface chemistry/morphology to study the interaction between surfaces and the CHO (Epithelial Chinese hamster ovary) cells. The materials used were SU-8 2005 (epoxy electron resist from Microchem), PDMS (polydimethylsiloxane from Down Corning), DLC (Diamond like carbon, ta-C (tetrahedral amorphous carbon)). Ordinary cover slip glass was used as reference. Samples with flat surfaces for each genuine material were produced. As surface modification techniques we used electron-beam lithography, ion implantation and plasma modification. For surface modification by electron beam lithography we have used SU-8 2005 as material and hexagonal cavities with inscribed diameters of 12, 80, 270 and 580 µm were used as different scale patterns. For surface modification by plasma processing we have used DLC (ta-C) thin film as material, deposited by cathodic arc plasma gun. The DLC (ta-C) surfaces were modified by hollow cathode plasma gun fed up with oxygen or sulfur hexafluoride gas. Silver ion implantation was made for SU-8 2005 using a low cost Inverted Ion Source using Ag energy of - 4 keV and dose of 1.0 x 10^{16} cm^{-2}. We have also produced a hybrid SU-8/PDMS sample. For that, we deposited a SU-8 thin film on PDMS bulk piece and did SU-8 lithography with hexagonal cavities pattern. Is this way, we obtained hexagons with SU-8 walls 64 µm wide and with inscribed diameter of 134 µm made of PDMS. Thus, we ended up with a total of 12 different samples. CHO cells were purchased from the American Tissue Culture Collection (ATCC). Cells were cultured in tissue culture flasks (25 cm^2) in a humidified atmosphere at 37 ºC with 5% CO_2 (by volume). The cells were grown in F-10 Ham's medium (Gibco, Invitrogen) supplemented with 10% by volume fetal bovine serum (Gibco, Invitrogen) and 1% (by volume) of antibiotics solution (penicillin/streptomycin). Cultures were passaged every 24h by a dilution factor of ½. Confluent cells were detached with trypsin and suspended in fresh media. Cell suspension was counted using a Neubauer chamber and seeded in 12-well cell culture plate (TPP) at a density of 1.2 × 10^4 cells per well (at a concentration of 1 × 10^6 cells/mL). Substrates were incubated for 24 h. Prepared substrates were immersed for 30 min in alcohol 70% to sterilize them before use in cell experiments. The flat surfaces were analysed based on the morphology of the cell attached to the surfaces by shape factor [1].

RESULTS: In the case of flat surfaces, CHO cell presented the best spreading on the SU-8 surface, followed by DLC (ta-C) surface, while PDMS was the worst situation, due to low wettability of this material. In the case of microstructured surfaces, SU-8 containing hexagonal microcavities of 12 µm proved to be the most adverse situation to CHO cell growth, probably because of the steep topography with cavities size lower than the CHO cells size. Instead, SU-8 containing hexagonal microcavities of 80 µm was the most favorable surface to CHO cell growth, even compared to reference glass. All surfaces were not cytotoxic.

DISCUSSION & CONCLUSIONS: CHO cell presented optimized and controlled attachment to the SU-8 2005 surface by introduction of micro scale hexagonal cavities of 80µm, with results comparable to the reference glass.

REFERENCES: [1] A. K. Shah, R. K. sinha, N. J. Hickok, R. S. Tuan (1999) *Bone*, **24(5)**:499–506.

Indirect rapid prototyping of small-scale medical devices

RD Boehm[1], B Chen[1], SD Gittard[1,2], HA Scott[2], BN Chichkov[2], NA Monteiro-Riviere[3,4], A Nasir[4,5], RJ Narayan[1]

[1] *Joint Department of Biomedical Engineering, University of North Carolina and North Carolina State University, Chapel Hill, NC 27599, USA.*

[2] *Laser Zentrum Hannover e. V., Hollerithalle 8, 30419 Hannover, Germany*

[3] *Center for Chemical Toxicology Research and Pharmacokinetics, Department of Clinical Sciences, North Carolina State University, Raleigh, NC 27695, USA.*

[4] *Department of Dermatology, University of North Carolina, Chapel Hill, NC 27599, USA.*

[5] *Wake Research Associates, 3100 Duraleigh Rd Ste 304, Raleigh, NC 27612, USA.*

INTRODUCTION: Two photon polymerization involves spatial and temporal overlap of photons to initiate chemical reactions, which lead to photopolymerization of photosensitive materials within well-defined volumes.[l] A large variety of inexpensive photosensitive materials (e.g., polymers and Ormocer® materials) may be processed with two photon polymerization. Two photon polymerization can be performed in a conventional manufacturing environment; no cleanroom facilities are needed. We have previously used two photon polymerization to create microneedles, tissue engineering scaffolds, and other medical devices. An indirect rapid prototyping approach known as two photon polymerization-micromolding has also been used to create tissue engineering scaffolds and microneedles. In this study, tissue barbs were prepared out of an acrylate-based polymer using two-photon polymerization-micromolding; details on the approach and the results can be found in Boehm et al.[2]

METHODS: Three types of tissue barbs were fabricated using two-photon polymerization-micromolding: two-pronged tissue barbs (these barbs contain two arrows pointing in opposite directions of one another on either side of the barb backbone), eight-pronged tissue barbs (these barbs contain two rows of four arrows pointing in opposite directions of one another on either side of the barb backbone), and sixteen-pronged tissue barbs (these barbs contain two rows of eight arrows pointing in opposite directions of one another on either side of the barb backbone). Master tissue barbs were prepared using an acrylate-based polymer known as e-Shell 300 (Envisiontec GmbH, Gladbeck, Germany) using two-photon polymerization. To prepare replica tissue barbs, e-shell 300 was placed within polydimethylsiloxane molds that were created from the two-photon polymerization-fabricated master structures.

RESULTS: Scanning electron micrographs were used to obtain size measurements of replica tissue barbs. In general, good correspondence was noted between the features of the tissue barbs and the corresponding computer-aided design (.STL) files. Since e-shell 300 exhibits fluorescence when exposed to near ultraviolet light, it may be used to observe tissue barb position and functionality. Confocal laser scanning microscopy was used to examine shallow penetration of cadaveric porcine skin by the barb tips. Blue fluorescence was noted in localized regions near the barb tip; this result was attributed to small pieces of e-Shell 300 (e.g., debris associated with tissue barb processing) that became separated from the tissue barbs during tissue penetration. The tissue barbs exhibited alignment within the laceration site; the long axis of the tissue barb became aligned with the plane of the linear laceration. This alignment served to minimize barb tip-tissue interaction.

DISCUSSION & CONCLUSIONS: Two photon polymerization and micromolding may be used for high fidelity replication of medical devices with microscale features. We anticipate that tissue barbs prepared using this approach may be used for sutureless tissue joining.

REFERENCES: [1] R. J. Narayan, A. Doraiswamy, D. B. Chrisey, et al (2010) *Mater Today* **13**:44-46. [2] R. D. Boehm, B. Chen, S. D. Gittard, et al (2013) *J Adhesion Sci Technol* **DOI:**10.1080/01694243.2012.693828.

ACKNOWLEDGEMENTS: This work was supported by National Science Foundation Grant 0936110.

A comparative study of femtosecond and nanosecond laser microcutting of AZ31 magnesium alloy stents

AG Demir, B Previtali

Department of Mechanical Engineering, Politecnico di Milano, Milan, Italy

INTRODUCTION: Magnesium alloy stents constitute an interesting solution for metallic cardiovascular stents due to their biocompatibility and biodegradability in human body. Laser microcutting is the industrially accepted method for stent manufacturing. However the laser-material interaction should be well investigated to control the quality characteristics of the microcutting process that concern the surface roughness, chemical composition and microstructure of the final device. The main laser characteristics that determine the final cut quality are the pulse duration and laser wavelength. In a generic comparison shorter wavelengths and shorter pulse durations are favourable for better laser micromachining quality. Longer pulsed lasers operating in µs-ns range are widely used in the industry; on the other hand it is more recent that industrial-grade solutions are available for ps-fs pulsed lasers. The present work demonstrates microcutting of stents in AZ31 with a new fs laser system, and compares the results with stents cut via a ns laser system.

METHODS: Laser microcutting was studied on AZ31 tubes with 2.5 mm outer diameter and 0.2 mm of wall thickness. Two laser systems were employed for a comparative study, namely ns-pulsed system characterized by high pulse energy, lower peak power (up to 10 kW) and relatively low pulse repetition rate (20-80 kHz), and fs-pulsed system characterized by low pulse energy (up to 0.075 mJ), high peak power (up to 60 MW) and high pulse repetition rate (single shot to 400 kHz). The two laser systems have wavelengths comparably similar in terms of absorption by metallic materials (see Table 1). With both lasers Ar was used as assist gas. The focused beam of the ns laser had a diameter of 23 µm, whereas the fs laser had 32 µm focused beam diameter. The cut stent mesh was designed within the multi-disciplinary research project of biodegradable Mg stents at the Politecnico di Milano [1].

RESULTS: Figure 1 exhibits the cut kerf of as cut stents. The ns pulse duration is long enough to generate heat diffusion in the bulk of the material, which generates cutting conditions governed by a combination of direct vaporization, vaporization from melt, and melt expulsion. On the other hand, fs pulse duration is short enough to interact with the material below the lattice cooling temperature, which enables microcutting conditions based on non-thermal ablation [2]. Due to this fact the cut kerf of the ns laser shows melt and recast areas. As a matter of fact, separation of scrap is achieved by kerf cleaning via chemical etching. The kerf realized by the fs laser shows a powder-like structure deposited on the kerf, whereas no melt is visible. Scrap separation is achieved by cleaning in an ultrasonic bath with acetone.

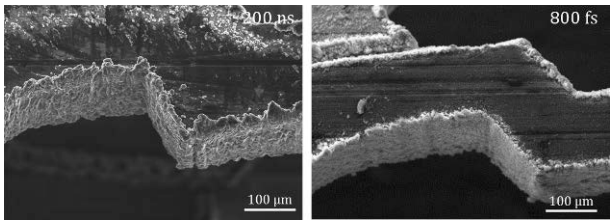

Fig. 1: Comparison of the kerf quality of the AZ31 stents cut with ns (left) and fs (right) pulsed lasers.

Table 1. The main characteristics of the used laser sources.

Laser source	Wavelength	Pulse duration	Max Energy
IPG YLP 1/500/50	1064 nm	200 ns	1 mJ
Rofin StarFemto	1552 nm	800 fs	0.075 mJ

CONCLUSIONS: The recent industrial grade fs lasers show great potential in terms of improving the cut quality on Mg stents. A more comprehensive study is undergoing to identify the benefits of different pulse duration regimes, which is the apparent point of debate today in laser micromachining.

REFERENCES: [1]W. Wu et al (2010) *Ann Biomed Eng* **38** (9): 2829–2840. [2] B.N. Chichkov et al (1996) *Appl. Phys. A* **63**:109-115.

ACKNOWLEDGEMENTS: The authors acknowledge the support from Rofin Baasel Lasertech Gmbh for their availability to use the fs laser system.

Nitrogen doping in biomaterials by extreme ultraviolet (EUV) surface modification for biocompatibility control

IU Ahad[1,2], B Budner[1], H Fiedorowicz[1], A Bartnik [1], D Brabazon [2]

[1] *Institute of Optoelectronics, Military University of Technology, 00-908 Warsaw, Poland*
[2] *Advanced Processing Technology Research Centre, School of Mechanical and Manufacturing Engineering, Faculty of Engineering & Computing, Dublin City University, Dublin 9, Ireland*

INTRODUCTION: Various studies show that employment of nitrogen coatings on certain biomaterials can noticeably increase the degree of biocompatibility (particularly for vascular repair) [1]. Chemical and laser ablation surface modification techniques are used for introduction or enrichment of nitrogen. However alteration of bulk material is reported which is undesirable for biomedical engineering applications. Extreme Ultraviolet (EUV) radiation with low penetration depth (less than 100 nm) can be successfully utilized to avoid bulk properties alteration. In this study Polyvinyl fluoride (PVF) and Polytetrafluoroethylene (PTFE) were treated by EUV radiation in the presence of ionized nitrogen. X-ray photoelectron spectroscopy (XPS) measurements demonstrate a notable amount of nitrogen on treated polymer surfaces.

METHODS: In this study a 10-Hz laser-plasma EUV source is used. This source is based on a double-stream gas-puff target, irradiated with the 3 ns/0.8J Nd:YAG laser pulse. The source is equipped with an auxiliary gas-puff valve to inject nitrogen into EUV – sample interaction region. Using a gold-plated grazing incidence ellipsoidal collector, an effective radiation focus and spectral coherence centered at 10±1 nm acquired. More detailed source setup information can be found in another place [2]. PTFE and PVF samples were irradiated by 50, 200, and 300 EUV shots and 50 and 200 EUV shots respectively. Pristine and EUV irradiated samples were examined by x-ray photoelectron spectroscopy (XPS).

RESULTS & DISCUSSION: Direct photo-etching by EUV photons result in formation of micro and nanostructures onto the polymer sample surfaces. Moreover in the presence of reactive gas (such as nitrogen), chemical modification in surface layers observed. Table 1 summarized the XPS spectra results of pristine and EUV treated samples. Pristine samples of PTFE ad PVF do not contain nitrogen atoms. It can be observed that in case of PTFE samples, at 300 EUV shots N1s (0.67% atomic weight) along with O1s (0.57% atomic weight) incorporates on polymer surface. Whereas in case of PVF samples nitrogen atom incorporation is demonstrated at 200 EUV shots (N1s=3.36 % atomic weight) forming polar covalent bond with carbon.

Table 1. Summarized results from XPS spectra

Material	No. of shots	Element	Atomic Weight %
PTFE	Pristine sample	C1s	24
		F1s	74
	50	C1s	23.17
		F1s	76.83
	200	C1s	24.99
		F1s	75.01
	300	C1s	29.46
		F1s	70.54
		O1s	0.57
		N1s	0.67
PVF	Pristine sample	C1s	66.73
		F1s	31.43
		O1s	1.85
	50	C1s	64.59
		F1s	34.74
		O1s	0.67
	200	C1s	76.6
		F1s	13.3
		O1s	6.74
		N1s	3.36

CONCLUSIONS: Nitrogen enrichment or doping in polymeric biomaterials is possible through EUV surface modification. EUV photons carry enough energy to simultaneously ionized and excite nitrogen gas molecules. This results in incorporation of nitrogen atoms in polymer chain as demonstrated by results therefore biocompatibility enhancement is foreseen.

REFERENCES: [1] W.-H. Liao et al. (2012) *J. Biomed. Mater. Res., Part A* **100(11)**:3151–6 [2] A. Bartnik et al. (2011) *Nucl Instrum Meth A* **647**:125–131

ACKNOWLEDGEMENTS: With the support of the Erasmus Mundus programme of the European Union and the 7th Framework Programme's Laserlab Europe project (Nr 284464).

Properties of nanostructured real surfaces for implants

J Fojt[1], V Filip[1], L Joska[1], H Moravec[1], J Fencl[2]

[1] *Institute of Chemical Technology, Prague, Czech Republic* [2] *Beznoska Ltd., Kladno, Czech Republic*

INTRODUCTION: The Ti-6Al-4V alloy currently belongs to the most frequently applied group of materials in implantology. Considering interaction with body environment, it is bioinert. Therefore, the research activities are focused on the formation of bioactive surface that would allow faster healing of the implant and its earlier loading. One of the possible ways is the formation of tubular nanostructure. Literature describes this process in detail mostly for smooth surfaces. Considering possible applications in implantology, areas with a relatively rough surface are used on the implant and it is desirable to nanostructure such inhomogeneous surface. The aim of this work was to create nanostructures of variable parameters on the Ti-6Al-4V alloy surface in the state modelling the implant. Created nanostructured surfaces were in-vitro tested from their use in medical applications point of view.

METHODS: Disc-shaped specimens of Ti-6Al-4V alloy were used, their surface was jet-blasted with corundum to Ra=5.6 ?m. Nanostructures were prepared by electrochemical oxidation in an ammonium sulphate and ammonium fluoride-based electrolyte. Various types of exposures were chosen to achieve a range of dimensions of nanostructures. Nanostructures were studied by scanning electron microscopy and photoelectron spectroscopy. Dimensions of nanostructures were primarily determined on polished specimens, final state of jet-blasted surfaces was difficult to precisely assess and did not provide sufficient data for statistical analysis. Adhesion of nanotubes was tested by pull-of method according to ASTM F1147-99 and ASTM C633-79 standards. The interaction of nanostructures with simulated body fluid (SBF) was periodically monitored by electrochemical impedance spectroscopy.

RESULTS: Nanostructures of tubular character were formed on all specimens. The most frequent diameters of tubes were 20 nm, 40 nm, or 110 nm, depending on the exposure conditions. Their length ranged from 230 nm to 640 nm. The formed nanostructures contained titanium, aluminium and vanadium oxides and fluorine bound in the tube bulk. Nanostructures strongly adhered to the surface; the strength necessary for tearing the tested couples off was on the level of 40 MPa. Nanostructures with parameters comparable with those of the polished specimens were formed on jet-blasted specimens.

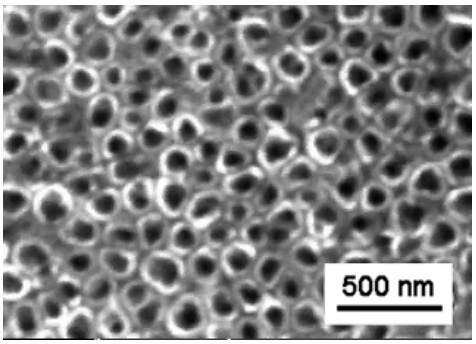

Fig. 1: Nanostructured surface of Ti-6Al-4V alloy.

The exposure in simulated body fluid indicated a positive impact of nanostructures, in terms of interaction with SBF, on both smooth and blasted surfaces. Non-nanostructured specimens showed behaviour typical for a passive material, the state of the surface has not practically changed during the exposure in SBF. On the contrary, hydroxyapatite precipitated on the nanostructured specimens. The most significant changes were identified for specimens with nanotubes of the largest diameters on both polished and jet-blasted surfaces. The impedance spectra indicated surface changes - precipitation of the compound - in the area of low and medium frequencies.

DISCUSSION & CONCLUSIONS:
Nanostructures were formed on specimens with a significantly inhomogeneous jet-blasted surface. Dependency between the resulting nanostructure parameters and the exposure conditions was determined. Considering the interaction with simulated body fluid, the nanostructures with the largest diameter of tubes (~100 nm) appeared to be the best. Gradual precipitation of hydroxyapatite from the simulated body fluid was well detectable by electrochemical impedance spectroscopy.

ACKNOWLEDGEMENTS: The works were carried out as a part of the TE 01020390 project, which is financially supported by Technology Agency of the Czech Republic.

Designing hydroxyapatite coating topography at the micro and nano level

C Petzold[1], H Haugen[1], KA Gross[2]

[1]*Department of Biomaterials, Institute for Clinical Dentistry, University of Oslo, Norway*

[2]*Institute of Biomaterials and Biomechanics, Riga Technical University, Latvia*

INTRODUCTION: Hydroxyapatite (HA), as an orthopaedic implant coating, has an intrinsic biocompatibility [1], but attention has never been directed to the topography for influencing the cell response. Here we report on a coating surface composed of more repeatable building blocks; flattened droplets that stack together to build up the coating. The entire topographical map of the surface requires information on the microscopic and nanoscale elements. This work shows how the micro and nano-topography can be measured for surface ordering to provide a favourable biological response.

METHODS: A narrow particle size range was flame sprayed to achieve a similar degree of melting. This allowed the desired melt viscosity to be set for depositing well-flattened droplets. The topography of thermal spray HA coated titanium surfaces was reported with atomic force microscopy (AFM; Asylum Research, Santa Barbara, USA) for height of the individual splats and HA crystal size on the splat surfaces. Splat heights were determined from profiles of scans of 50 x 50 μm^2 (N=23). Height differences were analysed manually from the smoothened profile data (N=119 edges). For crystal size analysis, entire splats were imaged at 50 µm side length (N=5). Crystal sizes were measured manually with 1 μm^2 or 25 μm^2 sized images if possible and correlated to their respective positions: centre (C), edge (E), or transition zone (T).

RESULTS: 1. Splat profiles. The mean splat height was calculated to be 0.99 µm ± 0.62 µm. Two characteristics of splats were observed; a flattened disk with a raised centre and splats with a lowered centre compared to the edges. Splat edges were usually steep. 2. HA crystal size. The grain sizes in the different positions increased in the order E < T < C. Significant differences were found between E and T, and E and C.

DISCUSSION & CONCLUSIONS: Splats had a steep border, in correlation with XRD data that suggested a crystalline structure of the HA with a crystal alignment perpendicular to the sprayed surfaces. The steepness of the splat borders was not precisely determined due to the limitation of the method (tip angle 18°). The valley depths were underestimated if narrower than the AFM-tip, in which case, the tip may not have reached the bottom of the valley. The HA crystals were larger at the centre of splats, indicating a slower cooling compared to the areas closer to the borders. Grain sizes in the C-areas were difficult to measure due to their larger size. Thus, the grain size measured for position C underestimates the actual size, as only relatively small grains could be analyzed. In conclusion, the results of the AFM analysis correlate well with results of XRD measurements, showing HA crystals perpendicular to the base surface. This is the first time that the splat height and surface topography have been measured on an oriented coating to understand the features that are exposed to proteins and cells. An oriented array of crystals has a similarity to the crystals in tooth enamel, but have a variability attributed to the different cooling rate across the diameter of the splat.

REFERENCES: [1] 1. T. Kokubo, H.-M. Kim, M. Kawashita, et al (2004), *J. Mater. Sci.: Mater. Med.* **15**:99-107

Controlling MSC self-organization by Laser-Assisted Bioprinting

E Pagès, M Rémy, M Medina, B Guillotin, R Devillard, F Guillemot

Inserm U1026, Université Bordeaux Segalen - BioTis, Bordeaux Cedex 33076, France

INTRODUCTION: Laser assisted bioprinting (LAB) is an emerging technology in tissue engineering (TE). LAB allows to print cells and liquid materials with a cell-level resolution, which is comparable to the complex histology of living tissues [1], what opens new horizons for studying morphogenetic process. By giving tissue engineers control on cell density and organization, LAB potentially holds promise to fabricate living tissues with biomimetic physiological functionality.

In this context, and because human mesenchymal stem cells (MSCs) have the capacity to be differentiated in many cell lineages, our work aims at evaluating the influence of their spatial patterning on self-organization processes.

METHODS: Cells used in these experiments are human adipose derived stem cells (ADSCs) and mouse bone marrow precursors transfected with Td-tomato (D1T). Bioinks are made from cells suspended into culture medium (DMEM F12) and biopaper is a collagen type I hydrogel layer. The laser pulse energy is 27 µJ (determined from previous experiments). Printing parameters are controlled to tune cell pattern features: distance between two cell islets, number of cells per islet and distance between cell lines. Cell viability, adhesion and differentiation are evaluated at different time points after bioprinting.

RESULTS: After LAB, cell viability is 97%, cells are able to adhere to collagen and to differentiate in adipocytes and chondrocytes as observed after staining with Oil red O and Alcian Blue (Fig. 1).

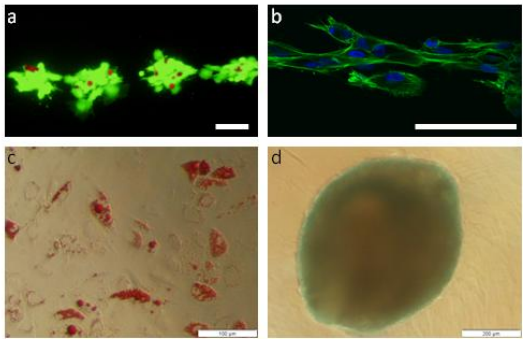

Fig. 1: Observation of cell viability (a), cell spreading (b), adipocyte and chondrocyte cell differenciation (resp. c and d) after bioprinting. Scale bar: 100µm

For a distance of 250 µm between 2 cell islets, cell migration occurs and a continuous line is formed at 24 h. When this islet-to-islet distance is larger than 250 µm, cells keep isolated till 72 h (Fig. 2). When this distance equals 250 µm, and the number of cells by islet is about 10, thin and continuous cell fibres are observed after 24 h, (data not shown). These fibres remain stable till 72 h but can be disturbed when other cell lines are closer than 1000 µm. Interestingly, by reducing the islet-to-islet distance in both directions to 250 µm, cells form a homogeneous layer at 48 h (Fig. 3).

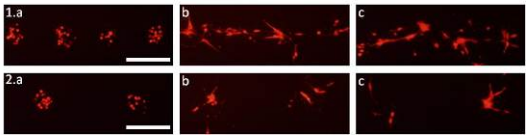

Fig. 2: Initial islet-to-islet distances (250 and 500 µm, raws 1 and 2) influence cell self-organization at 1, 24 and 72 h (a, b, c). Scale bar: 200µm

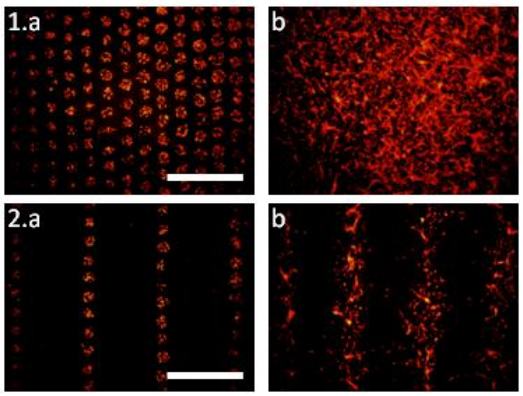

Fig. 3: Distance between cell lines (250 and 1000 µm, raws 1 and 2) induces formation of specific cell patterns at 1h (a) and 48h (b). Scale bar: 1000µm

DISCUSSION & CONCLUSIONS: Printed cells self-organize depending on the number of cells at vicinity. Accordingly, cell fibers or homogeneous cell layers can be obtained after 3 days in culture. Associated with the maintain for cell differentiation capacity, these results paves new opportunities to engineer complex tissues by LAB.

REFERENCES: [1]Guillotin, B., et al. (2010). *Biomaterials* **31(28)**:7250–7256.

ACKNOWLEDGEMENTS: R. Bareille for help in isolating ADSCs. ANR and Region Aquitaine for financial support.

Controlling wetting properties of AZ31 Mg alloy via laser surface structuring

AG Demir, V Furlan, N Lecis, B Previtali

Department of Mechanical Engineering, Politecnico di Milano, Milan, Italy

INTRODUCTION: For biomaterials and biomedical devices surface topography plays an important role on how material interacts with the body tissue. Laser micromachining constitutes a flexible option, as it allows different modality of surface machining ranging from ablation to annealing or remelting. As a consequence the properties of the surface can be changed in a controlled way. This work reports the use of a ns pulsed fibre laser for surface structuring to control the wetting properties of AZ31 Mg alloy. Such control is of great potential interest for the interaction of the biodegradable Mg alloy with the body tissue.

METHODS: Cold rolled AZ31 sheets (0.4 mm thick) were used for the study. A fibre laser source operating in ns regime (IPG Photonics YLP 1/100/50/50) was used for surface structuring. Beam manipulation was achieved with a scanner system, in ambient conditions without the use of shielding gas. Through preliminary investigations 5 different surface structures exhibiting surface roughness between R_a=0.2-4.3 µm were identified. Contact angle measurements were performed with Wilhemy plate method with distilled water. Moreover, the adhesion strength of the different surface oxide morphologies was evaluated by scratch testing.

RESULTS: Figure 1 shows the measured contact angles against the surface roughness values. The contact angle was effectively varied between 20°-70°, compared to the initial contact angle of 60° belonging to the non structured surface (R_a=0.25 µm). Within the first region of the plot in Figure 1 where the surface roughness varies between R_a=0.21-1 µm a clear drop in the contact angle is observed. This phenomenon can be explained by the increase of the real surface area stated by the Wenzel equation as:

$$cos(\theta_r) = R\, cos(\theta_f) \qquad (1)$$

where θ_f is the contact angle of an ideally flat surface, θ_r is the contact angle of a rough surface and R is the ratio between the real surface area, and the ideally projected one [1]. On the other hand in the range of R_a=1-4.3 µm an increase in the contact angle is visible. This is expected to be due to entrapment of gas phase within the surface but also due to the surface morphology which tends to generate sub-micron sized features, as explained by the the Casie-Baxter equation:

$$cos(\theta_r) = f_s\, cos(\theta_f) - f_g \qquad (2)$$

where f_s and f_v are the area fractions of the projecting solid and gas on the surface, respectively [2].

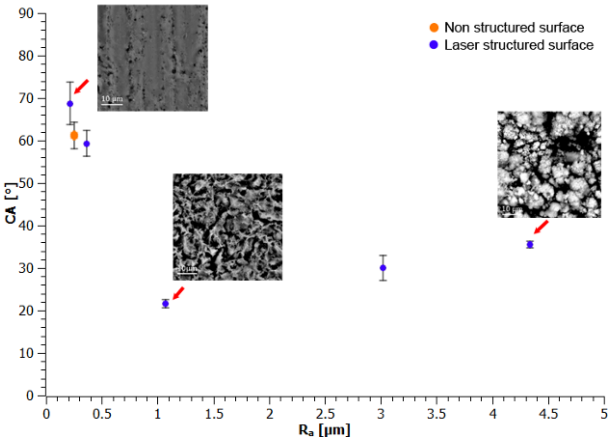

Fig. 1: Measured contact angle (CA) values as a function of average surface roughness (R_a) (error bars show standard deviation).

Scratch tests were used to evaluate, the critical load (Lc), defined as the load corresponding to which the oxide has been removed. The surface exhibiting the lowest contact angle showed similar Lc compared to the non structured surface with natural oxide layer (Lc ≅ 14 N).

CONCLUSIONS: The results confirm the possibility of varying the contact angle in the hydrophilic range with laser structuring. The use of a laser beam for surface structuring can be exploited to change the wetting properties of an entire medical device, or apply these changes only locally where needed with high precision and high resolution. Further research is ongoing on the effect of the surface structure for the application of biopolymer coatings.

REFERENCES: [1] R.N. Wenzel (1936) *Ind. Eng. Chem.* **28**:988–94. [2] A.B.D. Cassie, S. Baxter (1944) *Trans Faraday Soc* **40**:546–51

ACKNOWLEDGEMENTS: Fondazione CaRiTRO for partially funding the research (grant number 2011.0250).

Embryoid body culture of ES cells using gelatin/PEG micropatterned chips

K Nakazawa, T Hara, H Koga

Department of Life and Environment Engineering, The University of Kitakyushu, Japan

INTRODUCTION: Embryonic stem (ES) cells are pluripotent and possess self-renewal abilities; therefore, they have been used in various applications such as tissue engineering, regenerative medicine, pharmacological and toxicological studies, and fundamental studies of cell differentiation. The formation of embryoid bodies (EBs), which are cell aggregates of ES cells, is an initial step in ES cell differentiation, and EB culture has been widely utilized as a trigger for *in vitro* differentiation of ES cells. Among the various culture methods, micropatterned culture is a useful technique for regulating cell culture conditions because it can control the cellular micro-environment by regulating cell arrangement at a micro-scale. In this study, we fabricated a microchip, which the surface was modified with gelatin and polyethylene glycol (PEG), for the micropatterned culture of EBs, and we evaluated the effect of distance between EBs on the cell proliferation and differentiation properties of EBs.

METHODS: The microchip contained 37 gelatin spots (300 μm in diameter) in a triangular arrangement on a glass plate that served as the cell adhesion area; the region lacking the gelatin spots was modified with PEG to create the non-adhesion area. The chip was fabricated by microcontact printing method [1]. Three similar chips with pitches (the distance between the gelatin spots) of 500 μm (chip 500), 1000 μm (chip 1000), and 2000 (chip 2000) μm were designed to investigate the effect of distance between EBs on the properties of mouse EBs.

RESULTS & DISCUSSION: The ES cells inoculated on the chip adhered to the gelatin spots and formed a monolayer within 1 day of culture (Fig. 1a); thereafter, the ES cells gradually formed EBs on each gelatin spot by proliferation (Fig. 1b). The EBs remained on the gelatin spots of the chip throughout the culture period (Fig. 1c). The EB sizes gradually increased until 7 d of culture but remained almost constant thereafter (Fig. 2). Furthermore, the EB size increased with an increase in the pitch between the gelatin spots on the chip. These results indicated that the pitch between the EBs was positively correlated with the EB growth.

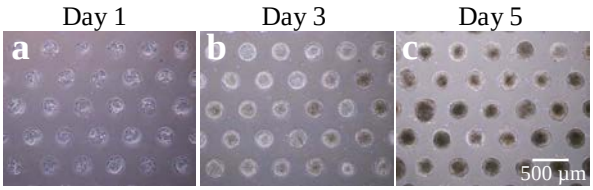

Fig. 1: EB formation on the microchip.

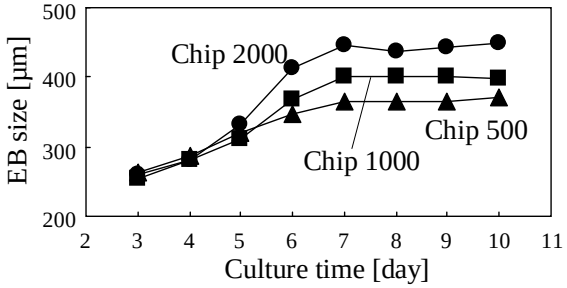

Fig. 2: Changes in the EB sizes on the chips.

To compare the properties of EBs formed under the three chip conditions, we measured the expression of marker genes at 10 d of culture by real-time PCR analysis. The expression levels of undifferentiated markers (Oct3/4 and Nanog) were the highest in the chip 500, but decreased in the chips 1000 and 2000 in that order. In contrast, the expression levels of differentiation markers (TTR, AFP, Nkx2.5, αMHC, and Flk1) were the highest in the chip 2000, but decreased in the chips 1000 and 500 in that order. These results suggested that cell differentiation rates were regulated by the pitch between the EBs. This effect may be related to the difference in culture environment under each condition. A shortage of oxygen and nutrients, and/or the accumulation of secretions by the neighboring EBs may occur, leading to regulation of cell differentiation in EBs.

CONCLUSIONS: We demonstrated that the distance between EBs affected to the proliferation and differentiation of ES cells in EBs.

REFERENCES: [1] Y. Sakai, Y. Yoshiura, K. Nakazawa (2011) *J Biosci Bioeng* **111**:85-91.

Protein binding functionalisation of plasma-derivatized silicone surfaces.

V Sharma [1], KA Blackwood[2], D Haddow[3] & JF Dye[1]

[1] RAFT Institute/UCL, UK. [2] RAFT Institute/Queensland University of Technology, AUS. [3] Altrika Ltd, UK.

INTRODUCTION: A major concern related to large area wounds is loss of barrier function. Silicone is a versatile material for medical applications, but is essentially bio-inert. The ability to bind proteins will allow functionalisation of silicone surfaces which may benefit wound healing and other biocompatible medical device applications. This study aimed to characterise target protein binding to derivatised silicone surfaces.

METHODS: Silicone sheets were derivatized with acrylic acid (AcA) or oxygen (O2) by plasma polymerisation (supplied by Altrika). Non-blocked polystyrene wells (PS) without any discs were used as reference. Discs of silicone sheets with fibrinogen (5-250 µg/ml) were incubated in pre-blocked ELISA wells. In some cases, the silicone surfaces were crossed linked with 2% glutaraldehyde (GTA). Bound fibrinogen (FBG) was detected by using an ELISA system. Total protein was measured using Bradford Ultra reagent (Novexin).

RESULTS: Optimal primary and secondary antibody concentrations were determined and FBG binding affinity and capacity to PS, O2 & AcA surfaces determined. FBG-silicone binding curves were characterized by saturation at around 150 µg/ml to all types, with the highest binding to AcA. Binding for PS samples saturated at around 50 µg/ml. GTA cross linked FBG was detected by a polyclonal anti-fibrinogen antibody. From total protein measurements approximate values for FBG binding were 1.27 µg/mm^2 (all of the silicone surfaces); 0.74 µg/mm^2 (PS). Release of protein by trypsinisation and slot-blot assay provided an alternative estimate of total bound protein. Silicone surfaces show 2x protein binding capacity than PS but with lower affinity. Bound protein was not removed from either surface, but binding could be reduced by co-incubating with non-ionic surfactant.

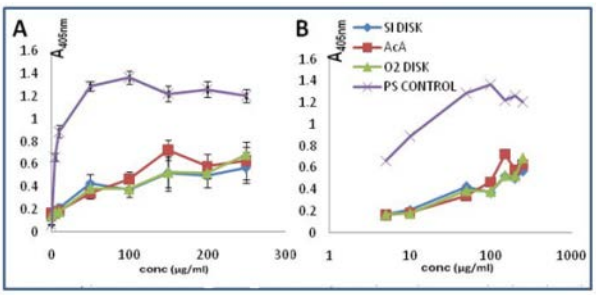

Fig. 1: ELISA characterisation of protein absorption on various silicone sheets coated with acrylic acid (AcA DISC), oxygen (O2 DISC) and non polymerized silicone (Si DISC). Non- blocked polystyrene wells without any discs were used as reference (PS CONTROL).

DISCUSSION & CONCLUSIONS: Silicone surfaces show nearly twice protein binding capacity than PS but with lower affinity. Currently, we are relating this to plasma resonance spectroscopic surface. Studies with surface extraction solutions to examine the robustness of this surface binding for practical functionalisation, and the effect of GTA crosslinking stabilisation are underway.

ACKNOWLEDGEMENTS: This work is supported by a TSB grant.

Pulsed Laser technologies for the transfer of levan nanostructures

F Sima[1], E Axente[1], LE Sima[2], U Tuyel[3], MS Eroglu[4,5], N Serban[1], C Ristoscu[1], SM Petrescu[2], E Toksoy Oner[3], IN Mihailescu[1]

[1] *Lasers Department, National Institute for Lasers, Plasma and Radiation Physics, Magurele, Romania* [2] *Department of Molecular Cell Biology, Institute of Biochemistry, Romanian Academy, Bucharest, Romania* [3] *Department of Bioengineering, Marmara University, Istanbul, Turkey* [4] *TUBITAK-UME, Chemistry Group Laboratories, Kocaeli, Turkey* [5] *Department of Chemical Engineering, Marmara University, Istanbul, Turkey*

INTRODUCTION: Matrix assisted pulsed laser evaporation (MAPLE) and combinatorial MAPLE (C-MAPLE) stand for advanced pulsed Laser technologies that permitted the fabrication of micro- or nano-arrays of wide-ranging biomaterials with applications in optoelectronics, biosensing, chemical sensing, biochemical analysis and for drug delivery systems and implant development [l,2]. Levan is a water soluble, strongly adhesive and film-forming long linear homopolymer of β(2-6) linked fructose residues with valuable applications [3]. The present study is focused on obtaining levan-based bioactive, nanostructured surfaces by use of pulsed laser techniques.

METHODS: Levan (L) or oxidized levan (OL) dissolved in DMSO were used as targets. In the experiments, a KrF* excimer laser source (λ = 248 nm, τ_{FWHM} = 25 ns) operating a repetition rate of 3 Hz was used for targets evaporation. The deposition substrates of Si(100) and optical glass slides were placed 4 cm apart and parallel to the targets and heated at 100°C. FTIR spectrometry analysis was carried out with Shimadzu 8400S equipped with an automated IR microscope 880 apparatus operating within the range (500-4000) cm^{-1}. SEM and AFM studies were conducted with Jeol JSM-5910 LV instrument at 20 kV and Park systems XE70 SPM Controller LSF-100 HS, respectively.

RESULTS: MAPLE deposited nanostructured thin films of L and OL showed a good adhesion to substrate and a uniform, homogenous nanostructured surface (Fig. 1A). C-MAPLE was applied to obtain a compositional library of L and OL in form of thin films. FTIR micro-spectroscopy confirmed the existence of a composition gradient along the length of the sample (Fig. 1B). Cell viability and proliferation studies confirmed the biocompatible behavior of the synthesized nanostructures [l, 2].

DISCUSSION & CONCLUSIONS: Levan polysaccharide proved to have high potential when applied by advanced pulsed laser technologies. Levan-based thin nanostructured bioactive surfaces were obtained without the use of plasticizers or pigments. C-MAPLE can rapidly generate discrete areas of organic film compositions with improved properties than starting materials.

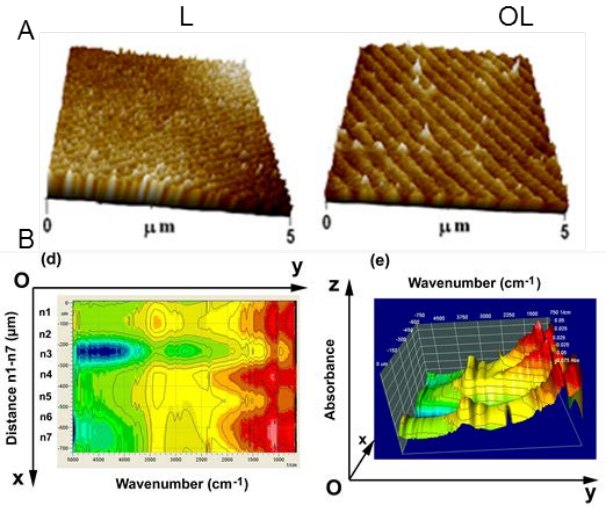

Fig. 1A: Typical AFM images of MAPLE deposited surfaces on Si. B: FTIR spectra recorded along the gradient of composition L to OL generated by C-MAPLE. FTIR micro-spectroscopy studies were carried out along 700 μm distance on zones (n1 to n7) defined by apertures of 100×100 μm^2 from the considered origin (O). 2D plot of absorption (y-axis) within the range (500-4000) cm^{-1}) over the distance of 700 μm (x-axis) and 3D representation of absorption versus distance on film, where the variation of the intensity is plotted along the z-axis. Blue is for weaker, yellow for intermediate while red is for stronger IR absorption.

REFERENCES: [1] F. Sima et al. (2011) *Biomacromolecules* **12**:2251 –56 [2] F. Sima et al. (2012) *Applied Physics Letters* **101**:233705 [3] A. Poli et al. (2009) *Carbohydrate Polymers* **78**:651.

ACKNOWLEDGEMENTS: This work was supported by the bilateral Contracts 109T614 and 112M330 between Turkey and Romania. CR, FS, NS and INM acknowledge the support of UEFISCDI (TE 82/2011). FS and LES acknowledge the financial support from the European Social Fund POSDRU 2007-2013 through POSDRU/89/1.5/S/60746.

Identification, production and characterization of phenoloxydases from marine organisms

B Maldonado[1], P Flammang[2], J Piette[1], C Van De Weerdt[1]

[1] *Molecular Biology and Genetic Engineering Unit, GIGA-R, University of Liège, Liège, Belgium*
[2] *Laboratoire de Biologie des Organisms Marins et Biomimétisme, Université de Mons-UMONS, Mons, Belgium*

INTRODUCTION: Adhesive proteins of marine origin have been extensively studied because of their great potential in the development of new adhesive compounds. However, very little is known about the enzymes involved in their specific post-translational modifications and the *in vivo* mechanisms involved in their maturation to reach their unique adhesive properties. The main goal of this study is to identify, isolate, produce and characterize the enzymes involved in the post-translational modifications of marine adhesive proteins. We especially focus on the study of the enzymes responsible for the transformation of tyrosine residues into DOPA and DOPA quinone in mussels (*Mytilus edulis*) and tube-worms (*Sabellaria alveolata*). These enzymes will also be used for the *in vitro* modification of recombinant adhesive proteins. Our findings should improve the yields of post-translational modification reactions in the new bio-inspired adhesive compounds for which these modifications are essential.

METHODS: Specimens of *Mytilus edulis* were obtained from the supplier "La Marée" (Herstal, Belgium). They were maintained in an aerated aquarium at 13°C for 10 days. Isolation of *M. edulis* phenoloxydase was performed as described in Hellio *et al*. (2000)[1] with a modified lysis buffer (not including 0.5 mM DTT). The extract was analyzed by electrophoresis on polyacrylamide gels under native conditions (Biorad) to maintain enzymatic activity. The presence of phenoloxydase was confirmed by overnight incubation of the native gels with 5 mM L-DOPA in 0.1 M phosphate buffer pH 6.8. Commercial mushroom tyrosinase (Sigma) was used as positive control. Phenoloxydase activity was also measured spectrophotometrically using the method of Pomerantz (1963)[2]. The extract was incubated at 25°C with 10 mM L-DOPA in 50 mM phosphate buffer pH 6.8. The phenoloxydase activity was followed by monitoring the increase of absorbance at 475 nm.

RESULTS: As shown in Figure 1 and Table 1, *M. edulis* tyrosinase was successfully isolated.

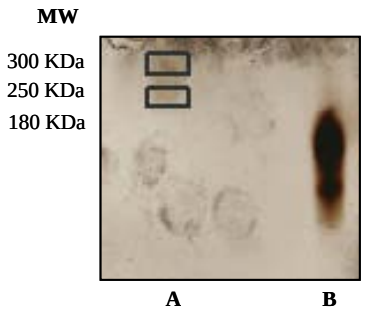

Fig. 1: Analysis by non-denaturating gel eletrophoresis of the tyrosinase extract of M. edulis. A: M. edulis extract incubated with 5 mM L-DOPA. B: Commercial mushroom tyrosinase (Sigma) incubated with 5 mM L-DOPA (10 µg, positive control). Molecular weight markers are shown on the left of the panel.

Table 1. Tyrosinase activity assay

Sample	OD 475nm 30 min	OD 475 nm 60 min
Negative control	0.06	0.07
M. edulis extract	0.20	0.35
Mushroom tyrosinase (10 µg)	0.66	0.75

DISCUSSION & CONCLUSIONS: Preliminary results in *M. edulis* are promising. Isolation of *S. alveolata* tyrosinase will also be started soon. The active bands identified in the native gels will be partially sequenced by mass spectrometry. From the peptide sequences obtained, we will look for similarities with sequences of enzymes already identified in databases. The sequences of the enzymes of interest will be cloned in a suitable vector for recombinant protein production in *E. coli*. Once production is optimized, the recombinant enzymes produced will be purified from bacterial extracts by chromatographic methods and they will be characterized at biochemical, biophysical and functional level.

REFERENCES: [1] C. Hellio, N. Bourgougnon and Y Le Gal (2000) Biofuling 16:235-244.
[2] S. Pomerantz (1963) J Biol Chem 238: 2351-2357.

Effect of histidine on the surface of chitosan beads after adsorption of copper ions

CRA Mahl, MM Beppu

Department of Materials Engineering and Bioprocess, Chemical Engineering School, University of Campinas, Campinas, Brazil

INTRODUCTION: Several chelating agents have been used pharmacologically to treat adverse effects of heavy metals to human health. In this work, chitosan in contact with histidine is investigated as a potential system to capture metal ions. Chitosan beads with and without the presence of histidine were analyzed by SEM and FTIR techniques in order to observe changes on its surface.

METHODS: To obtain chitosan beads a solution of 2.5 w/w chitosan (Sigma, 85% deacetylation, USA) was dropped at constant rate with in a solution of sodium hydroxide (NaOH 1 mol / L) (Synth, Brazil) under stirring regular. The beads remained during 24 h and then it was washed with distilled water until reaching a neutral pH.

Preparation of (chitosan+copper) beads: the chitosan beads were placed in contact with a solution of copper nitrate $CuNO_3.3H_2O$ (Vetec, Brazil) until reached equilibrium (100 h).

Preparaton of (chitosan+histidine+copper) beads: the chitosan beads were placed in a solution of histidine (100µM) for 24 h. Thereafter filtered and placed in a solution of copper nitrate until reached equilibrium (100 h).

The experiments were carried out at 25°C using a thermostatic bath (Dubnoff, NT 232, Brazil) with stirring of 150 rpm. The pH was fixed at 5.0. The chitosan beads (Chi, Chi+Cu(II) and (Chi+His) + His, were characterized by FTIR(Thermo Scintific, Nicolet 6700 (E.U.A)) and SEM (Leo 440i / 6070, Cambridge, England).

RESULTS: Significant changes in the FTIR spectra were found at the frequency of 1365 cm^{-1} which correspond to amino groups of chitosan. After copper adsorption and addition of histidine, occurs a remarkable change in this stretch. It suggests that histidine is inserting nitrogenated groups in chitosan. A study, in which histidine is functionalized on chitosan membranes crosslinked with glutaraldehyde, reported the same behavior, showing that histidine acts adding the amino groups at chitosan [1]. Under SEM, a microporous and heterogeneous structure was observed. But the morphology of pores changed after adsorption histidine or copper ions. This fact denotes that both agents change the chitosan matrix microstructure, producing different morphology after freeze-drying (method used to prepare SEM samples).

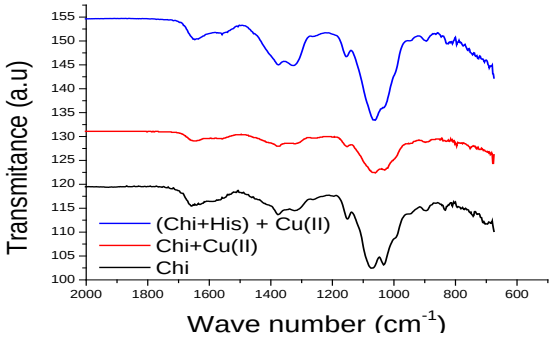

Fig.1-FTIR spectra of Chi, Chi+Cu(II) e (Chi+His) + Cu(II).

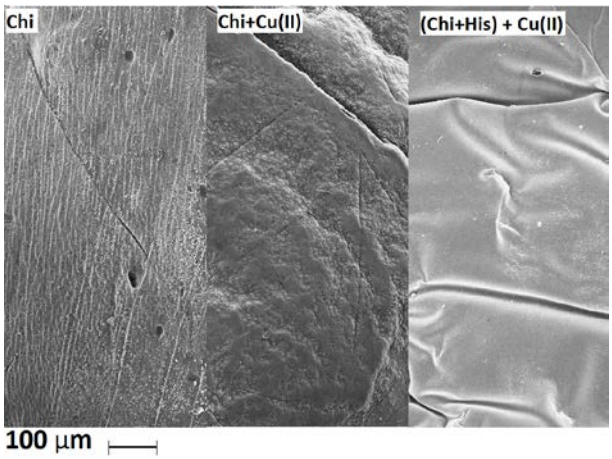

Fig.2- SEM micrographs of (A)Chi, (B)Chi+Cu(II) e (C)(Chi+His) + Cu(II).

DISCUSSION & CONCLUSIONS: The addition of histidine showed a possible change in the structure of chitosan beads. FTIR analysis showed that histidine is inserting amino groups in chitosan and MEV analysis indicated a change in the porous surfaces of matrices.

REFERENCES: [1]M.M.Beppu *et al* (2004) *J Membr Sc.*, 240.

ACKNOWLEDGEMENTS: FAPESP, CAPES and CNPQ.

Evaluation of *in vitro* calcification of pristine and sulfonated chitosan for use on stents

CS Campelo[1], MM Beppu[2], RS Vieira[1]

[1]*Department of Chemical Engineering, Universidade Federal do Ceará, CEP 60455-760, Fortaleza-CE, Brazil* [2]*Faculdade de Engenharia Química, Universidade Estadual de Campinas, Caixa Postal 6066, CEP 13081-970, Campinas, SP, Brazil*

INTRODUCTION: In the recent years, significant effort has been devoted to develop biomaterials for applications with blood contact, such as the production of artificial hearts, catheters, endovascular stents, hemodialysis membranes, chemical sensors and vascular implants. According to the World Health Organization (WHO), 17.3 million people died in 2008 from diseases related to cardiovascular problems, and it is estimated that by 2030, this number will increase to 23.6 million. Stents are devices used in patients with atherosclerosis since the 1980s. Although it minimizes problems caused by angioplasty, stents are subject to corrosion and other problems arising from its implementation. Metallic stents can be coated by thin polymer layers, which must have the following properties: a) bio and hemocompatibility; b) low cytotoxicity and no carcinogenic effects; c) chemical stability; d) easy processability and acceptable cost. Calcification is a process of calcium phosphate and other calcium compounds formation, which has been largely investigated and is the most important and undesirable cause of failure of heart valves. Chitosan is a natural polymer that has attracted attention in recent years due to excellent biocompatibility, biodegradability, affinity to biomolecules, and wound-healing activity. These properties may be increased through changes in the structure of chitosan, such as the addition of sulfonated groups. This modification can be done by the reaction of chitosan with sulfonic sodium salt, using methanol as reaction medium. In this context, this study evaluated the influence of sulfonated chitosan on the calcification mechanism to which the material is exposed when implanted in a patient.

METHODS: Chitosan membranes were obtained as described by Beppu [1]. Sulfonated chitosan were obtained as described by Amiji [2]. The calcification assays were performed following the methodology described by Aimoli [3]. The calcification characterization was conducted by SEM/EDS (Leo 440i / 6070, Cambridge, England).

RESULTS: From SEM, it was possible to observe clusters of calcium either for natural and modified chitosan membranes. However, a higher number of deposits were observed for pristine membranes. The EDS results (area and punctual) did not indicate presence of phosphorus, in both membranes, indicating that possibly there was no formation of calcium phosphate.

DISCUSSION & CONCLUSIONS: SEM showed some deposits on the surface of the studied membranes. Pristine chitosan membranes showed well-defined deposits, with size ranging from 2.5 to 10 micrometres. These deposits were analysed by EDS, and showed the presence of only Na, Ca and Cl, in addition to C and O, mainly for sulfonated chitosan. In this case, no calcium phosphates (typical compound of the process of calcification) was found. This can be explained by the presence of amino and sulfonated groups on chitosan chains, for pristine and sulfonated chitosan, respectively [4]. Amino groups are originally cationic hence are positively charged. These groups can create electron repulsion in Ca^{2+}, difficulting their deposition on the membrane. Sulfonate groups have a negative charge and is expected that they would attract Ca^{2+}. However, the anionic nature of the sulfonate causes a local pH reduction which results in the dissolution of the formed deposits [5]. These two mechanisms would be responsible for the associated delay in the nucleation process, contributing to the anticalcifying activity.

REFERENCES: [1] M.M. Beppu and C.C. Santana, Mater. Sci. Eng., 23 C (2003) 651; [2].M. M. Amiji (1998) *Colloids Surfaces B: Biointerfaces* **10**:263–271. [3] C. G. Aimoli, M. A. Torres, M. M. Beppu (2006) *Mater Sci and Eng C* **26**:78-86. [4] K. D. Park, W. K. Lee et al. (1997) *Biomaterials* **18**:47-51. [5] W. K. Lee, K. D. Park et al. (2001) *J Biomed Mater Res (Appl Biomater)* **58**:27-35.

Physico-chemical properties of synthetic SPIONs in comparison with magnetosomes

K Mireles[1], M Talantikit[1], TD Samani[1], M Mohammadi[2], E Sacher[3], LH Yahia[1]

[1]Laboratoire d'Innovation et d'Analyse de Bioperformance [2]Department de génie informatique et génie logiciel [3]Regroupement Québecois de Matériaux de Pointe. École Polytechnique de Montréal C.P. 5079, Succursale Centre-ville, H3C 3A7, Montréal, Québec, Canada

INTRODUCTION: Recent advances in nanotechnology have led to the development of magnetic nanoparticles (NMs) as iron oxide, including magnetite (Fe_3O_4), for drug delivery, magnetic resonance imaging (MRI), repair tissue, hyperthermia and cell separation. Many synthetic methods are often non-uniform size, incomplete crystallinity inhomogeneous composition and aggregate easily due to the magnetic attraction. Recently, an interesting alternative to these synthetic nanomaterials, called magnetosomes, was found in magnetotactic bacteria. The synthesis of magnetosomes by a biological process promises benefits in terms of controlling the crystal size and morphology, and superparamagnetic behavior at room temperature.

OBJECTIVE:

Compare synthetic Iron Oxide NPs with natural magnetosomes, in order to obtain a relation between their morphology, magnetic and physico-chemical properties, for propose as vehicle of delivering nitric oxide (NO) anti-biofilm.

METHODS: Magnetosomes: The bacteria used for the isolation of magnetosomes was Magnetococcus sp. MC-1. It was grown in a chemoheterolitriphic liquid media under microaerobic conditions. The bacteria were extracted from the culture media by centrifugation and the magnetosomes were isolated by using a magnet and the buffer as then aspirated leaving the only magnetosomes. The magnetosomes were washed and re-suspended in a solution containing 20% SDS (to destroy the possible proteins found in the surface of the magnetosome) using an agitator. The same method using a magnet and aspiration to isolate the magnetosome was used and putted finally in water.

The synthesis of the SPIONs with positive, negative and bare charge was doing according with the methodology reported by Sophie Laurent [1] and the following materials:

Positive NP: Aminopropyltriethoxysilane (APTES), Methanol, Acetone, Glycerol.

Negative SPION: DMF, Acetone, Water, Ether, NaOH solution, Neodymium magnet

Bare SPION: FeCl2.4H2O, FeCl3.6H2O, NaOH, Diethyleneglycol, HNO3 solution, Neodymium magnet

RESULTS: The morphology and size distribution were analyzed by transmission electron microscopy (TEM), where SPIONs with positive, negative and bare change and sizes around 10nm are compare with necklace-like chains of magnetosomes with sizes of NPs around 83nm and length of approximately 0.4 - 0.8 μm.

In order to complete the comparison of properties X-ray photoelectron spectroscopy (XPS) was used to make a detailed analysis of the surface, describe the functional groups on the surface of our NPs and corroborate with Fourier Transform Infrared (FTIR). Finally by vibrating sample magnetometer (VMS) we compare the values of saturation magnetization that were found around of 10 000 Oe at room temperature and confirm the superparamagnetic behavior of iron oxide nanoparticles and the ferromagnetic behavior of magnetosomes.

DISCUSSION & CONCLUSIONS: The results presented in this paper show promise for applications in the development of vehicle of delivering nitric oxide (NO) anti-biofilm, in agreement with the present superparamagnetic behavior, the uniform size and surface analysis.

REFERENCES: [1] S. Laurent et al (2012) *PLoS ONE*, **7(1)**:1-9

ACKNOWLEDGEMENTS: We are grateful to FQRNT which subsidizes the project.

Research on electrochemical properties SiO_2 layer, intended for contact with blood, deposited by sol-gel method

M Basiaga[1], W Walke[1], Z Paszenda[1], P Karasiński[2], J Szewczenko[1]

[1] *Faculty of Biomedical Engineering, Department of Biomaterials and Medical Engineering Devices, Silesian University of Technology, Zabrze, Poland.* [2] *Faculty of Electrical Engineering, Department of Optoelectronics, Silesian University of Technology, Gliwice, Poland*

INTRODUCTION: One of the ways how to increase hemocompatibility of the surface of titanium and its alloys is application of sol-gel method to create thin oxide layers based on such elements as: Ti, Si. An advantage of this method is low temperature at which the layer is created, which guarantees invariability of mechanical properties of metallic substrate. Data taken from subject-matter literature present, though, a number of undefined phenomena that accompany creation of oxide layers with participation of silicon on the surface of metallic biomaterial. One of the ways how to verify applicability o such surface modification is electrochemical tests [1, 2].

METHODS: Stock material for tests was titanium Grade 4 and titanium alloy Ti67. Samples were subject to surface treatment – mechanical polishing (Ra = 0,12 μm) and then SiO_2 layer was applied with the employment of sol-gel method (v = 3.0 cm/min, T = 430 °C, t = 60 min) [2]. In order to evaluate electrochemical characteristics of surface modified that way, pitting corrosion resistance test were performed as well as impedance measurement. The tests were made in artificial blood plasma at the temperature of T = 37 ±1°C with application of measurement system AutoLab PGSTAT 302N equipped with FRA2 module (Frequency Response Analyser).

RESULTS: Determined anodic polarisation curves proved the presence of a passive range to the value of the potential E = +4 V irrespective of the type of material and conditions of creating the layer – fig 1a. Rapid increase of anodic current density that would prove that pitting corrosion process was initiated was not observed in the analysed measurement range. Polarisation resistance Rp, determined additionally with application of Stern method, was within the range for: titanium Grade4: 350 – 380 kΩcm^2; modified titanium Grade4: 3350 – 3400 kΩcm^2, whereas for: titanium alloy Ti67: 520 – 540 kΩcm^2 modified titanium alloy Ti67: 3950 – 4000 kΩcm^2. Obtained results showed that the most favourable variant is modification SiO_2 for titanium alloy Ti67. Then, performed impedance tests confirmed good properties that protect biomaterial from artificial blood plasma impact. Maximum values of phase angles in a wide range of frequencies, presented in Bode diagrams, irrespective of the applied variant, are similar and equal $\theta \approx 80°$. Inclinations $\log|Z|$ in the whole range of frequency changes are close to -1, which proves capacitive character of the oxide layer – fig. 1b. Next, obtained large impedance values $|Z| > 10^6$ Ωcm^2 in the range of the smallest frequencies show good dielectric and protective properties of the oxide layers.

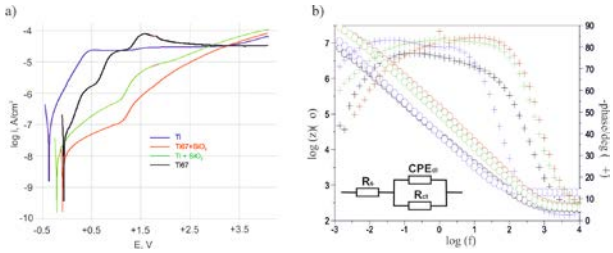

Fig. 1: Results of electrochemical properties: a) corrosion resistance, b) EIS study

DISCUSSION & CONCLUSIONS: Suggestion of proper variants of surface treatment with application of sol-gel method is of a long-range importance and will contribute to preparation of technological conditions with precise parameters of oxide layers creation on titanium implants used in the environment of human blood.

REFERENCES: [1]S.Shibli, S.Mathai (2008) Development and bio-electrochemical characterization of a novel TiO_2–SiO_2 mixed oxide coating for titanium implants. *Journal of Material Science* 19:2971–2981 [2]P.Karasiński, J.Jaglarz, M.Reben, E.Skoczek, J.Mazur (2011) Porous silica xerogel films as antireflective coatings – Fabrication and characterization. *Optical Materials* 33:1989-1994.

ACKNOWLEDGEMENTS: The project was funded by the National Science Centre allocated on the basis of the decision No. 2011/03/B/ST8/06499

Novel hybrid membrane of chitosan/ polycaprolactone for tissue engineering

GBC Cardoso[1-2], ABM Silva[4], M Sabino[3], AR Santos Jr[4] and CAC Zavaglia[1-2]

[1] State University of Campinas, Materials Engineering Department, Campinas, Brazil [2] Biofabris, Campinas, Brazil [3] Chemical Department, Grup B5IDA, Universidad Simón Bolívar, Caracas-Venezuela [4]Federal University of ABC, Santo André, São Paulo, Brazil

INTRODUCTION: Rotary jet spinning is a simple process to produce 3D structure that does not require high-voltage electric. Using this novel technique is possible to obtain non woven fibers and 3D scaffolds with different kinds of polymers, blends and composites, with a high porosity [1]. Poly(ε-caprolactone) (PCL), well-known semicrystalline aliphatic polyester used extensively and FDA-approved for biomedical applications, it has low surface energy and therefore does not interact strongly with soft tissues, and also has a slow degradation rate (up to 6 to 36 months). Its highly crystalline structure is beneficial to its mechanical properties, but complicates the processing and reduces tissue interactions. In other hand, the biopolymer chitosan (CH) ensures not only biodegradation but also its natural characteristic of being an antimicrobial agent and guaranty biocompatibility with cell culture. Furthermore, CH has the same charge as self-assembled PCL scaffolds, preventing ionic binding of chitosan to a PCL surface. The aims of this research were to investigate the potential use in tissue engineering of the 3D hybrid structure: Chitosan membrane/Polycaprolactone mesh.

METHODS: For the rotatory jet spinning were used the polymer polycaprolactone (Mw. 80 KDa-Aldrich) and Chloroform (Merck), as solvent [2]. Through this 3D structure is created a biodegradable membrane by casting technique, using Chitosan (from shrimp shells, Aldrich), and finally in this way was generated a 3D hybrid structure: membrane-interconnected filaments. The samples were characterized by differential scanning calorimetry and scanning electron microscopy. All the samples: PCL and chitosan films, PCL mesh and chitosan/PCL membrane were tested in vitro, using Vero cells during the periods of 1, 3 and 5 days. Images were captured using a Nikon light microscope 80i [3].

RESULTS: As proof-of-principle we produced rotatory jet spinning using the low cost homemade equipment. We produced PCL fibers with high porosity surface (Fig 1a), therefore this fact may influence at the cell adhesion and proliferation. Also, analysing the SEM images was possible to note the full coating of the biomaterial with chitosan; the fibers were coated resulting into a roughness surface (Fig 1b). Also the literature shows that the PCL blended with CH improves water absorption capability, which is desirable property in many biomedical applications [3;4]. The DSC analysis demonstrates the main peaks of PCL and CH of the blend, showing the presence of the polymers and the absence of the solvents used. The analysis of cytotoxicity by direct exposure of Vero cells showed that these 3D structures show biocompatibility and non toxicity.

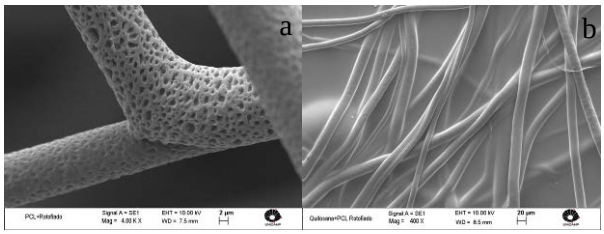

Fig. 1: Images: a) PCL fibers by rotatory jet spinning-scale 2µm; b) Chitosan membrane-polycaprolactone mesh- scale 20 µm.

DISCUSSION & CONCLUSIONS: The rotatory jet spinning was investigated and successfully used to produce PCL 3D porous mesh. Also, the technique of casting promoted the combination of PCL mesh with CH membrane. Finally, the successful addition of cells is creating an even more versatile and biocompatible 3D hybrid structure.

REFERENCES: [1] Badrossamay, M. R., Mcilwee, H. A., Goss, J. A. (2010) *Nano Letter*, **10**: 2257. [2] Mikos, A.G., Temenoff, J.S. (2000), *EJB Electronic Journal of Biotechnology* **3**:1-6. [3] Santos Jr., A.R., Barbantib, S H., Duek E.A.R., Wadad, M.L.F. (2009) *Materials Research*, **12**:257-263. [4] Hoque ME, San WY, Wei F, Li SM, Huang MH, Vert M,Hutmacher DW (2009) *Tissue Eng A* **15(10)**:3013. [5]Cruz DMG, Coutinho DF, Martinez EC, Mano JF, Ribelles JLG, Sanchez MS (2008) *J Biomed Mater Res B* **87B(2)**:544.

Corresponding author: guicardoso@fem.unicamp.br; amaliabapm@gmail.com; msabinog@gmail.com; arnaldo.santos@ufabc.edu.br; zavagl@fem.unicam.br.

Comparative study of the adhesion of biochemical complex macromolecules and chemical scales to reverse osmosis membrane surfaces

N Kang[1], J Lee[1,2], MH Jung[3], YH Lee[1]

[1] *Center for Water Resource Cycle, Korea Institute of Science and Technology*
[2]*Department of Environmental Engineering, Konkuk University*
[3] *Department of Physics, Sogang University, South Korea*

INTRODUCTION: In recent years, the use of reverse osmosis (RO) membranes in advanced wastewater reclamation has been extensively applied. The treated secondary wastewater effluent, which is the feed source for reclamation process, contains a considerable amount of divalent cations (i.e., Ca^{2+}, Mg^{2+}) and dissolved organic macromolecules. The presence of divalent cations has been reported to form scales with various anions and complex macromolecules with the constituents of dissolved organic matters, which are having significantly adhesive properties to membrane surface. In our study, the effects of feed solution chemistry (species of cations and anions, pH) and dissolved organic composition on the adhesion of biochemically formed complex macromolecules and chemical scales to RO membrane surfaces were specifically investigated.

METHODS: The polyamide thin-film composite RO membranes (BW30LE, Filmtec, USA) were selected. The membrane flux experiment was carried out in a custom-built lab-scale RO membrane filtration system which had three cross-flow cell units [1]. Membrane fouling was initiated by adding dissolved organics (BSA, alginate) and/or divalent cations (Ca^{2+}, Mg^{2+}) to the feed. The resultant flux profile was used to analyse the adhesion behaviour of biochemical complex macromolecules and chemical scales under the influence of different solution chemistries.

RESULTS: The presence of divalent ions reduces the electrostatic repulsion among dissolved organic molecules (BSA and alginate) and between the molecules and the membrane surface. The interaction of BSA and alginate with Ca^{2+} and Mg^{2+} resulted in a significant adhesion of biochemical complex macromolecules to the membrane surface. The morphology of the fouled membranes examined using SEM was shown in Fig. 1.

The flux profiles for the various foulant compositions are shown in Fig. 2. The fouled membrane by the adhesion of biochemical complex macromolecules resulted in a significant initial flux decline because of the interaction of BSA and alginate molecules with divalent cations which formed a gel-type fouling layer on the membrane surface (Fig. 1).

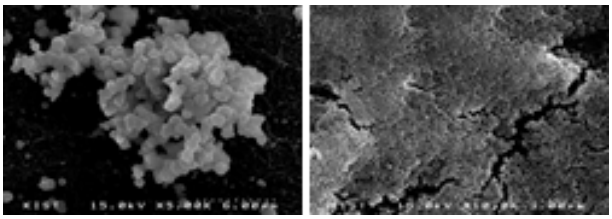

Fig. 1: SEM Images of fouled RO membranes by the adhesion of chemical scales (left) and biochemical complex macromolecules (right).

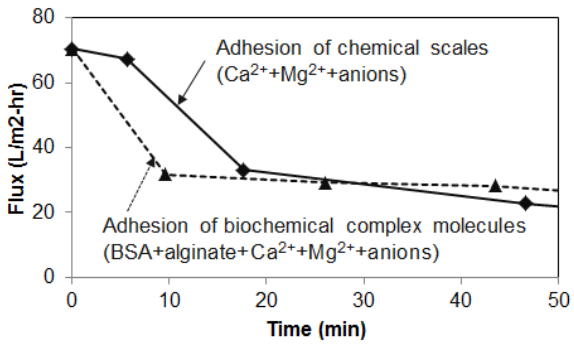

Fig. 2: RO membrane flux profiles.

DISCUSSION & CONCLUSIONS: This study has shown that the membrane fouling by the adhesion of chemical scales could be significantly enhanced by the adhesion of biochemical complex macromolecules in the presence of organic biomolecules.

REFERENCES: [1] C. Park, Y.H. Lee, S. Lee, S. Hong (2008) *Desalination* **220**:335-344.

ACKNOWLEDGEMENTS: This research was based on work supported by Center for Water Resource Cycle at KIST and by KEITI (Korea Environmental Industry & Technology Institute) (Project No. 192-091-001).

Fabrication and characterization of bioactive porous coatings on tantalum through micro-arc oxidation process

YC Li[1], YT Liu[2], KC Kung[2], TM Lee[3,4*], CC Wang[1]

[1] *Institute of Manufacturing Information and Systems, National Cheng Kung University, Taiwan*
[2] *Department of Materials Science and Engineering, National Cheng Kung University, Taiwan*
[3] *Institute of Oral Medicine, National Cheng Kung University, Taiwan*
[4] *Medical Devices Innovation Center, National Cheng Kung University, Taiwan*

INTRODUCTION: Titanium (Ti) and its alloys are ideally suited for implants due to their good biocompatibility. However, Ti lacks the level of osseointegration required for implant longevity. Recently, tantalum (Ta) is gaining more attention for new usages of metallic biomaterial. Ta can serve as a substitute for Ti, providing biological characteristics suitable substrates for osteoblast growth [1]. Implant covered with a porous surface that allows bone ingrowth fixation. In addition, the presence of bioactive CaP coatings improve a direct bone-implant contact the healing process [2]. The aim of this study was to fabricate porous CaP-containing coatings on the Ta surface using the MAO technique and evaluate the coatings topography, phase, and chemical composition.

METHODS: The pure tantalum disks with a size of ϕ12.7×2 mm were used as substrates, and in accordance with the specification of ASTM F560-08. The surfaces of the disks were polished with SiC papers to #1500 and ultrasonically cleaned with acetone, ethanol and distilled water prior to micro-arc oxidation treatment. The electrolyte solution contains $Ca(CH_3COO)_2•H_2O$ and $NaH_2PO_4•H_2O$. Ta disks were treated at an applied pulse voltage of 400 V, a pulse frequency of 1000 Hz and a duty ratio of 50% for 1.5 min. The surface morphology were observed by SEM (JEOL JSM-6390LV) with EDX (INCA 350 Oxford) for chemical analysis.

RESULTS: Fig. 1(a-b) presents the surface morphologies of Ta and Ta-MAO specimens. The surface of the Ta became rough and porous following spark discharges at a high applied voltage. These pores are well separated and distributed homogeneously over the surface. As shown in Fig. 1(c), the EDX spectra of Ta-MAO specimen exhibited that coatings included calcium, phosphorus, tantalum, and oxygen. Fig. 2 illustrates the roughness and wettability of various specimens. The contact angle of the Ti and Ta specimens were 56° and 43°, respectively. In contrast, the contact angle of the Ta-MAO specimen was 23°, which indicated that Ta-MAO specimens were hydrophilic and had a high surface energy. The Ra value of the Ta-MAO specimens was 0.7 μm, showing an increase with roughness.

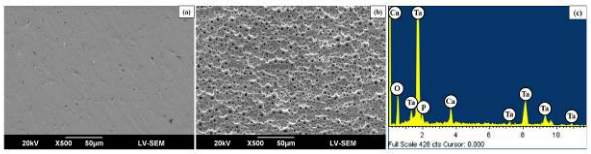

Fig. 1: Microstructures of (a) pure Ta; (b) Ta-MAO. (c) EDX spectra taken for the Ta-MAO.

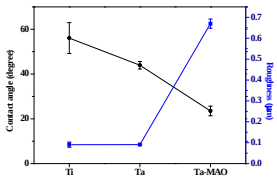

Fig. 2: The roughness and contact angles measured for various specimens

DISCUSSION & CONCLUSIONS: MAO integrates morphological and chemical modification in a single process. The Ta substrates were oxidized through process, whereupon a porous layer spontaneously grew on the surface. A well-controlled surface texture on implant surface can promote osseointegration [3]. Ta-MAO surface is hydrophilic, which may alter the population of proteins adsorbed thereby promote better cell–material interactions [4]. So this modified Ta is an improved alternative to untreated Ta for bone repair applications.

REFERENCES: [1] D.M. Findlay et al (2004) *Biomaterials* **25**:2215-27. [2] Z. Lin et al (2007) *J Biomed Mater Res A* **83**:1165-75. [3] P.R. Klokkevold et al (1997) *Clin Oral Impl Res* **8**:442-7. [4] V.K. Balla et al (2010) *Acta Biomaterialia* **6**:2329-34.

ACKNOWLEDGEMENTS: This work was financially supported by the National Science Council, Taiwan (NSC 100-2221-E-006-263)

Characteristics of calcium phosphate coated on titanium oxide nanotube arrays: an *in vitro* study

KC Kung[1], YT Liu[1], JL Chen[2], TM Lee[2,3], TS Lui[1]

[1] *Department of Materials Science and Engineering, National Cheng Kung University, Taiwan*
[2] *Institute of Oral Medicine, National Cheng Kung University, Taiwan*
[3] *Medical Devices Innovation Center, National Cheng Kung University, Taiwan*

INTRODUCTION: The different geometrical shapes of TiO_2 nanotubes have a wide range of relevant applications. Moreover, TiO_2 nanotubes are useful for improving cell functions of osteoblasts [1]. Calcium phosphate (CaP) of bioceramics could form a bone-like apatite on implant surfaces and improves osseointegration. Although TiO_2 nanotubes in physicochemical and biological performance and CaP coatings on titanium surface have been studied [2], it was seldom reported that CaP were coated on nanotube arrays. The aim of this study is to investigate the characteristics and biological responses of TiO_2 nanotube arrays coated with calcium phosphate.

METHODS: Disks of medical grade titanium were selected as substrate. The electrolyte was 1 M phosphoric acid (H_3PO_4) aqueous solution with the addition of 1 wt % hydrofluoric acid (HF). The specimen was used as the anode, and a Pt plate was used as the cathode. The samples were treated with an applied constant voltage of 10 V. CaP coatings were deposited onto nanotube arrays surface by RF sputtering. For heat treatment, the specimens were heated at temperature of 500°C in the vacuum tubefurnace. The physicochemical properties were evaluated by SEM, EDS, and XRD equipments. The biological properties were evaluated by *in vitro* tests, in term of the cell morphology and cell proliferation.

RESULTS: The surface morphology of sputtering CaP on nanotube arrays with vacuum heating treatment was shown in Figure 1(a). The three-dimensional structures with open pores were observed on the specimen. The Ca and P elements were distributed on nanotube arrays, as shown in Fig. 1(b). The XRD patterns showed that nanotube arrays were amorphous phase. Figure 2 shows the SEM of cell morphologies on nanotube arrays with sputtering CaP and heat treatment after 3 and 12 h of cell culture. Cells began to spread at two sides at 3-h culture, and flattened at 12-h culture. Besides, the significant increase in cell numbers as function of time was observed on the specimens throughout culture period.

Figure 1 Figure 2

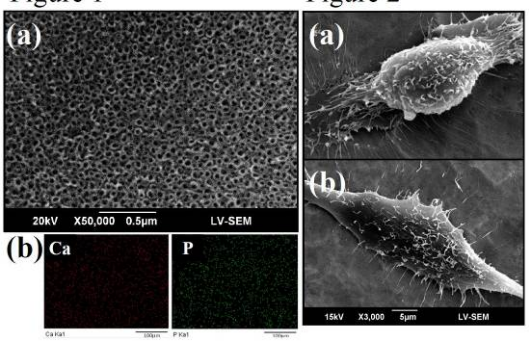

Fig. 1:. (a) The specimen morphology, and (b) Elemental distributions.
Fig. 2: Cell morphologies on the specimens. (a) 3 h, and (b) 12 h.

DISCUSSION & CONCLUSIONS: The 3D structures with open pores were observed on the specimen, and Ca and P were uniformly sputtered on the nanotube arrays. The nanotube surface showed the excellent cell adhesion, and an abundant amount of extracellular matrix (ECM) between the neighboring cells were observed with filopodia extensions [3]. The nanotube arrays could provide a template for the cell adhesion and proliferation. Besides, the small diameter of nanotube showed the better cell behavior [4]. This study indicated that cell activity can be significantly enhanced on nanotube arrays with sputtering CaP and heat treatment. Moreover, nanotube arrays with sputtering CaP and heat treatment can be designed to support cell functions on the implant.

REFERENCES: [1] J. Park et al (2007) *Nano Lett.* **7**:1686-91. [2] C. Yao et al (2008) *JBMR* **85A**:157-66. [3] K. Das et al (2009) *JBMR* **90A**:225-37. [4] J. Park et al (2009) *Small* **5**:666-71.

ACKNOWLEDGEMENTS: The authors would like to thank Medical Devices Innovation Center of NCKU (Grant D101-21008).

Matrix engineering for stem cells function: mesenchymal stem cells characteristics on a FGF2-immobilized surface

J Kang[1], J Kang[1], Y Kim[2], S Heon Kim[1]

[1] Center for Biomaterials, Korea Institute of Science and Technology, Seoul, Korea. [2] Department of Chemical Engineering, Soongsil University, Seoul

INTRODUCTION: Mesenchymal stem cells (MSCs) hold great promise as an important cell source for regenerative medicine because they can be easily isolated and expanded. In stem cell and tissue engineering research, studies involving cellular adhesion to an artificial ECM (art-ECM) have recently heightened [1]. Recently, we demonstrated that HSPG on cell membrane are involved in the cell adhesion via the heparin-binding region of fibronectin [2]. In this study, a MBP-FGF2 fusion protein was synthesized as a HSPG targeting matrix for stem cell adhesion and was characterized based upon immobilization and biochemical and biological activities.

METHODS: MBP-FGF2 adsorption onto polystyrene (PS) surface was determined by AFM and XPS analysis. The percent of cells adhered was determined from the amount of protein measured by the BCA assay (Pierce). For an inhibitory cell adhesion assay, 96-well PS plates coated with proteins were incubated with a given concentration of heparin for 1h at 37°C followed by the cell adhesion assay. BMSCs were used after being cultured for 5 days on PS-MBP-FGF2 or PS-FN for differentiation, FACS, real time-PCR, and glycoanalysis

RESULTS: MBP-FGF2 was adsorbed onto PS surface in a monolayered manner. The immobilized FGF2 bound soluble heparin. Bone marrow MSCs (BMSC) were adhered to PS-MBP-FGF2. The adhesion was inhibited by heparin but not FGFR receptor antagonist and a potent inhibitor of FGFR, PD173074. This result means that the adhesion is mediated by HS but not FGF receptor. Morphologies of hASCs on PS-MBP-bFGF were significantly different from ones on FN surface. BMSCs cultured on PS-MBP-FGF2 were inhibited to differentiate into osteogenic and adipogeneic cells as compared to PS-FN. MSC markers were down-regulated in BMSC cultured on PS-MBP-FGF2 compared to PS-FN.

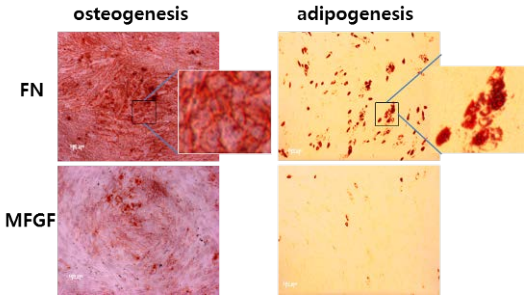

Fig. 1: Differentiation of BMSC on FN- or MBP-FGF2 coated surface

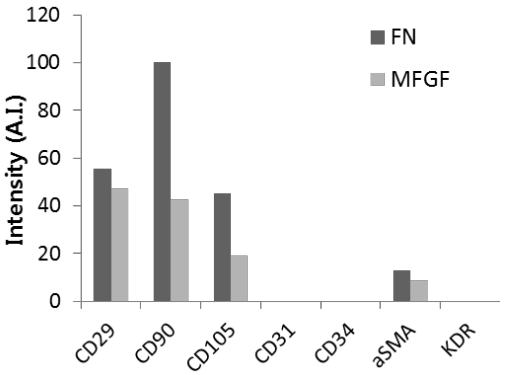

Fig. 2: Surface markers of BMSC on FN- or MBP-FGF2 coated surface

DISCUSSION & CONCLUSIONS: In conclusion, we propose that cell adhesion mechanisms strongly influence stem cell differentiation and that surfaces displaying immobilized FGF can serve as an artificial matrix for regulating integrin-mediated signaling and stem cell differentiation through FGF-heparin interaction.

REFERENCES: [1]Mauney JR, Volloch V, Kaplan DL . Biomaterials (2005) **26**:6167-75. [2]Park I-S, Han M, et al., *Biomaterials* (2009) **30**:6835–43.

ACKNOWLEDGEMENTS: This study was supported by the Korea Science and Engineering Foundation (KOSEF) grant funded by the Korea government.